

1-28-2015

ENVIRONMENTAL RADIATION DOSE ASSESSMENT AND VALIDATION FOR URANIUM HEXAFLUORIDE STORAGE MANAGEMENT

Shiaw-Der Su

Follow this and additional works at: https://digitalrepository.unm.edu/ne_etds

Recommended Citation

Su, Shiaw-Der. "ENVIRONMENTAL RADIATION DOSE ASSESSMENT AND VALIDATION FOR URANIUM HEXAFLUORIDE STORAGE MANAGEMENT." (2015). https://digitalrepository.unm.edu/ne_etds/11

This Dissertation is brought to you for free and open access by the Engineering ETDs at UNM Digital Repository. It has been accepted for inclusion in Nuclear Engineering ETDs by an authorized administrator of UNM Digital Repository. For more information, please contact disc@unm.edu.

Shiaw-Der Su

Candidate

Nuclear Engineering

Department

This dissertation is approved, and it is acceptable in quality and form for publication:

Approved by the Dissertation Committee:

Adam Alexander Hecht, Chairperson

Cassiano Richardo Endres de Oliveira

Shuang (Sean) Luan

Rick Kohrt

**ENVIRONMENTAL RADIATION DOSE
ASSESSMENT AND VALIDATION FOR
URANIUM HEXAFLUORIDE STORAGE MANAGEMENT**

by

SHIAW-DER SU

B.S., Nuclear Engineering, National Tsing Hua University, 1968
M.S., Nuclear Engineering, Purdue University, 1971

DISSERTATION

Submitted in Partial Fulfillment of the
Requirements for the Degree of

**Doctor of Philosophy
Engineering**

The University of New Mexico
Albuquerque, New Mexico

December, 2014

ACKNOWLEDGEMENTS

I heartily acknowledge Dr. Adam Alexander Hecht, my advisor and dissertation chair, for his constructive and professional advice and guidance in the course of completing this doctoral research and dissertation. I am sincerely grateful for his constant support and positive feedback.

I also thank my committee members, Dr. Cassiano Ricardo Endres de Oliveira, Dr. Shuang (Sean) Luan, and Mr. Rick Kohrt, for their support pertaining to this research, and assistance in my academic development and achievement. Gratitude is extended to URENCO USA in Eunice, New Mexico for the sponsorship of this research and use of their technical data, and to their technical staff for supporting field measurements and data collection.

And finally to my dear wife, Shi-Ju (Pearl), your love is the greatest gift of all. I am forever indebted to you for your patience, support, sacrifices and encouragement throughout the years in my pursuit of a doctorate degree.

**ENVIRONMENTAL RADIATION DOSE ASSESSMENT AND VALIDATION FOR
URANIUM HEXAFLUORIDE STORAGE MANAGEMENT**

by

Shiaw-Der Su

B.S., Nuclear Engineering, National Tsing Hua University, 1968

M.S., Nuclear Engineering, Purdue University, 1971

Ph.D., Engineering, The University of New Mexico, 2014

ABSTRACT

This research entailed development and application of an efficient indirect Monte Carlo simulation methodology for performing environmental radiation dose assessment for storage of a large number (thousands) of uranium hexafluoride (UF_6) cylinders in an outdoor storage area. The primary objective was to substantially improve the Monte Carlo computational efficiency by an order of magnitude or better as compared to the previous time-consuming methodology using the direct, standard simulation approach. The collateral objective was to support onsite storage of UF_6 cylinders at uranium enrichment facilities, addressing dose impacts on storage capacity, footprint requirements, and cylinder placement in terms of spacing, array and stacking.

The research was carried out in four sequential phases: Phase 1 – UF_6 radiation source term development; Phase 2 – single UF_6 cylinder dose evaluation for parameter selection; Phase 3 – multiple UF_6 cylinder dose assessment methodology development and application; and Phase 4 – validation of computational efficiency and dose simulations.

Phases 1 and 2 were a prerequisite for Phase 3 to provide the necessary data and input for use in Phase 3. The results of the single and multiple cylinder dose calculations from Phases 2 and 3 were validated in Phase 4 including quantification of computational efficiency. The analytical tools for the research consisted of the ORIGEN-S module in the SCALE 6.1.2 code package for source term calculations, the MAVRIC module in SCALE 6.1.2 for source importance data generation, and MCNP5 (v1.60) for radiation dose calculations.

The indirect Monte Carlo simulation process developed from Phase 3 was applied to a case study involving different storage configurations to investigate the dose trend and sensitivity to storage capacity, and dose impacts to storage management. The case study produced the results of the neutron and photon dose rates from multiple UF₆ cylinders in various storage arrays and stacks for impact analysis and demonstration of regulatory compliance at environmental locations such as the site boundary.

The computational efficiency of the indirect Monte Carlo dose simulations was quantified in terms of figure of merit, confirming the accomplishment of the objective for substantial improvement over the direct, standard approach. In addition, comparison of the dose rate results for single and multiple cylinders from this research against the field measurements and other calculations available validated the environmental dose assessment with respect to the degree of accuracy and conservatism. As a result of this research, future related work was identified and recommended for further development and enhancement.

TABLE OF CONTENTS

LIST OF FIGURES	xiii
LIST OF TABLES	xvi
ACRONYMS AND ABBREVIATIONS	xxi
1. INTRODUCTION	1
1.1 RESEARCH OBJECTIVES	3
1.2 RESEARCH SCOPE	4
1.3 MANUSCRIPT ORGANIZATION	5
2. DESCRIPTION OF UF ₆ CYLINDER STORAGE	7
2.1 UF ₆ CYLINDER DESCRIPTION	7
2.2 UF ₆ CYLINDER STORAGE AND STACKING.....	10
2.3 UUSA ENRICHMENT FACILITY DESCRIPTION	12
2.4 UUSA UBC STORAGE PAD DESCRIPTION.....	13
3. UF ₆ DIRECT RADIATION SOURCE TERMS	16
3.1 BASES AND ASSUMPTIONS.....	17
3.2 METHODOLOGY	20
3.2.1 Radioactive Decay Calculation.....	21
3.2.2 Neutron Source Calculation.....	22
3.2.3 Photon Source Calculation.....	25
3.3 CALCULATIONAL INPUTS/NOMEMCLATURE.....	26
3.4 DETAILED CALCULATION	27
3.4.1 Uranium Isotopic Concentrations	27
3.4.2 Nuclide Masses per kg of UF ₆	28

3.4.3	ORIGEN-S Calculations	29
3.4.4	Photon Source Correction for UF ₆ Matrix Bremsstrahlung.....	31
3.5	NEUTRON SOURCE TERM PER UNIT BASIS	33
3.6	UNCORRECTED PHOTON SOURCE TERM PER UNIT BASIS.....	36
3.7	CORRECTED PHOTON SOURCE TERM PER UNIT BASIS	37
3.8	RADIATION SOURCE TERM PER FILLED CYLINDER	38
3.9	TIME-DEPENDENT PHOTON SOURCE FOR FILLED FEED CYLINDER	41
3.10	TIME-DEPENDENT PHOTON SOURCE FOR EMPTY FEED CYLINDER	43
3.11	COMPARISON WITH PREVIOUS CALCULATIONS.....	45
3.12	KEY OBSERVATIONS	49
4.	SINGLE CYLINDER DOSE EVALUATION.....	51
4.1	PREVIOUS WORK.....	52
4.2	BASES AND ASSUMPTIONS.....	54
4.3	EVALUATION METHODOLOGY	55
4.4	TECHNICAL INPUTS	57
4.4.1	Model 48Y Cylinder Physical Parameters	57
4.4.2	Material Densities and Compositions	58
4.4.3	Neutron and Photon Source Strengths and Energy Spectra.....	59
4.4.4	Neutron and Gamma-Ray Dose Conversion Factors.....	60
4.4.5	Nuclear Cross Section Data	62
4.5	EVALUATION DETAILS	63
4.5.1	UF ₆ Material Density Calculation.....	63
4.5.2	Neutron Source Energy Spectrum of Importance.....	64

4.5.3	Photon Source Energy Spectrum of Importance.....	65
4.6	MCNP CALCULATIONS	67
4.6.1	Physical Models	67
4.6.2	Dose Rate Calculations.....	69
4.7	EVALUATION RESULTS	71
4.7.1	Energy Response Factors	71
4.7.2	Average Radial Contact Dose Rate versus U-235 Concentration	72
4.7.2	Average Radial Contact Photon Dose Rate versus Time.....	74
4.7.3	Neutron Results for a Single Filled Feed Cylinder.....	76
4.7.4	Photon Results for a Single Filled Feed Cylinder.....	78
4.7.5	Photon-to-Neutron Dose Ratio for a Single Filled Feed Cylinder.....	81
4.7.6	Photon Results for a Single Empty Feed Cylinder	84
4.8	KEY OBSERVATIONS AND PARAMETER SELECTION	86
5.	MULTIPLE CYLINDER DOSE ASSESSMENT METHODOLOGY	89
5.1	OVERVIEW	91
5.2	PREVIOUS WORK.....	93
5.3	SOURCE IMPORTANCE DATA GENERATION.....	96
5.3.1	Photon Source Position Biasing.....	96
5.3.2	Source Energy Biasing.....	105
5.3.3	Source Direction Biasing	106
5.4	INDIRECT MONTE CARLO SIMULAITONS	107
5.4.1	Key Parameters	108
5.4.2	Case Study	109

5.4.3	First-Step Process.....	110
5.4.4	Second-Step Process	116
6.	MULTIPLE CYLINDER DOSE RESULTS AND IMPACTS.....	119
6.1	NEUTRON DOSE RATES FOR FILLED FEED CYLINDERS	119
6.2	PHOTON DOSE RATES FOR FILLED FEED CYLINDERS	124
6.3	TOTAL DOSE RATES FOR FILLED FEED CYLINDERS	129
6.4	DOSE SENSITIVITY TO ARRAY SIZE AND STACKING.....	133
6.5	DOSE IMPACTS FOR FILLED FEED CYLINDERS.....	138
6.6	MANAGEMENT OF EMPTY FEED CYLINDER STORAGE	140
6.6.1	Equivalent Number of Freshly Emptied Cylinders.....	141
6.6.2	Dose Assessment for Empty Feed Cylinders.....	144
6.6.3	Storage Management Considerations	146
7.	VALIDATION OF COMPUTATIONAL EFFICIENCY	149
7.1	NEUTRON CALCULATIONS.....	149
7.2	PHOTON CALCULATIONS.....	152
7.3	DOSE ESTIMATES FROM SINGLE-STACK CALCULATIONS	154
7.4	COMPARISON WITH UUSA CALCULATION.....	161
8.	VALIDATION OF DOSE SIMULATIONS	163
8.1	MEASURED DOSE RATE DATA FOR SINGLE CYLINDERS	163
8.1.1	Single Cylinder Measurements at UUSA	163
8.1.2	Single Cylinder Radiation Surveys at UUSA	166
8.1.3	Single Tails Cylinder Measurements at Capenhurst.....	167
8.1.4	Single Feed Cylinder Measurements at Cameco	168

8.2	CALCULATED DOSE RATES FOR SINGLE CYLINDERS	169
8.2.1	UUSA Calculation	169
8.2.2	UD Calculation	171
8.2.3	Cameco Calculation	172
8.3	SUMMARY OF SINGLE CYLINDER COMPARISON	172
8.4	UUSA UBC STORAGE PAD MEASUREMENTS AND CALCULATION	174
8.4.1	UBC Storage Pad Measurements.....	174
8.4.2	UBC Storage Pad Dose Calculation	177
9.	CONCLUSIONS AND FUTURE WORK.....	183
9.1	CONCLUSIONS ON SOURCE TERMS.....	183
9.2	CONCLUSIONS ON SINGLE CYLINDER DOSE EVALUATION.....	184
9.3	CONCLUSIONS ON MULTIPLE CYLINDER DOSE ASSESSMENT	185
9.4	CONCLUSIONS ON VALIDATION.....	187
9.5	FUTURE WORK.....	188
	APPENDICES	190
	APPENDIX A ORIGEN-S COMPUTER FILES AND SAMPLE INPUT	191
A.1	ORIGEN-S CASES AND COMPUTER FILES	191
A.2	SAMPLE ORIGEN-S INPUT LISTING.....	192
A.2.1	Input File <i>nu.inp</i> – Natural Uranium with UO ₂ Bremsstrahlung	192
A.2.2	Input File <i>nu.inp</i> – Natural Uranium without UO ₂ Bremsstrahlung	192
A.2.3	Input File <i>nu1.inp</i> – Progeny Inventory for Empty Feed Cylinder.....	193
A.2.4	Input File <i>nu.inp</i> – Progeny Photon Source for Empty Feed Cylinder.....	193
	APPENDIX B NEUTRON AND PHOTON SOURCE DATA.....	195

APPENDIX C	FLUX-TO-DOSE RATE CONVERSION FACTORS	212
APPENDIX D	MCNP COMPUTER FILES FOR SINGLE CYLINDERS	214
D.1	MCNP CASES AND COMPUTER FILES FOR SINGLE CYLINDERS	214
D.2	SAMPLE MCNP INPUT LISITNG	215
D.2.1	Input File <i>feed_n1.txt</i>	215
D.2.2	Input File <i>feed_p1.txt</i>	217
D.2.3	Input File <i>empty_p1.txt</i>	219
APPENDIX E	CALCULATED DOSE RATES FOR SINGLE CYLINDERS	222
APPENDIX F	MAVRIC COMPUTER FILES AND INPUT LISTING	232
F.1	MAVRIC CASES AND COMPUTER FILES	232
F.2	MAVRIC INPUT LISITNG	232
F.2.1	Input File <i>d10x10p.inp</i>	232
F.2.2	Input File <i>d30x30p.inp</i>	234
APPENDIX G	MCNP COMPUTER FILES FOR FILLED CYLINDER ARRAY	237
G.1	MCNP CASES AND COMPUTER FILES	237
G.2	SAMPLE MCNP INPUT LISITNG	239
G.2.1	Input File <i>t100x100n01.txt</i>	239
G.2.2	Input File <i>t100x100n02.txt</i>	241
G.2.3	Input File <i>t100x100p01.txt</i>	242
G.2.4	Input File <i>t100x100p02.txt</i>	257
APPENDIX H	MCNP DOSE RATE MAPS AND RELATIVE ERRORS	260
APPENDIX I	EMPTY FEED CYLINDER DOSE ASSESSMENT	279
I.1	CUMULATIVE RELATIVE DOSE FROM EMPTY FEED CYLINDERS	279

I.2	MCNP CASES AND COMPUTER FILES FOR EMPTY FEED CYLINDERS	283
I.3	SAMPLE MCNP INPUT LISITNG	283
I.3.1	Input File <i>t10x10e01.txt</i>	283
I.3.2	Input File <i>t10x10e02.txt</i>	286
APPENDIX J	UUSA UBC STORAGE PAD DOSE CALCULATION	288
J.1	MCNP CASES AND COMPUTER FILES FOR VALIDATION USE	288
J.2	MCNP INPUT LISITNG	288
J.2.1	Input File <i>d100x8p01.txt</i>	289
J.2.2	Input File <i>d100x8p02.txt</i>	292
REFERENCES	294

LIST OF FIGURES

Figure 2-1 Physical Illustration of Model 48G Cylinder	8
Figure 2-2 Physical Illustration of Model 48Y Cylinder	9
Figure 2-3 Double Stacking of UF ₆ Storage Cylinders.....	11
Figure 2-4 UUSA Enrichment Facility Layout.....	12
Figure 3-1 UF ₆ Neutron Yield as a Function of U-235 Concentration in Weight Percents ...	34
Figure 3-2 Neutron Yield by Uranium Isotope.....	35
Figure 3-3 Neutron Source Term Comparison between UUSA and UNM Calculations	47
Figure 3-4 Photon Source Term Comparison between ORIGEN-2 (UUSA) and ORIGEN-S (UNM).....	48
Figure 4-1 Schematic of a Model 48Y Cylinder.....	57
Figure 4-2 Homogenized Source Geometry	68
Figure 4-3 Slumped Source Geometry	68
Figure 4-4 Average Radial Surface Dose Rates for Filled Cylinder versus U-235 Concentration.....	73
Figure 4-5 Time-dependent Average Contact Dose Rates for Filled and Empty Feed Cylinders	75
Figure 4-6 Radial Dose Rate Profile and Photon/Neutron Dose Ratio (Homogenized Geometry).....	83
Figure 4-7 Axial Dose Rate Profile and Photon/Neutron Dose Ratio (Homogenized Geometry).....	83
Figure 4-8 Photon Dose Rate Profiles for a Single 48Y Feed Cylinder	85

Figure 5-1 Source Sampling Importance Data – 10x10 Double Stacking (48Y Filled Feed Cylinders).....	101
Figure 5-2 Source Sampling Importance Data – 30x30 Double Stacking (48Y Filled Feed Cylinders).....	102
Figure 5-3 Normalized Relative Photon Source Importance for 10x10 Array.....	104
Figure 5-4 Normalized Relative Photon Source Importance for 30x30 Array.....	104
Figure 5-5 10x10 Filled Feed Cylinder Array – Single, Double and Triple Stacks	112
Figure 5-6 30x30 Filled Feed Cylinder Array – Single, Double and Triple Stacks	113
Figure 5-7 100x100 Filled Feed Cylinder Array – Single, Double and Triple Stacks	114
Figure 5-8 Triple Stacked 10x10 Array Model for 2 nd Step MCNP Calculation	118
Figure 6-1 Radial Neutron Dose Rate Profile for 10x10 Array.....	121
Figure 6-2 Radial Neutron Dose Rate Profile for 30x30 Array.....	122
Figure 6-3 Radial Neutron Dose Rate Profile for 100x100 Array.....	123
Figure 6-4 Radial Photon Dose Rate Profile for 10x10 Array.....	126
Figure 6-5 Radial Photon Dose Rate Profile for 30x30 Array.....	127
Figure 6-6 Radial Photon Dose Rate Profile for 100x100 Array.....	128
Figure 6-7 Radial Total Dose Rate Profile for 10x10 Array	130
Figure 6-8 Radial Total Dose Rate Profile for 30x30 Array	131
Figure 6-9 Radial Total Dose Rate Profile for 100x100 Array	132
Figure 6-10 Neutron Dose Sensitivity to Array Size and Stacking at 105 m	134
Figure 6-11 Neutron Dose Sensitivity to Array Size and Stacking at 205 m	135
Figure 6-12 Photon Dose Sensitivity to Array Size and Stacking at 105 m.....	136
Figure 6-13 Photon Dose Sensitivity to Array Size and Stacking at 205 m.....	137

Figure 6-14 Time-dependent Photon Dose Rate Profile for an Empty Feed Cylinder	143
Figure 6-15 Number of Freshly Emptied Cylinders Needed for Equivalent Dose	143
Figure 6-16 Photon Dose Rate Profile Comparison for Empty and Filled Cylinders	145
Figure 6-17 Dose Rate Comparison for Empty and Filled Feed Cylinder Storage Arrays ..	148
Figure 8-1 UUSA UBC Storage Pad Validation Model	181
Figure H-1 Single-Stack 10x10 Array Neutron Dose Rate Map and Relative Error	261
Figure H-2 Double-Stack 10x10 Array Neutron Dose Rate Map and Relative Error	262
Figure H-3 Triple-Stack 10x10 Array Neutron Dose Rate Map and Relative Error	263
Figure H-4 Single-Stack 30x30 Array Neutron Dose Rate Map and Relative Error	264
Figure H-5 Double-Stack 30x30 Array Neutron Dose Rate Map and Relative Error	265
Figure H-6 Triple-Stack 30x30 Array Neutron Dose Rate Map and Relative Error	266
Figure H-7 Single-Stack 100x100 Array Neutron Dose Rate Map and Relative Error	267
Figure H-8 Double-Stack 100x100 Array Neutron Dose Rate Map and Relative Error	268
Figure H-9 Triple-Stack 100x100 Array Neutron Dose Rate Map and Relative Error	269
Figure H-10 Single-Stack 10x10 Array Photon Dose Rate Map and Relative Error	270
Figure H-11 Double-Stack 10x10 Array Photon Dose Rate Map and Relative Error	271
Figure H-12 Triple-Stack 10x10 Array Photon Dose Rate Map and Relative Error	272
Figure H-13 Single-Stack 30x30 Array Photon Dose Rate Map and Relative Error	273
Figure H-14 Double-Stack 30x30 Array Photon Dose Rate Map and Relative Error	274
Figure H-15 Triple-Stack 30x30 Array Photon Dose Rate Map and Relative Error	275
Figure H-16 Single-Stack 100x100 Array Photon Dose Rate Map and Relative Error	276
Figure H-17 Double-Stack 100x100 Array Photon Dose Rate Map and Relative Error	277
Figure H-18 Triple-Stack 100x100 Array Photon Dose Rate Map and Relative Error	278

LIST OF TABLES

Table 2-1 Model 48G and 48Y Storage Cylinder Parameters	8
Table 3-1 U-235 Concentrations and Cylinder Types	27
Table 3-2 Cylinder Parameters	27
Table 3-3 Nuclear Data	27
Table 3-4 Uranium Isotopic Concentrations and UF ₆ Mass Distributions	29
Table 3-5 Bremsstrahlung Radiation Yield Data	32
Table 3-6 Effective Atomic Numbers for UO ₂ and UF ₆	33
Table 3-7 UF ₆ Neutron Source Term per Filled Cylinder for Various U-235 Weight Percents	39
Table 3-8 UF ₆ Photon Source Term per Filled Cylinder for Various U-235 Weight Percents	40
Table 3-9 Time-dependent UF ₆ Photon Source Term for 48Y Filled Feed Cylinder	42
Table 3-10 Time-dependent UF ₆ Photon Source Term for 48Y Empty Feed Cylinder	44
Table 4-1 Model 48Y Cylinder Parameters	58
Table 4-2 Material Densities and Compositions	59
Table 4-3 Full and Partial Neutron Energy Spectra for Filled 48Y Feed Cylinder	65
Table 4-4 Full and Partial Photon Energy Spectra for 48Y Feed Cylinder	66
Table 4-5 Average Radial Surface Dose Rates for Filled Cylinder versus U-235 Concentration	73
Table 4-6 Time-dependent Average Contact Dose Rates for Filled and Empty Feed Cylinders	75

Table 5-1 MAVRIC Photon Source Importance for 10x10 Array (48Y Filled Feed Cylinders)	103
Table 5-2 MAVRIC Photon Source Importance for 30x30 Array (48Y Filled Feed Cylinders)	103
Table 5-3 Unbiased and Biased Neutron Source Energy Distributions (48Y Filled Feed Cylinder)	106
Table 5-4 Unbiased and Biased Photon Source Energy Distributions (48Y Filled Feed Cylinder)	106
Table 5-5 Cylinder Storage Arrangements for Case Study	109
Table 5-6 Application of Photon Source Importance Data to Case Study	115
Table 6-1 Radial Neutron Dose Rate Profile for 10x10 Array	121
Table 6-2 Radial Neutron Dose Rate Profile for 30x30 Array	122
Table 6-3 Radial Neutron Dose Rate Profile for 100x100 Array	123
Table 6-4 Radial Photon Dose Rate Profile for 10x10 Array	126
Table 6-5 Radial Photon Dose Rate Profile for 30x30 Array	127
Table 6-6 Radial Photon Dose Rate Profile for 100x100 Array	128
Table 6-7 Radial Total Dose Rate Profile for 10x10 Array	130
Table 6-8 Radial Total Dose Rate Profile for 30x30 Array	131
Table 6-9 Radial Total Dose Rate Profile for 100x100 Array	132
Table 6-10 Storage Pad Setback Distance Requirements	139
Table 6-11 Radial Photon Dose Rates for Empty Feed Cylinders	145
Table 6-12 Dose Rate Comparison for Empty and Filled Feed Cylinder Storage Arrays	148
Table 7-1 Neutron Computational Efficiency for Triple-stacked 100x100 Array	151

Table 7-2 Photon Computational Efficiency for Triple-stacked 100x100 Array	153
Table 7-3 Neutron Dose Estimates from Single-stack Calculations.....	157
Table 7-4 Photon Dose Estimates from Single-stack Calculations	158
Table 7-5 Average Surface Neutron Dose Rates from First-Step MCNP Calculations	159
Table 7-6 Average Surface Photon Dose Rates from First-Step MCNP Calculations.....	160
Table 7-7 Comparison of Computational Efficiency between UNM and UUSA Cases	162
Table 8-1 Comparison with TLD and EAD Measurements at UUSA for Filled 48Y Feed Cylinders.....	165
Table 8-2 Comparison with TLD and EAD Measurements at UUSA for Filled 48Y Tails Cylinders.....	165
Table 8-3 Comparison with Photon Radiation Surveys at UUSA.....	167
Table 8-4 Comparison with Single Tails Cylinder Measurements at Capenhurst.....	167
Table 8-5 Single Feed Cylinder Measurements at Cameco.....	169
Table 8-6 UNM and UUSA MCNP Calculated Dose Rates for a Single 48Y Filled Feed Cylinder.....	170
Table 8-7 UNM and UD MCNP Calculated Dose Rates for a Single 48Y Cylinder	171
Table 8-8 Comparison with Single Filled Feed Cylinder Neutron Dose Rates at Cameco..	172
Table 8-9 Photon Measurements at UUSA UBC Storage Pad	176
Table 8-10 Comparison between Case Study and UBC Storage Pad Calculation	180
Table 8-11 Comparison with Photon Measurements at UUSA UBC Storage Pad.....	182
Table A-1 ORIGEN-S Case Description and Computer Files for Filled Tails and Feed Cylinders.....	191
Table A-2 ORIGEN-S Case Description and Computer Files for Empty Feed Cylinders...	191

Table B-1 Neutron Yield by Isotope.....	195
Table B-2 UF ₆ Neutron Source Term at 0.2% U-235.....	196
Table B-3 UF ₆ Neutron Source Term at 0.3% U-235.....	197
Table B-4 UF ₆ Neutron Source Term at 0.4% U-235.....	198
Table B-5 UF ₆ Neutron Source Term at 0.5% U-235.....	199
Table B-6 UF ₆ Neutron Source Term at 0.711% U-235.....	200
Table B-7 Uncorrected UF ₆ Photon Source Term at 0.2% U-235.....	201
Table B-8 Uncorrected UF ₆ Photon Source Term at 0.3% U-235.....	202
Table B-9 Uncorrected UF ₆ Photon Source Term at 0.4% U-235.....	203
Table B-10 Uncorrected UF ₆ Photon Source Term at 0.5% U-235.....	204
Table B-11 Uncorrected UF ₆ Photon Source Term at 0.711% U-235.....	205
Table B-12 Corrected UF ₆ Photon Source Term at 0.2% U-235.....	206
Table B-13 Corrected UF ₆ Photon Source Term at 0.3% U-235.....	207
Table B-14 Corrected UF ₆ Photon Source Term at 0.4% U-235.....	208
Table B-15 Corrected UF ₆ Photon Source Term at 0.5% U-235.....	209
Table B-16 Corrected UF ₆ Photon Source Term at 0.711% U-235.....	210
Table B-17 Neutron Source Term Comparison for Filled Cylinders	211
Table B-18 Photon Source Term Comparison for Filled Cylinders	211
Table C-1 ANSI/ANS-6.1.1-1977 Dose Conversion Factors.....	212
Table C-2 ANSI/ANS-6.1.1-1991 Dose Conversion Factors.....	213
Table D-1 MCNP Case Description and Computer Files for a Single Feed Cylinder	214
Table E-1 Neutron and Photon Energy Response Factors for a Filled Cylinder	223
Table E-2 Photon Energy Response Factors for an Empty Cylinder.....	224

Table E-3 Neutron Dose Rate Results for a Single Filled Feed Cylinder	225
Table E-4 Effect of Concrete Pad on Neutron Dose Rates	226
Table E-5 Effect of Ground Scattering on Neutron Dose Rates	226
Table E-6 Secondary Photon Dose Rates due to Neutron Interactions	227
Table E-7 Effect of ANSI/ANS-6.1.1-1991 Standard on Neutron Dose Rates	227
Table E-8 Photon Dose Rate Results for a Single Filled Feed Cylinder	228
Table E-9 Effect of Concrete Pad on Photon Dose Rates.....	229
Table E-10 Effect of Ground Scattering on Photon Dose Rates.....	229
Table E-11 Comparison of Photon Dose Rates between Full and Partial Spectra	230
Table E-12 Effect of ANSI/ANS-6.1.1-1991 Standard on Photon Dose Rates.....	230
Table E-13 Photon Dose Rate Results for a Single Empty Feed Cylinder	231
Table F-1 MAVRIC Case Description and Computer Files	232
Table G-1 MCNP Cases in First-Step Process for Cylinder Arrays	237
Table G-2 MCNP Cases in Second-Step Process for Cylinder Arrays	238
Table I-1 Cumulative Relative Dose from Empty Feed Cylinders.....	280
Table I-2 MCNP Photon Cases for Empty Feed Cylinders	283
Table J-1 MCNP Photon Cases for Empty Feed Cylinders.....	288

ACRONYMS AND ABBREVIATIONS

ALARA	As Low As Reasonably Achievable
AP	Anterior-Posterior
ANL	Argonne National Laboratory
ANS	American Nuclear Society
ANSI	American National Standards Institute
CADIS	Consistent Adjoint Driven Importance Sampling
CFR	Code of Federal Regulations
CPU	Central Processing Unit
CTC	Center-to-Center (spacing)
CTME	MCNP Computer Time Cutoff
DOE	U.S. Department of Energy
DOT	U.S. Department of Transportation
DU	Depleted Uranium
DUF ₆	Depleted Uranium Hexafluoride
EAD	Electronic Alarming Dosimeter
ENDF	Evaluated Nuclear Data File
EPA	U.S. Environmental Protection Agency
FOM	Figure of Merit
GB	Giga Bytes
GHz	Giga Hertz
HP	Hewlett Packard
ICRP	International Commission on Radiological Protection

ID	Inner (or Inside) Diameter
LANL	Los Alamos National Laboratory
LWR	Light Water Reactor
MAVRIC	MONACO with Automated Variance Reduction for Importance Calculations
MCNP	Monte Carlo Neutral Particle transport code
NCRP	National Council on Radiation Protection
NEF	National Enrichment Facility
nps	Number of Particle Histories (used in MCNP)
NRC	U.S. Nuclear Regulatory Commission
NU	Natural Uranium
ORIGEN	Oak Ridge Isotope GENERation code
ORNL	Oak Ridge National Laboratory
PC	Personal Computer
RAB	Restricted Area Boundary
RAM	Random Access Memory
RSICC	Radiation Safety Information Computational Center
SCALE	Standardized Computer Analysis for Licensing Evaluation
SAR	Safety Analysis Report
SF	Spontaneous Fission
sqrt	square root
SWU	Separative Work Unit
TFSI	Thermo Fisher Scientific Inc.
TLD	ThermoLuminescent Dosimeter

UBC	Uranium By-product Cylinder
UD	Urenco Deutschland
UK	United Kingdom
UNM	The University of New Mexico
U.S.	United States (of America)
UUSA	URENCO USA
wt %	weight percents

1. INTRODUCTION

Uranium hexafluoride (UF_6 , also commonly known as hex) is a chemical compound of hexavalent uranium and fluorine converted from U_3O_8 (also known as yellow cake) at a conversion facility to allow for further process. This conversion is an integral part of the nuclear fuel cycle. UF_6 can be a solid, liquid or gas depending on the occurring range of temperature and pressure. At room temperature, UF_6 is a solid white, dense crystalline material that resembles rock salt.

After conversion, UF_6 is the process gas used by the gaseous diffusion and centrifuge enrichment plants to increase the concentration or enrichment of the fissionable isotope U-235 from naturally occurring uranium ore. The enrichment process with UF_6 offers two unique features. First, it can conveniently be used as a gas for processing, as a liquid for homogenization and sampling, and as a solid for storage and transport. Second, with only one natural isotope in fluorine, all the isotopic separative capacity of the enrichment process is expended to enrich the concentration of the lighter uranium isotopes.

As a part of the front-end of the nuclear fuel cycle, commercial uranium enrichment facilities typically enrich natural uranium hexafluoride, which contains approximately 0.711 wt % U-235, to a final product with up to 5 wt % U-235 for light-water-reactor (LWR) fuel fabrication. Enrichment to higher U-235 concentrations is also achievable for other applications such as research reactor fuel and weapons material. The depleted uranium hexafluoride (DUF_6), with approximately 0.1 to 0.5 wt % U-235 is collected in certified containers for storage and eventual disposal or de-conversion. At the enrichment facilities, the UF_6 material is classified as follows, depending on the U-235 concentration in uranium:

- "Feed" (natural UF₆, feed stock for enrichment process)
- "Product" (enriched UF₆, withdrawn from enrichment process)
- "Tails" (depleted UF₆, withdrawn from enrichment process)

In the existing uranium enrichment facilities, handling and storage of UF₆ mostly use Model 48Y (48 inches in diameter) cylinders for feed and depleted UF₆, and Model 30B (30 inches in diameter) for enriched UF₆. A 48Y cylinder has a fill capacity of 12,501 kg UF₆, and a 30B cylinder can contain up to 2,277 kg UF₆ [USEC 1995, Table 2]. Other models of cylinders are also available and have been used previously such as Model 48G cylinders at the U.S. gaseous diffusion plants [ANL 2013].

Regardless of feed, product or tails material, UF₆ is typically stored as a solid in large carbon steel containers such as the afore-mentioned Models 48Y/G and 30B cylinders at the operating enrichment facilities for long term storage (for tails) or short term storage (for feed and product). These cylinders can be stored indoor or outdoor in accordance with the licensing requirements by the regulatory agency such as the U.S Nuclear Regulatory Commission (NRC).

At the URENCO USA (UUSA) Enrichment Facility (formerly National Enrichment Facility [NRC 2005]), 48Y feed and tails cylinders are allowed for storage on an outdoor concrete pad called Uranium By-product Cylinder (UBC) Storage Pad. Indoor storage is provided for 30B product cylinders inside the Cylinder Receipt and Dispatch Building covered by the Criticality Accident Alarm System as required by 10 CFR 70.24 [NRCa] and physical protection of special nuclear material per 10 CFR 73 [NRCc]. Outdoor storage of

product cylinders requires UUSA to address criticality and safeguards concerns for special nuclear material.

Uranium decays by alpha emission or spontaneous fission and UF_6 contained in cylinders emit both neutrons and photons as a function of enrichment or U-235 concentration. These neutron and photon sources contribute to radiation doses external to the cylinders. To model the dose from the cylinders at an external point, Monte Carlo simulations were performed. Source term determination representative of the real radiation source distribution and actual UF_6 matrix is the first step required in the onsite and offsite dose assessment for the UF_6 cylinders. These source terms are necessary for use in dose calculations and shielding analyses to ensure that the facility and storage pad are properly designed such that radiation doses to onsite personnel and the general public in unrestricted areas are within the regulatory limits. The dose to the general public at environmental locations such as the site boundary is the focus of this research for compliance with the environmental regulations.

The UF_6 source terms with an in-growth time of one year represent the maximum intensity. They are applicable to the dose calculations for a single cylinder and for the entire array of cylinders to obtain the maximum doses with respect to time. Time-dependent source terms are considered in this research to assess the impact to storage management, in particular, for empty feed cylinders.

1.1 RESEARCH OBJECTIVES

The main purpose of this research is to effectively assess environmental external radiation doses for an outdoor UF_6 cylinder storage yard or pad with application of an efficient Monte Carlo method to achieve the following objectives:

- Reducing dose simulation time
- Predicting dose trend for increasing storage capacity
- Maximizing storage capacity for a given footprint
- Demonstrating regulatory compliance with the site boundary dose limit
- Supporting onsite UF₆ storage management such as cylinder spacing, stacking and placement

1.2 RESEARCH SCOPE

To meet the objectives set forth in Section 1.1, this research consists of the following scope in four distinct phases:

- Phase 1 – UF₆ radiation source term development for Monte Carlo dose simulations for filled tails, filled feed, and empty feed cylinders using 48Y Model
- Phase 2 – Single cylinder dose evaluation by Monte Carlo simulations for calculating the dose rates from a single cylinder, and setting the key parameters for multiple cylinder dose assessment
- Phase 3 – Methodology development for efficient Monte Carlo simulations and application to cylinder array dose analysis
- Phase 4 – Quantification of computational efficiency and validation of dose simulations against field measurements and other calculations available

The work in Phases 1 and 2 is a prerequisite for Phase 3, as it provides the necessary input and information for use in dose analysis for multiple cylinders. Phase 3 is the heart of this research project to provide an efficient approach to dose calculations for arrays of

cylinders in different stacking configurations (one, two and three high). The results from Phase 3 are useful for quantifying computational efficiency, predicting dose trend, sizing storage space requirements, and devising an efficient and economical cylinder storage/placement scheme. Phase 4 involves quantification of computational efficiency, and the use of field radiation measurements and other calculations available for validation of the efficiency and accuracy of the dose calculations with the improved approach.

1.3 MANUSCRIPT ORGANIZATION

The following chapters describe the research efforts and results including discussion of previous work. Chapter 2 introduces the essential information on UF₆ cylinders and their storage related to this research. Chapter 3 defines and provides the UF₆ radiation source terms consisting of neutron and photon sources for filled tails, filled feed and empty feed 48Y cylinders as developed from Phase 1. Chapter 4 presents the dose rate results for a single cylinder, and sets the pertinent parameters from Phase 2 for use in the multiple cylinder dose assessment in Phase 3. As a result of the Phase 3 efforts, Chapter 5 provides the details of an efficient indirect Monte Carlo simulation approach to the dose assessment for various configurations and arrangements of UF₆ cylinder storage. The dose results of significance to this research are presented in Chapter 6, including dose impacts to management of filled and empty cylinder storage. As part of the scope in Phase 4, Chapter 7 validates the computational efficiency of the indirect Monte Carlo simulation method relative to the direct approach. Chapter 8, also part of Phase 4, compares the calculated dose results against the field measurements and other calculations for validation of the UF₆ source terms and application of the indirect Monte Carlo simulation method.

In addition, a concluding chapter is included as Chapter 9, summarizing the findings and interpretations and recommending future work. The computer files and supporting information are collected in the appendices.

2. DESCRIPTION OF UF₆ CYLINDER STORAGE

This chapter provides the supporting background information related to this research, including UF₆ cylinder physical description, storage and stacking with special focus on the UUSA Enrichment Facility in Eunice, New Mexico.

2.1 UF₆ CYLINDER DESCRIPTION

Model 48G and 48Y cylinders are typically used for storage of solid UF₆, which has a density of 5.1 g/cm³ [USEC 1995, Table 5] at room temperature. Model 48G cylinders with a thinner wall thickness were used in earlier times at the gaseous diffusion plants such as Portsmouth. Model 48Y cylinders are currently in use at the UUSA Enrichment Facility for tails storage. Table 2-1 provides the physical parameters and contents of Model 48G and 48Y cylinders. Figures 2-1 and 2-2 depict the physical configuration of a single cylinder for 48G and 48Y, respectively.

Cylinders are initially filled to a safe capacity, which is allowed to cool for several days. After cooling, UF₆ contracts and forms a solid that fills about 60% of the internal cylinder volume. During storage, a cylinder contains UF₆ solid in the bottom in slumped geometry and UF₆ gas at less than atmospheric pressure in the top 40% of the internal volume.

Table 2-1 Model 48G and 48Y Storage Cylinder Parameters

Description	Value for 48G	Value for 48Y
Nominal Diameter, in (cm)	48 (122)	48 (122)
Nominal Length, in (cm)	146 (370)	150 (380)
Shell Thickness, in (cm)	0.3125 (0.8)	0.625 (1.6)
Maximum Fill Limit, lb (kg)	28,000 (12,701)	27,560 (12,501)
Minimum Internal Volume, ft ³ (m ³)	139 (3.94)	142.7 (4.04)
Construction Material	Carbon steel	Carbon steel
Reference Source	USEC 1995, §6.10	USEC 1995, §6.9

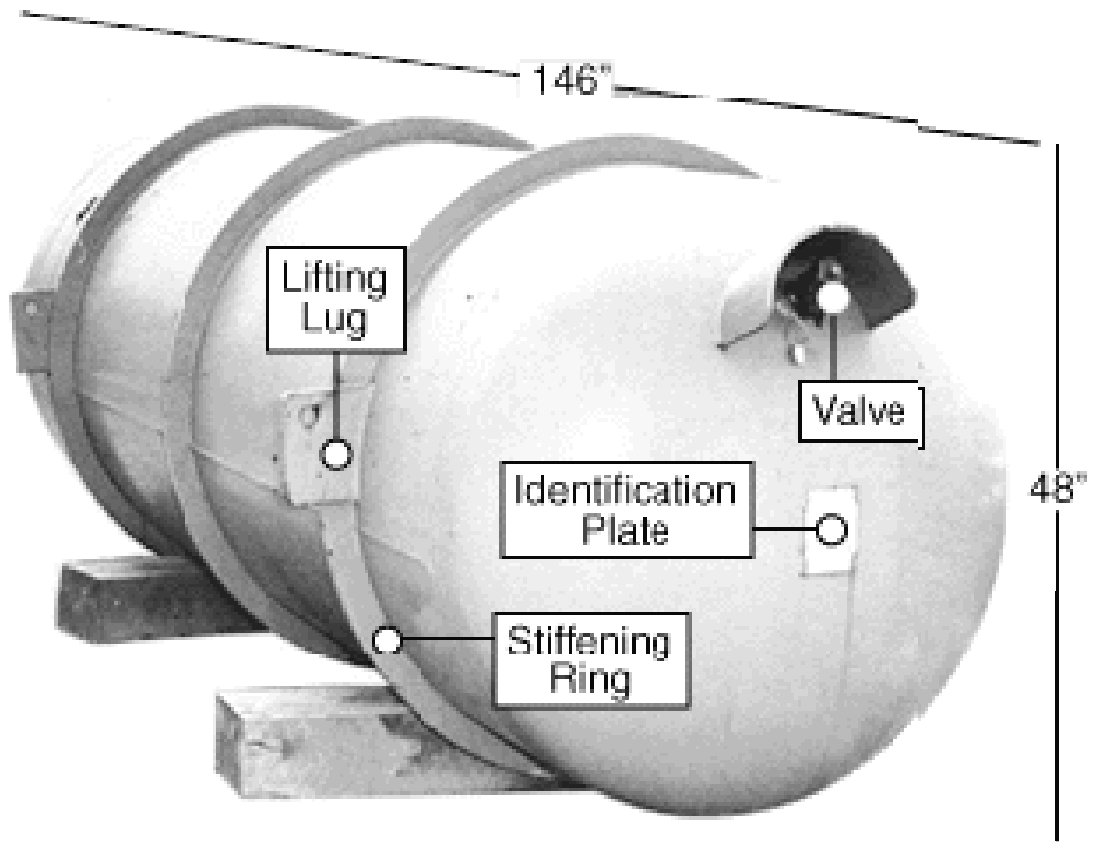


Figure 2-1 Physical Illustration of Model 48G Cylinder



Figure 2-2 Physical Illustration of Model 48Y Cylinder

2.2 UF₆ CYLINDER STORAGE AND STACKING

The uranium hexafluoride is stored in cylinders in large outdoor areas called storage yards or pad, which typically have a gravel or concrete base. The newer storage areas are built of concrete.

The cylinders in the storage area can be stacked one, two or three high. Figure 2-3 features a double stacking configuration at the various enrichment facilities in the U.S. Besides the current practice of double stacking, UUSA plans to use a unique triple stacking configuration to minimize the footprint required for the storage pad at their enrichment facility. The cylinders in the bottom stack are placed on concrete chocks, with some wooden chocks used in older yards as shown in Figure 2-1.

At the U.S. gaseous diffusion plants (Portsmouth and Paducah), the filled cylinder stacking is limited to two high, because of the use of Model 48G cylinders which have a thinner wall than Model 48Y. The switch to Model 48Y cylinders at commercial uranium enrichment facilities allows triple stacking, owing to a thicker wall to provide structural support. The arrangement of triple stacking offers the advantage of additional storage capacity within the boundary of a given footprint without significant environmental dose impacts.



UBC Storage Pad at the UUSA Enrichment Facility in Eunice, New Mexico



DUF₆ Cylinder Storage Yard at a Gaseous Diffusion Plant in the U.S. [ANL 2013]



DUF₆ Cylinder Storage Yard at the Portsmouth, Ohio Gaseous Diffusion Plant [ANL 2013]

Figure 2-3 Double Stacking of UF₆ Storage Cylinders

2.3 UUSA ENRICHMENT FACILITY DESCRIPTION

UUSA owns and operates a commercial uranium enrichment facility in Eunice, New Mexico to provide enrichment services to nuclear utilities. Figure 2-4 depicts the facility layout [UUSA 2012a, Fig. 9-4]. The distances from the facility to the site boundary (or fence line) vary from appropriately 400 to 1,000 m [NRC 2005, Table A.1-4], depending on the sector. The UBC Storage Pad is marked as Item 1 on Figure 2-4. The distance from the storage pad edge is about 1,200 ft (366 m) to the east site boundary and about 1,600 ft (488 m) to the north boundary [UUSA 2012c, Figure 14]. For this research, these distances were used for comparison with the required distances from the case study for arrays of cylinders.

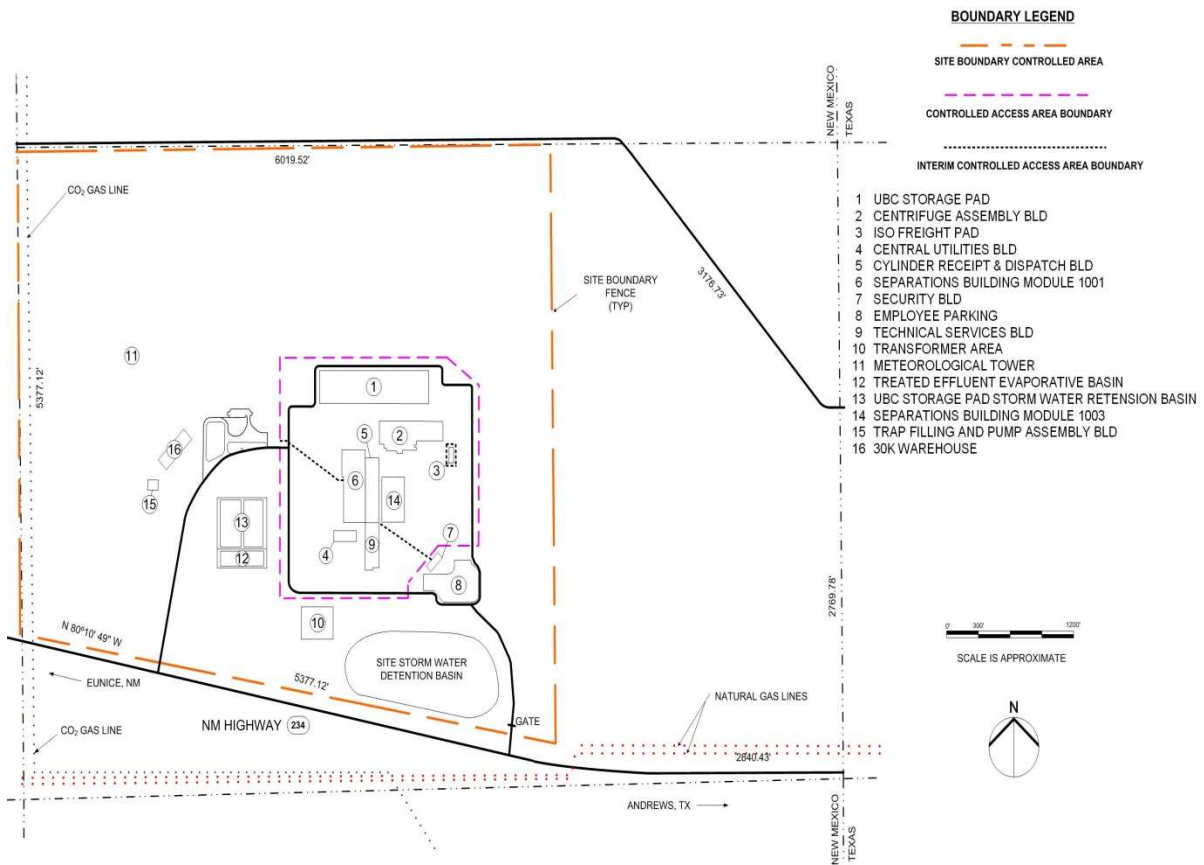


Figure 2-4 UUSA Enrichment Facility Layout

This uranium enrichment plant is based on a highly reliable gas centrifuge process, and has been in operation since June 2010 [LPES 2014, §1.0]. The plant is designed to separate a feed stream containing the naturally occurring proportions of uranium isotopes into a product stream - enriched in the uranium-235 (U-235) isotope and a tails stream - depleted in the U-235 isotope. The process, entirely physical in nature, takes advantage of the tendency of materials of differing density to segregate in a centrifuge. The chemical form of the working material of the plant, uranium hexafluoride (UF₆), does not require chemical transformations at any stage of the process. This process enriches natural UF₆, containing approximately 0.711% U-235 to a UF₆ product, containing U-235 enriched up to 5 wt%.

The current licensed nominal capacity of the facility is 3 million separative work units (SWU) per year [NRC2005, §1.1.3]. The SWU is a measurement in kilograms of the separative work (effort or energy) required to separate isotopes of uranium for use in nuclear power reactors or nuclear weapons. UUSA plans on expanding the facility to an eventual 10-million SWU capacity to meet future demands [UUSA 2012b].

The facility uses only two types of cylinders, namely, 48Y for the feed and tails material, and 30B for the product material. These cylinders meet the ANSI N14.1 standard [ANSI 2001], and the 10 CFR 71.73 [NRCb] and 49 CFR 173.420 [DOT] requirements for packaging and offsite transport.

2.4 UUSA UBC STORAGE PAD DESCRIPTION

The UUSA Enrichment Facility utilizes the UBC Storage Pad to store the expected volume of Uranium Byproduct Cylinders (depleted UF₆) produced by the facility. The cylinder contents are stored under vacuum in corrosion-resistant ANSI N14.1 Model 48Y cylinders. Additionally, the UBC Storage Pad provides limited buffered storage of full and

empty 48Y feed cylinders. Only the source material (depleted and natural UF₆) is stored in this area. The area does not allow for storage of special nuclear material (enriched UF₆) at this time.

The UBC Storage Pad can accommodate storage of approximately 15,730 cylinders under the current license from the NRC [NRC 2013, Condition 21]. The cylinders are stacked two high. Concrete saddles are used to store the cylinders approximately a few inches above ground level to avoid contact with soil.

An initial section of the storage pad has been constructed and in use for storage of filled tails, filled feed, and empty feed cylinders. The section features an array size of 129x8 cylinders (129 cylinders per row from east to west and 8 rows from north to south) with cylinder ends oriented in the north-south direction [UUSA 2010, §2.0]. For double stacking, the initial section can accommodate a total of $(129 \times 8) + (128 \times 8) = 2,056$ cylinders. Each upper cylinder (on the top level) sits and fits directly above the tight space between two lower cylinders (on the bottom level), thus reducing the total number of cylinders on the top level by one (see Figure 2-3). As of April 2014, approximately 1,600 cylinders have been placed on the pad, mostly in a double-stacked arrangement [Kohrt 2014].

To allow facility expansion with an increased SWU capacity, UUSA plans on expanding the UBC Storage Pad to accommodate up to 25,000 cylinders in triple stacking [UUSA 2013c, §1.0]. Additional sections will be constructed on the UBC Storage Pad to host this planned capacity.

Empty feed cylinders require a radiological cooling period in storage prior to reuse as tails cylinders, or for return to the customers. The cooling period is dependent upon the emitted dose, and is typically three months. An allowance has been made for six months of

storage of empty feed cylinders. For a 3-million SWU capacity, this output requires an allocated space for 354 empty feed cylinders [UUSA 2005, §3.4.11.3]. The storage space requirement is practically proportional to the SWU capacity. For example, facility expansion to a 10-million SWU capacity needs to provide sufficient storage space for 1,180 empty feed cylinders.

Under normal conditions, the primary radiological risk from tails (DUF_6) cylinder storage is direct radiation dose from exposure to low-level external radiation due to neutron and photon sources in DUF_6 . For environmental considerations, the U.S. Environmental Protection Agency regulations of 40 CFR 190.10(a) [EPA] require that the offsite dose at the site boundary (e.g., fence line as shown in Figure 2-4) be less than 25 mrem/year (0.25 mSv/year). This annual dose equates 2.85 $\mu\text{rem/h}$ for continuous residential occupancy (8,766 hours per year), or 12.5 $\mu\text{rem/h}$ for occupational business entities (based on 2,000 hours per year) [Sanders 2010]. Note that the conventional dose units of mrem and μrem rather than the International System of Units of mSievert or $\mu\text{Sievert}$ are used throughout this document for convenience and alignment with the common nuclear industry practice. Demonstration of regulatory compliance necessitates performance of radiation dose assessment with an appropriate radiation transport code such as MCNP [LANL 2008] and MAVRIC [ORNL 2011a].

3. UF₆ DIRECT RADIATION SOURCE TERMS

The direct radiation source term refers to the direct source causing external radiation doses to personnel as a result of radiation exposure. The direct radiation source type may be neutron radiation only, photon radiation only, or both neutron and photon radiation. The source term consists of the source intensity (number of photons or neutrons per second) and its associated energy spectrum from UF₆ as a volumetric source necessary for input into the Monte Carlo simulation code to calculate the neutron or photon dose.

UF₆ emits both neutron and photon radiation as a function of enrichment or U-235 concentration, and contributes to radiation doses external to the cylinders. Source term determination is the first step required in the onsite and offsite dose assessment for the UF₆ cylinders. These source terms are necessary for use in dose calculations and shielding analyses to ensure that the facility and storage pad are properly designed such that radiation doses to onsite personnel and the general public in unrestricted areas are within the regulatory limits.

This chapter determines and defines the radiation (neutron and photon) source terms and associated energy spectra for the following materials:

- "Feed" (natural UF₆)
- "Tails" (depleted UF₆)

The product material (enriched UF₆) is excluded, as its storage in an open outdoor area is prohibited without the approval of the U.S. Nuclear Regulatory Commission (NRC), and/or requires the use of an overpack which provides additional shielding. At present, the UUSA Enrichment Facility does not permit storage of product cylinders on the UBC Storage Pad.

Several previous UF₆ source term calculations were available for references or comparison. The initial UUSA calculations [AREVA 2003a and 2003b] used a manual approach for the UF₆ neutron yield, and ORIGEN-2 [Groff 1991] for the photon source. The calculations were updated in 2013 to support the facility expansion at UUSA [UUSA 2013b], using the ORIGEN-S module in the SCALE 6.1.2 code package [ORNL 2011b, 2011c, and 2013]. The 2013 updated calculations were largely based on an independent, unpublished study performed by the author at the University of New Mexico (UNM).

For this research, it was necessary to revise the previous calculations to incorporate the following changes:

- Focus on tails and feed cylinders for outdoor storage management
- Use of a standard SCALE built-in energy group structure for the nuclear cross section library
- Addition of the time-dependent photon source terms for both filled and empty feed cylinders
- Inclusion of several tails assays for sensitivity study

The following sections describe the details of the required source term calculations for filled tails, filled feed and empty feed cylinders to support UF₆ storage management.

3.1 BASES AND ASSUMPTIONS

The current practice at the commercial uranium enrichment facilities for producing enriched uranium for LWR fuel employs natural UF₆ as feed material, despite the fact that the feed material can have a different U-235 concentration. Natural uranium in the feed material contains 0.711 wt % U-235, which corresponds to an atomic abundance of 0.72% U-

235 [Baum 2002]. The UUSA Safety Analysis Report (SAR) also provides the same specification for natural UF_6 as feed material in the enrichment process [UUSA 2013a, §1.1].

In this research, the tails material was assumed to contain depleted uranium with 0.2 to 0.5 wt % U-235. The typical range of the tails assay is 0.2 to 0.34 wt % U-235 [UUSA 2004, §1.1.3.2], depending on the trade-off between SWU and tails assay. A higher tails assay requires less SWU. DUF_6 at the U.S. gaseous diffusion plants mostly contains 0.2 to 0.4% U-235 by weight [DOE 2001, p.1]. In a training module on Depleted Uranium [NRC 2008], it is also stated that “DU assays typically span the 0.2-0.4% range, with 0.2-0.3% being the most common”. The current tails specification at the UUSA facility is 0.1 to 0.5% U-235 [UUSA 2013a, §1.1.3.2]. The assumption of 0.2 to 0.5% U-235 by weight for tails assay covered the typical range and provided sufficient data points for studying the sensitivity of the source terms to the tails assay. Accordingly, the ORIGEN-S calculations for tails material included the cases for 0.2%, 0.3%, 0.4% and 0.5% U-235 assays.

For the convenience of scaling, the calculation basis used in the SCALE/ORIGEN-S runs was 1 kg of UF_6 , as the code accepts any useful calculation basis. With this basis, the total source strength in a given filled cylinder can be readily obtained by multiplying the unit source strength by the cylinder capacity. The self-shielding effect of UF_6 is a factor for the dose calculations but irrelevant for the source term calculations.

The in-growth time for the progenies (or daughter products) of the uranium isotopes was assumed to be one year. The progenies build up with time from the initial concentrations of the uranium isotopes with no daughter products, reaching equilibrium at one-year in-growth time, as demonstrated by a calculation with SCALE 6.1.2 [UUSA 2013, §7.2.1] and other references [e.g., AREVA 2003b] available. No further validation would be

necessary. This assumption affects photon sources only. The neutron sources are virtually time independent.

Besides primary gamma emission, the UF_6 photon source must include the component of bremsstrahlung radiation due to beta decay of the uranium progeny. For the contribution from this component, bremsstrahlung in the UO_2 matrix was initially assumed, as SCALE 6.1.2 lacks the option of calculating the bremsstrahlung radiation contribution for the actual UF_6 matrix. The option of the UO_2 matrix was used for conservatism to obtain the uncorrected photon sources terms first, which were subsequently corrected for the actual UF_6 matrix to remove the conservatism (see Section 3.7). This correction was specifically applicable to UF_6 in the filled feed and filled tails cylinders only.

A feed cylinder contains residual radioactivity from the daughter products of the uranium isotopes after being emptied in the process system which separates uranium from its progeny. However, the emptied cylinder contains little or no UF_6 to provide self-shielding, resulting in a much higher external dose rate than that for a filled cylinder.

The radiation source terms for an empty feed cylinder need to be treated differently from a filled feed or tails cylinder. An empty 48Y feed cylinder may contain an allowable “heel” quantity of UF_6 (22.68 kg) [USEC 1995, Table 3], but would be of no appreciable significance to the dose external to the cylinder because of the small quantity. Therefore, only the photon source term from the progeny of natural uranium is of importance to the dose assessment. The progeny in an empty cylinder was based on an initial maximum capacity of a filled feed cylinder with one-year growth of daughter products, followed by radioactive decay after being emptied. Since the empty feed cylinder is essentially absent of UF_6 , it

would be appropriate to use the water matrix available in ORIGEN-S for the bremsstrahlung radiation contribution to simulate the matrix for air and carbon steel with an empty cylinder.

3.2 METHODOLOGY

The source term calculation involves the determination of neutron and photon sources as a function of U-235 concentration for UF₆ contained in certified cylinders meeting the ANSI N14.1-2001 standard [ANSI 2001]. The calculation used the ORIGEN-S module [ORNL 2011b] in the SCALE code package [ORNL 2011c] with a patch to fix the nuclear decay data library for uranium. The patched version was released in February 2013 as SCALE 6.1.2 [ORNL 2013].

The code was obtained from Radiation Safety Information Computational Center (RSICC) at Oak Ridge National Laboratory (ORNL) under an export-controlled license for a single user (Computer Code Request No. 135966), and successfully installed on a Hewlett Packard laptop computer (Model: HP G71 Notebook PC).

ORIGEN (Oak Ridge Isotope GENERation code) has been developed and maintained as the depletion and decay module in the SCALE code system. This version, ORIGEN-S, maintains the capability of other versions to be used as a standalone code but has the added ability to utilize multi-energy-group cross sections processed from standard ENDF/B evaluations. ORIGEN-S applies a matrix exponential expansion model to calculate time-dependent concentrations, activities, and radiation source terms for a large number of isotopes simultaneously generated or depleted by neutron transmutation, fission, and radioactive decay. For this calculation, ORIGEN-S was used to determine the UF₆ neutron and photon source strengths and associated energy spectra.

ORIGEN-S performed the radioactive decay calculation for uranium isotopes to determine the nuclide concentration in grams and/or curies as a function of decay time, and automatically generated the resulting neutron and photon sources in the same run. The neutron source consists of the neutron yields from spontaneous fission and (α , n) reactions with fluorine in UF₆. The photon radiation includes photons arising from X-rays, gamma-rays, bremsstrahlung, spontaneous fission gamma rays, and gamma rays accompanying (α , n) reactions. The following subsections discuss the applicable methodology for the radioactive decay calculation (§3.2.1), neutron source calculation (§3.2.2) and photon source calculation (§3.2.3) as extracted from the ORIGEN-S user's manual [ORNL 2011b] for inclusion and completion.

3.2.1 Radioactive Decay Calculation

In determining the time dependence of nuclide concentrations, ORIGEN-S solves for the formation and disappearance of a nuclide by radioactive disintegration and neutron transmutation. For radioactive decay only as considered in this calculation, the time rate of change of the concentration for a particular nuclide, N_i , in terms of these production and removal processes can be written as

$$\frac{dN_i}{dt} = \sum_{j=1}^m l_{ij} \lambda_j N_j - \lambda_i N_i \quad (\text{Eq. 1})$$

where

N_i = atom density of nuclide i ,

λ_i = radioactive disintegration constant of nuclide i ,

l_{ij} = branching fractions of radioactive disintegrations from other nuclides j to nuclide i ,

Equation 1 is used to calculate the radioactivity (in curies) of the decay or daughter products of the uranium isotopes, which in turn, is used to determine the photon source strength and associated energy spectrum.

The radioactivity by nuclide or isotope is available from the ORIGEN-S output, but is not listed in this calculation as part of the results as the dose assessment only requires the source intensity and associated energy spectrum.

3.2.2 Neutron Source Calculation

The neutron source strengths and energy spectra computed by ORIGEN-S include neutrons produced from spontaneous fission, (α , n) reactions, and beta-delayed neutron emission. For UF_6 , there is no contribution from beta-delayed neutrons. The computational methods and neutron decay data were adopted from the Los Alamos National Laboratory code SOURCES-4B (LANL 2000). Only the homogeneous medium (α , n) option has been adopted. The method of computing the spontaneous fission neutron source is independent of the medium containing the fuel. However, (α , n) production varies significantly with the composition of the medium. ORIGEN-S includes three (α , n) options: (1) a UO_2 fuel matrix, (2) a borosilicate glass matrix, and (3) an arbitrary problem-dependent matrix defined by the user input compositions. This calculation used option (3). In this option, the code determined the matrix compositions (UF_6) from the input.

3.2.2.1 Spontaneous Fission Neutrons

In ORIGEN-S, spontaneous fission neutron sources and spectra are calculated using the half-life, spontaneous fission branching fraction, number of neutrons per fission (ν), and Watt fission spectrum parameters for 43 fissioning actinides. The half-lives used in the

calculation are obtained from the ORIGEN-S decay data library. All other data are obtained from a separate neutron source decay data library.

The spontaneous fission neutron energy spectrum is approximated by a Watt fission spectrum using two evaluated nuclide-dependent spectral parameters, A and B, such that

$$N_i(E) = Ce^{-E/A} \sinh \sqrt{BE} \quad (\text{Eq. 2})$$

where E is the neutron energy and C is a normalization constant.

3.2.2.2 (α , n) Reaction Neutrons

The (α , n) neutron source and spectra are strongly dependent on the constituent and light element content of the medium containing the alpha-emitting nuclides. Calculation of the source and energy spectra requires accurate knowledge of the slowing down of the alpha particles and the probability of neutron production as the α particle energy decreases in the medium. ORIGEN-S performs an (α , n) neutron source calculation for a homogeneous mixture in which the alpha-emitting nuclides are uniformly intermixed with the target nuclides. Since the dimensions of the target are much larger than the range of the alpha particles, all alpha particles are stopped within the mixture. The neutron yield from an alpha particle of energy E_α emitted by nuclide k in a homogeneous mixture with total atom number density N , and (α , n) target nuclide atom density N_i , can be determined as

$$Y_{i,k} = \frac{N_i}{N} \int_0^{E_\alpha} \frac{\sigma_i(E)}{S(E)} dE \quad (\text{Eq. 3})$$

where $S(E)$ is the total stopping power of the medium, and $\sigma_i(E)$ is the energy-dependent (α , n) reaction cross section for target nuclide i . ORIGEN-S uses this expression to calculate the neutron yield for each target nuclide and from each discrete-energy alpha particle emitted by all alpha-emitting nuclides in the material. The stopping power for compounds, rather than

pure elements, is approximated using the Bragg-Kleeman additivity rule [Attix 1986, p.178] based on the assumption that the stopping power per atom of compound is additive. The energy-dependent elemental stopping cross sections are determined as parametric fits to evaluated data. The values of $Y_{i,k}$ are determined using a discrete numerical approximation of the integral over the alpha particle energy in Eq. 3. The neutron yield from the alpha particle as it slows down in the medium is calculated by subdividing the maximum energy E_α into a number of discrete energy groups, or bins. The number of alpha energy groups can be set by the user using the input parameter NAG in the 81\$ array in ORIGEN-S. The neutron yield is determined for each discrete alpha energy bin using the average midpoint energy of the bin. The total neutron source is determined by multiplying the total alpha source strength for each alpha energy bin by the respective (α, n) yield value $Y_{i,k}$. This calculation is performed for each alpha particle and target nuclide in the medium.

The neutron spectra are calculated using nuclear reaction kinematics, assuming that the (α, n) reaction emits neutrons with an isotropic angular distribution in the center-of-mass system. The maximum and minimum permissible energies of the emitted neutron are determined by applying mass, momentum, and energy balance for each product nuclide energy level. The nuclear data libraries contain the necessary data for the ORIGEN-S calculation, including the product nuclide levels, the product level branching data, the (α, n) reaction Q values, the excitation energy of each product nuclide level, and the branching fraction of (α, n) reactions resulting in the production of product levels. The nuclear data used in the (α, n) source calculation are limited to alpha energies below 6.5 MeV. Any alpha particle exceeding this limit is assigned an energy value of 6.5 MeV and the calculation

proceeds. This limitation has no impact on the uranium isotopes whose alpha particles are all less than 6.5 MeV.

In the arbitrary matrix option, the code calculates the (α , n) neutron source and spectra using the source, target, and constituents determined using the material compositions in the problem. The neutron source calculation is performed assuming that the concentrations of the (α , n) target elements and matrix compositions remain constant during decay.

3.2.3 Photon Source Calculation

The gamma-ray source strengths and energy spectra computed by ORIGEN-S include photons arising from X-rays, gamma-rays, bremsstrahlung, spontaneous fission gamma rays, and gamma rays accompanying (α , n) reactions. Photons from X-rays and gamma rays emitted from the nucleus for all decay modes are stored in the gamma library as line-energy and intensity data. Continuum spectra from bremsstrahlung, spontaneous fission, and (α , n) interactions are represented as binned pseudo-line data.

The ability of ORIGEN-S to apply line-energy data allows photon energy spectra to be calculated in any user-specified energy group structure directly. When the data from photon data libraries are converted to multigroup yields by ORIGEN-S, the intensities of the photons are adjusted to conserve energy of the spectrum. The adjusted group intensity is given by

$$I_g = I_a(E_a / E_g) \quad (\text{Eq. 4})$$

where

I_a = actual photon intensity from the gamma library (photons per disintegration),

E_a = actual photon energy (MeV),

E_g = mean energy of the group (MeV),

I_g = group photon intensity (photons per disintegration).

If the actual photon energy E_a is near a group boundary, the group intensity may be split between two groups. To determine when this split occurs, a factor f is computed as

$$f = \frac{E_a - E_l}{E_u - E_l} \quad (\text{Eq. 5})$$

where

E_l = lower energy bound of the group (MeV),

E_u = upper energy bound of the group (MeV).

If $f \leq 0.03$, the intensity I_g is split equally between group g and the next lower energy group, unless group g is the lowest group. If $f \geq 0.97$, the intensity I is split equally between group g and the next higher energy group, unless group g is the highest group. If $0.03 < f < 0.97$, the intensity I_g is not split between adjacent groups.

If a nuclide decays by gamma emission but does not have evaluated spectral data in the photon library, the recoverable gamma energy determined from the ENDF/B decay evaluations is saved and the extra energy is accounted for by renormalizing the spectra. If this extra energy exceeds 1% of the total gamma energy from the spectrum, ORIGEN-S prints out a warning message.

3.3 CALCULATIONAL INPUTS/NOMEMCLATURE

The U-235 concentrations and storage cylinder types used for UF_6 are shown in Table 3-1. The “U-235 concentration or assay” used herein refers to the weight percents of the U-235 isotope in uranium. The cylinder parameters are given in Table 3-2. The nuclear data used in this calculation are provided in Table 3-3.

Natural uranium is composed of three radioactive isotopes: U-234, U-235 and U-238 with trace amounts of U-236. The specific isotopic content is not known, other than

enrichment. The ORNL/TM-12294 report [ORNL 1995, p. 20] gives a set of formulas that relates the amount of U-234, U-236, and U-238 to the amount of U-235 as follows:

- $W_{234} = 0.007731 * (W_{235})^{1.0837}$
- $W_{236} = 0.0046 * W_{235}$
- $W_{238} = 100 - W_{234} - W_{235} - W_{236}$

where W is weight percent (wt %).

Table 3-1 U-235 Concentrations and Cylinder Types

Description	U-235 Concentration	Cylinder Type	Reference
Feed Material	0.711 wt % U-235	Model 48Y	Section 3.1
Tails Material	0.2 to 0.5 wt % U-235	Model 48Y	Section 3.1

Table 3-2 Cylinder Parameters

Cylinder Type	Description	Value	Unit	Reference
48Y for Feed	Max Fill Limit	12,501 (27,560)	kg (lb)	USEC 1995, Table 2
	Feed Assay	0.711	wt % U-235	Section 3.1
48Y for Tails	Max Fill Limit	12,501 (27,560)	kg (lb)	USEC 1995, Table 2
	Tails Assay	0.2 to 0.5	wt % U-235	Section 3.1

Table 3-3 Nuclear Data

Nuclide	Atomic Mass	Half Life (years)	Reference
U-234	234.040946	2.455×10^5	Baum 2002
U-235	235.043923	7.038×10^8	Baum 2002
U-236	236.045562	2.342×10^7	Baum 2002
U-238	238.050783	4.468×10^9	Baum 2002
Fluorine	18.9984032	(stable)	Baum 2002

3.4 DETAILED CALCULATION

3.4.1 Uranium Isotopic Concentrations

The weight percents of the various uranium isotopes were calculated from the equations listed in Section 3.3, using the U-235 wt % as an input. As an example, the U-235

wt % in tails (depleted UF₆) is 0.3%. The weight percents for other pertinent uranium isotopes were calculated as:

$$W_{234} = 0.007731 * 0.3^{1.0837} = 0.002401593\%$$

$$W_{236} = 0.0046 * 0.3 = 0.001564\%$$

$$W_{238} = 100 - 0.002401593 - 0.3 - 0.001564 = 99.65603441\%$$

Table 3-4 provides the Excel-calculated weight percents of uranium isotopes for several U-235 concentrations by weight including 0.2, 0.3, 0.4 and 0.5% for tails, and 0.711% for feed. The calculated values for 0.3% and 0.711% U-235 agree reasonably well with the comparable NBL-SRM-969 primary traceable standards used at the Portsmouth Gaseous Diffusion Plant Nondestructive Assay Laboratory [McGinnis 2009, Table 1], except for U-236 which is immaterial to dose consequences because of trace quantities.

3.4.2 Nuclide Masses per kg of UF₆

Since the calculation basis for input to SCALE/ORIGEN-S was 1 kg of UF₆ (Section 3.1), it was necessary to determine the corresponding mass for each nuclide in UF₆. The associated nuclides include U-234, U-235, U-236, U-238 and F-19. For such determination, the average atomic mass for uranium for a given enrichment was calculated as follows:

$$\bar{A}_U = 100 / \sum_i W_i / A_i \quad (\text{Eq. 6})$$

where W_i and A_i are the weight percent and atomic mass for nuclide i, respectively, and i refers to U-234, U-235, U-236 and U-238.

For example, the average U atomic mass for tails at 0.3% assay is:

$$\frac{100}{\frac{0.002401593}{234.040946} + \frac{0.3}{235.043923} + \frac{0.001564}{236.045562} + \frac{99.65603441}{238.050783}} = 238.0415339$$

For 1 kg (or 1,000 g) of UF₆, the mass of UF₆ was converted to mass of just uranium by the mass fraction of U in UF₆:

$$1000 \text{ g UF}_6 * 238.0415339 / (238.0415339 + 6 * 18.9984032) = 676.19 \text{ g U}$$

Accordingly, 1 kg of UF₆ at 0.3% assay contains the following mass distribution:

U-234	676.19 g x 0.002096969/100 = 1.4180E-02 g
U-235	676.19 g x 0.003/100 = 2.0286E+00 g
U-236	676.19 g x 0.00138/100 = 9.3315E-03 g
U-238	676.19 g x 99.69652303/100 = 6.7414E+02 g
F-19	1000 g - 676.19 g = 3.2381E+02 g

The Excel-calculated UF₆ mass distribution for each U-235 concentration is also provided in Table 3-4, along with the uranium isotopic concentrations.

Table 3-4 Uranium Isotopic Concentrations and UF₆ Mass Distributions

Isotope	A	wt %				
		0.2	0.3	0.4	0.5	0.711
U-235	235.043923	0.2	0.3	0.4	0.5	0.711
U-234	234.040946	0.001351331	0.002096969	0.002864099	0.003647619	0.005342035
U-236	236.045562	0.00092	0.00138	0.00184	0.0023	0.0032706
U-238	238.050783	99.79772867	99.69652303	99.5952959	99.49405238	99.28038736
Total		100.000	100.000	100.000	100.000	100.000
U Average Atomic Mass		238.0446188	238.0415339	238.0384483	238.0353621	238.0288487
Isotope	A	g per kg UF ₆				
		0.2	0.3	0.4	0.5	0.711
U-total		6.7620E+02	6.7619E+02	6.7619E+02	6.7619E+02	6.7618E+02
U-235	235.043923	1.3524E+00	2.0286E+00	2.7048E+00	3.3809E+00	4.8076E+00
U-234	234.040946	9.1376E-03	1.4180E-02	1.9367E-02	2.4665E-02	3.6122E-02
U-236	236.045562	6.2210E-03	9.3315E-03	1.2442E-02	1.5552E-02	2.2115E-02
U-238	238.050783	6.7483E+02	6.7414E+02	6.7345E+02	6.7277E+02	6.7132E+02
F-19	18.9984032	3.2380E+02	3.2381E+02	3.2381E+02	3.2381E+02	3.2382E+02
Total UF ₆		1.0000E+03	1.0000E+03	1.0000E+03	1.0000E+03	1.0000E+03

3.4.3 ORIGEN-S Calculations

The UF₆ source terms were determined with the ORIGEN-S module in the SCALE 6.1.2 code system. The calculations produced the results of curie contents by nuclide,

neutron source strengths and energy spectra, and photon source strengths and energy spectra for five U-235 concentrations of 0.2, 0.3, 0.4 and 0.5% for tails, and 0.711% for feed by weight in uranium. The results of the source strengths and energy spectra are of particular interest to application in radiation dose calculations.

For the neutron source, the calculation included the contributions from (α , n) reactions and spontaneous fissions. The (α , n) reactions were based on the UF₆ matrix by inputting the composition of UF₆ by nuclide into ORIGEN-S. The standard SCALE 27-group structure [ORNL 2011c, Table S6.5.1] for neutrons was used for compatibility with SCALE applications to obtain the neutron source energy spectra. This group structure would facilitate source importance calculations with the MAVRIC module in SCALE to take advantage of the built-in nuclear cross section data library. The ORIGEN-S output provides the contributions from (α , n) reactions and spontaneous fissions, respectively as well as the total in terms of the source strength and energy spectrum. In addition, the neutron yield by isotope is available from the output files.

For a filled tails or feed cylinder, the photon source calculation with ORIGEN-S considered the cases with and without bremsstrahlung (shortened as brem) radiation contribution, using the standard 19-group structure [ORNL 2011c, Table S6.5.1] for photons. For the case with bremsstrahlung radiation, the UO₂ matrix was used per assumption in Section 3.1, as ORIGEN-S lacks the option of the UF₆ matrix. The use of the UO₂ matrix tends to over-estimate the bremsstrahlung radiation contribution for the UF₆ matrix, because the effective atomic number for UO₂ is greater than that for UF₆ (see Section 3.4.4), resulting in a conservative photon source term without correction. Correction to the bremsstrahlung

radiation component is necessary to remove the conservatism in the photon source, as discussed in Section 3.4.4.

The decay or in-growth times considered in the ORIGEN-S calculation included zero and one year. The zero year corresponds to the initial uranium concentrations, and thus only uranium isotopes are present (no progeny). The one-year decay is consistent with the assumption of one-year in-growth time for buildup of the progeny to reach equilibrium as a result of the uranium decay. Both zero and one year cases were used in Chapter 4 to show the change in the dose rate with time.

The ORIGEN-S calculations for filled cylinders consisted of a total of 10 cases for five different U-235 concentrations with two cases each. The computer input and output files for each case are listed in Table A-1 in Appendix A, along with the case description. The input file listing for the sample cases for natural UF₆ is also provided in Appendix A.

The ORIGEN-S calculations for an empty feed cylinder were treated differently as separately discussed in Section 3.10.

3.4.4 Photon Source Correction for UF₆ Matrix Bremsstrahlung

As indicated in Section 3.4.3, the ORIGEN-S-generated photon source terms for filled cylinders are conservative because of the use of UO₂ matrix for bremsstrahlung radiation. To remove this conservatism, the bremsstrahlung radiation component was manually corrected using the radiation yield data as a function of beta energy for high-Z materials to demonstrate the linearity with Z (atomic number) and insensitivity to energy.

Table 3-5 provides the bremsstrahlung radiation yield data as a function of beta energy for tin (Z=50), tungsten (Z=74) and lead (Z=82), as taken directly from *Introduction to Radiological Physics and Radiation Dosimetry* [Attix 1986, Appendix E]. The data show

that the yield is closely related to the atomic ratio and fairly independent of beta energy, especially for higher-Z materials such as tungsten and lead.

Table 3-5 Bremsstrahlung Radiation Yield Data

Beta Energy (MeV)	Radiation Yield			Tin/Lead Yield Ratio	Tungsten/Lead Yield Ratio
	<u>Tin (Z=50)</u>	<u>Tungsten (Z=74)</u>	<u>Lead (Z=82)</u>	<u>Z ratio=0.61</u>	<u>Z ratio=0.9</u>
0.1	6.584E-03	1.032E-02	1.162E-02	0.567	0.888
0.2	1.147E-02	1.865E-02	2.118E-02	0.542	0.881
0.5	2.224E-02	3.712E-02	4.241E-02	0.524	0.875
1.0	3.666E-02	6.030E-02	6.842E-02	0.536	0.881
1.5	4.998E-02	8.022E-02	9.009E-02	0.555	0.890
2.0	6.284E-02	9.856E-02	1.096E-01	0.573	0.899
2.5	7.534E-02	1.158E-01	1.277E-01	0.590	0.907

For charged particles such as betas in a given material or compound, an effective atomic number can be derived by use of elemental weight fractions as weighting factors [Attix 1986, p. 308]. Table 3-6 provides the Excel-calculated effective atomic numbers for UO₂ and UF₆ with a UF₆/UO₂ ratio of 0.7937. This ratio was rounded up to 0.8 as a correction factor to be applied to the UO₂ bremsstrahlung radiation, based on the observation of the yield data relationship in Table 3-5. This factor is higher than the arbitrary factor of 0.6 assumed in the previous UUSA calculation [AREVA 2003b, §5.3(a)] which lacks a technical basis. Note that the bremsstrahlung correction is applicable to the filled cylinders containing UF₆ only. The photon source term in the empty feed cylinders which are absent of UF₆ does not require such correction, as discussed in Sections 3.1 and 3.10.

Table 3-6 Effective Atomic Numbers for UO₂ and UF₆

UO₂ Effective Atomic Number (DU used for slight conservatism)					
	<u>Element</u>	<u>Atomic Number, Z</u>	<u>Atomic Mass</u>	<u>Weight Fraction, f</u>	<u>Z x f</u>
	U	92	238.0402998	0.88150	81.0983
	O	8	15.9994	0.11850	0.9480
Effective Z					82.0463
UF₆ Effective Atomic Number (DU used for slight conservatism)					
	<u>Element</u>	<u>Atomic Number, Z</u>	<u>Atomic Mass</u>	<u>Weight Fraction, f</u>	<u>Z x f</u>
	U	92	238.0402998	0.67619	62.2096
	F	9	18.9984032	0.32381	2.9143
Effective Z					65.1239

3.5 NEUTRON SOURCE TERM PER UNIT BASIS

The neutron source term is independent of the decay time or in-growth time, as the progeny of the uranium isotope decay makes completely negligible contribution to neutron yields. However, the neutron yield is significantly dependent upon the U-235 enrichment or assay value. It increases with U-235 wt %, because of the increasing contribution from U-234 (α, n) reactions, which is a dominant component of the total neutron yield for higher U-235 concentrations, based on the ORIGEN-S output. Note that the enrichment process increases not only U-235 concentration, but also U-234 concentration simultaneously. Consideration of U-234 is a key factor in the determination of the UF₆ source terms. Table B-1 in Appendix B gives the neutron yield by isotope.

Figure 3-1 depicts the neutron source strength as a function of U-235 concentration using the data in Table B-1. The graph shows that the contribution from (α, n) reactions is approximately linear with U-235 concentration and the contribution from spontaneous fissions stays fairly constant (relatively insensitive to the U-235 parameter). The contribution from (α, n) reactions constitutes a significant component of the total neutron yield for a given U-235 concentration, and its relative contribution increases with the U-235

concentration. The spontaneous fission neutron contribution is virtually all from U-238, because of its predominant weight fraction and abundance.

Figure 3-2 shows the neutron yield by isotope in column chart type with the (α, n) and spontaneous fission components indicated. Obviously, U-234 and U-238 are the principal contributors to the UF_6 neutron yield. The contributions from U-235 and U-236 are relatively minor or negligible.

The results of the neutron source terms on a per unit basis (i.e. per kg of UF_6), are presented in Tables B-2, B-3, B-4, B-5 and B-6 in Appendix B for 0.2%, 0.3%, 0.4%, 0.5% and 0.711% U-235, respectively, as extracted from the associated ORIGEN-S output files. The results include the source strengths and associated energy spectra plus the breakdown of the contributions from (α, n) reactions and spontaneous fissions (SF). Note that DU denotes the symbol for depleted U and NU for natural U.

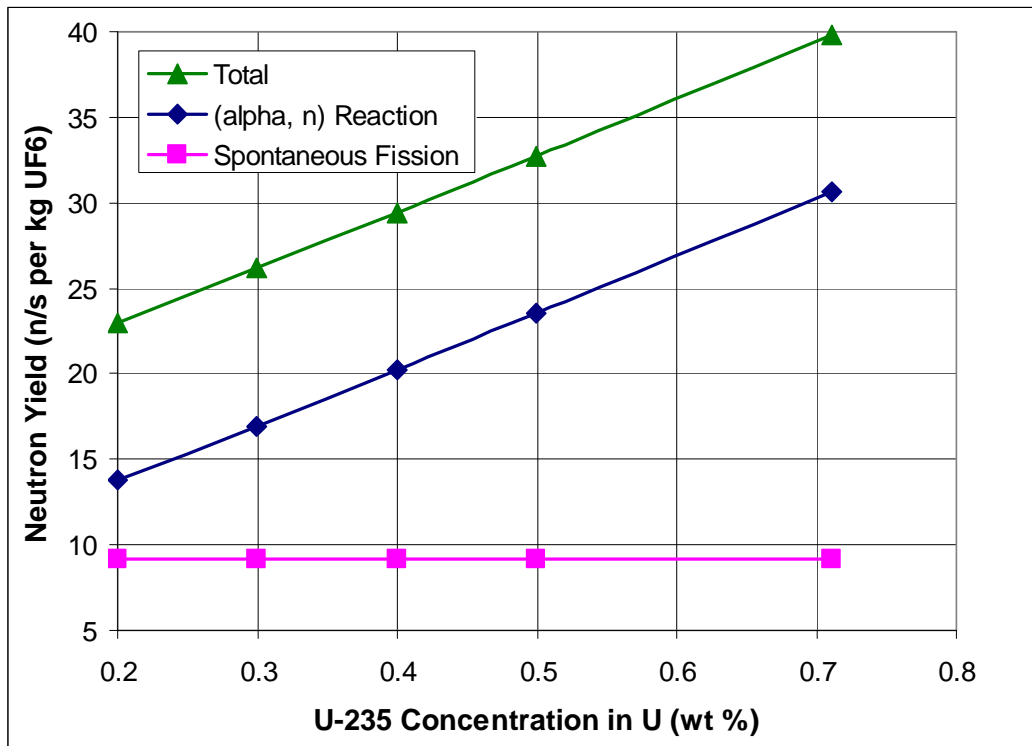


Figure 3-1 UF_6 Neutron Yield as a Function of U-235 Concentration in Weight Percents

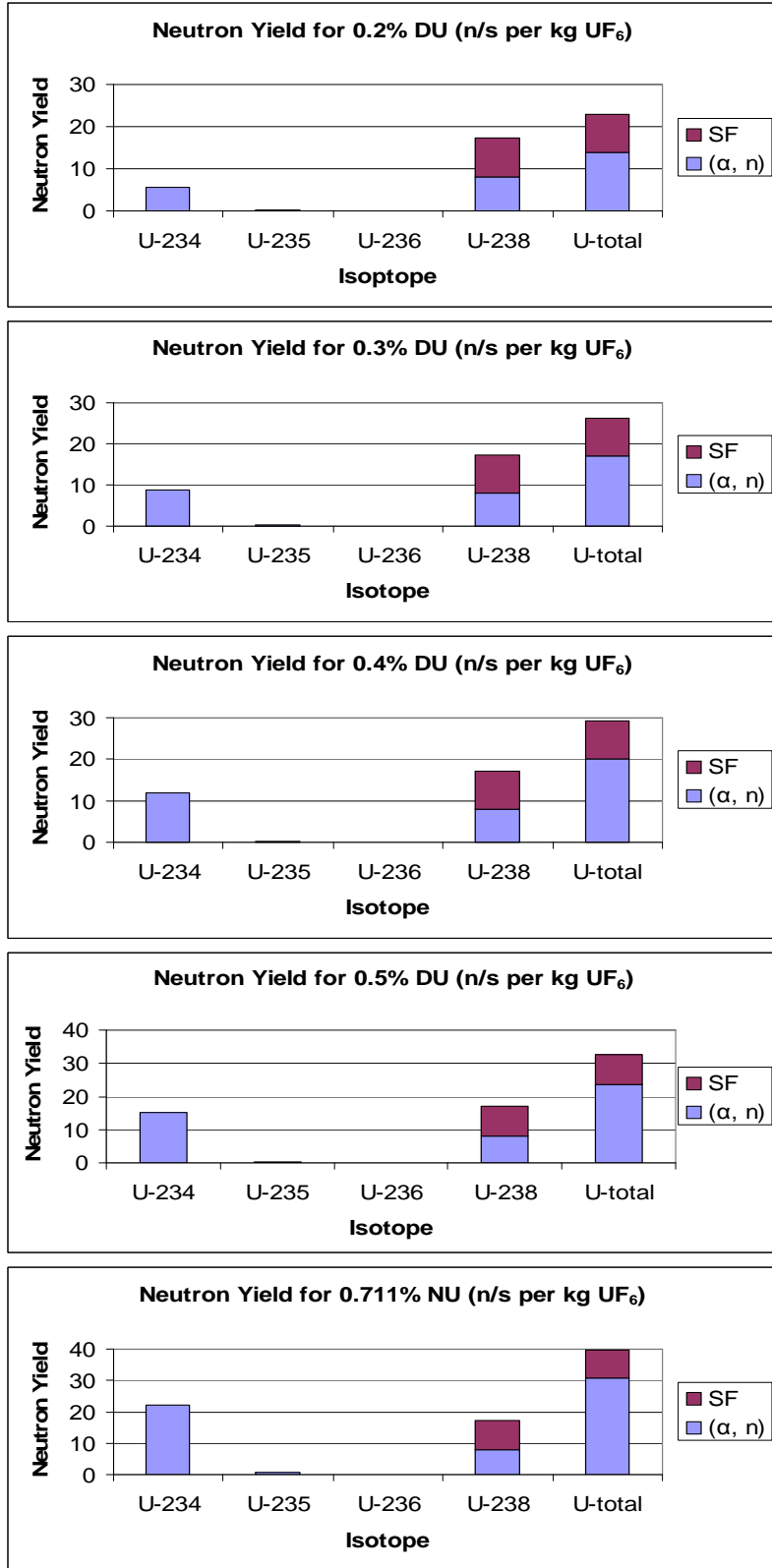


Figure 3-2 Neutron Yield by Uranium Isotope

3.6 UNCORRECTED PHOTON SOURCE TERM PER UNIT BASIS

As generated with ORIGEN-S, the results of the uncorrected photon source terms on a per unit basis (i.e. per kg of UF₆) based on the UO₂ bremsstrahlung, are presented in Tables B-7, B-8, B-9, B-10 and B-11 in Appendix B for 0.2%, 0.3%, 0.4%, 0.5% and 0.711% U-235, respectively. The results include the source strengths and associated energy spectra.

Unlike the neutron source term, the photon source term is sensitive to the decay or in-growth time. Initially (at zero year), only uranium isotopes contribute to the photon source term, as no progeny is present. After one-year in-growth time, the buildup of the decay products increases the photon source intensity considerably as demonstrated by the ORIGEN-S results. The use of the in-growth time of one year is appropriate for the maximum photon source intensity based on the ORIGEN-S test runs and previous validation.

As for the neutron source term, the U-235 concentration is a key parameter for the photon source intensity, which also increases with the U-235 wt% as a result of the increasing contribution from U-234. Again, U-234 must be included in the UF₆ source term determination, because of its significant contribution to both neutron and photon sources.

The photon source term for each U-235 wt % value includes the results with and without bremsstrahlung radiation. The bremsstrahlung contribution is very important for the photon source term. For the option of the conservative UO₂ matrix used in the ORIGEN-S calculation, the ratio of the total photon source strength with bremsstrahlung to that without bremsstrahlung decreases as the U-235 wt % increases. It should be noted that the bremsstrahlung contribution calculated with ORIGEN-S is highly conservative (over-estimated) for UF₆, as the effective atomic number for UF₆ is less than that for UO₂ (see Section 3.4.4). The bremsstrahlung correction for UF₆ is provided in Section 3.7.

3.7 CORRECTED PHOTON SOURCE TERM PER UNIT BASIS

As stated in Section 3.6, the photon source term generated with ORIGEN-S requires correction for the bremsstrahlung radiation contribution in the actual UF₆ matrix rather than the assumed UO₂ matrix used in ORIGEN-S. Without correction, the use of the UO₂ matrix would be conservative but overestimate the bremsstrahlung radiation component of the photon source term.

The steps for correcting the UO₂ bremsstrahlung for the UF₆ matrix are described below:

- Obtain the net UO₂ bremsstrahlung contribution for each energy group as follows:
Net UO₂ bremsstrahlung = difference of ORIGEN-S results with and without UO₂ bremsstrahlung
- Correct the net UO₂ bremsstrahlung contribution for the UF₆ matrix by a factor of 0.8 for each group (see Section 3.4.4) to obtain the net UF₆ bremsstrahlung contribution.
- Calculate the adjusted total photon source intensity for each energy group by adding the contributions for no bremsstrahlung and the net UF₆ bremsstrahlung.

Using the above procedure, Tables B-12 through B-16 in Appendix B provide the corrected photon source terms per unit basis. The results include the cases for 0.2%, 0.3%, 0.4%, 0.5% and 0.711% U-235. The corrected photon source terms were used to obtain the photon source intensity and energy spectra for each cylinder (Section 3.8), and to calculate the photon doses from UF₆ cylinders.

3.8 RADIATION SOURCE TERM PER FILLED CYLINDER

With the results of the neutron and corrected photon source terms per kg of UF₆ available from Sections 3.5 and 3.7 respectively, the source term per cylinder for the maximum fill limit of 12,501 kg UF₆ (Table 3-2) can be easily calculated as follows:

48Y Filled Feed or Tails Cylinder

$$\text{Source per cylinder} = (\text{intensity per kg UF}_6) \times (12501 \text{ kg UF}_6 \text{ per cylinder})$$

For a filled cylinder, the source terms per cylinder are provided in Table 3-7 for neutrons and Table 3-8 for photons for the various U-235 concentrations. For both neutrons and photons, the energy spectra are fairly similar for different U-235 concentrations. The principal contributors to the neutron source are U-234 and U-238. The photon source arises from Th-231, Th-234, Pa-234, Pa-234m, U-234, U-235 and U-238. The UF₆ self-shielding effect is a factor for dose calculations, but irrelevant for the source term generation which only treats the decay of uranium isotopes.

As stated earlier, the neutron source terms are independent of the decay time. The photon source terms are given for the one-year growth time to reach equilibrium and for the case with bremsstrahlung corrected for the UF₆ matrix. These results are necessary for subsequent dose calculations with the MCNP code, as the code requires the source input in terms of the total source strength per cylinder and its associated energy spectrum to obtain an absolute dose value.

Table 3-7 UF₆ Neutron Source Term per Filled Cylinder for Various U-235 Weight Percents

Group	Energy Boundaries (MeV)	Neutron Source Intensity (n/s per cylinder)				
		48Y Tails (0.2%)*	48Y Tails (0.3%)*	48Y Tails (0.4%)*	48Y Tails (0.5%)*	48Y Feed (0.711%)*
1	1.00E-11 - 1.00E-08	3.055E-13	4.583E-13	6.110E-13	7.637E-13	1.086E-12
2	1.00E-08 - 3.00E-08	8.647E-13	1.298E-12	1.729E-12	2.161E-12	3.074E-12
3	3.00E-08 - 5.00E-08	2.178E-07	2.175E-07	2.173E-07	2.170E-07	2.166E-07
4	5.00E-08 - 1.00E-07	9.192E-07	9.182E-07	9.173E-07	9.163E-07	9.144E-07
5	1.00E-07 - 2.25E-07	3.777E-06	3.773E-06	3.769E-06	3.765E-06	3.758E-06
6	2.25E-07 - 3.25E-07	5.832E-06	5.825E-06	5.820E-06	5.814E-06	5.802E-06
7	3.25E-07 - 4.14E-07	2.569E-06	2.566E-06	2.563E-06	2.560E-06	2.555E-06
8	4.14E-07 - 8.00E-07	2.413E-05	2.410E-05	2.408E-05	2.405E-05	2.400E-05
9	8.00E-07 - 1.00E-06	1.843E-05	1.840E-05	1.839E-05	1.836E-05	1.833E-05
10	1.00E-06 - 1.13E-06	7.478E-06	7.471E-06	7.463E-06	7.456E-06	7.439E-06
11	1.13E-06 - 1.30E-06	1.568E-05	1.566E-05	1.564E-05	1.563E-05	1.559E-05
12	1.30E-06 - 1.86E-06	6.105E-05	6.099E-05	6.093E-05	6.087E-05	6.074E-05
13	1.86E-06 - 3.06E-06	1.703E-04	1.814E-04	1.925E-04	2.041E-04	2.293E-04
14	3.06E-06 - 1.07E-05	1.764E-03	1.841E-03	1.921E-03	2.003E-03	2.180E-03
15	1.07E-05 - 2.90E-05	8.658E-03	9.712E-03	1.080E-02	1.190E-02	1.430E-02
16	2.90E-05 - 1.01E-04	6.491E-02	7.061E-02	7.647E-02	8.246E-02	9.541E-02
17	1.01E-04 - 5.83E-04	1.008E+00	1.091E+00	1.176E+00	1.263E+00	1.451E+00
18	5.83E-04 - 3.04E-03	1.155E+01	1.239E+01	1.325E+01	1.413E+01	1.603E+01
19	3.04E-03 - 1.50E-02	1.248E+02	1.323E+02	1.399E+02	1.476E+02	1.644E+02
20	1.50E-02 - 1.11E-01	2.971E+03	3.147E+03	3.327E+03	3.509E+03	3.905E+03
21	1.11E-01 - 4.08E-01	2.730E+04	2.943E+04	3.162E+04	3.385E+04	3.869E+04
22	4.08E-01 - 9.07E-01	9.132E+04	1.027E+05	1.144E+05	1.264E+05	1.523E+05
23	9.07E-01 - 1.42E+00	8.097E+04	9.613E+04	1.117E+05	1.276E+05	1.620E+05
24	1.42E+00 - 1.83E+00	3.582E+04	4.279E+04	4.997E+04	5.730E+04	7.314E+04
25	1.83E+00 - 3.01E+00	3.305E+04	3.654E+04	4.014E+04	4.380E+04	5.174E+04
26	3.01E+00 - 6.38E+00	1.533E+04	1.530E+04	1.529E+04	1.528E+04	1.524E+04
27	6.38E+00 - 2.00E+01	5.819E+02	5.813E+02	5.807E+02	5.802E+02	5.789E+02
Total	1.00E-11 - 2.00E+01	2.875E+05	3.269E+05	3.673E+05	4.085E+05	4.978E+05

*U-235 wt % in uranium in parentheses

Table 3-8 UF₆ Photon Source Term per Filled Cylinder for Various U-235 Weight Percents

Group	Energy Boundaries (MeV)	Photon Source Intensity (p/s per cylinder)				
		48Y Tails (0.2%)*	48Y Tails (0.3%)*	48Y Tails (0.4%)*	48Y Tails (0.5%)*	48Y Feed (0.711%)*
1	1.00E-02 - 4.50E-02	3.737E+10	3.863E+10	3.993E+10	4.125E+10	4.408E+10
2	4.50E-02 - 1.00E-01	2.091E+10	2.106E+10	2.123E+10	2.139E+10	2.174E+10
3	1.00E-01 - 2.00E-01	8.408E+09	9.034E+09	9.662E+09	1.029E+10	1.161E+10
4	2.00E-01 - 3.00E-01	2.473E+09	2.505E+09	2.536E+09	2.568E+09	2.635E+09
5	3.00E-01 - 4.00E-01	1.690E+09	1.690E+09	1.689E+09	1.688E+09	1.685E+09
6	4.00E-01 - 6.00E-01	1.162E+09	1.161E+09	1.160E+09	1.159E+09	1.157E+09
7	6.00E-01 - 8.00E-01	1.147E+09	1.145E+09	1.144E+09	1.143E+09	1.141E+09
8	8.00E-01 - 1.00E+00	8.854E+08	8.847E+08	8.837E+08	8.828E+08	8.808E+08
9	1.00E+00 - 1.33E+00	5.289E+08	5.284E+08	5.279E+08	5.274E+08	5.262E+08
10	1.33E+00 - 1.66E+00	7.872E+07	7.863E+07	7.856E+07	7.848E+07	7.831E+07
11	1.66E+00 - 2.00E+00	9.500E+07	9.491E+07	9.481E+07	9.471E+07	9.451E+07
12	2.00E+00 - 2.50E+00	1.588E+05	1.585E+05	1.584E+05	1.583E+05	1.579E+05
13	2.50E+00 - 3.00E+00	1.824E+04	1.823E+04	1.821E+04	1.820E+04	1.816E+04
14	3.00E+00 - 4.00E+00	1.639E+04	1.638E+04	1.636E+04	1.635E+04	1.631E+04
15	4.00E+00 - 5.00E+00	5.532E+03	5.527E+03	5.522E+03	5.517E+03	5.507E+03
16	5.00E+00 - 6.50E+00	2.220E+03	2.218E+03	2.215E+03	2.214E+03	2.209E+03
17	6.50E+00 - 8.00E+00	4.354E+02	4.350E+02	4.345E+02	4.342E+02	4.333E+02
18	8.00E+00 - 1.00E+01	9.536E+01	9.527E+01	9.517E+01	9.508E+01	9.488E+01
19	1.00E+01 - 2.00E+01	1.753E+00	1.750E+00	1.749E+00	1.748E+00	1.744E+00
Total	1.00E-02 - 2.00E+01	7.474E+10	7.682E+10	7.893E+10	8.107E+10	8.563E+10

*U-235 wt % in uranium in parentheses

3.9 TIME-DEPENDENT PHOTON SOURCE FOR FILLED FEED CYLINDER

To compare the time-dependent photon source term and associated dose rate with an empty feed cylinder, an additional ORIGEN-S calculation for a filled feed cylinder was performed for the case of natural UF₆ for 0.0, 0.1, 0.2, 0.3, 0.5, 0.7, 1.0 and 2.0 year decay. The input and output files are *nu_a.inp* and *nu_a.out* for the run with UO₂ bremsstrahlung; and *nu_na.inp* and *nu_na.out* for the run with no bremsstrahlung, respectively. Table 3-9 lists the resulting photon source terms with correction of bremsstrahlung radiation for the UF₆ matrix in the same manner as described in Section 3.7. It is apparent that the assumption of the one-year in-growth time is valid for reaching equilibrium and maximum photon source terms, as the values for 1.0 and 2.0 year decay are identical at least to four significant figures.

Note that only the photon source term is time dependent. The neutron source term stays virtually constant, independent of the in-growth or decay time.

The time-dependent photon source term is useful for determining the corresponding time-dependent dose rate, which is important for management of cylinder storage especially for strategic placement of empty feed cylinders (see subsequent discussion in Section 3.10).

Table 3-9 Time-dependent UF₆ Photon Source Term for 48Y Filled Feed Cylinder

Gp.	Energy Boundaries (MeV)	Photon Source Intensity (p/s per cylinder)							
		0 year*	0.1 year*	0.2 year*	0.3 year*	0.5 year*	0.7 year*	1.0 year*	2.0 year*
1	1.00E-02 – 4.50E-02	1.167E+10	3.355E+10	4.040E+10	4.280E+10	4.393E+10	4.407E+10	4.408E+10	4.408E+10
2	4.50E-02 – 1.00E-01	7.166E+08	1.461E+10	1.924E+10	2.087E+10	2.162E+10	2.172E+10	2.174E+10	2.174E+10
3	1.00E-01 – 2.00E-01	4.474E+09	9.131E+09	1.075E+10	1.131E+10	1.157E+10	1.161E+10	1.161E+10	1.161E+10
4	2.00E-01 – 3.00E-01	2.406E+08	1.798E+09	2.342E+09	2.533E+09	2.623E+09	2.633E+09	2.635E+09	2.635E+09
5	3.00E-01 – 4.00E-01	4.564E+06	1.098E+09	1.480E+09	1.613E+09	1.676E+09	1.684E+09	1.685E+09	1.685E+09
6	4.00E-01 – 6.00E-01	2.568E+05	7.523E+08	1.016E+09	1.108E+09	1.151E+09	1.156E+09	1.157E+09	1.157E+09
7	6.00E-01 – 8.00E-01	2.885E+05	7.419E+08	1.001E+09	1.092E+09	1.135E+09	1.140E+09	1.141E+09	1.141E+09
8	8.00E-01 – 1.00E+00	0.000E+00	5.728E+08	7.731E+08	8.432E+08	8.762E+08	8.804E+08	8.808E+08	8.808E+08
9	1.00E+00 – 1.33E+00	1.211E+05	3.422E+08	4.619E+08	5.037E+08	5.235E+08	5.259E+08	5.262E+08	5.262E+08
10	1.33E+00 – 1.66E+00	0.000E+00	5.092E+07	6.873E+07	7.496E+07	7.790E+07	7.826E+07	7.831E+07	7.831E+07
11	1.66E+00 – 2.00E+00	5.173E+04	6.147E+07	8.295E+07	9.046E+07	9.402E+07	9.445E+07	9.451E+07	9.451E+07
12	2.00E+00 – 2.50E+00	3.135E+04	1.136E+05	1.424E+05	1.525E+05	1.573E+05	1.578E+05	1.579E+05	1.579E+05
13	2.50E+00 – 3.00E+00	1.816E+04	1.816E+04	1.816E+04	1.816E+04	1.816E+04	1.816E+04	1.816E+04	1.816E+04
14	3.00E+00 – 4.00E+00	1.631E+04	1.631E+04	1.631E+04	1.631E+04	1.631E+04	1.631E+04	1.631E+04	1.631E+04
15	4.00E+00 – 5.00E+00	5.507E+03	5.507E+03	5.507E+03	5.507E+03	5.507E+03	5.507E+03	5.507E+03	5.507E+03
16	5.00E+00 – 6.50E+00	2.209E+03	2.209E+03	2.209E+03	2.209E+03	2.209E+03	2.209E+03	2.209E+03	2.209E+03
17	6.50E+00 – 8.00E+00	4.333E+02	4.333E+02	4.333E+02	4.333E+02	4.333E+02	4.333E+02	4.333E+02	4.333E+02
18	8.00E+00 – 1.00E+01	9.488E+01	9.488E+01	9.488E+01	9.488E+01	9.488E+01	9.488E+01	9.488E+01	9.488E+01
19	1.00E+01 – 2.00E+01	1.744E+00	1.744E+00	1.744E+00	1.744E+00	1.744E+00	1.744E+00	1.744E+00	1.744E+00
Total	1.00E-02 – 2.00E+01	1.711E+10	6.270E+10	7.761E+10	8.284E+10	8.528E+10	8.560E+10	8.563E+10	8.563E+10

*In-growth time after filling

3.10 TIME-DEPENDENT PHOTON SOURCE FOR EMPTY FEED CYLINDER

As indicated earlier, the empty feed cylinders contain photon sources from the daughter products of the uranium isotopes. The photon source term for the empty cylinders were treated differently from that for the filled tails or feed cylinders. First, an ORIGEN-S run was made with a fully loaded feed cylinder (containing 12,501 kg UF₆) for one-year in-growth time to determine the radionuclide inventory (in grams) of the natural uranium progeny (daughter products). This inventory represents the maximum source term for the natural uranium progeny at the time of emptying. Second, the resulting progeny inventory was input into a subsequent ORIGEN-S run to obtain the photon source strength and energy spectrum as a function of time from the time of emptying ($t = 0$) up to 2 years.

The same 19-group structure for photons was used for the empty cylinders as for the filled cylinders. However, the bremsstrahlung radiation for the water matrix option available in ORIGEN-S was selected for equivalent treatment of bremsstrahlung in air and carbon steel associated with an empty cylinder. Unlike the filled cylinders, the photon source for the empty cylinders decreases with time after emptying.

Tables A-1 in Appendix A lists and describes the input and output files used to calculate the photon source term for the empty cylinders. Table 3-10 provides the time-dependent photon source terms.

Table 3-10 Time-dependent UF₆ Photon Source Term for 48Y Empty Feed Cylinder

Gp.	Energy Boundaries (MeV)	Photon Source Intensity (p/s per cylinder)							
		0 year*	0.1 year*	0.2 year*	0.3 year*	0.5 year*	0.7 year*	1.0 year*	2.0 year*
1	1.00E-02 - 4.50E-02	8.869E+09	2.336E+09	8.171E+08	2.858E+08	3.501E+07	4.337E+06	2.450E+05	6.279E+04
2	4.50E-02 - 1.00E-01	1.116E+10	3.689E+09	1.290E+09	4.512E+08	5.520E+07	6.760E+06	2.997E+05	1.408E+04
3	1.00E-01 - 2.00E-01	1.165E+09	3.930E+08	1.374E+08	4.807E+07	5.880E+06	7.204E+05	3.225E+04	2.000E+03
4	2.00E-01 - 3.00E-01	4.135E+08	1.439E+08	5.032E+07	1.760E+07	2.160E+06	2.717E+05	2.042E+04	1.157E+04
5	3.00E-01 - 4.00E-01	2.394E+08	8.372E+07	2.928E+07	1.024E+07	1.258E+06	1.591E+05	1.284E+04	7.708E+03
6	4.00E-01 - 6.00E-01	2.187E+08	7.651E+07	2.676E+07	9.359E+06	1.145E+06	1.403E+05	6.383E+03	6.554E+02
7	6.00E-01 - 8.00E-01	7.389E+08	2.585E+08	9.041E+07	3.162E+07	3.868E+06	4.733E+05	2.061E+04	6.304E+02
8	8.00E-01 - 1.00E+00	7.219E+08	2.526E+08	8.834E+07	3.089E+07	3.779E+06	4.623E+05	1.996E+04	3.427E+02
9	1.00E+00 - 1.33E+00	4.426E+08	1.549E+08	5.416E+07	1.894E+07	2.317E+06	2.835E+05	1.229E+04	2.808E+02
10	1.33E+00 - 1.66E+00	6.539E+07	2.288E+07	8.001E+06	2.798E+06	3.423E+05	4.193E+04	1.871E+03	1.345E+02
11	1.66E+00 - 2.00E+00	9.267E+07	3.242E+07	1.134E+07	3.965E+06	4.851E+05	5.943E+04	2.669E+03	2.191E+02
12	2.00E+00 - 2.50E+00	5.748E+04	2.013E+04	7.055E+03	2.486E+03	3.354E+02	7.838E+01	5.355E+01	8.661E+01
13	2.50E+00 - 3.00E+00	2.593E-01	3.032E-01	3.550E-01	4.068E-01	5.182E-01	6.218E-01	7.772E-01	1.295E+00
14	3.00E+00 - 4.00E+00	6.175E-02	7.219E-02	8.450E-02	9.680E-02	1.233E-01	1.479E-01	1.848E-01	3.078E-01
15	4.00E+00 - 5.00E+00	4.849E-05	4.939E-05	4.976E-05	4.993E-05	5.014E-05	5.031E-05	5.054E-05	5.139E-05
16	5.00E+00 - 6.50E+00	1.398E-05	1.424E-05	1.435E-05	1.440E-05	1.446E-05	1.450E-05	1.457E-05	1.482E-05
17	6.50E+00 - 8.00E+00	1.779E-06	1.813E-06	1.827E-06	1.834E-06	1.841E-06	1.847E-06	1.856E-06	1.887E-06
18	8.00E+00 - 1.00E+01	2.424E-07	2.473E-07	2.492E-07	2.501E-07	2.512E-07	2.520E-07	2.532E-07	2.574E-07
19	1.00E+01 - 2.00E+01	2.860E-09	2.921E-09	2.945E-09	2.956E-09	2.969E-09	2.979E-09	2.992E-09	3.042E-09
Total	1.00E-02 - 2.00E+01	2.413E+10	7.444E+09	2.603E+09	9.105E+08	1.114E+08	1.371E+07	6.741E+05	1.005E+05

*Decay time after emptying

3.11 COMPARISON WITH PREVIOUS CALCULATIONS

UUSA previously performed a UF₆ source term calculation to support the license application of the National Enrichment Facility (NEF) in Eunice, New Mexico. The calculation included the neutron and photon source terms [AREVA 2003a and 2003b]. For direct comparison with this calculation, additional ORIGEN-S runs [UUSA 2013b] were executed with the same energy group structures as used in the original UUSA calculation. The ORIGEN-S calculations supporting this research are identified here as the UNM calculations.

For the neutron source, UUSA used the neutron yield data in the paper on *Neutron Production in UF₆ from the Decay of Uranium Nuclide* (Wilson 1981) to manually calculate the total source strengths from both (α , n) reactions and spontaneous fissions. However, an assumption was made for the (α , n) reaction neutron energy spectrum, based on an Am-241 – fluorine source. Am-241 produces alpha particles at an average energy of about 5.5 MeV, while uranium isotopes produce alpha particles between 4.1 and 4.8 MeV [Baum 2002]. Since the neutron energy produced by an (α , n) reaction is a function of the alpha particle energy, the Am-241-F (α , n) energy spectrum is harder than a U-F (α , n) spectrum. Table B-17 in Appendix B compares the neutron results between the UUSA and UNM calculations for tails at 0.34% U-235 and for feed at 0.711% of relevance to this research. The comparison is shown graphically in Figure 3-3. The agreement for the spontaneous fission contribution is excellent. However, the (α , n) reaction contribution is higher with the UNM ORIGEN-S calculation using the problem-dependent matrix of UF₆ for the stopping power, which represents a more rigorous treatment of the neutron yield. Fissioning in uranium was accounted for in the MCNP dose calculations, not in the ORIGEN-S neutron source terms.

For the photon source, the original UUSA calculation used the stand-alone code ORIGEN-2 [Groff 1991] to calculate the source intensity per MTU (metric ton uranium). These photon results can be converted into photons/s per cylinder by the following multipliers:

48Y Tails Cylinder (0.34% U-235)

$$(12501 \text{ kg UF}_6/\text{cylinder}) \times (0.67619 \text{ U/UF}_6) \times (1/1000 \text{ MT/kg}) = 8.4584 \text{ MTU/cylinder}$$

48Y Feed Cylinder (0.711% U-235)

$$(12501 \text{ kg UF}_6/\text{cylinder}) \times (0.67618 \text{ U/UF}_6) \times (1/1000 \text{ MT/kg}) = 8.4529 \text{ MTU/cylinder}$$

The converted ORIGEN-2 photon source terms are presented in Table B-18 in Appendix B and compared with the corresponding UNM ORIGEN-S results. The graphical comparison is shown in Figure 3-4. The two separate calculations with different codes (ORIGEN-2 and ORIGEN-S) agree reasonably well with respect to the total source strength, but there are some minor differences in the energy spectrum. The UNM ORIGEN-S calculation reflects the updated nuclear decay data library with ENDF/B-VII.1 used in the SCALE 6.1.2 code system with better accuracy.

It needs to be noted that the photon energy group structure used in Table B-18 is different from that in Table 3-9. The 19-group structure in Table 3-9 omits photons emitted between 0.0 and 0.01 MeV, which are included in the 18-group structure in Table B-18. Consequently, the total photon source strength for the 19-group structure is less than that for the 18-group structure. The omission of photons between 0.0 and 0.01 MeV results in no dose impacts, because of negligible contributions from these weak photons.

In addition to the UUSA calculation, the neutron source strength for a feed cylinder from this calculation is in excellent agreement with the Cameco calculation, which gives a value of

5.0×10^5 n/s per cylinder (Cameco 2009, §B.3.2) versus the ORIGEN-S calculated quantity of 4.98×10^5 n/s, thus validating the neutron source intensity (strength) for feed material. No spectral data were available from Cameco for comparison.

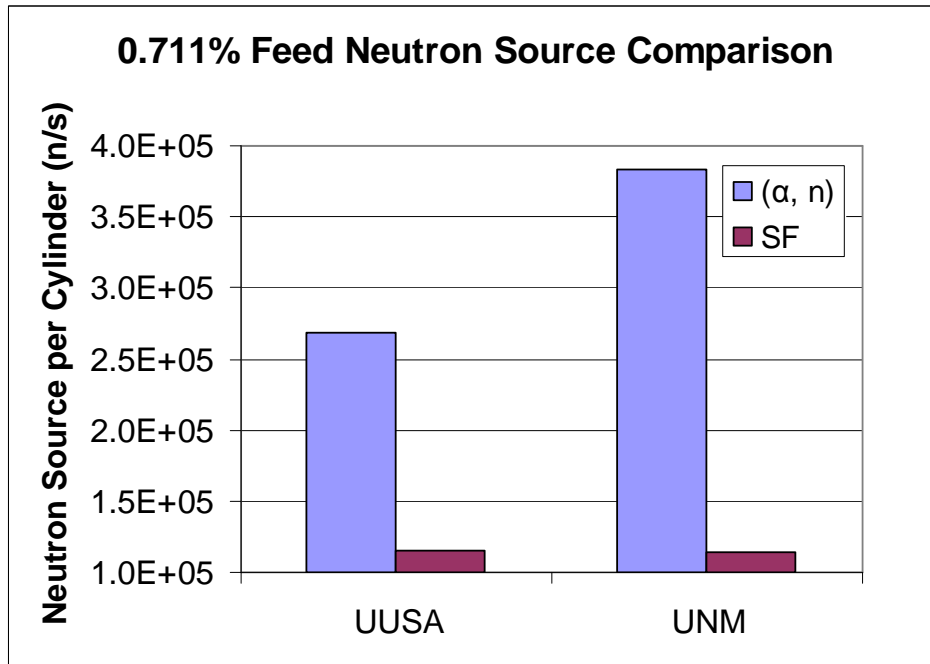
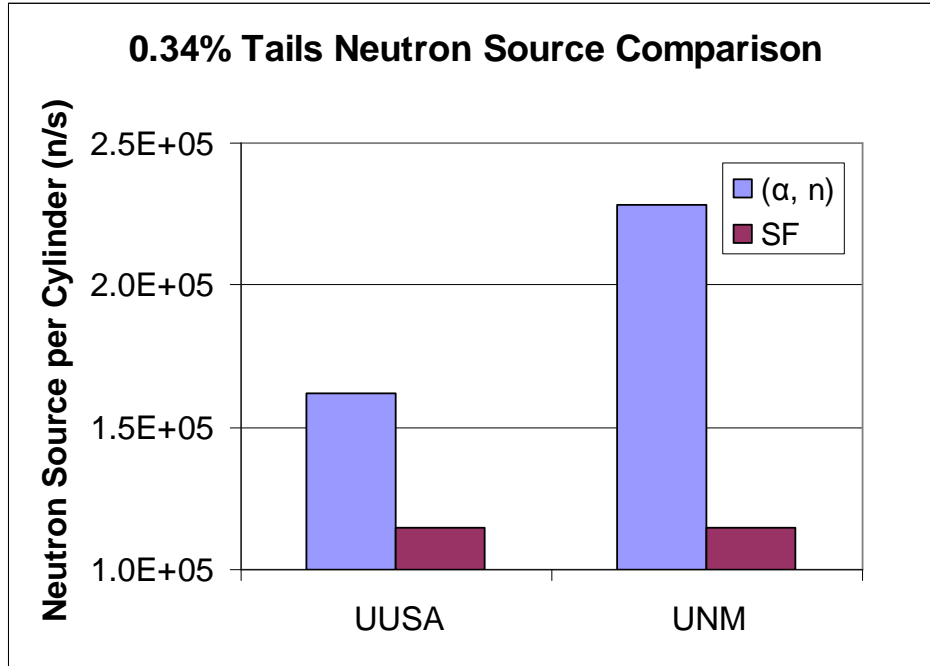


Figure 3-3 Neutron Source Term Comparison between UUSA and UNM Calculations

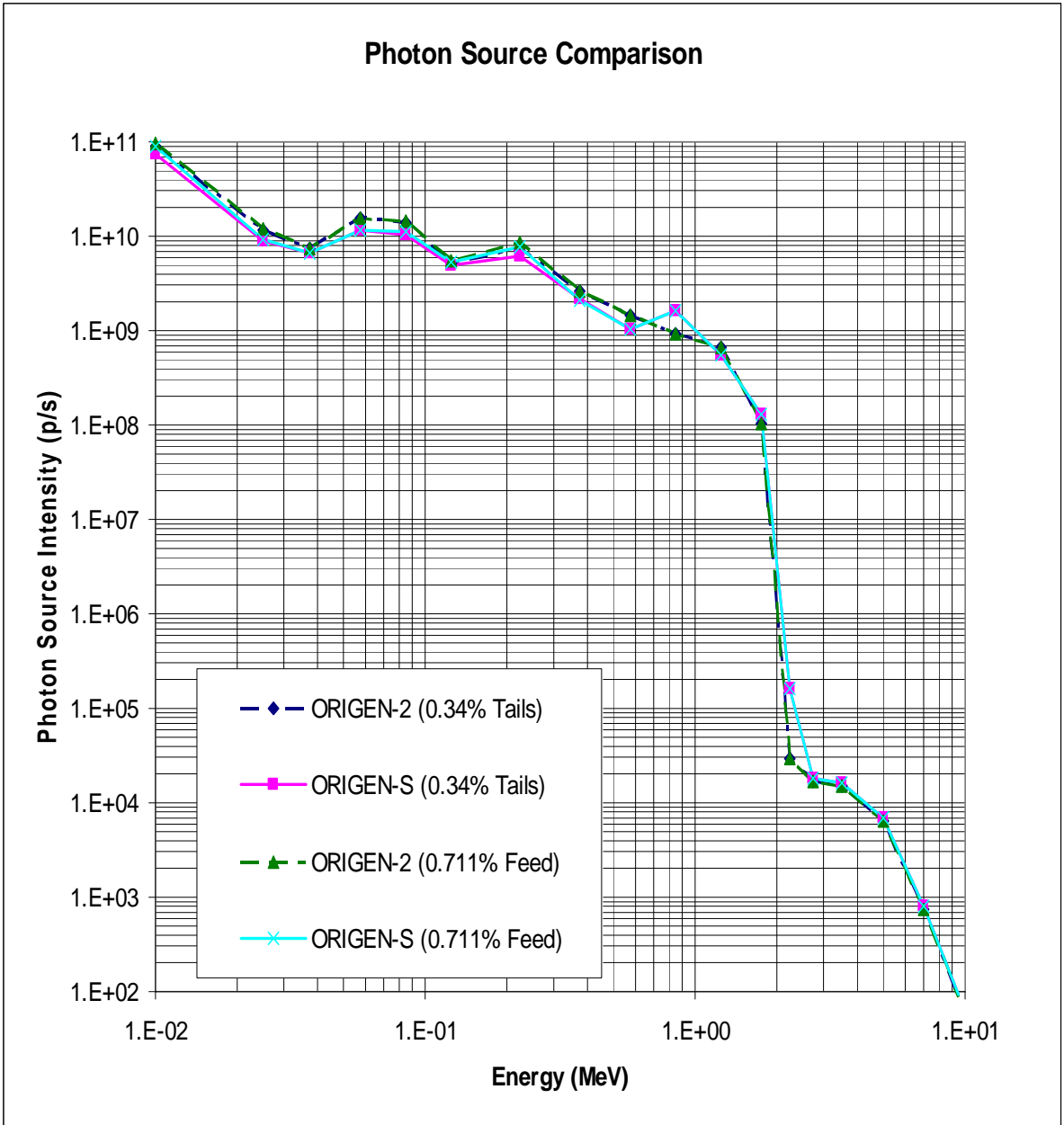


Figure 3-4 Photon Source Term Comparison between ORIGEN-2 (UUSA) and ORIGEN-S (UNM)

3.12 KEY OBSERVATIONS

The UF_6 radiation source terms were determined with the ORIGEN-S module in the SCALE code system (SCALE 6.1.2), and validated with additional calculations and comparison with previous similar calculations with a different methodology or code. The results include the total source strengths and associated energy spectra for both neutrons and photons as a function of U-235 concentration. These results reflect the change in the methodology and the updated nuclear decay data library for improved accuracy, and compare favorably with the previous calculations. These results are necessary for use in subsequent radiation dose assessment described in Chapters 4 and 5.

The results from this phase (Phase 1) led to the following key observations:

- U-234 Significance – Despite its relatively small quantity, U-234 is an important or principal contributor to both neutron and photon source terms, and must be included in the calculation.
- In-Growth Time – The in-growth time affects the photon source terms as a result of the buildup of the daughter products (progenies) from radioactive decay of uranium isotopes. The one-year in-growth time is appropriate for reaching the maximum photon source intensity. The neutron source term is independent of the in-growth time.
- U-235 Effect – Both neutron and photon source strengths increase with U-235 concentration, because of the accompanying increasing contribution from U-234. The neutron source is more sensitive to U-235 concentration than the photon source. For the neutron source, the U-235 concentration mainly affects the (α , n) reaction contribution, but poses little impact on the spontaneous fission contribution.

- Bremsstrahlung Contribution – Bremsstrahlung radiation is a significant part of the photon sources. Neglect of this contribution would grossly underestimate the photon source term and resulting radiation dose.
- Filled versus Empty Cylinders – Filled cylinders contain both neutron and photon sources, whereas only the photon source is present in empty cylinders. The neutron source is time independent. On the other hand, the photon source changes with time, reaching equilibrium after one-year in-growth for filled cylinders, but decaying rapidly for empty cylinders. Time dependence is a factor that must be considered in storage management of empty cylinders.

4. SINGLE CYLINDER DOSE EVALUATION

To gain an in-depth understanding of radiation transport associated with UF_6 , this research first evaluated the effects of the source geometry, concrete/ground scattering, dose conversion factors, secondary photon contributions, and photon energy spectrum for a single cylinder. The results of this evaluation provided the necessary input and results for use in the multiple cylinder dose assessment, and for validation of the source terms determined in Chapter 3.

The evaluation involved the calculations of radiation dose rates for UF_6 contained in a certified Model 48Y cylinder meeting the ANSI N14.1-2001 standard [ANSI 2001], including both neutron and photon dose rates, as Model 48Y is currently in use at uranium enrichment facilities for tails and feed material pertaining to this research. The calculations used the neutron and photon source terms for UF_6 generated from Phase 1 work as described in Chapter 3.

The dose calculations utilized the MCNP code (MCNP5, v1.60) [LANL 2010] for neutron and photon transport contained in the computer code package CCC-810 [RSICC 2013]. The code was obtained from Radiation Safety Information Computational Center (RSICC) at Oak Ridge National Laboratory (ORNL) under an export-controlled license for a single user (Computer Code Request Number 1418158), and successfully installed on a Toshiba laptop computer (Model: Satellite C855-S5115 Notebook PC). The nuclear data associated with MCNP5, v1.60 are based mainly on the ENDF/B-VII.0 library. Although a newer version of MCNP (MCNP6.1) is also available in the same code package, the test

results for UF_6 doses from MCNP5, v1.60 and MCNP6.1 are practically identical. Accordingly, the choice of MCNP5, v1.60 was appropriate for this research.

The neutron and photon dose rates were separately calculated with the MCNP code, using the ANSI/ANS-6.1.1-1977 dose conversion factors to obtain the reference results. The calculations included a case study on the effect of the newer ANSI/ANS-6.1.1-1991 dose conversion factors.

The reference calculations covered the radial and axial dose rates for both homogenized and slumped source geometry at the points of interest (at contact, 1, 5, 10, 20, 50, 100 m, etc). The F5 tallies (for point detectors) were used to score the fluxes, which were then converted internally in MCNP to the dose rate results.

In addition, the homogenized geometry was treated as a base case for evaluation of the various effects including concrete pad scattering, ground soil scattering, adequacy of the partial photon energy spectrum, and secondary photon contributions due to neutron reactions. For the parameter evaluation, the calculations considered the radial dose rates only for the sake of saving computer run times as similar effects would be expected in the axial direction.

Details of the single cylinder dose evaluation follow.

4.1 PREVIOUS WORK

UUSA has performed calculations of dose rates from a single filled 48Y cylinder, including both photon and neutron contributions [UUSA 2013, §7.1]. For a filled tails cylinder containing 0.34% U-235 by weight, the dose rates calculated with MCNP, v1.40 [LANL 2005] were 1.56 mrem/h at contact (0.11 n + 1.45 p), and 0.48 mrem/h (0.03 n + 0.45 p) at one meter from the side surface. The corresponding dose rates for a filled feed cylinder were 1.63 mrem/h at contact (0.16 n + 1.47 p), and 0.49 mrem/h (0.05 n + 0.44 p) at one

meter from the side surface. Note that the neutron and photon dose components were obtained from the associated MCNP output files.

The UUSA calculation used the ANSI/ANS-6.1.1-1977 flux-to-dose rate conversion factors [ANS 1977, pp 4 and 5] to convert the particle flux to the dose rate in units of rem/h or mrem/h. This version of the conversion factors is conservative relative to the newer ANSI/ANS-6.1.1-1991 [ANS 1991, Tables 4 and 5] standard, and compliant with 10 CFR 20 [NRCd, Table 1004(b).2] for neutrons.

The UUSA calculations neglected the scattering effect of the concrete pad or ground soil, which would make additional dose contributions at close-in distances but decrease the doses at larger distances. Furthermore, the calculations focused on filled cylinders only. The empty feed cylinder was purposely excluded with the assumption that these empty cylinders would be strategically placed on the storage pad with sufficient shielding by the surrounding filled cylinders to minimize its dose impact to a negligible level.

The author conducted an independent, unpublished study in the Summer 2013 semester at the University of New Mexico (UNM) for a single filled feed cylinder containing natural UF₆. The study evaluated the effects of the source geometry, concrete/ground scattering, secondary photon contributions, partial vs. full photon energy spectrum, and flux-to-dose rate conversion factors. The study concluded that it would be acceptable to select the homogenized source geometry and ANSI/ANS-6.1.1-1977 dose conversion factors for conservatism, simulate the concrete pad with ground soil, and use a partial energy spectrum of importance for dose calculations.

The conclusions from this independent study are applicable to the current research. However, for completeness and in view of the change in the energy group structures for

neutron and photon source terms, it was deemed desirable and necessary to repeat the single cylinder evaluation for selection of appropriate parameters for use in Phase 3 work on the multiple cylinder dose assessment.

The single cylinder dose evaluation belongs to Phase 2 of this research, using the source terms generated from ORIGEN-S (Phase 1), and feeding the results to the multiple cylinder dose assessment (Phase 3) and validation of dose simulations for a single cylinder (Phase 4). This chapter describes the research efforts expended in this phase.

4.2 BASES AND ASSUMPTIONS

For the reference condition, the formation of UF_6 in the feed or tails cylinder was assumed to be uniform and homogeneous in the internal volume of the cylinder. During filling, UF_6 tends to form an annulus on the inner surface of the cylinder as a result of circumferential cooling to desublime (change from gas to solid) UF_6 , and then gradually settles in the bottom portion of the cylinder as a slumped geometry. The slumped geometry is more realistic than the assumed homogenized geometry. The dose calculations for the slumped geometry are useful for comparison with measurements, but are less conservative than for the homogenized geometry.

The UF_6 cylinders were placed horizontally on a concrete pad with localized supporting chocks or stillages, since the cylinders are normally handled and stored horizontally on their sides with the valve oriented at the 12 o'clock position which is at the top of the end flange (see Figure 2-1, §2.2). A concrete pad is typically used for storage of cylinders on supporting chocks or stillages so that the cylinders are at approximately 6 inches above the pad (see Figure 2-1, §2.2) to avoid direct contact with ground soil.

For ease of modeling, both axial ends of the cylinder were assumed to be flat. In actuality, the cylinder ends are physically rounded. The assumption of flat ends poses insignificant modifications to the actual geometry, as the overall axial length of the cylinder is very long (146.75 inches without skirts – see Figure 4-1, §4.4.1).

Modeling of the cylinder neglected the stiffening rings and skirted ends (see Fig. 4-1, §4.4.1). These items are localized parts with little or no effect on the dose rates at the points of interest. The absence of these items simplifies modeling and provides slight conservatism.

The material for the concrete pad was taken to be ordinary concrete. Ordinary concrete is the material of choice for the concrete pad, because of its wide commercial availability. The exact compositions of ordinary concrete vary from source to source and from batch to batch. For this study, the standard compositions from ANSI/ANS-6.4-1997 [ANS 1997, Table 5-1] were used.

Both ground soil and environmental air were assumed to be dry. The dry condition lacks moisture and represents a conservative assumption for dose calculations (in particular for neutrons), as moisture (containing hydrogen) can thermalize neutrons with a subsequent softer energy spectrum and lower dose results.

4.3 EVALUATION METHODOLOGY

This evaluation involved the calculations of radiation dose rates for UF_6 contained in a certified cylinder meeting the ANSI N14.1-2001 standard [ANSI 2001], including both neutron and photon dose rates. The calculations used the UF_6 source terms generated with the ORIGEN-S module in the SCALE code package as described in Chapter 3 for filled tails, filled feed and empty feed cylinders.

The dose calculations were performed with the MCNP code (MCNP5, v1.60) for neutron and photon transport [LANL 2008 and LANL 2010]. MCNP is a general-purpose Monte Carlo N-Particle code developed by Los Alamos National Laboratory (LANL) that can be used for neutron, photon, electron, or coupled neutron/photon/electron transport, including the capability to calculate eigenvalues for critical or subcritical systems. The code treats an arbitrary three-dimensional configuration of materials in geometric cells bounded by first- and second-degree surfaces and fourth-degree elliptical tori. The code provides the necessary processed cross section data libraries for radiation transport problems.

Several versions of MCNP exist. The latest production version is MCNP6.1 distributed by RSICC at ORNL [RSICC 2013]. The code package for MCNP6.1 also contains its preceding version, MCNP5, v1.60. For this evaluation, MCNP5, v1.60 was retained to calculate neutron, primary photon and secondary photon dose rates, as this version produced practically the same results as MCNP6.1 but ran modestly faster than MCNP6.1. The nuclear data associated with MCNP5, v1.60 are based mainly on the ENDF/B-VII.0 library. The MCNP software used was: (a) appropriate for this fixed source calculations, and (b) applied only within the range of validation as documented in the MCNP manual [LANL 2008]. This manual is essentially a user guide, and contains the necessary instructions for preparation of inputs and execution of the code.

A number of convenient variance reduction techniques are available in MCNP for improving statistics and computational efficiency. The techniques used for this evaluation included: cell importance and source energy biasing. Because of the simplicity of the geometric model for a single cylinder, the Monte Carlo simulations were fairly

straightforward without the need for more advanced variance reduction schemes to achieve satisfactory statistics within reasonable computer times.

4.4 TECHNICAL INPUTS

This section describes the technical inputs used for the single cylinder dose evaluation. The required inputs for the MCNP dose calculations include physical data such as geometric dimensions and material data (densities and compositions), neutron and photon source terms, flux-to-dose rate conversion factors, and nuclear cross section data. The reference sources for these inputs are appropriately cited.

4.4.1 Model 48Y Cylinder Physical Parameters

A physical configuration of the 48Y cylinder is illustrated in Figure 4-1. Table 4-1 lists the pertinent physical parameters including the dimensions, capacity, and materials used.

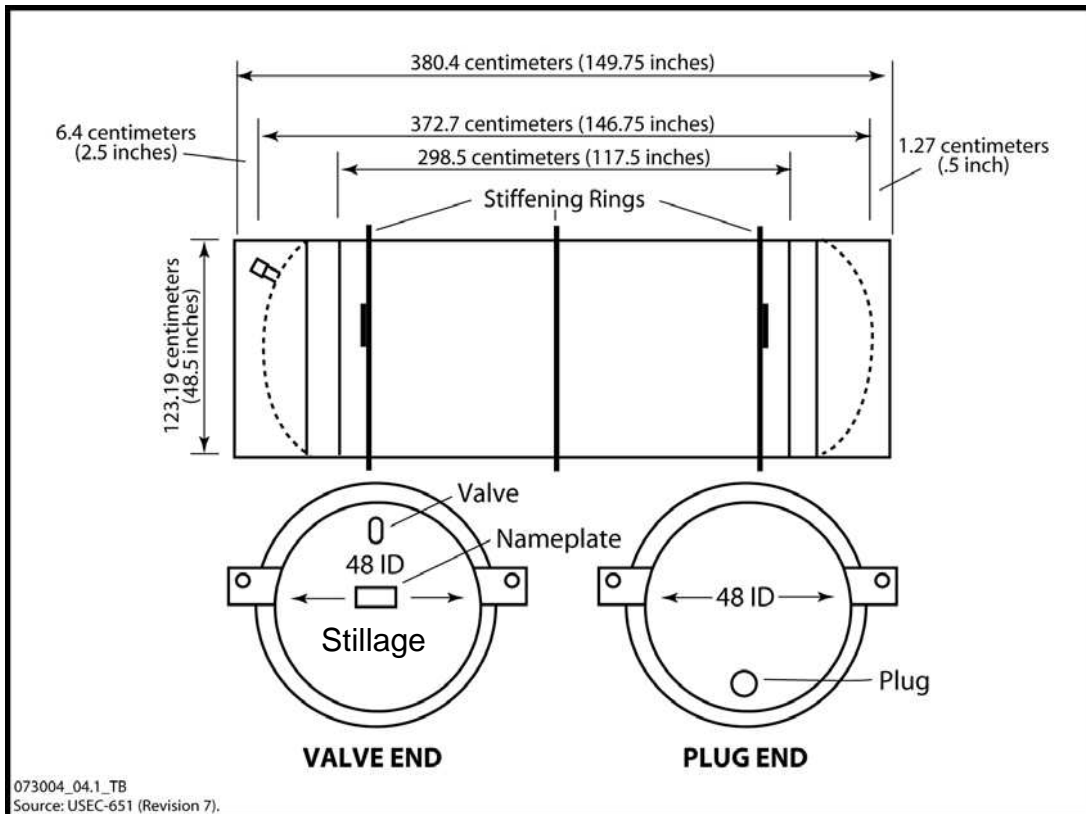


Figure 4-1 Schematic of a Model 48Y Cylinder

Table 4-1 Model 48Y Cylinder Parameters

Description	Value	Units	Reference
48Y cylinder ID	48	Inches	ANSI 2001, Fig. 9
48Y cylinder outside length	146.75	Inches	ANSI 2001, Fig. 9
48Y shell thickness	0.625	Inches	ANSI 2001, Fig. 9
Maximum UF ₆ fill limit	27560 (12501)	Pounds (kg)	ANSI 2001, Table 1
Minimum internal volume	142.7	ft ³	ANSI 2001, Table 1
Shell construction material	A516 Steel	N/A	ANSI 2001, §6.12.5
Height above pad or ground	6	Inches	Cameco 2009, §3.1

4.4.2 Material Densities and Compositions

The physical model contains the following five materials:

- Source material inside the cylinder UF₆
- Cylinder shell construction material A516 carbon steel
- Storage pad Ordinary concrete
- Ground Bulk soil
- Environment Dry air

Table 4-2 contains the material data used as input into the dose rate calculations, including the appropriate references cited. The material compositions used here for concrete, soil and air are reasonably consistent with those cited in *Engineering Compendium on Radiation Shielding* [Jaeger 1975]

It should be recognized that slight variations in the material compositions are conceivable with different references. The differences are typically within the numerical round-off. Shielding calculations are insensitive to these minor differences in the material compositions, which produce insignificant effect on the results relative to the typical calculational uncertainty.

Table 4-2 Material Densities and Compositions

Material	Density (g/cm ³)	Wt. % Range or as Noted	Wt. % Used or as Noted	Reference
UF ₆	5.1 (solid)	N/A	Composition input by atom as follows: F: 6 U:1	USEC 1995, Table 5
A516 Carbon Steel	7.85	C: 0.26(max) Mn: 0.60 – 1.20 P: 0.035(max) S: 0.04(max) Si: 0.15 – 0.40 Fe: balance	Fe: 100	ASM International 1990, Table 6
Concrete (cured)	2.35	H: 0.55(typical) O: 49.83(typical) Si: 31.57(typical) Ca: 8.26(typical) Na: 1.70(typical) Mg: 0.26(typical) Al: 4.55(typical) S: 0.13(typical) K: 1.91(typical) Fe: 1.23(typical)	H: 0.55 O: 49.83 Si: 31.57 Ca: 8.26 Na: 1.70 Mg: 0.26 Al: 4.55 S: 0.13 K: 1.91 Fe: 1.23	ANSI/ANS-6.4-1997, Table 5-1 [ANS 1997]
Bulk Soil	1.6	O: 44 - 49 Si: 22 - 36 Ca: 1 - 7 Na: 2.4 – 2.5 Mg: 0.1 - 3 Al: 6 - 10 K: 1.5 - 3 Fe: 2 - 10	O: 46.5 Si: 29 Ca: 4 Na: 2.45 Mg: 1.55 Al: 8.0 K: 2.25 Fe: 6.0	Engineering ToolBox 2013
Dry Air	0.0012*	N ₂ : 78.084 O ₂ : 20.946 CO ₂ : 0.033 Ar: 0.934 note: these values are <i>volume %</i> directly from the reference	N: 75.521 O: 23.177 C: 0.014 Ar: 1.288 note: these values are <i>wt.%</i> converted from <i>volume %</i>	Weast 1985, pp. F-10, F-156

*Air density rounded from 0.001204 to 0.0012 g/cm³.

4.4.3 Neutron and Photon Source Strengths and Energy Spectra

The dose rate calculations required the radiation source input including the source strengths and energy spectra for both neutron and photon sources associated with UF₆. The required sources for use in the single cylinder dose evaluation were for a filled tails cylinder, a filled feed cylinder, and an empty feed cylinder. The filled tails and feed cylinders contain both neutron and photon sources, while only the photon source is present in the empty feed cylinder. Chapter 3 describes the generation of the source terms used in this evaluation.

The neutron source strength and associated energy spectrum for the filled tails and feed cylinders include the contributions from both spontaneous fission and (α, n) reactions. The neutron source data used in this evaluation are provided in Table 3-7 (§3.8) for the filled tails cylinder as a function of U-235 concentration, and for the filled feed cylinder. The full neutron energy spectrum was modified to a partial spectrum of importance to the dose

calculations, as subsequently described in Section 4.5.2. This modification improved the computational efficiency by ignoring the non-contributing groups.

Table 3-8 in Section 3.8 lists the photon source strengths and associated energy spectra for the filled tails and feed cylinders, based on the bremsstrahlung radiation yield for the actual UF₆ matrix. As for the neutron source, the full photon energy spectrum was modified to a partial spectrum of importance to the dose calculations, as subsequently described in Section 4.5.3. The modification was more significant for photons as it eliminated a large number of non-contributing weak photons at low energies.

For the empty feed cylinder, Table 3-10 in Section 3.10 provides the time-dependent photon source data following emptying. The empty feed cylinder contains residual radioactivity from the daughter products of the uranium isotopes after separation of progeny from uranium in the enrichment process system.

4.4.4 Neutron and Gamma-Ray Dose Conversion Factors

The calculated neutron and photon fluxes in units of particles/cm²-s need to be converted to dose rates in mrem/h, using the appropriate dose conversion factors. There are two sets of dose conversion factors available from the ANSI/ANS standards, including the ANSI/ANS-6.1.1-1977 [ANS 1977] and ANSI/ANS-6.1.1-1991 [ANS 1991] standards. The differences between these standards are discussed herein.

The ANSI/ANS-6.1.1-1977 standard is typically used for regulatory compliance with 10 CFR 20 [NRCd]. It provides the conversion factors for ambient dose equivalent, which is an operational quantity to be measured by radiation survey instruments. This standard considers the quality factors for biological effects, but excludes the relevant stochastic risk weighting factors for the various organs or tissues. Therefore this standard is more

conservative (producing higher doses) than the corresponding newer ANSI/ANS-6.1.1-1991 standard. The resulting doses from this standard relate closely to the response of radiation monitors (measured doses). Table C-1 in Appendix C lists the neutron and photon dose conversion factors as converted to the units of interest from ANSI/ANS-6.1.1-1977. For neutrons, the conversion factors are consistent with the recommendations in NCRP-38 [NCRP 1971].

The ANSI/ANS-6.1.1-1991 standard is different from the ANSI/ANS-6.1.1-1977 standard in that the 1991 standard is for the purpose of determining effective dose equivalent, taking into account the biologically relevant quantity generally consistent with ICRP 51 [ICRP 1987]. This standard provides the dose conversion factors in units of 10^{-12} Sv-cm², which can be easily converted to mrem/h per particles/cm²-sec with a multiplier of $(10^{-12}) \times (10^5 \text{ mrem/Sv}) \times (3600 \text{ s/h}) = 3.6 \times 10^{-4} \text{ mrem-s/Sv-h}$. The conversion factors given in Table C-2 in Appendix C include this multiplier for each energy group. Since the hypothetical phantom orientation is unknown, the most conservative dose factors in anterior-posterior (AP) exposure mode are used as provided in Table C-2. The resulting effective dose equivalent based on ANSI/ANS-6.1.1-1991 is less than the corresponding ambient dose equivalent based on ANSI/ANS-6.1.1-1977 (see further subsequent discussion in Sections 4.7.3.5 for neutrons and 4.7.4.5 for photons).

Other sets of dose conversion factors such as ICRP-21 [ICRP 1971] and ICRP-74 [ICRP 1997] exist for different applications. As quoted from the MCNP report [LANL 2008, Appendix H], “Although the various conversion factor sets differ from one another, it seems to be the consensus of the health physics community that they do not differ significantly from most health physics applications where accuracies of 20% are generally acceptable. Some of

the differences in the various sets are attributable to different assumptions about source directionality, phantom geometry, and depth of penetration. The neutron quality factors, derived primarily from animal experiments, are also somewhat different.” Moreover, the conversion factor sets are subject to change based on the actions by authoritative entities.

4.4.5 Nuclear Cross Section Data

This evaluation deals with five materials – UF₆, A516 carbon steel, environmental air, ordinary concrete, and ground bulk soil identified as materials 1, 2, 3, 4, and 5 respectively. They are specified on the Mn card in the MCNP input, where n is the material number. For example, m1 is the UF₆ source material. The material property can be entered on the cell card in terms of atom density (atoms/b-cm) or physical density (g/cm³). In this evaluation, the physical density was used for each material and entered in g/cm³ with a preceding negative sign as required by the code.

The Mn card also specifies the isotopic composition of the materials in the cells, which in turn, determines the cross-section data sets to be used for the problem. For each constituent in the material, (ZAID, fraction) is entered as a pair. ZAID identifies the nuclear data library, and fraction is the atomic fraction (or weight fraction if negative). In this evaluation, all of the neutron cross sections were taken from the library ended with .70c for continuous-energy neutron interaction data based on ENDF/B-VII.0 at 293.6 K. Fractions can be un-normalized or normalized, provided the relative fractions are correct. This temperature is appropriate to use, as it corresponds closely to an ambient condition.

In photon (MODE P) problems, one photoatomic interaction table is required for each element as the photoatomic data is atomic in nature. The photoatomic data need to be identified by element only. For example, ZAID entries of 92235 and 92238 are treated as

92000. The absence of the library identifier extension in ZAID implies that MCPLIB04 photon library based on ENDF/B-VI, Release 8 (latest photon data library in MCNP5, v1.60) is used for photon transport.

In coupled neutron-photon problems (MODE N P), specifying a particular isotope on a material card will invoke the neutron set for that isotope and the corresponding photon set for that element. For example, an entry of “92235.70c” on a material card will cause MCNP to use ZAID=92235.70c (U-235) for neutron data and 92000.04p (uranium element) for photon data. An entry of “92235” without an extension (library identifier) will still use ZAID=92235.70c for neutron data and 92000.04p for photon data, as the first match found in the MCNP cross section directory file *xmdir* is used. However, it is usually preferable to include the library identifier extension in ZAID for proper identification and future reference.

4.5 EVALUATION DETAILS

This section provides the calculation details including the necessary calculations for obtaining the inputs into MCNP such as UF₆ material densities, and partial energy spectra of importance. In addition, the physical models and dose-rate calculation details are described.

4.5.1 UF₆ Material Density Calculation

For the filled tails and feed cylinders, this evaluation considered two distinct cases of the source geometry, namely, homogenized and slumped geometry. The UF₆ source material densities are different for these geometry types as calculated below:

Homogenized Geometry

Cylinder inner radius = 24 in. = 60.96 cm (Table 4-1, half of ID)

Cylinder inside length = 145.55 in. = 369.57 cm (Table 4-1 less wall thickness)

Cylinder internal volume = $\pi \cdot (60.96)^2 \cdot 372.75 \text{ cm}^3 = 4.3146 \times 10^6 \text{ cm}^3$

Cylinder fill limit = 12,501 kg = 1.2501×10^7 g (Table 4-1)

Homogenized UF₆ density = $(1.2501 \times 10^7 \text{ g}) / (4.3146 \times 10^6 \text{ cm}^3) = 2.897 \text{ g/cm}^3$

Slumped Geometry

Certified minimum volume = $142.7 \text{ ft}^3 = 4.0408 \times 10^6 \text{ cm}^3$ (Table 4-1)

Solid density = 5.1 g/cm^3 (Table 4-2)

Maximum possible fill = $(5.1 \text{ g/cm}^3) * (4.0408 \times 10^6 \text{ cm}^3) = 2.0608 \times 10^7 \text{ g} = 20,608 \text{ kg}$

Fill volume fraction = $(12,501 \text{ kg}) / (20,608 \text{ kg}) = 0.6066$

Arc height for 60.66% fill volume = 71.215 cm (from automated calculator)

UF₆ density = $(2.897 \text{ g/cm}^3) / (0.6066) = 4.776 \text{ g/cm}^3$

4.5.2 Neutron Source Energy Spectrum of Importance

The neutron source term presented in Table 3-7 in Section 3.8 is for the full 27 energy group structure. For radiation dose calculations, it is time-consuming and unnecessary to include the non-contributing energy groups. The dose contributors arise predominantly from high-energy neutrons. Consideration of neutron energies greater than 0.015 MeV (group 20 and higher) is sufficient for dose calculations. These groups already represent 99.96% of the total neutron source strength. The remaining groups amounting to merely 0.04% are inconsequential to the resulting neutron dose, owing to lower energies with smaller dose conversion factors.

Based on the neutron source data in Table 3-7, Table 4-3 lists the partial neutron energy spectrum for a filled 48Y feed cylinder used in the MCNP calculation, along with the full spectrum for reference. Consideration of neutron energies greater than 0.015 MeV is also acceptable for filled tails cylinders.

Table 4-3 Full and Partial Neutron Energy Spectra for Filled 48Y Feed Cylinder

Group	Neutron Energy (MeV)	Full Energy Spectrum		Partial Energy Spectrum	
		Source Intensity (n/s per cylinder)	Normalized Fraction	Source Intensity (n/s per cylinder)	Normalized Fraction
1	1.00E-11 - 1.00E-08	1.086E-12	2.182E-18		
2	1.00E-08 - 3.00E-08	3.074E-12	6.175E-18		
3	3.00E-08 - 5.00E-08	2.166E-07	4.351E-13		
4	5.00E-08 - 1.00E-07	9.144E-07	1.837E-12		
5	1.00E-07 - 2.25E-07	3.758E-06	7.549E-12		
6	2.25E-07 - 3.25E-07	5.802E-06	1.166E-11		
7	3.25E-07 - 4.14E-07	2.555E-06	5.133E-12		
8	4.14E-07 - 8.00E-07	2.400E-05	4.821E-11		
9	8.00E-07 - 1.00E-06	1.833E-05	3.682E-11		
10	1.00E-06 - 1.13E-06	7.439E-06	1.494E-11		
11	1.13E-06 - 1.30E-06	1.559E-05	3.132E-11		
12	1.30E-06 - 1.86E-06	6.074E-05	1.220E-10		
13	1.86E-06 - 3.06E-06	2.293E-04	4.606E-10		
14	3.06E-06 - 1.07E-05	2.180E-03	4.379E-09		
15	1.07E-05 - 2.90E-05	1.430E-02	2.873E-08		
16	2.90E-05 - 1.01E-04	9.541E-02	1.917E-07		
17	1.01E-04 - 5.83E-04	1.451E+00	2.915E-06		
18	5.83E-04 - 3.04E-03	1.603E+01	3.220E-05		
19	3.04E-03 - 1.50E-02	1.644E+02	3.303E-04		
20	1.50E-02 - 1.11E-01	3.905E+03	7.845E-03	3.905E+03	7.848E-03
21	1.11E-01 - 4.08E-01	3.869E+04	7.772E-02	3.869E+04	7.775E-02
22	4.08E-01 - 9.07E-01	1.523E+05	3.059E-01	1.523E+05	3.061E-01
23	9.07E-01 - 1.42E+00	1.620E+05	3.254E-01	1.620E+05	3.256E-01
24	1.42E+00 - 1.83E+00	7.314E+04	1.469E-01	7.314E+04	1.470E-01
25	1.83E+00 - 3.01E+00	5.174E+04	1.039E-01	5.174E+04	1.040E-01
26	3.01E+00 - 6.38E+00	1.524E+04	3.061E-02	1.524E+04	3.063E-02
27	6.38E+00 - 2.00E+01	5.789E+02	1.163E-03	5.789E+02	1.163E-03
Total	1.00E-11 - 2.00E+01	4.978E+05	1.000E+00	4.976E+05	1.000E+00

4.5.3 Photon Source Energy Spectrum of Importance

The photon source term presented in Table 3-8 in Section 3.8 is for the full 19 energy group structure. As for neutron dose calculations, it is time-consuming and unnecessary to include the non-contributing energy groups. The photon dose contributors arise predominantly from the energy groups between 0.045 and 2.0 MeV (groups 2 through 11)

(see validation in Section 4.7.4.4). These important groups represent only 48.5% of the total photon source strength. However, the remaining groups amounting to 51.5% contribute insignificantly to the resulting photon dose, as photons of lower energies (<0.045 MeV) are too weak to be penetrating and photons of higher energies (>2.0 MeV) are too low in intensity to significantly contribute.

Based on the photon source data in Table 3-8, Table 4-4 lists the partial photon energy spectrum for a filled 48Y feed cylinder used in the MCNP calculation, along with the full spectrum for reference. Again, consideration of these important photon energy groups is also applicable to filled tails cylinders.

Table 4-4 Full and Partial Photon Energy Spectra for 48Y Feed Cylinder

Group	Photon Energy (MeV)	Full Energy Spectrum		Partial Energy Spectrum	
		Source Intensity (p/s per cylinder)	Normalized Fraction	Source Intensity (p/s per cylinder)	Normalized Fraction
1	1.00E-02 - 4.50E-02	4.408E+10	5.148E-01		
2	4.50E-02 - 1.00E-01	2.174E+10	2.539E-01	2.174E+10	5.233E-01
3	1.00E-01 - 2.00E-01	1.161E+10	1.356E-01	1.161E+10	2.794E-01
4	2.00E-01 - 3.00E-01	2.635E+09	3.077E-02	2.635E+09	6.342E-02
5	3.00E-01 - 4.00E-01	1.685E+09	1.968E-02	1.685E+09	4.056E-02
6	4.00E-01 - 6.00E-01	1.157E+09	1.351E-02	1.157E+09	2.785E-02
7	6.00E-01 - 8.00E-01	1.141E+09	1.332E-02	1.141E+09	2.746E-02
8	8.00E-01 - 1.00E+00	8.808E+08	1.029E-02	8.808E+08	2.120E-02
9	1.00E+00 - 1.33E+00	5.262E+08	6.145E-03	5.262E+08	1.266E-02
10	1.33E+00 - 1.66E+00	7.831E+07	9.145E-04	7.831E+07	1.885E-03
11	1.66E+00 - 2.00E+00	9.451E+07	1.104E-03	9.451E+07	2.275E-03
12	2.00E+00 - 2.50E+00	1.579E+05	1.844E-06		
13	2.50E+00 - 3.00E+00	1.816E+04	2.121E-07		
14	3.00E+00 - 4.00E+00	1.631E+04	1.905E-07		
15	4.00E+00 - 5.00E+00	5.507E+03	6.431E-08		
16	5.00E+00 - 6.50E+00	2.209E+03	2.580E-08		
17	6.50E+00 - 8.00E+00	4.333E+02	5.060E-09		
18	8.00E+00 - 1.00E+01	9.488E+01	1.108E-09		
19	1.00E+01 - 2.00E+01	1.744E+00	2.037E-11		
Total	1.00E-02 - 2.00E+01	8.563E+10	1.000E+00	4.155E+10	1.000E+00

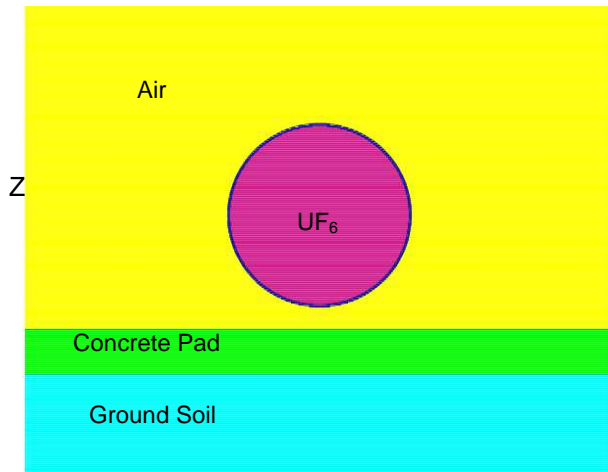
4.6 MCNP CALCULATIONS

The UF_6 radiation dose rates from a single feed cylinder were determined with MCNP5, version 1.60. The calculations produced the results of radial and axial dose rate profiles as a function of distance from the outer surface of the cylinder. This section covers the physical models considered and dose rate calculation details.

4.6.1 Physical Models

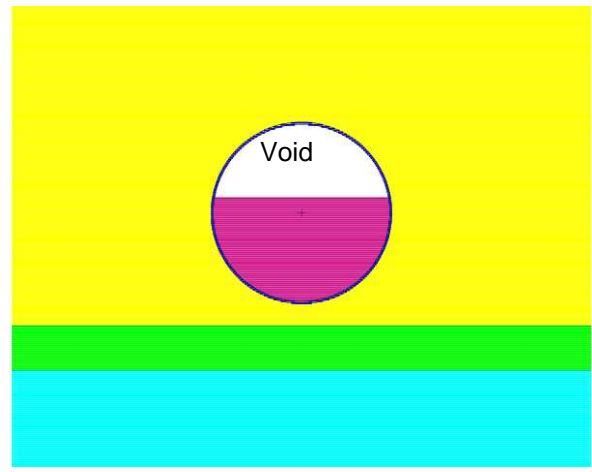
Homogenized and slumped source geometries were used. Figure 4-2 depicts the geometry models of the homogenized source geometry used for the MCNP calculation in the Y-Z and X-Z planes, respectively. Figure 4-3 displays the corresponding models of the slumped source geometry. The models include the physical dimensions and material densities for use as input into MCNP. The differences between the two geometry types are in the spatial source distribution and UF_6 density as indicated.

For consistency with the Cameco calculation [Cameco 2009, §3.1], the dose points were located at contact (0.02 m) and at 1, 5, 10, 20, 50 and 100 m from the outer surface of the cylinder. Additional points at 0.305 m (1 ft), 2 m and 200 m were included for use in comparison with other calculations or measurements. The points for the radial dose rate profile were placed at the mid-height of the cylinder, while those for the axial dose rate profile were located along the cylinder centerline.



Y Axis
(Y-Z Plane)

Homogenized Geometry



Y Axis
(Y-Z Plane)

Slumped Geometry



X Axis
(X-Z Plane)

Figure 4-2 Homogenized Source Geometry



X Axis
(X-Z Plane)

Figure 4-3 Slumped Source Geometry

Physical Dimensions

Cylinder ID = 48 in. = 121.92 cm
 Cylinder shell thickness = $\frac{5}{8}$ in. = 1.5875 cm
 Cylinder inner length = 145.5 in. = 369.57 cm
 Concrete pad thickness = 12 in. = 30.48 cm
 Cylinder height above pad = 6 in. = 15.24 cm

Material Densities

UF_6 (homogenized) = 2.897 g/cm³
 UF_6 (slumped) = 4.775 g/cm³
 Air = 0.0012 g/cm³
 Ordinary concrete = 2.35 g/cm³
 Bulk soil = 1.6 g/cm³
 Void = 0.0 g/cm³

4.6.2 Dose Rate Calculations

The neutron and photon dose rates were separately calculated with the MCNP code, using the ANSI/ANS-6.1.1-1977 dose conversion factors to obtain the reference results. The calculations included a case study on the effect of the ANSI/ANS-6.1.1-1991 dose conversion factors.

For filled tails and feed cylinders, the calculations were first performed to determine the effect of the U-235 concentration (wt %) on the average contact dose rates on the inner and outer surfaces of the cylinder. The calculations used the one-year in-growth time for the maximum source terms, and were carried out on a group-by-group basis. For each energy group, the dose calculation with MCNP5, v1.60 determined an energy response factor in units of mrem/h per n/s or p/s of the source for this group. These MCNP calculations were simple and identical to other single cylinder calculations with the exception of a single energy group used with a unit source to obtain the energy response factor. The MCNP input and output files for these runs are listed in Table E-1 in Appendix E. The energy response factors for the groups of importance were then used to calculate the dose rate with the Excel spreadsheet for each source of concern. In so doing, only a set of energy response factors was necessary for dose calculations from any source with the same energy group structure.

The above calculations provided the results for selection of the filled cylinder type for the single cylinder dose evaluation to study the effects of the parameters of interest. Based on these results, the bounding filled feed cylinder was chosen for the dose evaluation (see discussion in Section 4.7.1). The results also served to devise a source energy biasing scheme to increase the importance of more contributing energy groups for use in the subsequent dose calculations to improve computational efficiency.

The time-dependent dose rates were also calculated for a single filled feed cylinder and a single empty feed cylinder to compare the change in the average surface dose rate with time between these cylinder types. The calculations were accomplished in the same manner as for the average contact dose rate versus U-235 concentration (wt %), using the appropriate energy response factors developed from the MCNP5, v1.60 run for each important energy group. For the empty cylinder, the interior of the cylinder could be treated as air or void with no appreciable difference in the dose results. The time-dependent dose results would be useful in effective management of empty cylinders on the outdoor storage pad.

For the selected filled feed cylinder, the reference calculations covered the radial and axial dose rates for both homogenized and slumped source geometry at the points of interest (at contact, 0.305, 1, 2, 5, 10, 20, 50, 100 and 200 m). The F5 tallies (for point detectors) were used to score the fluxes, which were then modified internally in MCNP by the dose response function to produce the dose rates.

In addition, the homogenized geometry was treated as a base case for evaluation of the various effects including concrete pad scattering, ground soil scattering, adequacy of the partial photon energy spectrum, and secondary photon contributions due to neutron reactions. For this evaluation, the calculations considered the radial dose rates only for the sake of saving computer run times, as similar effects are expected in the axial direction.

For an empty filled cylinder, the reference calculations covered the radial and axial dose rates for the homogenized source geometry only. As for the filled cylinder, the detector points were located at contact, 0.305, 1, 2, 5, 10, 20, 50, 100 and 200 m from the side or end surface of the cylinder. The dose rate profiles for the empty feed cylinder corresponded to

the time immediately after emptying (separation of progeny from natural uranium) for comparison with those for the filled feed cylinder.

The MCNP calculations for the selected filled feed cylinder consisted of a total of 6 cases for neutrons and a total of 6 cases for photons. The computer input and output files for each case are listed in Table D-1 in Appendix D, along with the case description and Central Processing Unit (CPU) time for each case. Appendix D also lists the sample input files for the neutron and photon cases. Only one MCNP run was made for the empty feed cylinder. Its associated input and output files are included in Table D-1 in Appendix D with listing of the input file.

4.7 EVALUATION RESULTS

This section presents the results of the single cylinder dose evaluation including the following items of interest:

- Energy response factors for filled and empty cylinders
- Average radial surface dose rate as a function of U-235 assay from 0.2 to 0.711%
- Average surface dose rate as a function of time from 0 to 2 years
- Neutron dose rate results for a single filled feed cylinder
- Photon dose rate results for a single filled feed cylinder
- Photon-to-neutron dose ratios for a single filled feed cylinder
- Radial and axial photon dose rate profiles for a single empty feed cylinder

4.7.1 Energy Response Factors

Table E-1 in Appendix E provides the neutron and photon energy response factors for a filled cylinder in units of mrem/h per n/s or p/s for the important energy groups. The

photon energy response factors for an empty feed cylinder are presented in Table E-2. Note that the empty feed cylinder contains no neutron source because of the absence of UF_6 .

The energy response factors were obtained from the MCNP output files for the reference case with the homogeneous source geometry, concrete pad, ground scattering and ANSI/ANS-6.1.1-1977 dose conversion factors. The MCNP calculations produced two sets of the energy response factors for the inside and outside surfaces of the cylinder, respectively.

The factors in Tables E-1 and E-2 became the required inputs into the Excel spreadsheet for calculations of the average surface dose rates presented in Sections 4.7.2 and 4.7.3. The dose contribution from each group is simply the product of the energy response factor and the corresponding source intensity.

4.7.2 Average Radial Contact Dose Rate versus U-235 Concentration

Using the energy response factors in Table E-1 for the filled cylinder together with the source data in Tables 3-7 for neutrons and 3-8 for photons in Chapter 3, Table 4-5 provides the resulting average radial contact dose rates on the inside and outside surfaces of the cylinder as a function of U-235 wt% in uranium (N for neutrons, P for photons and T for total). Figure 4-4 plots the corresponding results.

As expected, the neutron dose rate for the filled cylinder increases with the U-235 concentration but represents a small fraction of the total dose rate. The photon dose rate remains fairly constant with the U-235 concentration. The increase in the total dose rate from 0.2% to 0.711% U-235 is minor. The use of a filled feed cylinder would be conservative and bounding for all tails cylinders in the dose evaluation.

Another observation of the results is that the carbon steel shell of the cylinder attenuates photons more significantly than neutrons. The dose reduction factors from the inside surface to the outside surface are about 1.7 for neutrons, and 3.2 to 3.5 for photons.

Table 4-5 Average Radial Surface Dose Rates for Filled Cylinder versus U-235 Concentration

U-235 (wt %)	Dose Rate (mrem/h)					
	Inside - N	Inside - P	Inside - T	Outside - N	Outside - P	Outside - T
0.2	0.195	4.961	5.156	0.116	1.533	1.649
0.3	0.222	4.965	5.187	0.132	1.532	1.664
0.4	0.250	4.968	5.218	0.148	1.531	1.679
0.5	0.279	4.971	5.250	0.165	1.530	1.695
0.711	0.340	4.977	5.317	0.202	1.537	1.739

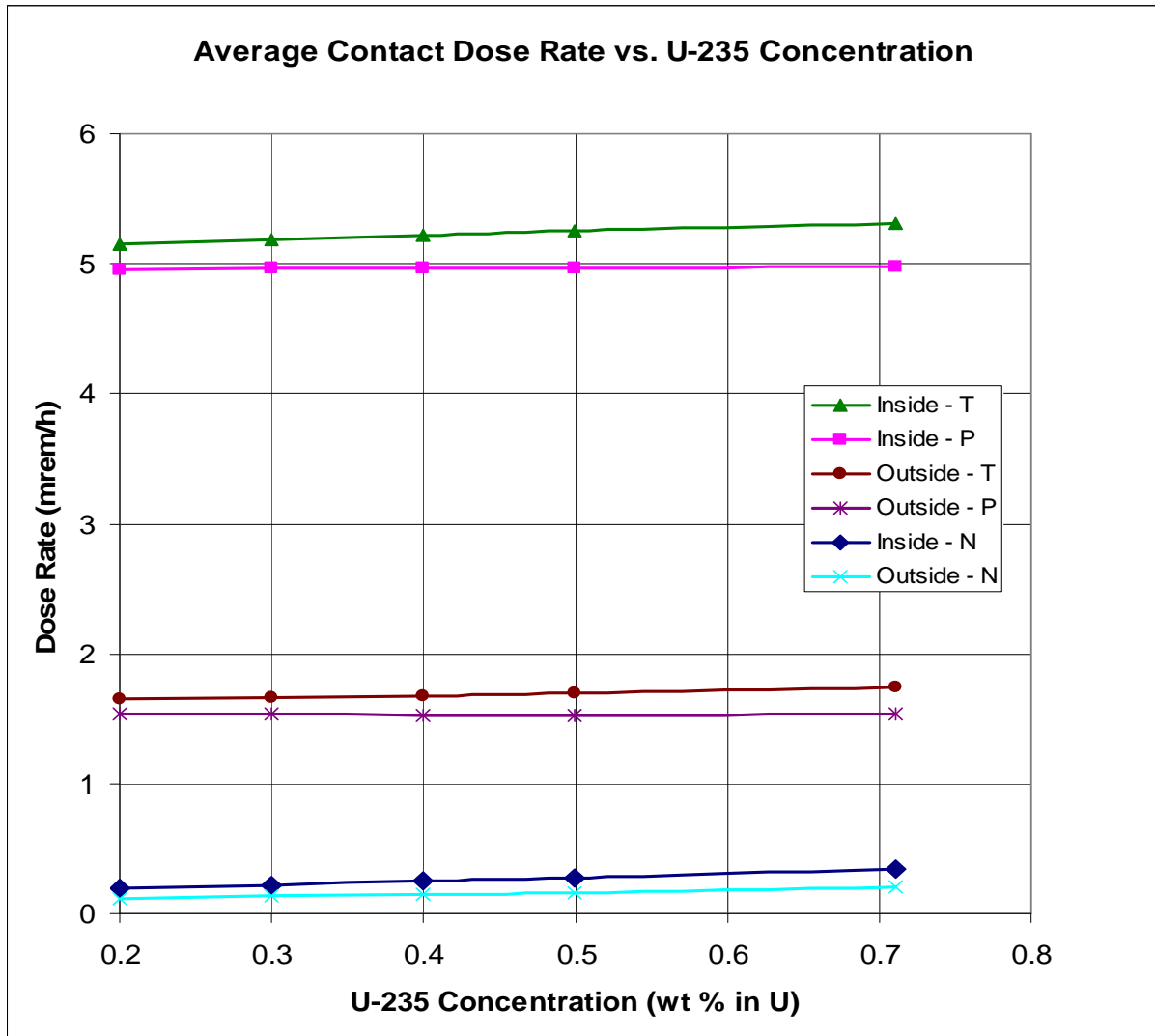


Figure 4-4 Average Radial Surface Dose Rates for Filled Cylinder versus U-235 Concentration

4.7.2 Average Radial Contact Photon Dose Rate versus Time

Using the photon energy response factors in Table E-1 for the filled cylinder and Table E-2 for the empty cylinder together with the photon source data in Tables 3-9 and 3-10 in Chapter 3, Table 4-6 provides the resulting average radial contact dose rate on the outside surface of the filled feed cylinder as a function of time after filling (N for neutrons, P for photons and T for total). Table 4-6 includes the same results for the empty feed cylinder on both inside and outside surfaces after emptying. Figure 4-5 plots the corresponding results.

For the filled feed cylinder, the photon dose rate increases with time after filling as a result of the buildup of the daughter products from uranium decay. On the other hand, the photon dose rate decreases with time after emptying, owing to the decay of the daughter products following separation from uranium.

As observed from Table 4-6, the freshly emptied feed cylinder (at $t = 0$) has a much higher dose rate than the filled feed cylinder because of the absence of UF_6 which self shields. However, the emptied cylinder dose rate decreases rapidly with time. After three months from emptying (called cooling period), the dose rate from an empty feed cylinder is comparable to that from a filled feed cylinder. Effective management of UF_6 cylinder storage must take the dose impact of the empty cylinders into account.

Table 4-6 Time-dependent Average Contact Dose Rates for Filled and Empty Feed Cylinders

<u>Time (y)</u>	<u>Contact Dose Rate (mrem/h)</u>				
	<u>Filled - Outside - N</u>	<u>Filled - Outside - P</u>	<u>Filled - Outside - T</u>	<u>Empty - Inside - P</u>	<u>Empty - Outside - P</u>
0.0	0.202	0.003	0.205	9.862E+01	2.072E+01
0.1	0.202	0.995	1.196	3.375E+01	7.246E+00
0.2	0.202	1.341	1.543	1.180E+01	2.534E+00
0.3	0.202	1.462	1.664	4.128E+00	8.862E-01
0.5	0.202	1.520	1.722	5.051E-01	1.084E-01
0.7	0.202	1.526	1.728	6.194E-02	1.329E-02
1.0	0.202	1.527	1.729	2.850E-03	6.049E-04
2.0	0.202	1.527	1.729	2.746E-04	5.171E-05

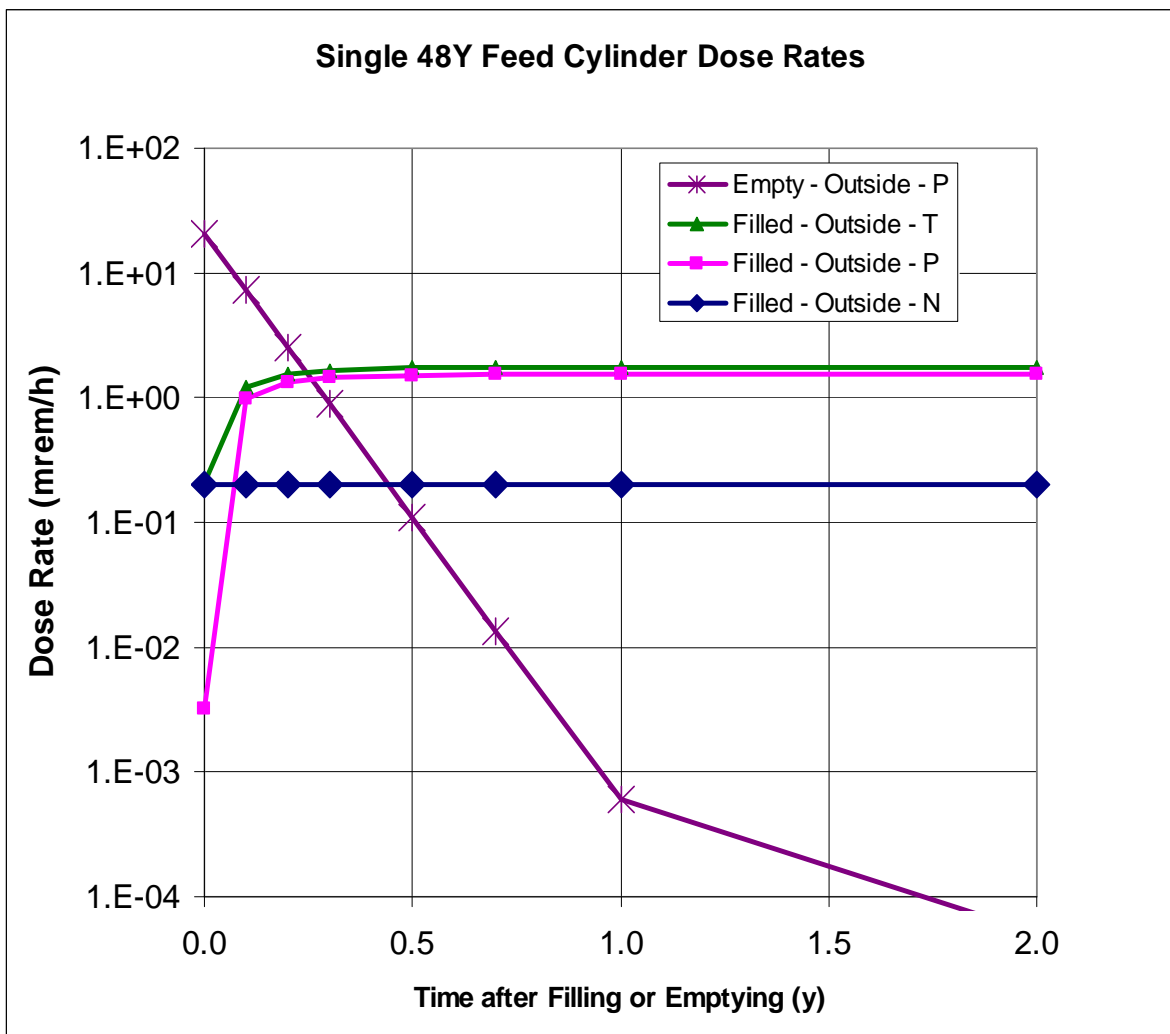


Figure 4-5 Time-dependent Average Contact Dose Rates for Filled and Empty Feed Cylinders

4.7.3 Neutron Results for a Single Filled Feed Cylinder

Based on the results in Section 4.7.1, the conservative and bounding filled feed cylinder was selected for the dose evaluation to determine the pertinent parameters for use in the multiple cylinder dose assessment in Phase 3 (Chapters 5 and 6). This section presents the neutron results for a single filled feed cylinder.

4.7.3.1 Radial and Axial Neutron Dose Rate Profiles

The results of the radial and axial neutron dose rates are presented in Table E-3 in Appendix E based on the ANS/ANSI-6.1.1-1977 dose conversion factors. The associated statistical relative errors are indicated in parentheses. The results include the cases for the homogenized and slumped geometry with concrete pad and ground scattering.

The relative statistical error (fractional standard deviation) associated with each calculated dose rate is less than the acceptance criterion of 0.05 as specified in the MCNP manual [LANL 2008, Table 2.5] except at the axial point of 200 m. Additional run time with more particle histories is deemed necessary at this particular point to achieve statistically satisfactory results.

The homogenized geometry produces higher dose rates than the slumped geometry, thus validating the conservatism stated in Section 4.2. However, the results for the slumped geometry (a more realistic UF₆ formation) should be used for comparison with measurements. The homogenized geometry may be used for conservative calculations, which are preferable in demonstrating regulatory compliance.

Another observation of interest is that the radial dose rate profile is generally higher than the corresponding axial dose rate profile as expected, because the solid angle subtended by the source is larger radially than axially.

4.7.3.2 Effect of Concrete Pad

The effect of the concrete pad on neutron doses was evaluated by replacing concrete with bulk soil on the MCNP cell card. The evaluation considered the radial dose rates only, as the effect on the axial dose rates was expected to be similar at the same elevation. Further, the conservative homogenized source geometry was used for the evaluation.

Table E-4 in Appendix E lists the neutron dose results with and without the concrete pad for comparison. The neutron dose rates are lower with the concrete pad, and the dose ratio varies with distance. The dose decrease with concrete is attributable to the presence of hydrogen in concrete which softens the energy spectrum, with lower resulting doses.

4.7.3.3 Effect of Ground Scattering

The effect of ground scattering on neutron doses was evaluated by replacing bulk soil with air on the MCNP cell card. The evaluation considered the radial dose rates only, as the effect on the axial dose rates was expected to be similar at the same elevation. Further, the conservative homogenized source geometry was used for the evaluation.

Table E-5 in Appendix E lists the neutron dose results with and without ground scattering for comparison. The ground scattering effect generally increases the doses and varies with distance. Peaking is observed at the close-in distances (<5 m distance), followed by a diminishing effect to a dose ratio of almost 1.0 (no effect) at 50 m. Beyond 50 m, it is conceivable that ground scattering may reduce doses as a result of softening of the energy spectrum at large distances due to attenuation in air and ground soil.

4.7.3.4 Secondary Photon Contributions

Neutron interactions with the materials in the model produce secondary photons, which may or may not contribute to the overall radiation doses. To evaluate this

contribution, the MCNP code was run in a coupled neutron and photon transport mode (MODE N P) to tally the photon dose rates. For this evaluation, the homogenized geometry as used for Case n1 was selected.

Table E-6 in Appendix E lists the neutron and secondary photon dose rate results for comparison. The secondary photon dose is on the order of 1% of the neutron dose. This contribution is practically insignificant relative to uncertainties. Further its contribution to the total dose (neutron plus primary photon) dose would not be appreciable, as the neutron dose component is relatively small. Therefore, the secondary photon contributions can be ignored in future calculations.

4.7.3.5 Effect of ANSI/ANS-6.1.1-1991 Neutron Dose Conversion Factors

The effect of the ANSI/ANS-6.1.1-1991 standard was evaluated by using the neutron dose conversions from this standard for Case n1, which is for the homogenized geometry. Again, the evaluation considered the radial dose rates only.

Table E-7 in Appendix E lists the neutron dose rate results with the ANSI/ANS-6.1.1-1977 and ANSI/ANS-6.1.1-1991 standards. The dose ratio is generally 0.41, meaning that the effective dose equivalent for neutrons from the ANSI/ANS-6.1.1-1991 standard is about 41% of the ambient dose equivalent from the ANSI/ANS-6.1.1-1977 standard. It should be noted that the effective dose equivalent includes biologically relevant quantities such as tissue/organ weighting factors, whereas the ambient dose equivalent corresponds to the response of radiation monitoring.

4.7.4 Photon Results for a Single Filled Feed Cylinder

This section presents the photon results from the evaluation of a single filled feed cylinder, which is a bounding type for the dose assessment.

4.7.4.1 Radial and Axial Photon Dose Rate Profiles

The results of the radial and axial photon dose rates are presented in Table E-8 in Appendix E, based on the ANS/ANSI-6.1.1-1977 photon dose conversion factors. The associated statistical relative errors are indicated in parentheses. The calculated photon dose rates have a relative statistical error of less than 0.05 at all points, meeting the acceptance criterion for point detector tallies as specified in the MCNP manual [LANL 2008, Table 2.5]. The results include the cases for the homogenized and slumped geometry with the concrete pad and ground scattering.

As for the neutron doses, the homogenized geometry produces higher photon dose rates than the slumped geometry, thus again validating the conservatism stated in Section 4.2. The dose ratio of the homogenized geometry to the slumped geometry is greater for photons than for neutrons, because of the large self-shielding factor of UF_6 for photons. Further, like the neutron doses, the radial photon dose rate profile is generally higher than the corresponding axial dose rate profile as expected, because the solid angle subtended by the source is larger radially than axially.

The results for the slumped geometry (more realistic UF_6 formation) should be used for comparison with measurements. The conservative results for the homogenized geometry are preferable for demonstrating regulatory compliance.

4.7.4.2 Effect of Concrete Pad

The effect of the concrete pad on photon doses was evaluated by replacing concrete with bulk soil on the MCNP cell card. The evaluation considered the radial dose rates only, as the effect on the axial dose rates was expected to be similar at the same elevation. Further, the conservative homogenized source geometry was used for the evaluation.

Table E-9 in Appendix E lists the photon dose results with and without the concrete pad for comparison. The photon dose rates are practically the same with and without the concrete pad. These results are not surprising for photons, since both concrete and soil contain mainly silicon and oxygen and there is a sufficient thickness of material used for scattering off concrete or soil.

4.7.4.3 Effect of Ground Scattering

The effect of ground scattering on photon doses was evaluated by replacing bulk soil with air on the MCNP cell card. The evaluation considered the radial dose rates only, as the effect on the axial dose rates was expected to be similar at the same elevation. Further, the conservative homogenized source geometry was used for the evaluation.

Table E-10 in Appendix E lists the photon dose results with and without ground scattering for comparison. The ground scattering effect varies with distance, and generally increases the doses at close-in distances. Peaking is observed at the close-in distances (<10 m distance), followed by a diminishing effect to a dose ratio of less than 1 (negative effect) at 50 m. Beyond 50 m, it is conceivable that ground scattering may reduce doses as a result of softening of the energy spectrum at large distances due to attenuation through the media.

4.7.4.4 Effect of Full Photon Energy Spectrum

To verify the acceptability of using a partial photon energy spectrum of importance as given in Section 4.5.3, a calculation was performed using the full energy spectrum for the case of the homogenized geometry (same as Case p1 except for the energy spectrum). This case required two principal changes to the MCNP input, including the energy spectrum and tally multiplier. The full energy spectrum covers the entire energy range of the 19-group structure from 0.01 to 20.0 MeV. The tally multiplier for each dose point is the associated

total photon source strength of 8.563×10^{10} photons/s per cylinder (see Table 4-4) for all 19 groups versus 4.155×10^{10} photons/s for the partial spectrum (see Table 4-4).

Table E-11 in Appendix E lists the radial photon dose rate results for both partial and full energy spectra for comparison. The dose differences between these two spectra are within statistical uncertainties, implying that the use of the partial energy spectrum of importance is acceptable and appropriate for the photon dose calculations.

4.7.4.5 Effect of ANSI/ANS-6.1.1-1991 Photon Dose Conversion Factors

The effect of the ANSI/ANS-6.1.1-1991 standard was evaluated by using the photon dose conversions from this standard for Case p1, which is for the homogenized geometry. Again, the evaluation considered the radial dose rates only.

Table E-12 in Appendix E lists the photon dose rate results with the ANSI/ANS-6.1.1-1977 and ANSI/ANS-6.1.1-1991 standards. The photon dose ratio is generally 0.85, meaning that the effective dose equivalent for photons from the ANSI/ANS-6.1.1-1991 standard is about 85% of the ambient dose equivalent from the ANSI/ANS-6.1.1-1977 standard. It should be noted that the effective dose equivalent includes biologically relevant quantities such as tissue/organ weighting factors, whereas the ambient dose equivalent corresponds to the response of radiation monitoring.

4.7.5 Photon-to-Neutron Dose Ratio for a Single Filled Feed Cylinder

Using the conservative neutron and photon dose rates for the homogenized geometry in Sections 4.7.4.1 and 4.7.4.2, respectively, the photon-to-neutron dose ratio as a function of distance is plotted in Figure 4-6 for the radial direction and Figure 4-7 for the axial direction.

In general, the photon/neutron dose ratio decreases with distance, except for locations near the cylinder surface where skyshine effects are still insignificant. As the distance

increases, skyshine becomes relatively more important for neutrons than for photons, increasing the relative contribution from neutrons which in turn, decreases the photon/neutron dose ratio.

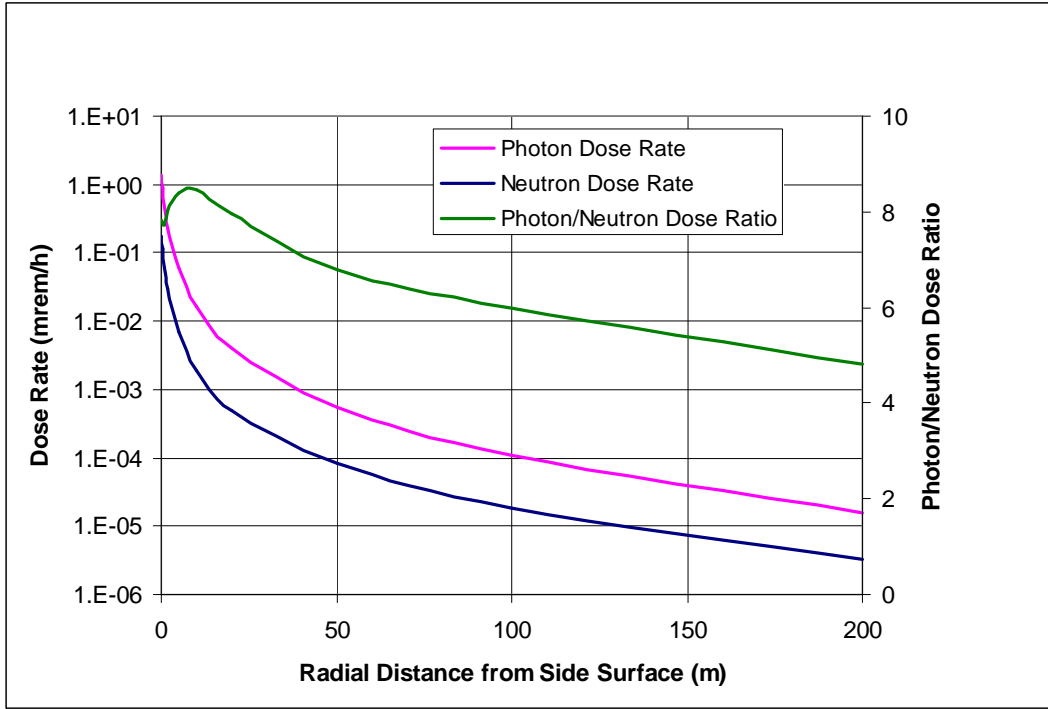


Figure 4-6 Radial Dose Rate Profile and Photon/Neutron Dose Ratio (Homogenized Geometry)

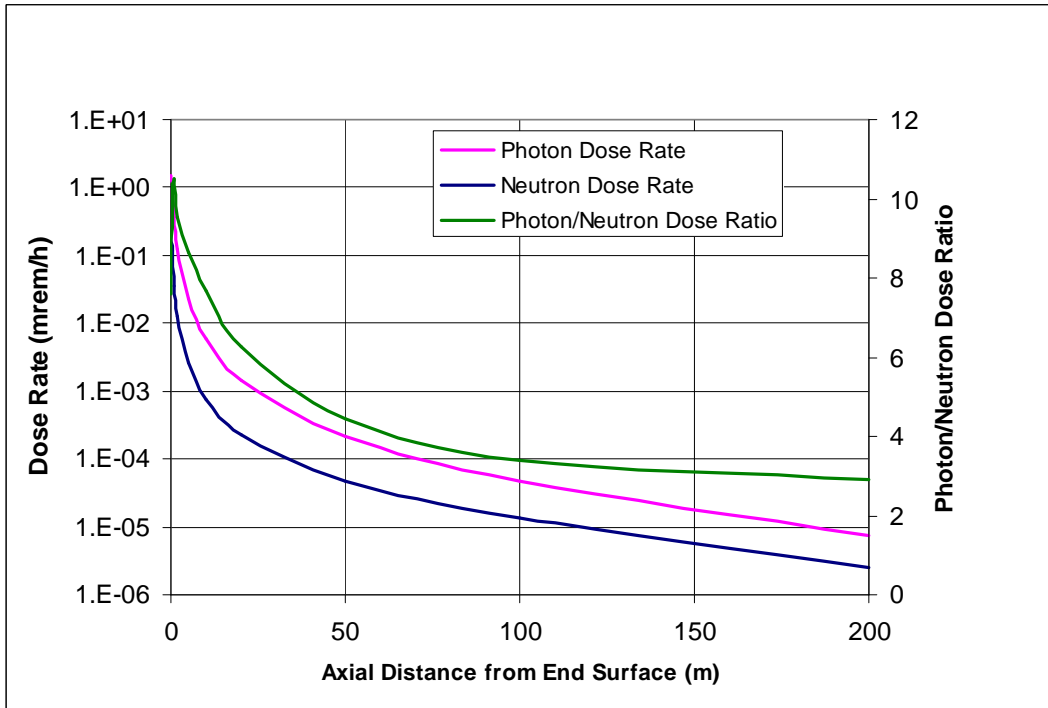


Figure 4-7 Axial Dose Rate Profile and Photon/Neutron Dose Ratio (Homogenized Geometry)

4.7.6 Photon Results for a Single Empty Feed Cylinder

Table E-13 in Appendix E provides the photon dose rate profiles for a freshly emptied feed cylinder (at $t = 0$), using the ANSI/ASN-6.1.1-1977 dose conversion factors, concrete pad and ground scattering with the assumption of a spatially uniform source distribution in the internal volume of the cylinder. It needs to be recognized that localized dose peaking could occur at or near the cylinder because of possible non-uniformity of the daughter product deposits on the inside surface of an empty cylinder. For large distances, the peaking effect becomes gradually diminished to no impact when the distance is relatively large so that the source in the cylinder could be viewed as a point source.

As for the filled feed cylinder, the calculated photon dose rates for the empty feed cylinder have a relative statistical error of less than 0.05 at all points, meeting the acceptance criterion for point detector tallies as specified in the MCNP manual [LANL 2008, Table 2.5]. The radial dose rates are also generally higher than the corresponding axial dose rates. However, the radial-to-axial dose ratio at 1 m and beyond is less for the empty cylinder than for the filled cylinder, because of the lack of self-shielding by UF_6 as present in the filled cylinder.

Figure 4-8 plots the radial and axial dose profiles for a single freshly emptied feed cylinder. For comparison purposes, the plot includes the same profiles for the filled feed cylinder. The larger radial-to-axial dose ratio for the filled feed cylinder is apparent from the plot.

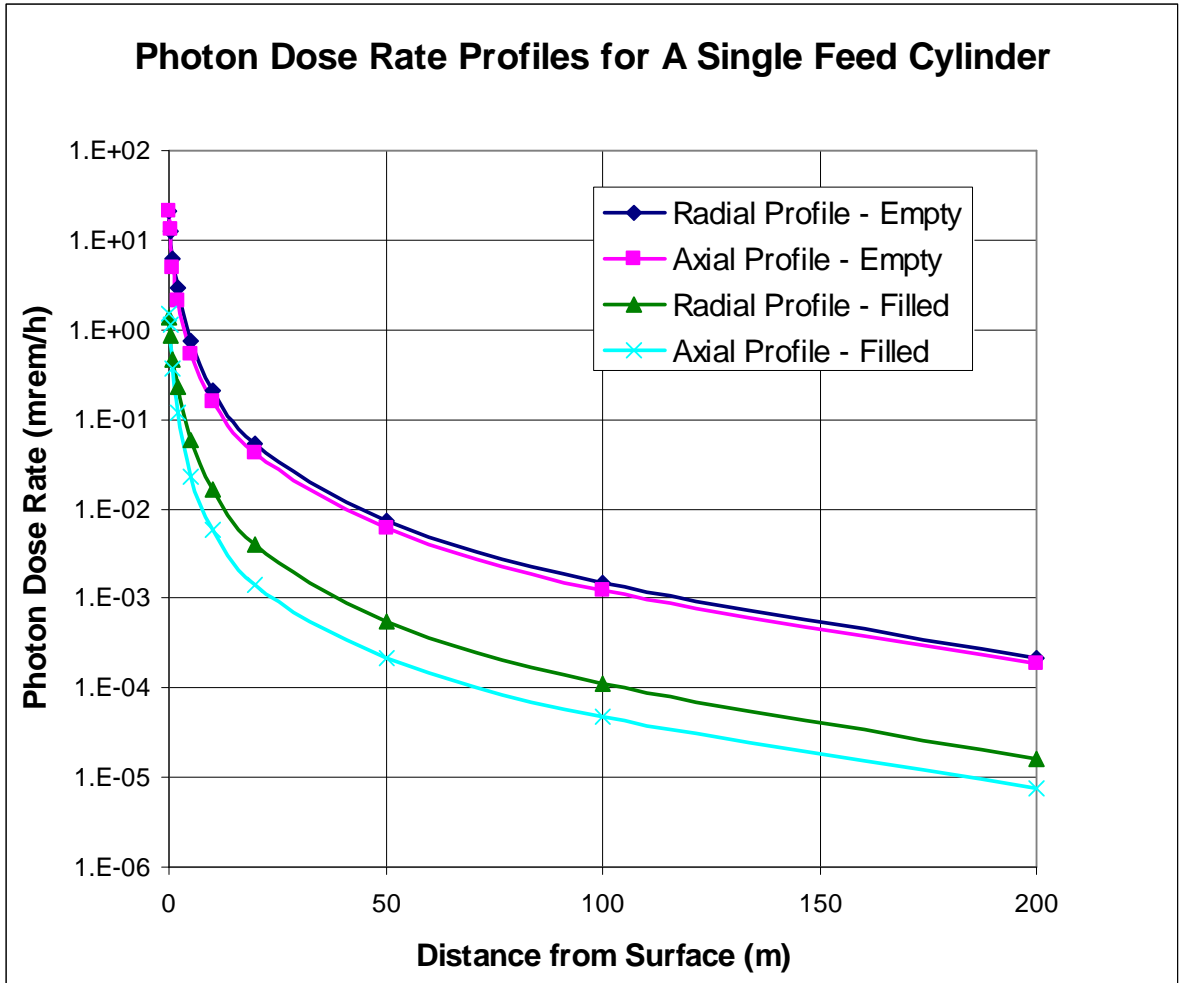


Figure 4-8 Photon Dose Rate Profiles for a Single 48Y Feed Cylinder

4.8 KEY OBSERVATIONS AND PARAMETER SELECTION

In summary, the UF₆ radiation dose rates from a single 48Y feed cylinder were determined with the MCNP code (MCNP5, v1.60), and used for the selection of the pertinent parameters for the subsequent multiple cylinder dose assessment described in Chapter 5. The calculations considered the conservative homogenized source geometry and nearly realistic slumped source geometry. The results include the radial and axial dose rate profiles for both neutrons and photons. For an in-depth understanding of radiation transport associated with the neutron and photon sources from UF₆, the study also evaluated the effects of concrete pad scattering, ground soil scattering, secondary photon contributions, partial photon energy spectrum and flux-to-dose rate conversion factors.

As deduced from the results in this evaluation, the following key observations are noted:

- Feed Cylinder Dose Rates – The filled feed cylinder gives a slightly higher total dose rate than any tails cylinder, thus representing a bounding type suitable for the multiple cylinder dose assessment to demonstrate regulatory compliance. The empty feed cylinder when freshly emptied is associated with a higher dose rate than the filled feed cylinder by about one order of magnitude, requiring special attention in storage management to address dose impacts.
- Source Geometry – The assumed homogenized source geometry produce more conservative (higher) dose rates than the nearly realistic slumped source geometry. The former is appropriate for conservative calculations, while the latter aligns closely with the field measurements. Hence, the homogenized source geometry is appropriate for the multiple cylinder dose assessment to preserve conservatism.

- Radial vs. Axial Dose Rate Profile – The radial dose rates are generally greater than the corresponding axial dose rates. Orientation of the cylinders will affect the site boundary doses when multiple cylinders are included in the dose calculations. The case study in Phase 3 for multiple cylinders uses the radial direction for dose assessment.
- Effect of Concrete Pad – The presence of the concrete pad has a tendency of reducing the neutron dose rates because of the moisture content in concrete softening the neutron energy spectrum. However, the effect on the photon dose rates is insignificant or inconsequential. Replacement of concrete with ground soil would lead to some conservatism in the neutron dose rate, but its impact on the total dose rate is minor because of a relatively small neutron dose component. To save the computer time by eliminating the concrete body, the concrete pad was treated as ground soil in the multiple cylinder dose assessment.
- Effect of Ground Soil Scattering – The ground soil scattering effect is more significant for neutrons than for photons, as the albedo coefficients are greater for neutrons. The effect varies with distance, peaking at a distance of 1 to 5 m and then dropping to no or reducing effect at 50 m and beyond. Inclusion of the ground scattering may increase or decrease the dose, depending on the distance from the source. The multiple cylinder dose assessment should include the ground scattering to accurately calculate the dose rates at various distances.
- Secondary Photon Contributions – The secondary photon dose rate from neutron interactions is on the order of 1% of the corresponding neutron dose rate, and can be ignored in future calculations as its contribution to the overall dose rate will be even

lower. The multiple cylinder dose assessment described in Chapter 5 disregards the secondary photon contributions.

- Partial vs. Full Photon Energy Spectrum – The partial photon energy spectrum for energies between 0.045 and 2.0 MeV is adequate for photon dose calculations, as the dose results for the partial and full spectra are practically identical within statistical uncertainties. Therefore, the multiple cylinder dose assessment only needs to use the partial energy spectrum to eliminate unnecessarily consuming computer time to track non-contributing histories from unimportant energy groups.
- Effect of Flux-to-Dose Rate Conversion Factors – The use of the ANSI/ANS-6.1.1-1977 standard results in ambient dose equivalents, whereas the ANSI/ANS-6.1.1-1991 standard yields effective dose equivalents. The effective dose equivalent is 41% of the ambient dose equivalent for neutrons, and 85% for photons. For compliance with 10 CFR 20, the ANSI/ANS-6.1.1-1977 standard must be used in the multiple cylinder dose assessment.
- Photon-to-Neutron Dose Ratio – At each point, the neutron dose is relatively lower than the photon dose. Except for points near the cylinder surface, the photon/neutron dose ratio decreases with distance, indicating skyshine radiation contributions become increasingly more important for neutrons than for photons. For environmental considerations, it is necessary to include the neutron contribution in the overall dose assessment besides the principal photon component.

5. MULTIPLE CYLINDER DOSE ASSESSMENT METHODOLOGY

The single cylinder dose evaluation presented in Chapter 4 shows that the contact dose rate is on the order of 2 mrem/h for a filled tails or feed cylinder, and 20 mrem/h for a freshly emptied feed cylinder. These low radiation doses are manageable on a single cylinder basis to meet the as-low-as-reasonably-achievable (ALARA) requirements in 10 CFR 20 [NRCd]. Consideration of multiple cylinders would increase the dose contributions significantly, particularly at the far fields such as the site boundary. The multiple cylinder dose assessment is the focus of this chapter, using an efficient Monte Carlo simulation method to achieve statistically acceptable results within reasonable computer times.

The UF₆ cylinder storage yard or pad accommodates thousands of cylinders that are typically stacked two high as shown in Figure 2-3 in Chapter 2. At a given receptor, multiple cylinders will make contributions to the radiation dose. The magnitude of the dose contribution from each cylinder varies, depending on the location of the cylinder. The close-in cylinders are expected to contribute more significantly than the distant cylinders. Additionally, the cylinders on the top stack are the principal dose contributors, as the top stack provides some shielding for the bottom stack.

Dose calculations for multiple cylinders are challenging by virtue of the large quantity of cylinders, UF₆ self-shielding effect, skyshine radiation contributions and site boundary distance factor, representing a deep-penetration shielding problem. The storage of different types of cylinders including filled tails, filled feed and empty feed cylinders also adds a certain degree of complexity, because of substantial dose contributions from a

relatively small quantity of empty feed cylinders. The weak photon radiation sources from UF_6 introduce an additional complication to the problem.

At the UUSA Enrichment Facility, several dose calculations are available for arrays of cylinders on the UBC Storage Pad to demonstrate regulatory compliance. The cylinder stacking configurations considered in the calculations included single, double and triple stacks. The calculations used the MCNP code (MCNP5 v1.40) [LANL 2005] without specific importance sampling or biasing for the source distributions (position, energy and direction). The standard, unbiased approach (except the convenient built-in variance reduction features such as cell importance) was a time-consuming process, requiring over 100 hours CPU time for a typical case (Table 8-9 in Chapter 8). Other shortcomings with this approach included limited results only for a few detector points, lengthy input, and poor statistics at large distances.

To improve the computational efficiency with the MCNP code, it is essential to develop an optimized approach with importance sampling for reducing the CPU time by an order of magnitude or better as compared to the direct, unbiased method. The approach taken in this research involved assignment of an importance to different particles based on how much they would contribute to the final answer. In so doing, more time can be spent on important particles with less time wasted on unimportant particles. The degree of optimization depends on the accuracy of the importance sampling. A more accurate importance sampling scheme will certainly lead to a better degree of optimization. The intent of this research is to reach a good estimate of particle importance parameters, but not a perfectly optimized scheme which is practically unattainable or probably theoretically unsolvable.

5.1 OVERVIEW

The work in Phase 1 (Chapter 3) and Phase 2 (Chapter 4) was a prerequisite for this phase (Phase 3), as it provided the necessary input and data for use in dose analysis for multiple cylinders. Phase 3 was the heart of this research project to provide an efficient Monte Carlo approach to dose simulations for arrays of cylinders in different stacking configurations.

The dose calculations for multiple cylinders used the same Monte Carlo method as for a single cylinder, namely MCNP5, v1.60. For a single cylinder, the Monte Carlo calculations are fairly straightforward without requiring sophisticated variance reduction techniques, because of the absence of geometric complexity. The situation is distinctly different for multiple cylinders, especially for thousands of cylinder in a storage yard. The direct standard Monte Carlo calculations for this case would be very time-consuming, as indicated earlier. Fortunately, a number of variance reduction techniques are available in the MCNP code, provided the user enters appropriate weighting factors or biasing schemes as inputs for importance sampling. Therefore, the key to an efficient Monte Carlo calculation for deep penetration problems requires development of an importance sampling scheme.

The MAVRIC sequence [ORNL 2011a] in the SCALE code package is available to generate a space and energy-dependent importance map (weight windows) for biasing during radiation transport and a mesh-based biased source distribution. MAVRIC is based on the CADIS (Consistent Adjoint Driven Importance Sampling) methodology. MAVRIC automatically performs a quick three-dimensional, discrete ordinates calculation using DENOVO [ORNL 2011a, §S6.B] to find the adjoint flux as a function of position and energy, which forms the basis for the importance map and biased source distribution. The

adjoint flux or function is a measure of the “importance” of a particle (neutron or photon) in contributing to the response of the detector [Bell 1970, §6.1d]. In this research, the importance and biasing data from the output of MAVRIC were processed, analyzed and converted into a form suitable for input into MCNP to perform a forward Monte Carlo calculation. The joint application of discrete ordinates and Monte Carlo radiation transport offers an efficient solution to deep penetration or thick shielding problems to achieve satisfactory statistics in reasonable computer times.

The improved approach was used to study the environmental doses from multiple filled cylinders in the storage yard or on the UBC pad. The study considered different variations of stacking configurations including single, double and triple stacks. For each stacking configuration, the dose calculations consisted of the following three co-planar arrays: 10 x 10, 30 x 30, and 100 x 100 for approximately an order of magnitude increase in cylinder quantity from case to case. These cases (a total of 9 for neutrons and 9 for photons) would provide sufficient data points for determining the dose effects of cylinder quantity and stacking configuration to establish a reasonable trend of the dose with respect to the storage capacity.

For completeness, the multiple cylinder dose assessment was extended to address the effect of storage of empty feed cylinders on the pad in light of significant dose contributions from these cylinders. Since the empty cylinders contain no UF₆ for self shielding, the dose calculations could be accomplished without using the source importance data with respect to position.

5.2 PREVIOUS WORK

The past and existing UF₆ cylinder storage yards at the U.S. gaseous diffusion plants including East Tennessee Technology Park in Tennessee, Portsmouth in Ohio and Paducah in Kentucky [DOE 2001] typically relied on radiation monitoring as part of regular surveillance and maintenance activities to meet the ALARA dose requirements and comply with the regulations. Radiation measurements are useful and beneficial, as they provide actual field data and eliminate the need for detailed dose calculations. This approach is viable for the existing storage yards with cylinder inventory at or near the capacity, as external radiation levels around the yards are not expected to change noticeably with time.

For new uranium enrichment facilities, the storage yards or pads must be designed and licensed for an allocated capacity. The design process requires detailed dose assessment for demonstration of regulatory compliance and receipt of regulatory approval in the licensing process. The external dose requirements include onsite doses to facility workers and offsite doses to the general public at the site boundary. The latter requirement (offsite doses) is the concern for environmental dose compliance, and therefore constitutes the main thrust for this research.

The UUSA Enrichment Facility in Eunice, New Mexico is currently the only newer commercial facility in the U.S. In support of the initial licensing application to the NRC, UUSA calculated the annual dose equivalent from the UBC Storage Pad, based on an occupancy factor of 2000 hours per year at the site boundary where no full-time residents are present [AREVA 2003d]. The calculation assumed a storage capacity of 15,727 filled tails (DUF₆) 48Y cylinders, and 354 empty feed cylinders [AREVA 2003d, Table 3]. Double stacking was used. The dose calculations were carried out with an old version of the MCNP

code, namely MCNP4C [RSICC 2000] in a direct approach without specific biasing schemes to speed up the calculations.

The lack of validation in the initial calculations necessitated incorporation of conservative calculational uncertainties to account for such factors as Monte Carlo sampling error, photon skyshine uncertainties at large distances [NSE 1993], neutron dose conversion factors and potential uncharacterized source variables [AREVA 2003c]. As such, these calculations applied an upper limit multiplier on both dose equivalent and source uncertainty to normalization of nominal MCNP results. The resulting multipliers were about a factor of 2 for photon doses and 10 for neutron doses. These multipliers were conservative for regulatory compliance but unduly excessive (particularly for neutrons), imposing an economic penalty on the storage pad footprint requirements.

In 2010, UUSA performed a sensitivity study with MCNP5, v1.40 to evaluate the dose impacts of the variations of the UBC Storage Pad cylinder arrangements in one, two and three stacks high [UUSA 2010]. The study took a direct time-consuming approach without additional variance reduction techniques beyond the convenient features offered by the code. The radiation source terms from the initial dose calculation were used without updating in this study. Thus, the afore-mentioned conservative multipliers were applied to the MCNP dose results, resulting in overestimates of dose equivalents to both workers and the general public as previously calculated.

To support the planned UBC Storage Pad expansion, UUSA prepared a new calculation in 2012 [UUSA 2012c], which retained the same source terms as used in the two previous calculations [AREVA 2003d and 2010] but removed the unnecessarily conservative dose multipliers. The calculational approach with MCNP5, v1.40 remained intact, using the

direct time-consuming simulation method. For bounding purposes, the calculations assumed storage of all 48Y filled feed cylinders (slightly higher dose rates than the filled tails cylinders), but neglected consideration of empty feed cylinders. This calculation concluded that an expansion of the capacity of the UBC Storage Pad to host 25,000 48Y filled cylinders (tails and feed) in a triple stacked arrangement would be feasible, and would not require any additional mitigations provided that adequate distances were maintained from the pad edge to the site boundary.

At the request of the NRC for additional information on the UUSA planned facility expansion, another calculation was completed in 2013 [UUSA 2013c] to evaluate the direct radiation dose equivalent contribution from the UF₆ storage on the UUSA site to the workers involved in the construction activities due to the expansion to 10-million SWU capacity. This calculation reflected the updated source terms [UUSA 2013b] generated with ORIGEN-S and omitted the unnecessary conservative dose multipliers. However, the dose calculation with MCNP5, v1.40 employed the same time-consuming approach as before, encountering difficulties in attaining statistically satisfactory results at large distances.

All of the previous MCNP dose calculations for multiple cylinders with a direct approach suffered the common drawbacks of a time-consuming process, possible lengthy input, limited output of results, and unsatisfactory statistics at large distances. Development of an efficient approach would be vital and beneficial to perform the dose assessment for multiple cylinders for management of UF₆ cylinder storage in a cost-effective manner. Towards this goal, this chapter provides the details of the development and application of an indirect Monte Carlo simulation approach to the multiple cylinder dose problems.

5.3 SOURCE IMPORTANCE DATA GENERATION

As commonly known, the dose contribution varies with the position, energy and direction of the source particle. More contributions are expected from the closer and higher-energy source particles traveling in the direction towards the detector points of interest. The importance of each source particle is thus a function of its dose contribution. Weighting can then be applied to the source particles based on their importance to the resulting dose, forming a biased source distribution for random sampling.

For each particle type (photon or neutron), separate sets of source importance are normally necessary because of different radiation transport characteristics. However, for the case of UF₆ cylinders, equal position weighting was applied to the neutron source in each cylinder without biasing, as the UF₆ material is a poor neutron attenuator. A test run using the neutron source importance data generated with MAVRIC in the MCNP neutron dose calculation failed to improve the computational efficiency (discussed in Section 7.1). Consequently, source position biasing was applied to the photon source only for which the importance data were generated and used in the MCNP calculations.

This section discusses the generation of photon source importance data with respect to position, and covers energy and direction biasing for neutrons and photons for application to the MCNP dose calculations.

5.3.1 Photon Source Position Biasing

The photon source position importance data were generated with the MAVRIC module in the SCALE 6.1.2 code package. The data generation included the 10x10 and 30x30 cylinder arrays in double stacking only. The importance data for the top layer of double stacking was applicable to the single stack as well as the top layer of triple stacking,

in view of similar relative importance characteristics. In addition, the importance data for the bottom layer of double stacking were used for both middle and bottom layers of triple stacking, as source sampling from these layers would be small, relative to the top layer. For the 100x100 array, extrapolations and approximations were used for extension beyond 30 cylinders. Any normalized importance value of less than 0.001 was taken as 0.001 without appreciable loss of computation efficiency.

For a square array size (in terms of cylinder quantity) as used for the case study in this research, the importance data generation considered the radial direction to focus on the higher radial dose rate profile as evaluated in Section 4.7.4.1 for a single cylinder. For the axial direction, a separate set of importance data would need to be generated. Alternatively, the radial importance data could be applied to the axial direction without significant loss of computational efficiency, since the use of radial biasing would avoid over-biasing in the axial direction and accommodate large variations in source importance with detector positions (additional discussion in Section 8.4.2).

As selected from the single cylinder dose evaluation, the photon source term was taken for the bounding 48Y filled feed cylinder. To simplify the geometric model for MAVRIC, each cylinder was approximated by a square cross section with the cylinder wall neglected. This approximation facilitated the MAVRIC calculations to provide a clear graphical importance map for all cylinders modeled. The omission of the cylinder wall in the model was justified by the rationale that the importance data were on a relative rather than absolute basis and the small wall thickness relative to the UF₆ physical dimension would pose only minor effects on the relative importance data.

The source importance model assumed a center-to-center (CTC) cylinder spacing of 5 ft (152.4 cm) radially and 16 ft (~488 cm) axially, consistent with typical spacing for cylinder storage [OEPA 2004, Attachment A, p. 11]. The same spacing was also used in the subsequent dose calculations with the MCNP code (Section 5.4.1) for consistency. Based on the results from the single cylinder dose evaluation, the model simulated the concrete pad with ground soil, and included the effects of ground scattering and air skyshine. The ANS/ANSI-6.1.1-1977 dose conversion factors were entered as input for the photon dose response function required by the MAVRIC module.

As a matter of fact, the source importance depends on the detector location. Each detector location is associated with a specific set of importance data. It would be a tedious process to generate and apply detector-dependent importance data. Instead, a single set of data was generated at a representative detector location for use in the multiple cylinder dose assessment.

Since MARVIC performed the adjoint flux calculations to determine the source importance, it was necessary to select an appropriate adjoint source location (detector location in the forward transport mode) to be representative of the majority of environmental locations. A series of test runs were made with MARVIC by placing the adjoint source at various distances from the edge of the cylinder storage array. The resulting importance data were fed into the MCNP calculations to determine the figure of merit (the speed-up). The test results showed that an adjoint source located at 40 to 50 m from the edge of the cylinder array would be appropriate for environmental dose considerations.

The MAVRIC runs included the cases for 10x10 and 30x30 arrays in double stacking. The adjoint source was represented by a box with a large volume to cover the full axial

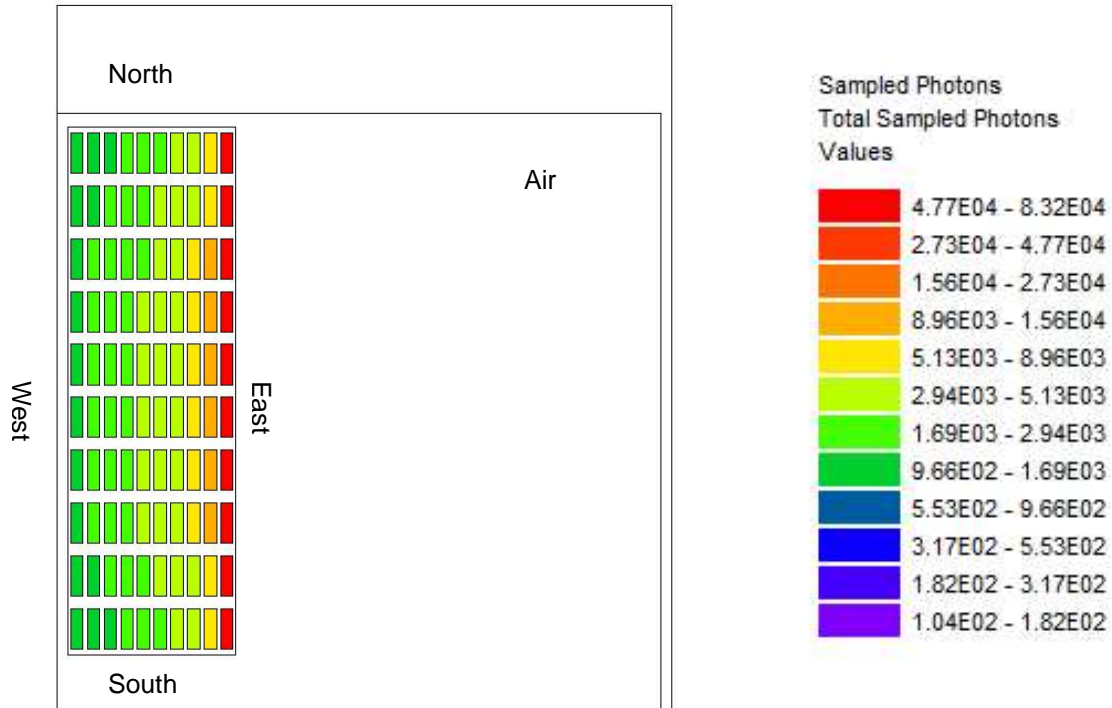
length of the cylinder array and a personnel height of 8 ft (~244 cm) located at the selected radial distance of 40 to 50 m from the edge of the cylinder array. The 8-ft height approximates the height of the cylinder array in double stacking. It is tall for an average person, but acceptable for increasing the mesh element volume for tally purposes because of insignificant vertical dose variations over this height. All the cylinders were modeled without considering geometric symmetry, as MAVRIC could not treat reflective boundaries. With the standard 19 energy group structure for the photon source (Table 3-8), the MAVRIC runs took advantage of the built-in cross section library for radiation transport calculations. Appendix F lists the associated input and output files in Table F-1, and provides the input file listing. Again, these cases are for the photon source only. No neutron source position biasing is necessary as indicated in Section 5.3.

The MAVRIC-produced photon source importance maps are displayed in Figure 5-1 for the 10x10 array and Figure 5-2 for the 30x30 array, including the importance for both top and bottom stacks. For orientation purposes, the X axis represents the west-east direction, and the Y axis refers to the south-north direction. The cylinder locations are identified by row in the south-north direction starting from 1 on the south. In each row, the cylinders are numbered from the west with the first cylinder on the west boundary and last cylinder on the east boundary.

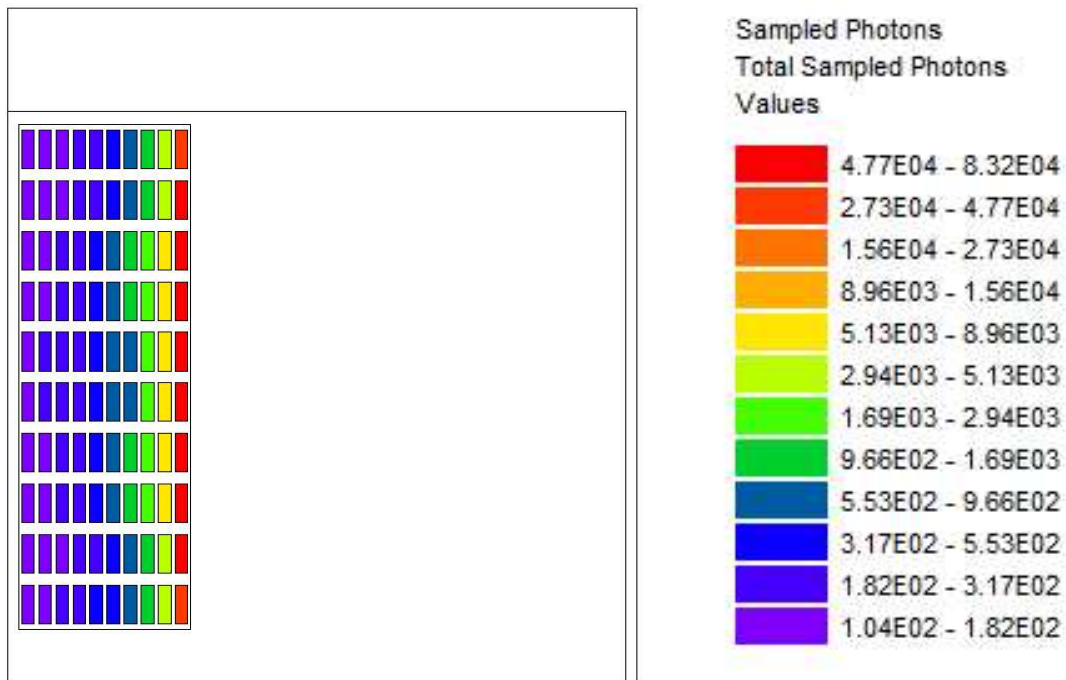
The corresponding relative importance data for the photon source by cylinder are provided in Table 5-1 for the 10x10 array and Table 5-2 for the 30x30 array. These data were in turn normalized to 1.0 for the last cylinder on the top stack as shown in Tables 5-1 and 5-2 and plotted in Figures 5-3 and 5-4.

It is apparent that the top stack is more important than the bottom stack which is shielded by the top stack, and the front cylinders are more important than the back cylinders, again due to shielding. The important data are fairly symmetric about the middle row (row #5 or 6 in the 10x10 array, and row #15 or 16 in the 30x30 array) in the south-north direction. For minimizing the input to the MCNP dose calculation, the importance data for the middle row were selected to be representative of all rows. This approach was approximate and reasonable, because of small variations in importance from one row to another. The use of single-row data saved efforts in entering different data on a cylinder-by-cylinder basis for little gain in computational efficiency.

The results for the 30x30 array were applicable to the 100x100 array without the need for another MARIC run, since the dose contributions from the front 30 cylinders were predominant, and the importance data for the back 70 cylinders could be approximated by extrapolation from the 30x30 array data or sampled equally with minor impact on computer times. The application of the photon source importance data with respect to position biasing for different storage configurations is discussed in Table 5-6 in Section 5.4.3.

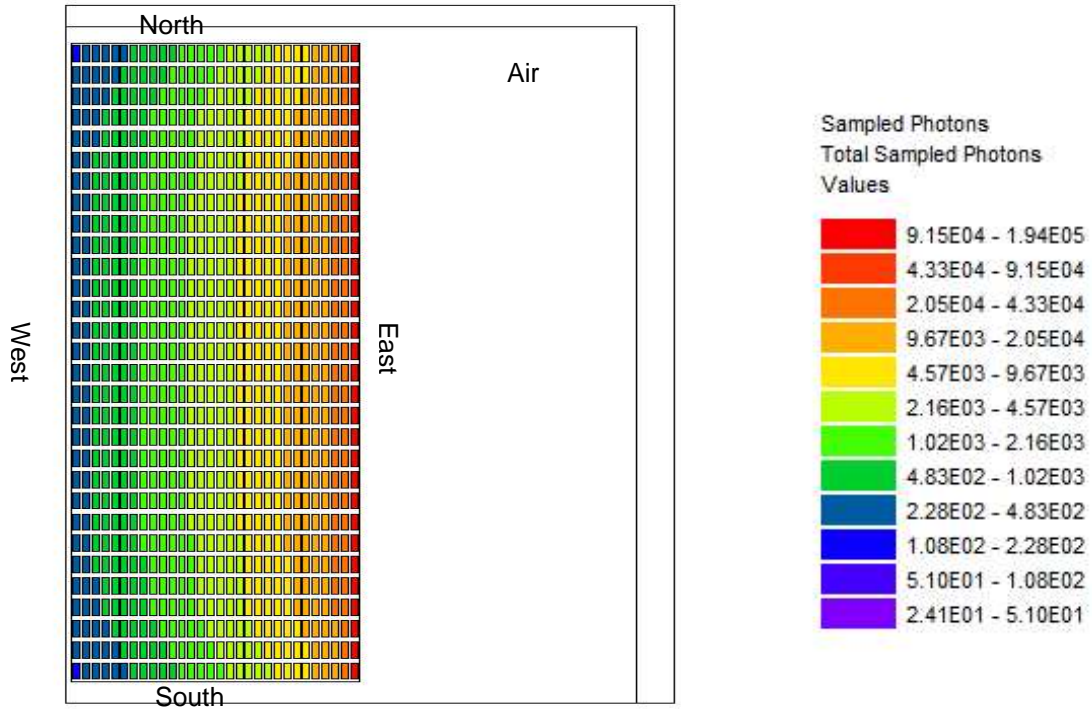


d10x10p – Photon Source Importance – Top Stack

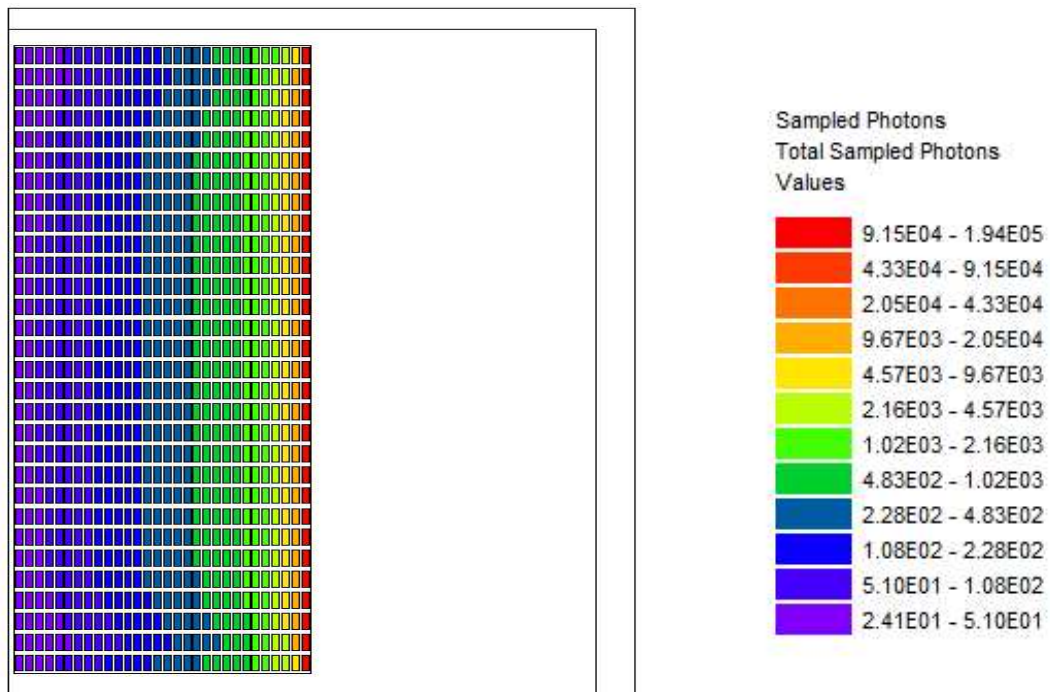


d10x10p – Photon Source Importance – Bottom Stack

Figure 5-1 Source Sampling Importance Data – 10x10 Double Stacking (48Y Filled Feed Cylinders)



d30x30p – Photon Source Importance – Top Stack



d30x30p – Photon Source Importance – Bottom Stack

Figure 5-2 Source Sampling Importance Data – 30x30 Double Stacking (48Y Filled Feed Cylinders)

Table 5-1 MAVRIC Photon Source Importance for 10x10 Array (48Y Filled Feed Cylinders)

Cylinder #	Relative Importance		Normalized Importance*	
	Top Stack	Bottom Stack	Top Stack	Bottom Stack
1 (West)	0.156	0.016	1.93E-02	1.97E-03
2	0.189	0.019	2.34E-02	2.29E-03
3	0.226	0.023	2.80E-02	2.83E-03
4	0.270	0.029	3.34E-02	3.63E-03
5	0.325	0.040	4.02E-02	4.93E-03
6	0.396	0.059	4.90E-02	7.29E-03
7	0.493	0.096	6.10E-02	1.19E-02
8	0.643	0.178	7.96E-02	2.20E-02
9	1.170	0.630	1.45E-01	7.80E-02
10 (East)	8.080	7.450	1.00E+00	9.22E-01

*Normalized to 1 for Cylinder #10 on the top stack

Table 5-2 MAVRIC Photon Source Importance for 30x30 Array (48Y Filled Feed Cylinders)

Cylinder #	Relative Importance		Normalized Importance*	
	Top Stack	Bottom Stack	Top Stack	Bottom Stack
1 (West)	3.99E-02	3.99E-03	2.38E-03	2.38E-04
2	4.66E-02	4.51E-03	2.78E-03	2.69E-04
3	5.41E-02	5.23E-03	3.22E-03	3.12E-04
4	6.27E-02	6.05E-03	3.74E-03	3.61E-04
5	7.25E-02	6.98E-03	4.32E-03	4.16E-04
6	8.38E-02	8.05E-03	4.99E-03	4.80E-04
7	9.68E-02	9.29E-03	5.77E-03	5.54E-04
8	1.12E-01	1.07E-02	6.67E-03	6.38E-04
9	1.29E-01	1.23E-02	7.69E-03	7.33E-04
10	1.49E-01	1.42E-02	8.88E-03	8.46E-04
11	1.72E-01	1.64E-02	1.03E-02	9.77E-04
12	1.99E-01	1.89E-02	1.19E-02	1.13E-03
13	2.30E-01	2.18E-02	1.37E-02	1.30E-03
14	2.66E-01	2.51E-02	1.59E-02	1.50E-03
15	3.07E-01	2.90E-02	1.83E-02	1.73E-03
16	3.54E-01	3.34E-02	2.11E-02	1.99E-03
17	4.09E-01	3.86E-02	2.44E-02	2.30E-03
18	4.73E-01	4.45E-02	2.82E-02	2.65E-03
19	5.46E-01	5.13E-02	3.25E-02	3.06E-03
20	6.30E-01	5.93E-02	3.75E-02	3.53E-03
21	7.28E-01	6.87E-02	4.34E-02	4.09E-03
22	8.41E-01	8.01E-02	5.01E-02	4.77E-03
23	9.72E-01	9.45E-02	5.79E-02	5.63E-03
24	1.13E+00	1.14E-01	6.72E-02	6.79E-03
25	1.31E+00	1.44E-01	7.81E-02	8.58E-03
26	1.53E+00	1.94E-01	9.14E-02	1.16E-02
27	1.82E+00	2.84E-01	1.08E-01	1.69E-02
28	2.22E+00	4.72E-01	1.32E-01	2.81E-02
29	3.32E+00	1.44E+00	1.98E-01	8.55E-02
30 (East)	1.68E+01	1.67E+01	1.00E+00	9.93E-01

*Normalized to 1 for Cylinder #30 on the top stack

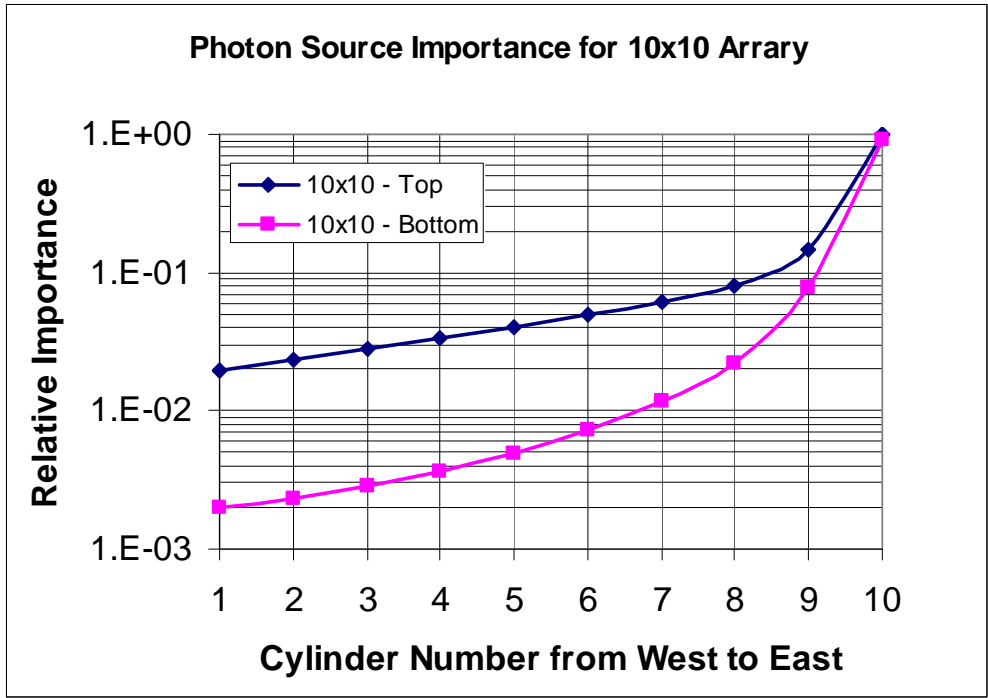


Figure 5-3 Normalized Relative Photon Source Importance for 10x10 Array

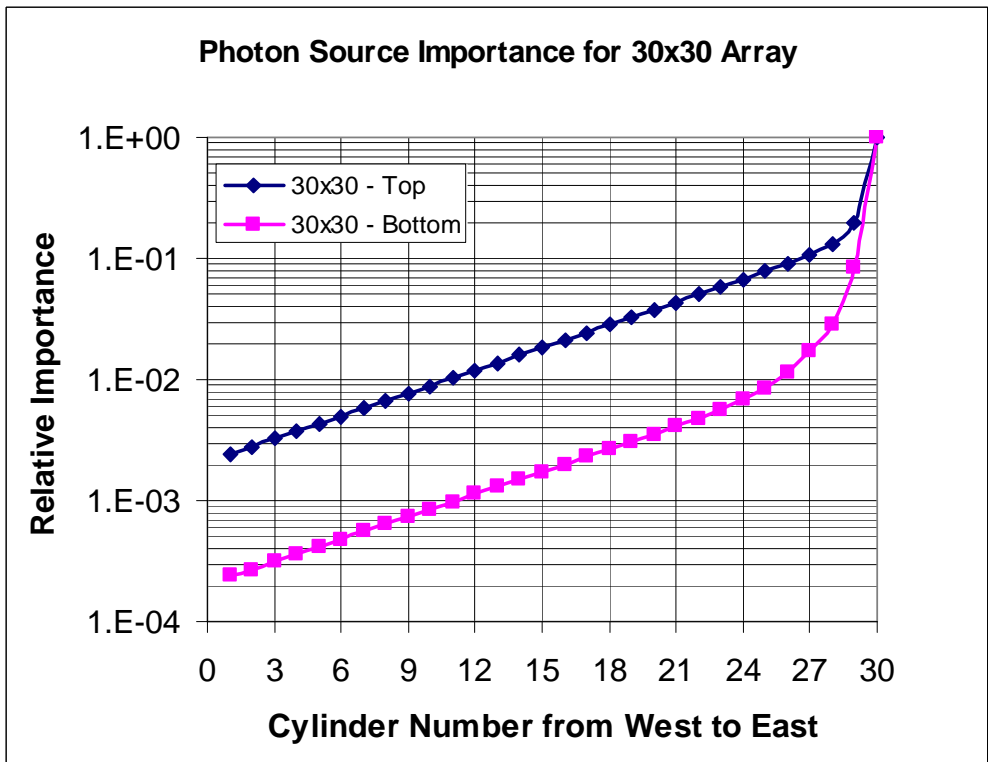


Figure 5-4 Normalized Relative Photon Source Importance for 30x30 Array

5.3.2 Source Energy Biasing

The source energy biasing was determined for, and applied to, both neutron and photon sources for the 48Y filled feed cylinder, based on the contribution from each energy group to the average contact dose rate on the outside surface of the cylinder. In other words, biasing was used to favor more contributing energy groups with higher weighting or importance. Although this biasing was constructed on the basis of the surface dose rate, its application to the entire problem with various receptors would be still beneficial, as non-penetrating photons from each cylinder were screened out or sampled with reduced frequency before reaching the external surface.

The biased source energy distributions for neutrons and photons were derived from the results of single cylinder dose calculations described in Sections 4.7.1 and 4.7.2 in Chapter 4 for a filled feed cylinder. The distribution included the important or contributing energy groups only as given in Tables 4-3 for neutrons and 4-4 for photons.

Table 5-3 presents the unbiased and biased neutron source energy distributions. The former is based on the energy spectrum of the actual source, while the latter represents a biasing scheme to favor the higher-energy neutrons.

Likewise, Table 5-4 provides the unbiased and biased photon source energy distributions, derived in the same manner as for neutrons. The energy biasing is more powerful for photons than for neutrons to filter out the low-energy photons, which contribute substantially to the total source intensity, but only slightly to the resulting dose outside the cylinder. On the other hand, the number of low-energy neutrons is relatively small with less profound biasing effects.

Table 5-3 Unbiased and Biased Neutron Source Energy Distributions (48Y Filled Feed Cylinder)

Group	Neutron Energy (MeV)	Unbiased Energy Spectrum		Biased Energy Spectrum	
		Source Intensity (n/s per cylinder)	Normalized Fraction	External Contact Dose Rate (mrem/h)	Normalized Fraction
20	1.50E-02 - 1.11E-01	3.905E+03	7.845E-03	3.071E-04	1.521E-03
21	1.11E-01 - 4.08E-01	3.869E+04	7.772E-02	5.339E-03	2.645E-02
22	4.08E-01 - 9.07E-01	1.523E+05	3.059E-01	4.344E-02	2.152E-01
23	9.07E-01 - 1.42E+00	1.620E+05	3.254E-01	7.393E-02	3.662E-01
24	1.42E+00 - 1.83E+00	7.314E+04	1.469E-01	3.808E-02	1.886E-01
25	1.83E+00 - 3.01E+00	5.174E+04	1.039E-01	2.982E-02	1.477E-01
26	3.01E+00 - 6.38E+00	1.524E+04	3.061E-02	1.034E-02	5.125E-02
27	6.38E+00 - 2.00E+01	5.789E+02	1.163E-03	5.946E-04	2.945E-03
Total	1.50E-02 - 2.00E+01	4.976E+05	1.000E+00	2.019E-01	1.000E+00

Table 5-4 Unbiased and Biased Photon Source Energy Distributions (48Y Filled Feed Cylinder)

Group	Photon Energy (MeV)	Unbiased Energy Spectrum		Biased Energy Spectrum	
		Source Intensity (p/s per cylinder)	Normalized Fraction	External Contact Dose Rate (mrem/h)	Normalized Fraction
2	4.50E-02 - 1.00E-01	2.174E+10	5.233E-01	1.212E-04	7.933E-05
3	1.00E-01 - 2.00E-01	1.161E+10	2.794E-01	2.282E-03	1.494E-03
4	2.00E-01 - 3.00E-01	2.635E+09	6.342E-02	2.104E-02	1.378E-02
5	3.00E-01 - 4.00E-01	1.685E+09	4.056E-02	5.568E-02	3.645E-02
6	4.00E-01 - 6.00E-01	1.157E+09	2.785E-02	1.250E-01	8.181E-02
7	6.00E-01 - 8.00E-01	1.141E+09	2.746E-02	2.943E-01	1.927E-01
8	8.00E-01 - 1.00E+00	8.808E+08	2.120E-02	3.983E-01	2.608E-01
9	1.00E+00 - 1.33E+00	5.262E+08	1.266E-02	3.960E-01	2.593E-01
10	1.33E+00 - 1.66E+00	7.831E+07	1.885E-03	8.990E-02	5.885E-02
11	1.66E+00 - 2.00E+00	9.451E+07	2.275E-03	1.448E-01	9.479E-02
Total	4.50E-02 - 2.00E+01	4.155E+10	1.000E+00	1.527E+00	1.000E+00

5.3.3 Source Direction Biasing

A built-in prescription is available in the MCNP code [LANL 2008, p 2-133] for the source direction biasing, which favors the direction towards the detector by sampling from a continuous exponential function with the following probability density function:

$$p(\mu) = Ce^{K\mu}$$

where C is a normalization constant equal to $K/(e^K - e^{-K})$, and $\mu = \cos\theta$ (θ is an angle relative to the biasing direction). In this study, the biasing (or favored) direction was the radial direction traveling from the west to the east, as the environmental receptors were located on the east side of the model.

The choice of the K value affects the biasing characteristics, with $K = 0.01$ for almost no biasing and $K = 3.5$ for very strong biasing [LANL 2008, Table 2.6]. K is typically about 1 per LANL 2008. This typical value was found suitable for this study after experimentation and confirmation with the test runs for different K values. The same direction biasing applied to both neutron and photon sources which are isotropic in nature.

5.4 INDIRECT MONTE CARLO SIMULATIONS

Section 5.2 describes the previous work which performed the dose assessment with a direct, time-consuming Monte Carlo simulation approach. The direct approach was a single-step once-through calculation, producing the results of interest in a single computer run.

This research took a different approach with indirect Monte Carlo simulations, involving a two-step process with the objective of improving computational efficiency. The first step used the Monte Carlo code to record the surface sources on the pertinent surfaces of a box enclosing all the cylinders on the storage pad. This step modeled all the cylinders explicitly, using the lattice or repeated structure feature. All the necessary parameters associated with the surface sources were written to a file, including (x, y, z) position, energy, direction cosines and weight. The resulting surface sources then became a set of new sources for the second step of the Monte Carlo simulation. In the second step, the box containing all the cylinders as used in the first step was treated as a black box (modeled as void with zero importance). Besides the black box, the model in the second step included environmental air

and ground soil only, greatly simplifying the geometry for Monte Carlo simulations. The results in the form of mesh tallies and associated relative errors were produced from the second step.

5.4.1 Key Parameters

As recapped from the single dose evaluation in Chapter 4, the key parameters selected for use in the multiple cylinder dose assessment are summarized below:

- Cylinder type – bounding 48Y filled feed cylinder
- UF_6 source geometry – homogenized and uniform within the cylinder internal volume for conservatism
- Receptors – located in the radial direction to yield higher doses
- Concrete pad – simulated by ground soil
- Ground soil scattering – included
- Skyshine radiation due to air scattering – included
- Secondary photon contributions – negligible and neglected
- Source energy spectra – important and contributing energy groups only
- Flux-to-dose rate conversion factors – use of the conservative and NRC-compliant ANSI/ANS-6.1.1-1977 standard

In addition, the center-to-center cylinder spacing was the same as used in the MAVRIC calculations of the photon source importance for consistency (Section 5.3.1), namely 5 ft (152.4 cm) radially and 16 ft (~488 cm) axially. The bottom cylinders had a ground clearance of 6 in. (15.24 cm) as assumed in the single cylinder evaluation. One difference from the MAVRIC model was that the MCNP model used the cylindrical geometry and included the cylinder wall.

Each cylinder in the storage array was modeled in the same manner as in the single cylinder evaluation for the reference case (Chapter 4), disregarding physical end rounding, skirted ends and local stiffening rings. To facilitate the use of a lattice for the repeated structures (cylinders), a slight modification to the cylinder stacking configuration was necessary with the assumption that the bottom of the upper cylinders was flush with the top of the lower cylinders. In reality, an upper cylinder sits and fits between two adjacent lower cylinders with about 5 in. (12.7 cm) overlap, based on a field measurement at the UUSA Enrichment Facility. However, the flush model would allow slightly more radiation streaming between cylinders with a larger gap than the actual arrangement, thus adding some conservatism in the dose assessment.

5.4.2 Case Study

To study the sensitivity of dose to the change in the storage capacity with respect to the array size and stacking arrangement, this research considered a number of cases as listed in Table 5-5 ranging from 100 to 30,000 cylinders on the storage pad. The cases included three storage arrays: 10x10, 30x30 and 100x100. For each array size, the cylinders were stacked one, two and three high. Neutron and photon doses were separately calculated with the MCNP code for each array size and stacking configuration.

Table 5-5 Cylinder Storage Arrangements for Case Study

Stacking	Number of Cylinders		
	10x10 Array	30x30 Array	100x100 Array
Single	100	900	10,000
Double	210 (10x10 top) (11x10 bottom)	1,830 (30x30 top) (31x30 bottom)	20,100 (100x100 top) (101x100 bottom)
Triple	300 (9x10 top) (10x10 middle) (11x10 bottom)	2700 (29x30 top) (30x30 middle) (31x30 bottom)	30,000 (99x100 top) (100x100 middle) (101x100 bottom)

The square arrays (in terms of the number of cylinders) were used here for the sensitivity study. The actual storage array would be most likely to deviate from the square arrangement. For example, the UUSA Enrichment Facility features a rectangular storage array as shown in Figure 2-3 in Chapter 2. The case study with the square arrays would provide the sensitivity results and quantify the computational efficiency of the indirect Monte Carlo simulation approach used in this research.

5.4.3 First-Step Process

The first-step process modeled all the cylinders explicitly with the surrounding air and ground soil. A box was constructed to closely contain all the cylinders and form the boundaries for writing the surface source file. Based on the orientation convention as indicated earlier in Figures 5-1 and 5-2, the pertinent surfaces were the top, east and north boundaries of the containing box. The sources on the other three surfaces (bottom, west and south) would be irrelevant, as scattering off these surfaces through the cylinders was accounted for on the scoring surfaces (top, east and north boundaries).

Figures 5-5, 5-6 and 5-7 depict the geometric models for the storage arrays of 10x10, 30x30, and 100x100 in one, two and three high, respectively. These plots were produced from the MCNP Plot Geometry Plotter [LANL 2008, Appendix B, §II] with the aid of the free Xming displayer server for the Microsoft Windows Operating Systems [Mair 2006] for MCNP plotting to function. The plots were generated and saved as postscript files viewable and printable with the free GSview graphical interface utility program [Lang 2012] under Microsoft Windows.

In the models, a unit cell was set up for each cylinder to build a lattice configuration, based on the radial and axial cylinder spacing given in Section 5.4.1. Each stack was

represented by a separate lattice of cylinders because of the offset between the upper and lower cylinders. It needs to be pointed out that the models took advantage of geometric symmetry about the X axis, requiring modeling of only one half of the rows of cylinders in the Y direction. With a reflective boundary on the south side for symmetry, the number of cylinders modeled in each case was one half of the actual number of cylinder considered. The multiplier used for the MCNP tally reflected the number of cylinders modeled in each respective case.

The material densities and compositions for the multiple cylinder dose assessment remained unchanged from the single cylinder dose evaluation (Section 4.4.2 in Chapter 4). The nuclear cross section data described in Section 4.4.5 were also applicable here.

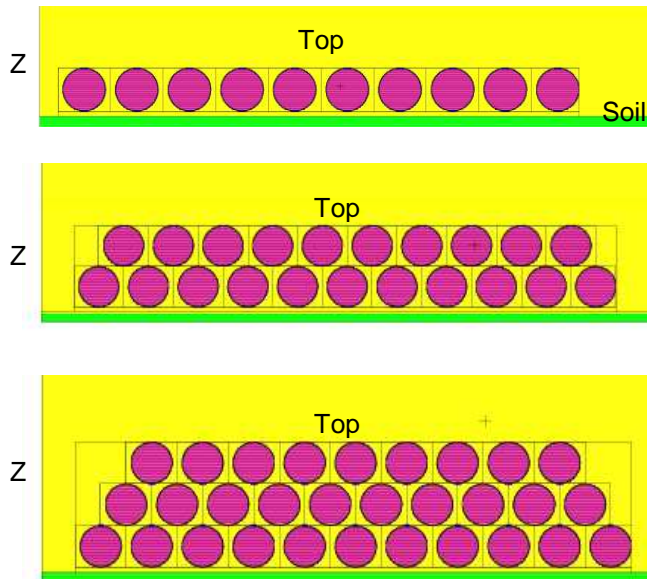
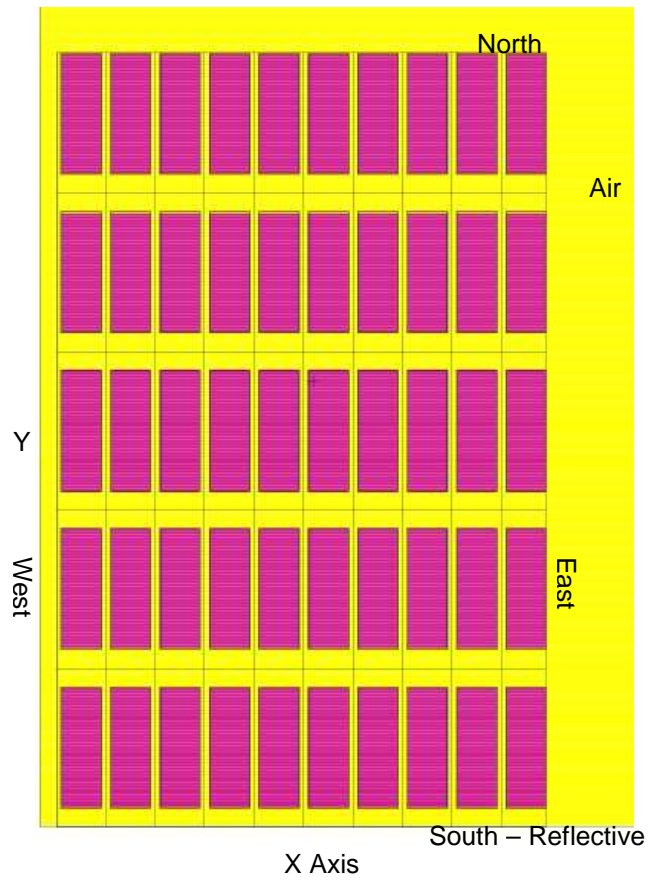


Figure 5-5 10x10 Filled Feed Cylinder Array – Single, Double and Triple Stacks

(See Figure 5-5 for direction, axis and material details)

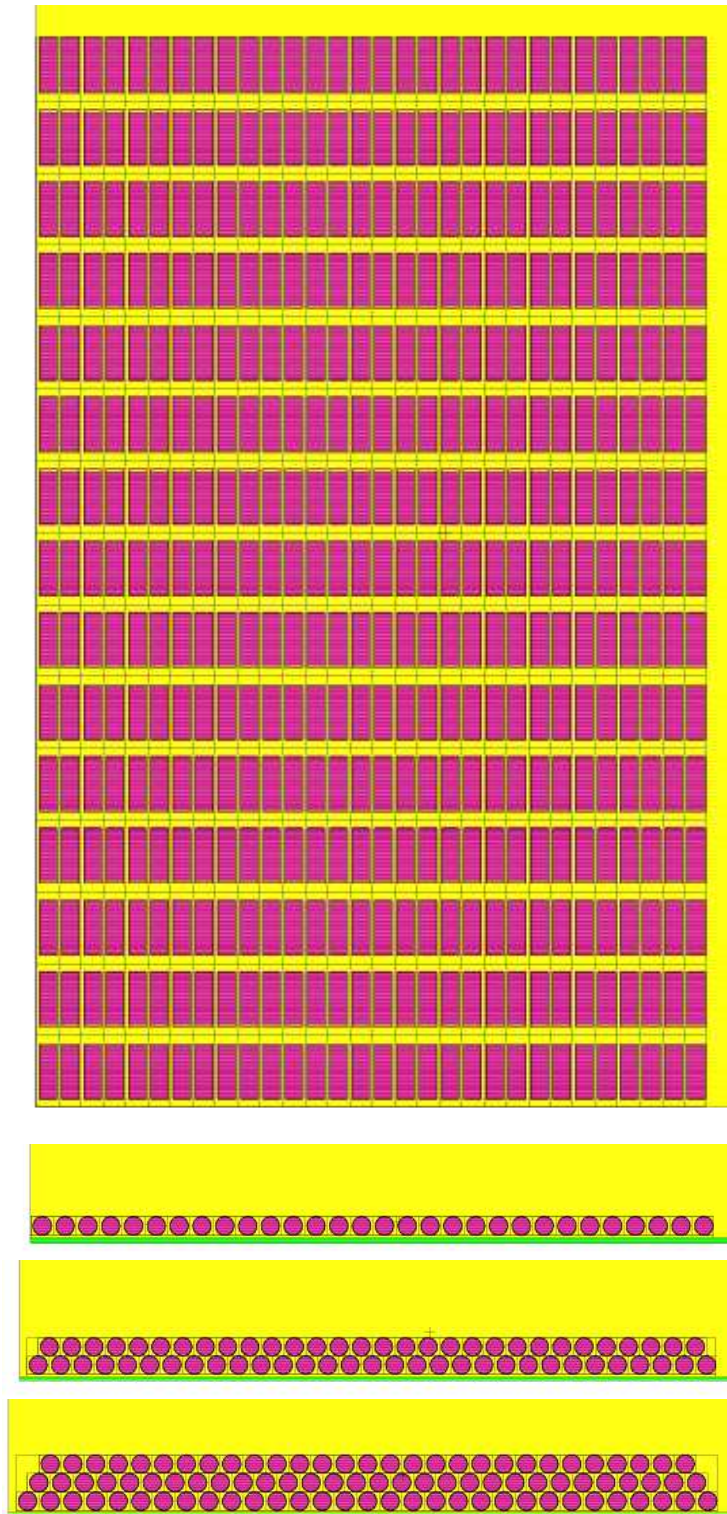


Figure 5-6 30x30 Filled Feed Cylinder Array – Single, Double and Triple Stacks

(See Figure 5-5 for direction, axis and material details)

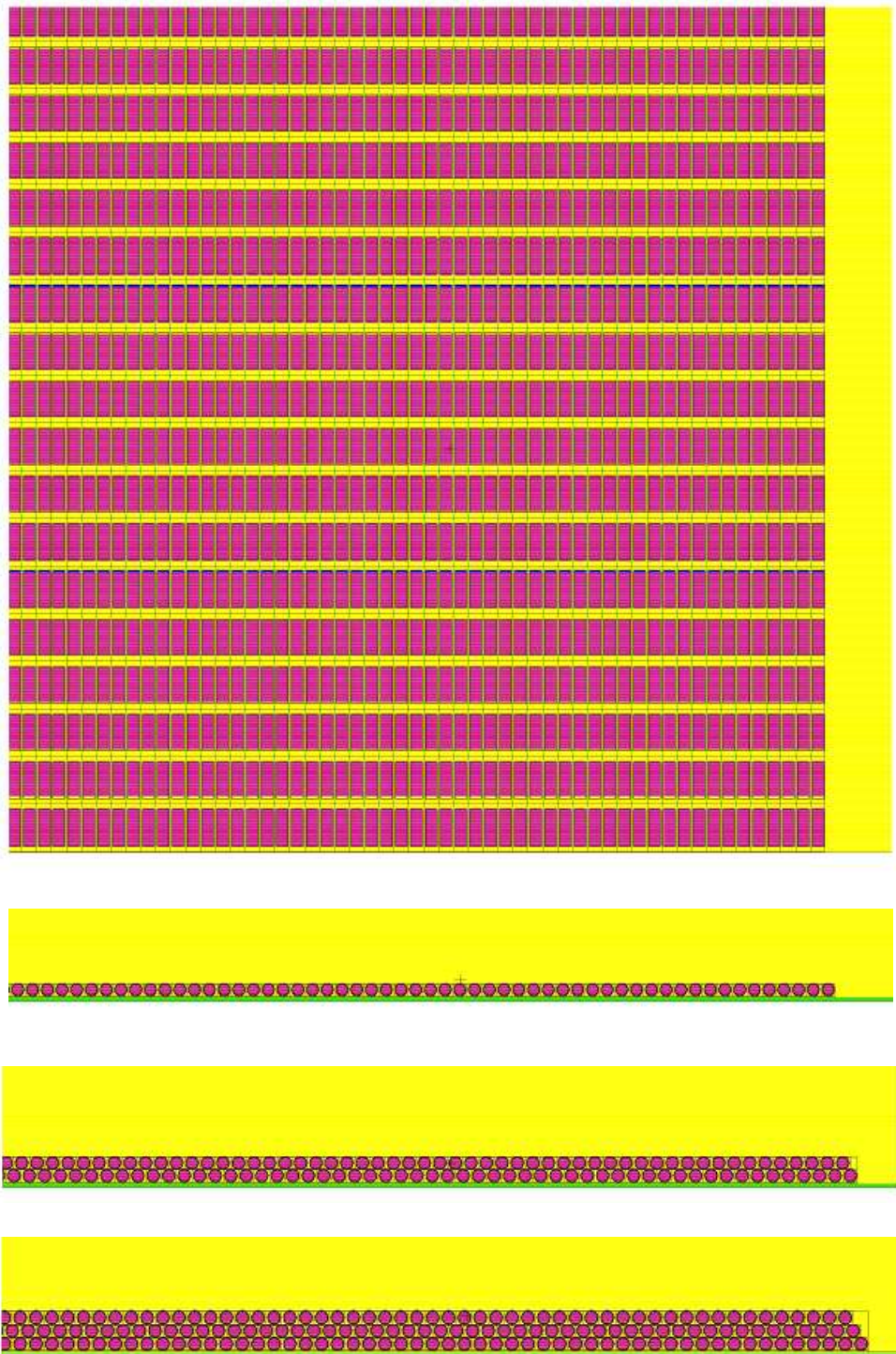


Figure 5-7 100x100 Filled Feed Cylinder Array – Single, Double and Triple Stacks

The MCNP5, v1.60 code was employed to write and save a surface source file for the tracks reaching the top, east and north faces of the cylinder-containing box. These faces corresponded to the top, east and north edges of the cylinder array. The sources on these surfaces would contribute to the doses in the radial direction on the east side of concern to the case study.

For the neutron calculations, the source energy and direction biasing schemes as described in Sections 5.3.2 and 5.3.3, respectively were applied to each case. The source position was unbiased with uniform sampling and equal weighting for each cylinder, as the source position biasing offered no special advantage for neutron transport.

For the photon calculations, the biased source distributions covered position, energy and direction (Sections 5.3.1, 5.3.2 and 5.3.3, respectively). The source importance data in Tables 5-1 and 5-2 were applied to the MCNP photon calculations as described in Table 5-6.

Table 5-6 Application of Photon Source Importance Data to Case Study

Storage Array	Stacking	Photon Source Importance Data Application
10x10	Single	Used the top stack data in Table 4-2 directly.
	Double	Used all the data in Table 4-2 directly.
	Triple	Used the top stack data in Table 4-2 for the top stack, and the bottom stack data in Table 4-2 for middle and bottom stacks.
30x30	Single	Used the top stack data in Table 4-3 directly.
	Double	Used the top stack data in Table 4-3 directly, but modified the bottom stack data to 0.001 for all normalized values < 0.001.
	Triple	Used the top stack data in Table 4-3 for the top stack and the modified bottom stack data for the middle and bottom stacks.
100x100	Single	Used the top stack data in Table 4-3 with extrapolation until the normalized importance dropped to 0.001. After that, the importance for all the remaining cylinders was taken as 0.001.
	Double	Applied the importance data for the 100x100 single stack to the top stack, and the modified 30x30 bottom stack data to the bottom stack.
	Triple	Applied the importance data for the 100x100 single stack to the top stack, and the modified 30x30 bottom stack data to the middle and bottom stacks.

The MCNP input and output files created from the first-step process are listed in Table G-1 in Appendix G along with the CPU time consumed, number of particle histories (nps) processed, and number of tracks written for the pertinent surfaces on the surface source file. The CPU time includes the input/output processing time and *CTME* entry for computer time cutoff in MCNP. For neutron cases, the *CTME* was set at 100 minutes for every case, sufficient to achieve satisfactory statistics. For photon cases, the *CTME* was set at 100, 200 and 300 minutes for single, double and triple stacking, respectively.

Appendix G provides the sample MCNP input files created in the first step process, including t100x100n01.txt and t100x100p01.txt for the triple-stacked 100x100 array neutron and photon cases for illustration purposes. Other cases are similar but relatively simpler with fewer cylinders modeled.

5.4.4 Second-Step Process

The dose results at the receptors of interest were produced from the second-step process. This process read the surface source file written and saved from the first-step process as the starting source. The geometric model for the second step was fairly simple, containing a zero-importance black box for the cylinders plus the surrounding environmental air and ground soil. The air region in the radial direction was subdivided into intervals with 100 m wide each for using the prescribed feature of cell importance available in MCNP. This feature controlled and maintained the particle population to be fairly constant in each air sub-cell for variance reduction purposes. Furthermore, sufficient air space was provided to account for air back-scattering. A reflective boundary was placed on the south boundary for geometric symmetry as modeled in the first step. Figure 5-8 illustrates the geometric model for the case of the 10x10 storage array in triple stacking. The models for other cases are

identical with the exception that the black cylinder box size varies, depending on the array size and stacking configuration.

The mesh tally was used to obtain the average dose rate in each mesh element with the MCNP5, v1.60 code. The mesh structure was constructed such that there were a large and adequate number of radial intervals (X direction) to produce the radial dose rate profile. In light of minor axial dose variations, coarse meshes were used for the axial direction (Y direction) to increase the scoring volumes for better statistics. For the vertical direction (Z direction), average tallies were made for a personnel level of 8 ft (~244 cm), as there was no appreciable vertical dose variation within this height from a plane source.

The mesh tallies could be generated for each contributing surface source individually or together. The breakdown by the contributing surface source provided the results for a quick and reasonable dose estimate from single stacking to double stacking or triple stacking (see discussion in Section 7.3).

The MCNP input and output files created in the second-step process are listed in Table G-2 in Appendix G, together with the surface source files used, CPU times consumed, and mesh tally files generated. The mesh tally files were then used to plot the two-dimensional dose maps and associated relative errors with the MCNPLOT Tally Plotter available in the MCNP code [LANL 2008, Appendix B, §III]. As for the MCNP Plot Geometry Plotter, the Xming Windows displayer server was used to generate the plots as postscript files, which were then opened and viewed with the GSview graphical interface utility program.

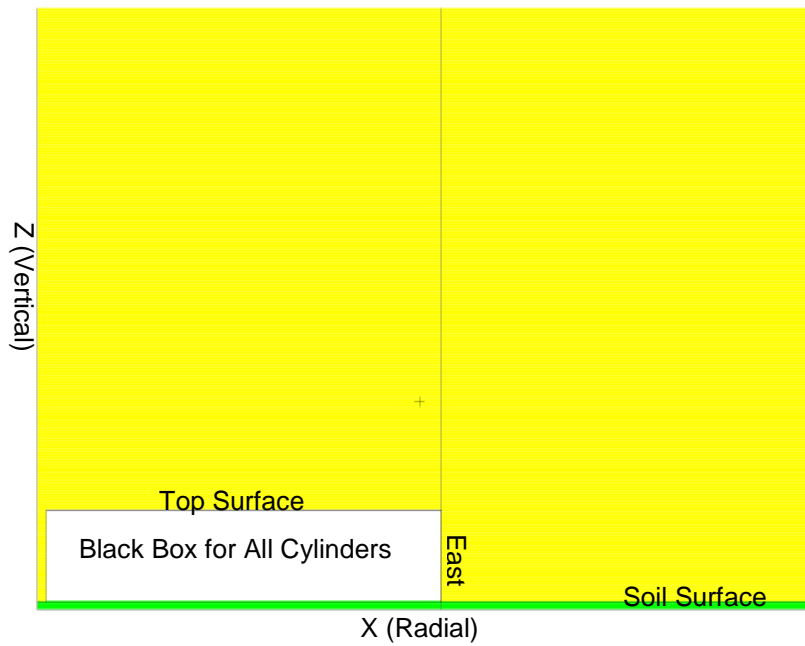
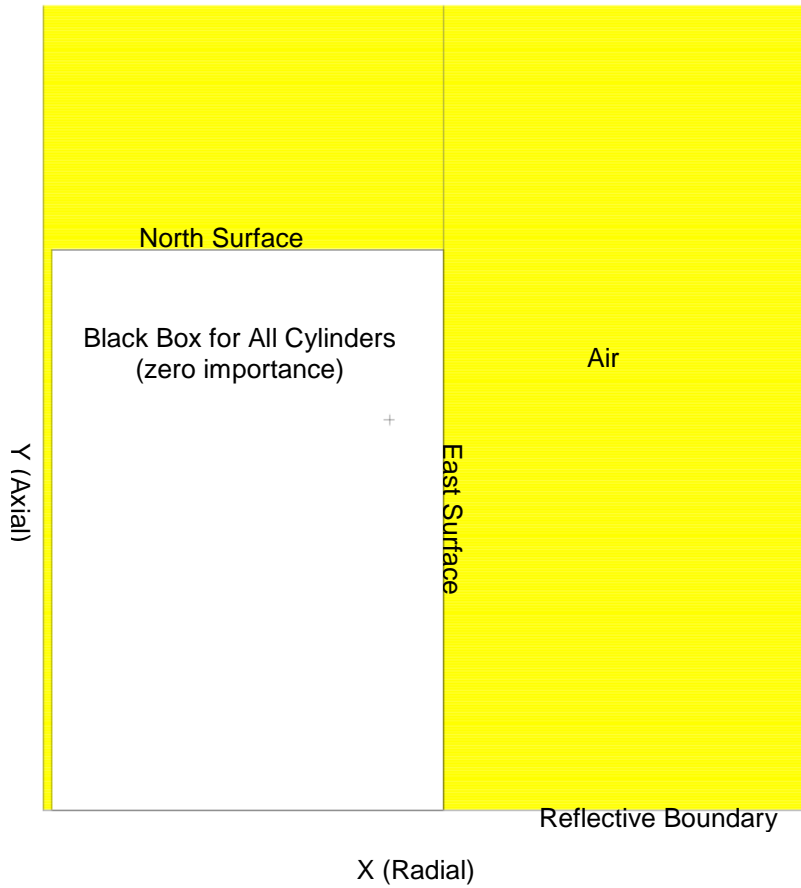


Figure 5-8 Triple Stacked 10x10 Array Model for 2nd Step MCNP Calculation

6. MULTIPLE CYLINDER DOSE RESULTS AND IMPACTS

The application of the methodology and process developed in Chapter 5 produced the neutron and photon dose rate results for different configurations of cylinder storage arrays. The dose assessment covered both filled and empty feed cylinders. The use of filled feed cylinders bounds filled tails cylinders, as their photon dose levels are practically the same, and the neutron dose level is slightly higher from the filled feed cylinders.

The multiple cylinder dose results presented and discussed in this chapter include the following items:

- Neutron dose rate results for filled feed cylinders
- Photon dose rate results for filled feed cylinders
- Total dose rate results for filled feed cylinders
- Photon dose rate results for empty feed cylinders

The dose levels impact cylinder storage management such as spacing, stacking, capacity, footprint and setback distances from the site boundary. This chapter includes a dose impact analysis to address these storage issues.

6.1 NEUTRON DOSE RATES FOR FILLED FEED CYLINDERS

The *runtpc* file created from the second step of the MCNP calculation for each case was used to plot the mesh tally results with the Z option on the MCNP execution line. Figures H-1 through H-9 in Appendix H reproduce the neutron dose rate maps and their associated relative errors for different arrays and stacking configurations of 48Y filled feed cylinders, as generated from the MCNP execution.

Using the mesh tally results from the second step of the MCNP calculations, the representative radial neutron dose rate profiles at the mid-plane are presented in Tables 6-1 through 6-3 and Figures 6-1 through 6-3 for the 10x10, 30x30 and 100x100 arrays, respectively. The dose sensitivity to the array size and stacking configuration is discussed in Section 6.3.

Based on Figures H-1 through H-9 in Appendix H, the neutron dose rate results are generally statistically acceptable in the radial direction out to 500 m from the edge of the nearest cylinder on the east side, as the associated relative errors meet the MCNP-prescribed criterion of 0.1 [LANL 2008, Table 2.5] for the tally over a volume element. As expected, the statistics are better in the radial direction than in the axial direction, as the neutron source direction biasing favored the particle histories moving in the radial direction.

The array sizes and stacking configurations affect the required CPU time to reach satisfactory statistics. In the first step of the MCNP calculations for neutrons, the same computer cutoff time with CTME = 100 minutes was used for all cases regardless of the array size or stacking configuration. For each array size, the resulting relative errors became larger (but still acceptable) as more stacks were placed, implying that more time would be required for the double and triple stacking configurations to achieve the same statistics as for the single stacking configurations.

In the MCNP mesh tally, the same number of axial intervals was used to cover the entire axial length of the cylinder array. This modeling approach increased the mesh element volume as the array size increased. The larger mesh element volumes enabled the 100x100 storage array to achieve very favorable statistics for all three stacking configurations with the same computer run time.

Table 6-1 Radial Neutron Dose Rate Profile for 10x10 Array

48Y Filled Feed Cylinder Storage - 10x10 Array - No Cell Source Biasing Neutron Dose Rate (mrem/h)						
Distance (m)	Neutron Dose Rate (mrem/h)			Relative Error		
	Single Stack	Double Stack	Triple Stack	Single Stack	Double Stack	Triple Stack
0	1.65E-01	1.83E-01	1.91E-01	0.0051	0.0064	0.0074
1	8.47E-02	1.23E-01	1.43E-01	0.0053	0.0066	0.0121
5	3.00E-02	5.08E-02	6.76E-02	0.0066	0.0088	0.0159
11	1.53E-02	2.64E-02	3.46E-02	0.0081	0.0110	0.0197
22	7.50E-03	1.27E-02	1.72E-02	0.0086	0.0135	0.0244
50	2.58E-03	4.01E-03	4.96E-03	0.0136	0.0208	0.0375
105	7.22E-04	1.08E-03	1.20E-03	0.0153	0.0278	0.0492
155	3.19E-04	4.76E-04	5.65E-04	0.0191	0.0308	0.0556
205	1.51E-04	2.13E-04	2.64E-04	0.0220	0.0313	0.0576
255	8.23E-05	1.29E-04	1.38E-04	0.0261	0.0425	0.0632
305	4.66E-05	6.58E-05	7.93E-05	0.0354	0.0417	0.0736
355	2.80E-05	3.44E-05	4.09E-05	0.0374	0.0460	0.0594
395	1.76E-05	2.17E-05	2.70E-05	0.0480	0.0459	0.0793

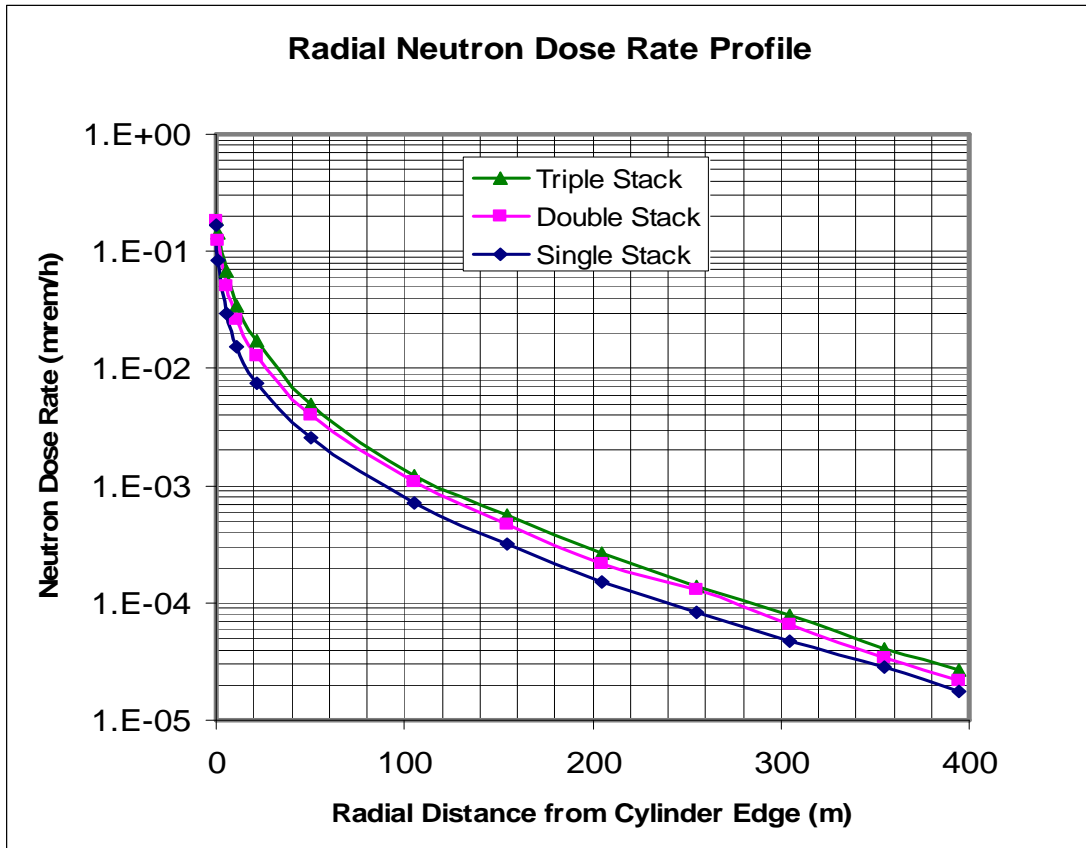


Figure 6-1 Radial Neutron Dose Rate Profile for 10x10 Array

Table 6-2 Radial Neutron Dose Rate Profile for 30x30 Array

48Y Filled Feed Cylinder Storage - 30x30 Array - No Cell Source Biasing Neutron Dose Rate (mrem/h)						
Distance (m)	Dose Rate (mrem/h)			Relative Error		
	Single Stack	Double Stack	Triple Stack	Single Stack	Double Stack	Triple Stack
0	1.81E-01	2.00E-01	2.15E-01	0.0100	0.0103	0.0126
1	1.05E-01	1.42E-01	1.66E-01	0.0077	0.0139	0.0243
5	5.11E-02	7.37E-02	8.98E-02	0.0082	0.0187	0.0204
11	3.40E-02	4.85E-02	6.04E-02	0.0078	0.0169	0.0231
22	2.31E-02	3.24E-02	3.94E-02	0.0077	0.0177	0.0240
50	1.21E-02	1.66E-02	1.87E-02	0.0098	0.0229	0.0283
105	4.58E-03	6.17E-03	7.09E-03	0.0107	0.0211	0.0354
155	2.27E-03	3.04E-03	3.29E-03	0.0134	0.0337	0.0367
205	1.16E-03	1.57E-03	1.67E-03	0.0153	0.0363	0.0366
255	6.26E-04	8.46E-04	9.08E-04	0.0170	0.0376	0.0409
305	3.52E-04	4.50E-04	5.10E-04	0.0191	0.0343	0.0437
355	2.02E-04	2.70E-04	2.92E-04	0.0240	0.0545	0.0557
395	1.25E-04	1.65E-04	1.72E-04	0.0249	0.0426	0.0594

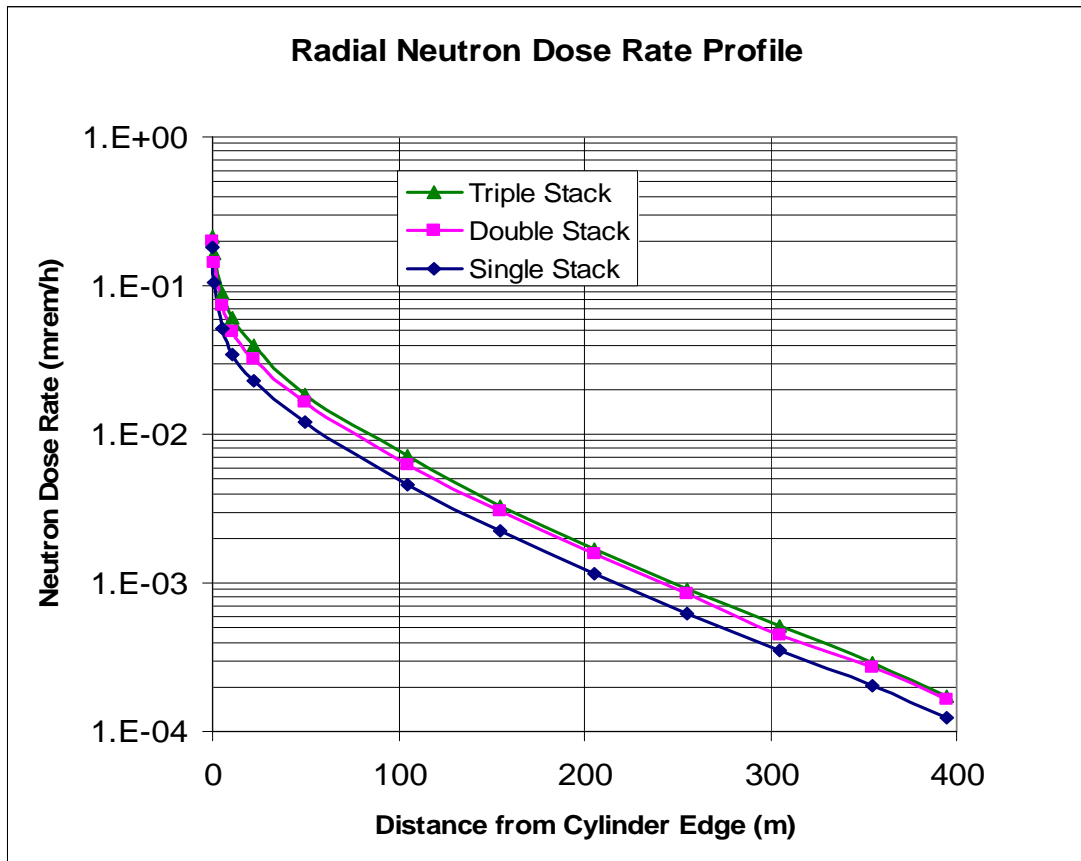


Figure 6-2 Radial Neutron Dose Rate Profile for 30x30 Array

Table 6-3 Radial Neutron Dose Rate Profile for 100x100 Array

48Y Filled Feed Cylinder Storage - 100x100 Array - No Cell Source Biasing Neutron Dose Rate (mrem/h)						
Distance (m)	Dose Rate (mrem/h)			Relative Error		
	Single Stack	Double Stack	Triple Stack	Single Stack	Double Stack	Triple Stack
0	2.09E-01	2.48E-01	2.58E-01	0.0155	0.0216	0.0205
1	1.46E-01	1.88E-01	2.24E-01	0.0130	0.0227	0.0336
5	9.72E-02	1.29E-01	1.43E-01	0.0124	0.0228	0.0280
11	7.77E-02	1.03E-01	1.15E-01	0.0114	0.0198	0.0309
22	6.12E-02	7.79E-02	8.95E-02	0.0091	0.0176	0.0288
50	4.02E-02	5.07E-02	5.56E-02	0.0102	0.0201	0.0292
105	1.98E-02	2.38E-02	2.71E-02	0.0105	0.0169	0.0315
155	1.10E-02	1.31E-02	1.42E-02	0.0117	0.0185	0.0297
205	6.23E-03	7.83E-03	8.54E-03	0.0144	0.0214	0.0355
255	3.73E-03	4.34E-03	4.67E-03	0.0147	0.0225	0.0302
305	2.19E-03	2.61E-03	2.66E-03	0.0169	0.0252	0.0322
355	1.27E-03	1.70E-03	1.70E-03	0.0181	0.0300	0.0403
395	8.13E-04	9.96E-04	1.04E-03	0.0214	0.0416	0.0413

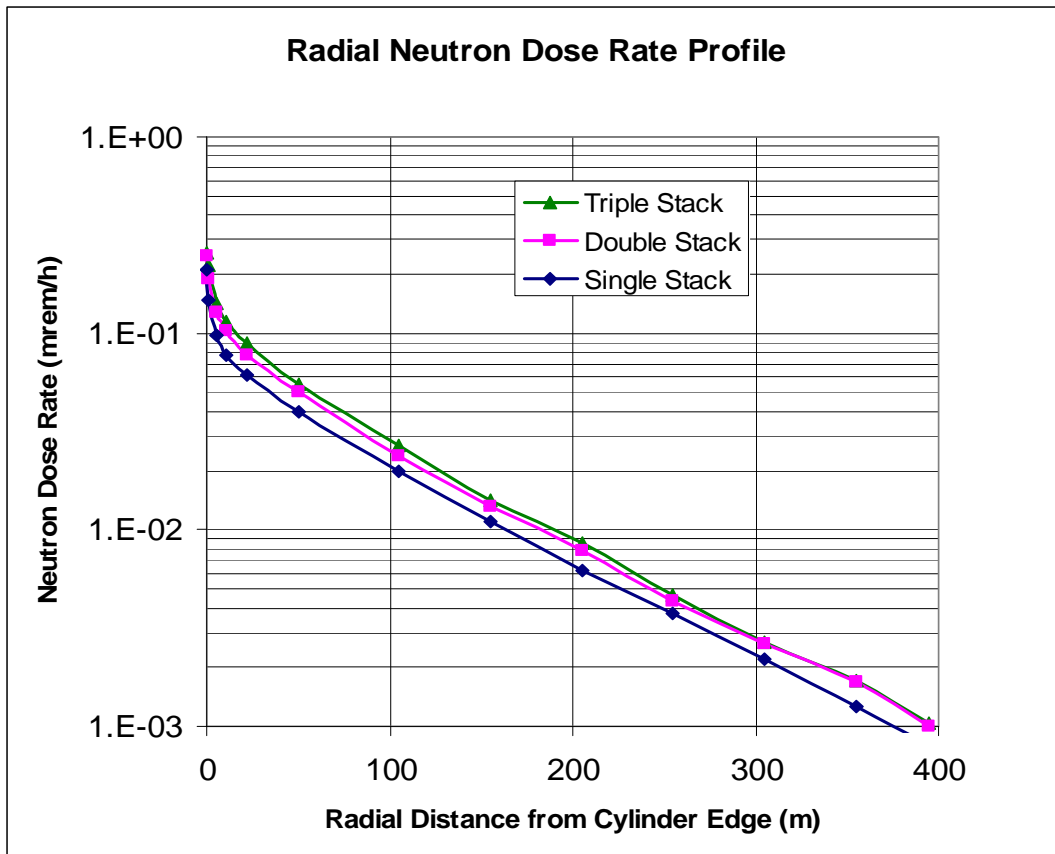


Figure 6-3 Radial Neutron Dose Rate Profile for 100x100 Array

6.2 PHOTON DOSE RATES FOR FILLED FEED CYLINDERS

As for the neutron cases, the *runtpc* file created from the second step of the MCNP calculation for each photon case was used to plot the mesh tally results with the Z option on the MCNP execution line. Figures H-10 through H-18 in Appendix H reproduce the photon dose rate maps and their associated relative errors for different arrays and stacking configurations of 48Y filled feed cylinders, as created from this MCNP execution.

Using the mesh tally results from the second step of the MCNP calculations, the representative radial photon dose rate profiles are presented in Tables 6-4 through 6-6 and Figures 6-4 through 6-6 for the 10x10, 30x30 and 100x100 arrays, respectively. The dose sensitivity to the array size and stacking configuration is discussed in Section 6.3.

The array sizes and stacking configurations affect the required CPU time to reach satisfactory statistics. In the first step of the MCNP calculations for photons, the same cutoff time was used for all array sizes for a given stacking configuration – 100 minutes for one high, 200 minutes for two high and 300 minutes for three high. All the cases achieved similar statistics with these run times.

The statistics for the photon dose rate results are less favorable than those for the neutron dose rate results despite more computer time consumed for the double and triple stacking configurations. This outcome was not surprising, because of the larger self-shielding effect of UF_6 for photons. In contrast to the neutron results, the statistics for photon results are considerably better in the radial direction than in the axial direction (see Figures H-10 through H-18 in Appendix H), as the photon calculations included the source position importance data besides the direction biasing to favor the particle histories moving in the

radial direction and receptors located on the east side. The neutron calculations did not consider the source position biasing, which was shown to be unnecessary.

The MCNP mesh tally used the same mesh structure for both neutrons and photons. Therefore, the neutron and photon results corresponded to the same mesh elements or detector locations.

Table 6-4 Radial Photon Dose Rate Profile for 10x10 Array

48Y Filled Feed Cylinder Storage - 10x10 Array Photon Dose Rate (mrem/h)						
Distance (m)	Photon Dose Rate (mrem/h)			Relative Error		
	Single Stack	Double Stack	Triple Stack	Single Stack	Double Stack	Triple Stack
0	1.13E+00	1.19E+00	1.21E+00	0.0020	0.0020	0.0042
1	5.26E-01	7.23E-01	8.26E-01	0.0032	0.0036	0.0038
5	1.56E-01	2.59E-01	3.41E-01	0.0091	0.0059	0.0061
11	7.09E-02	1.24E-01	1.71E-01	0.0147	0.0078	0.0086
22	2.95E-02	5.38E-02	7.52E-02	0.0076	0.0153	0.0135
50	8.19E-03	1.39E-02	1.85E-02	0.0295	0.0274	0.0229
105	1.80E-03	2.84E-03	3.77E-03	0.0217	0.0252	0.0261
155	7.50E-04	1.13E-03	1.45E-03	0.0366	0.0374	0.0426
205	3.66E-04	5.13E-04	6.96E-04	0.0332	0.0388	0.0653
255	1.73E-04	2.53E-04	3.70E-04	0.0339	0.0393	0.0501
305	1.04E-04	1.37E-04	2.07E-04	0.0413	0.0476	0.0559
355	6.02E-05	7.97E-05	1.09E-04	0.0481	0.0515	0.0557
395	3.70E-05	5.14E-05	7.54E-05	0.0502	0.0560	0.0829

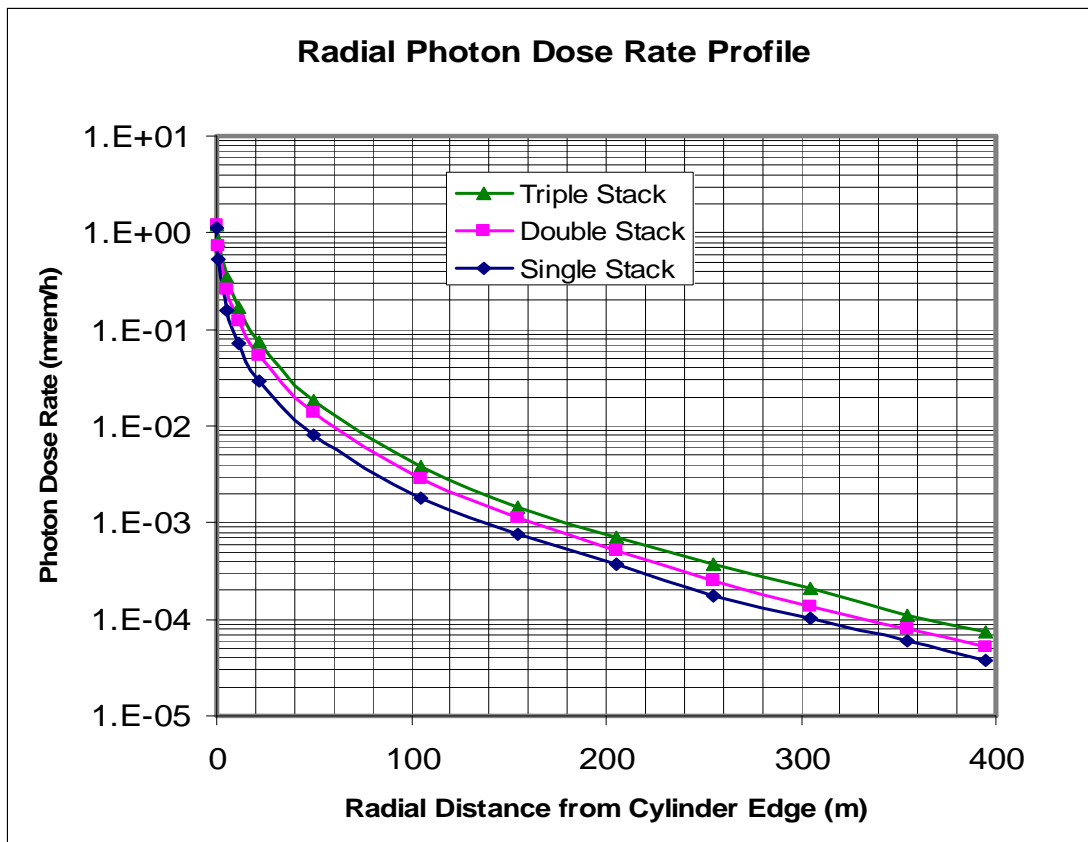


Figure 6-4 Radial Photon Dose Rate Profile for 10x10 Array

Table 6-5 Radial Photon Dose Rate Profile for 30x30 Array

48Y Filled Feed Cylinder Storage - 30x30 Array Photon Dose Rate (mrem/h)						
Distance (m)	Dose Rate (mrem/h)			Relative Error		
	Single Stack	Double Stack	Triple Stack	Single Stack	Double Stack	Triple Stack
0	1.13E+00	1.21E+00	1.23E+00	0.0023	0.0030	0.0024
1	5.47E-01	7.42E-01	8.47E-01	0.0037	0.0049	0.0046
5	1.81E-01	2.84E-01	3.76E-01	0.0125	0.0070	0.0085
11	9.66E-02	1.53E-01	2.03E-01	0.0098	0.0098	0.0087
22	5.30E-02	8.16E-02	1.08E-01	0.0130	0.0146	0.0124
50	2.41E-02	3.40E-02	4.35E-02	0.0194	0.0156	0.0215
105	9.04E-03	1.19E-02	1.42E-02	0.0301	0.0310	0.0236
155	4.23E-03	5.47E-03	6.15E-03	0.0314	0.0443	0.0296
205	2.01E-03	2.74E-03	2.98E-03	0.0315	0.0362	0.0245
255	1.12E-03	1.40E-03	1.68E-03	0.0412	0.0337	0.0273
305	6.77E-04	8.38E-04	9.55E-04	0.0484	0.0686	0.0308
355	3.64E-04	4.59E-04	5.30E-04	0.0416	0.0374	0.0365
395	2.51E-04	3.28E-04	3.63E-04	0.0589	0.0637	0.0510

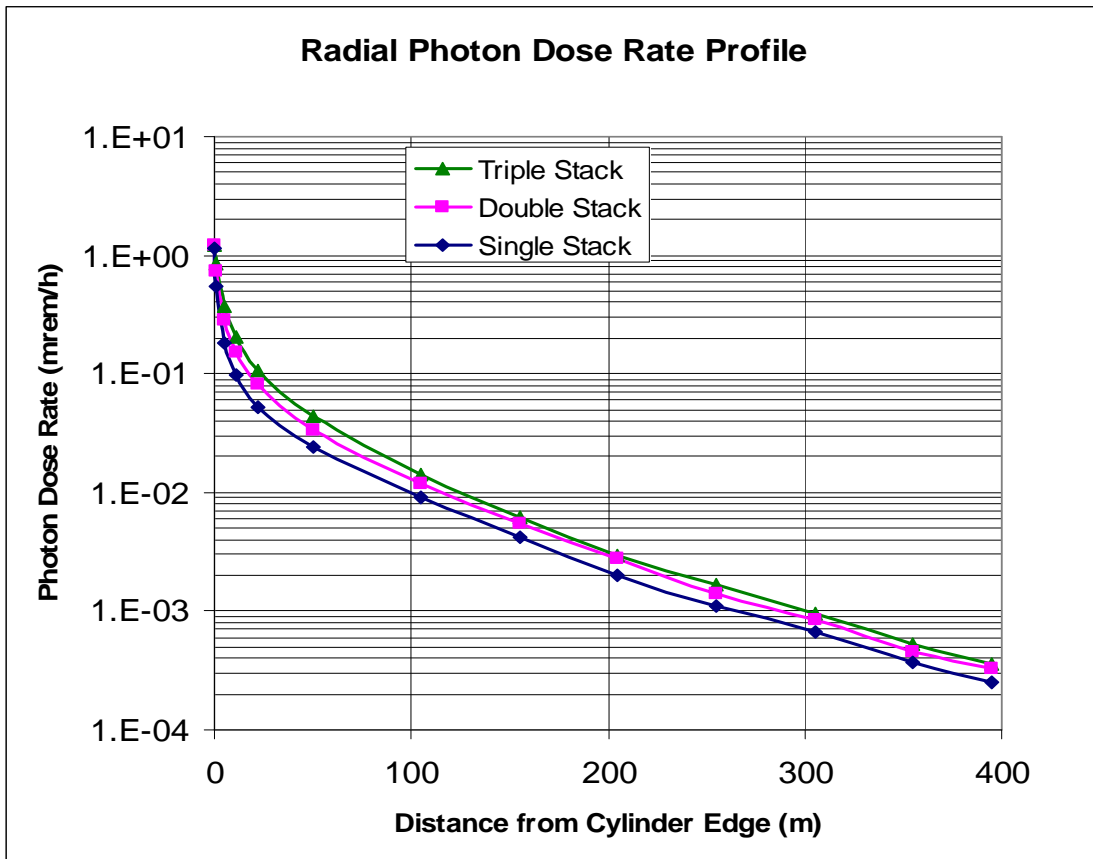


Figure 6-5 Radial Photon Dose Rate Profile for 30x30 Array

Table 6-6 Radial Photon Dose Rate Profile for 100x100 Array

48Y Filled Feed Cylinder Storage - 100x100 Array Photon Dose Rate (mrem/h)						
Distance (m)	Dose Rate (mrem/h)			Relative Error		
	Single Stack	Double Stack	Triple Stack	Single Stack	Double Stack	Triple Stack
0	1.16E+00	1.25E+00	1.27E+00	0.0048	0.0092	0.0046
1	6.00E-01	7.97E-01	8.71E-01	0.0074	0.0165	0.0085
5	2.43E-01	3.43E-01	4.13E-01	0.0172	0.0228	0.0163
11	1.60E-01	2.20E-01	2.47E-01	0.0301	0.0357	0.0113
22	1.07E-01	1.40E-01	1.60E-01	0.0237	0.0394	0.0212
50	6.19E-02	7.58E-02	8.89E-02	0.0355	0.0285	0.0461
105	2.98E-02	3.54E-02	3.86E-02	0.0333	0.0368	0.0301
155	1.68E-02	1.87E-02	2.20E-02	0.0414	0.0307	0.0423
205	9.05E-03	1.16E-02	1.20E-02	0.0370	0.0419	0.0305
255	5.42E-03	6.41E-03	6.99E-03	0.0364	0.0562	0.0325
305	3.57E-03	3.83E-03	4.35E-03	0.0441	0.0425	0.0394
355	1.92E-03	2.20E-03	2.47E-03	0.0382	0.0490	0.0820
395	1.22E-03	1.45E-03	1.55E-03	0.0386	0.0472	0.0443

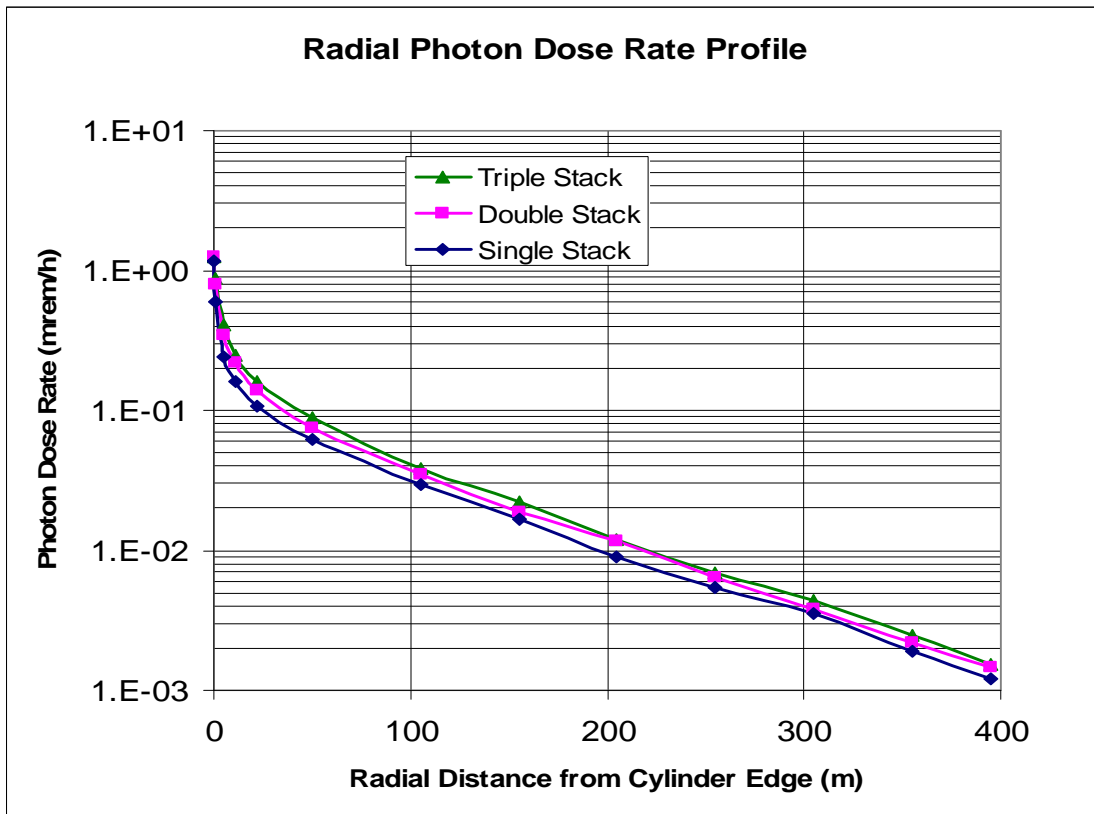


Figure 6-6 Radial Photon Dose Rate Profile for 100x100 Array

6.3 TOTAL DOSE RATES FOR FILLED FEED CYLINDERS

The neutron and photon dose rate results presented in Sections 6.1 and 6.2 were combined to give the total dose rate results as presented in Tables 6-7 through 6-9 and Figures 6-7 through 6-9. The tabulation includes the associated relative errors calculated as follows:

$$\sigma_t = \text{sqrt}[(D_n * \sigma_n)^2 + (D_p * \sigma_p)^2] / D_t$$

where D_t , D_n and D_p are the total, neutron and photon dose rates, respectively, and σ_t , σ_n and σ_p are the corresponding relative errors. All the relative errors meet the acceptance criterion of less than 0.1 as prescribed in the MCNP manual [LANL 2008, Table 2.5].

The photon dose is a principal component of the total dose. However, its relative importance decreases as the distance increases because of greater neutron skyshine contributions. This behavior is consistent with the observation for a single cylinder as discussed in Section 4.7.5 in Chapter 4.

The total dose rates are used in Section 6.5 to address the dose impacts to storage management of filled cylinders.

Table 6-7 Radial Total Dose Rate Profile for 10x10 Array

Filled Feed Cylinder Storage - 10x10 Array Total Dose Rate (mrem/h)						
Distance (m)	Total Dose Rate (mrem/h)			Relative Error		
	Single Stack	Double Stack	Triple Stack	Single Stack	Double Stack	Triple Stack
0	1.30E+00	1.37E+00	1.40E+00	0.0019	0.0019	0.0038
1	6.11E-01	8.45E-01	9.69E-01	0.0029	0.0034	0.0037
5	1.86E-01	3.10E-01	4.09E-01	0.0077	0.0053	0.0057
11	8.62E-02	1.51E-01	2.06E-01	0.0122	0.0070	0.0079
22	3.70E-02	6.65E-02	9.24E-02	0.0063	0.0129	0.0119
50	1.08E-02	1.79E-02	2.35E-02	0.0227	0.0223	0.0197
105	2.52E-03	3.91E-03	4.97E-03	0.0161	0.0216	0.0231
155	1.07E-03	1.60E-03	2.02E-03	0.0263	0.0287	0.0344
205	5.17E-04	7.31E-04	9.60E-04	0.0244	0.0299	0.0499
255	2.55E-04	3.69E-04	5.08E-04	0.0245	0.0306	0.0403
305	1.51E-04	2.05E-04	2.86E-04	0.0306	0.0386	0.0453
355	8.82E-05	1.15E-04	1.50E-04	0.0349	0.0423	0.0436
395	5.46E-05	7.30E-05	1.02E-04	0.0374	0.0440	0.0645

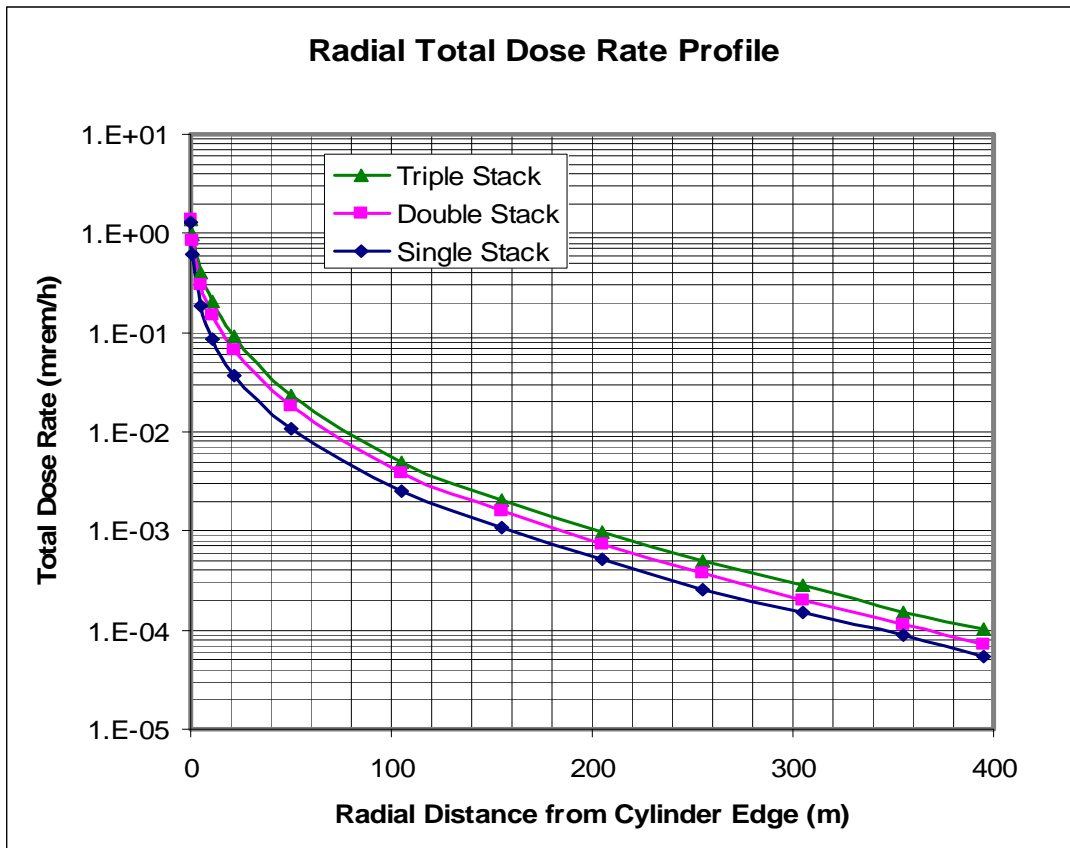


Figure 6-7 Radial Total Dose Rate Profile for 10x10 Array

Table 6-8 Radial Total Dose Rate Profile for 30x30 Array

Filled Feed Cylinder Storage - 30x30 Array						
Total Dose Rate (mrem/h)						
Distance (m)	Total Dose Rate (mrem/h)			Relative Error		
	Single Stack	Double Stack	Triple Stack	Single Stack	Double Stack	Triple Stack
0	1.31E+00	1.41E+00	1.45E+00	0.0024	0.0030	0.0028
1	6.52E-01	8.84E-01	1.01E+00	0.0033	0.0047	0.0055
5	2.32E-01	3.58E-01	4.66E-01	0.0099	0.0068	0.0079
11	1.31E-01	2.02E-01	2.63E-01	0.0075	0.0085	0.0085
22	7.61E-02	1.14E-01	1.47E-01	0.0094	0.0116	0.0111
50	3.62E-02	5.06E-02	6.22E-02	0.0133	0.0129	0.0173
105	1.36E-02	1.81E-02	2.13E-02	0.0203	0.0216	0.0197
155	6.50E-03	8.51E-03	9.44E-03	0.0210	0.0309	0.0231
205	3.17E-03	4.31E-03	4.65E-03	0.0207	0.0265	0.0205
255	1.75E-03	2.25E-03	2.59E-03	0.0271	0.0253	0.0228
305	1.03E-03	1.29E-03	1.47E-03	0.0325	0.0462	0.0252
355	5.66E-04	7.29E-04	8.22E-04	0.0281	0.0310	0.0307
395	3.76E-04	4.93E-04	5.35E-04	0.0402	0.0447	0.0395

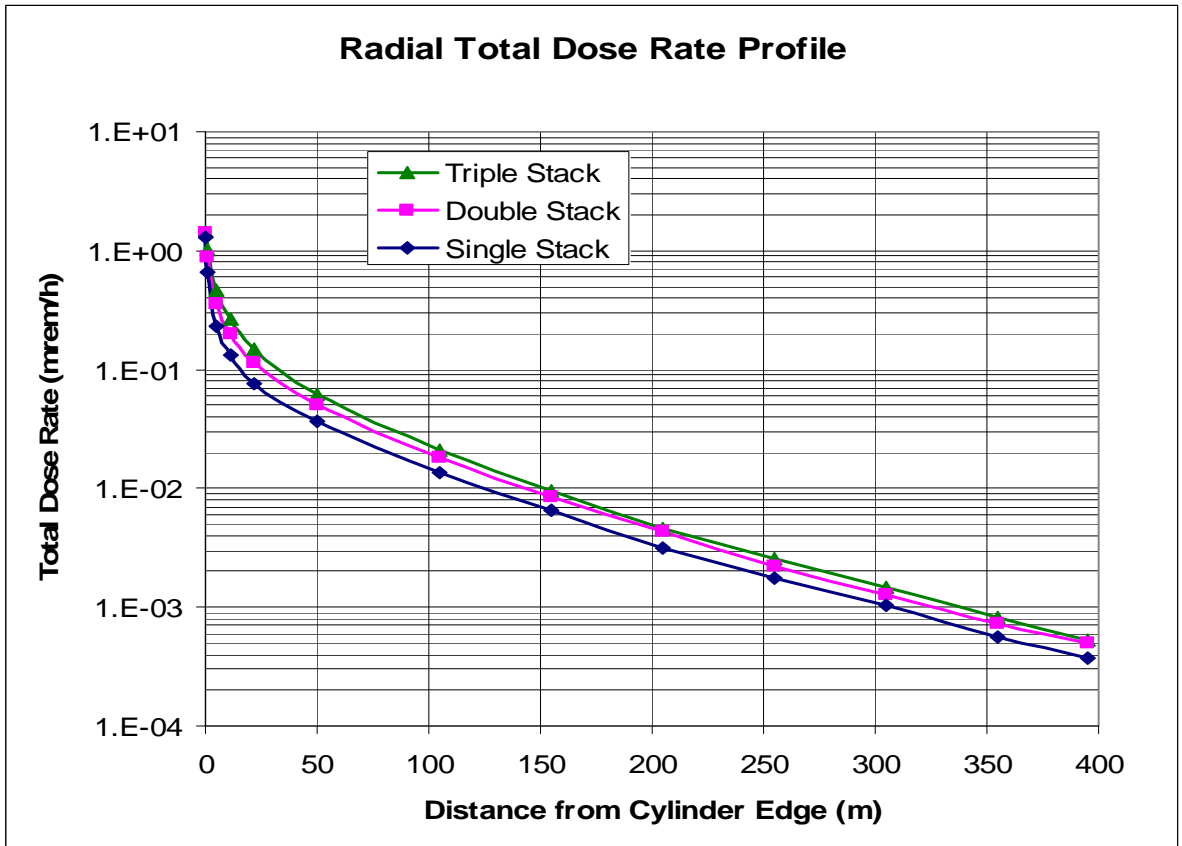


Figure 6-8 Radial Total Dose Rate Profile for 30x30 Array

Table 6-9 Radial Total Dose Rate Profile for 100x100 Array

Filled Feed Cylinder Storage - 100x100 Array Total Dose Rate (mrem/h)						
Distance (m)	Total Dose Rate (mrem/h)			Relative Error		
	Single Stack	Double Stack	Triple Stack	Single Stack	Double Stack	Triple Stack
0	1.37E+00	1.50E+00	1.53E+00	0.0047	0.0085	0.0052
1	7.46E-01	9.85E-01	1.10E+00	0.0065	0.0140	0.0096
5	3.40E-01	4.72E-01	5.56E-01	0.0128	0.0177	0.0141
11	2.38E-01	3.23E-01	3.62E-01	0.0206	0.0251	0.0125
22	1.68E-01	2.18E-01	2.50E-01	0.0154	0.0261	0.0171
50	1.02E-01	1.27E-01	1.45E-01	0.0219	0.0189	0.0305
105	4.96E-02	5.92E-02	6.57E-02	0.0204	0.0230	0.0219
155	2.78E-02	3.18E-02	3.62E-02	0.0254	0.0196	0.0282
205	1.53E-02	1.94E-02	2.05E-02	0.0227	0.0265	0.0231
255	9.15E-03	1.08E-02	1.17E-02	0.0224	0.0347	0.0229
305	5.76E-03	6.44E-03	7.01E-03	0.0281	0.0273	0.0273
355	3.19E-03	3.90E-03	4.17E-03	0.0241	0.0306	0.0513
395	2.03E-03	2.45E-03	2.59E-03	0.0247	0.0327	0.0313

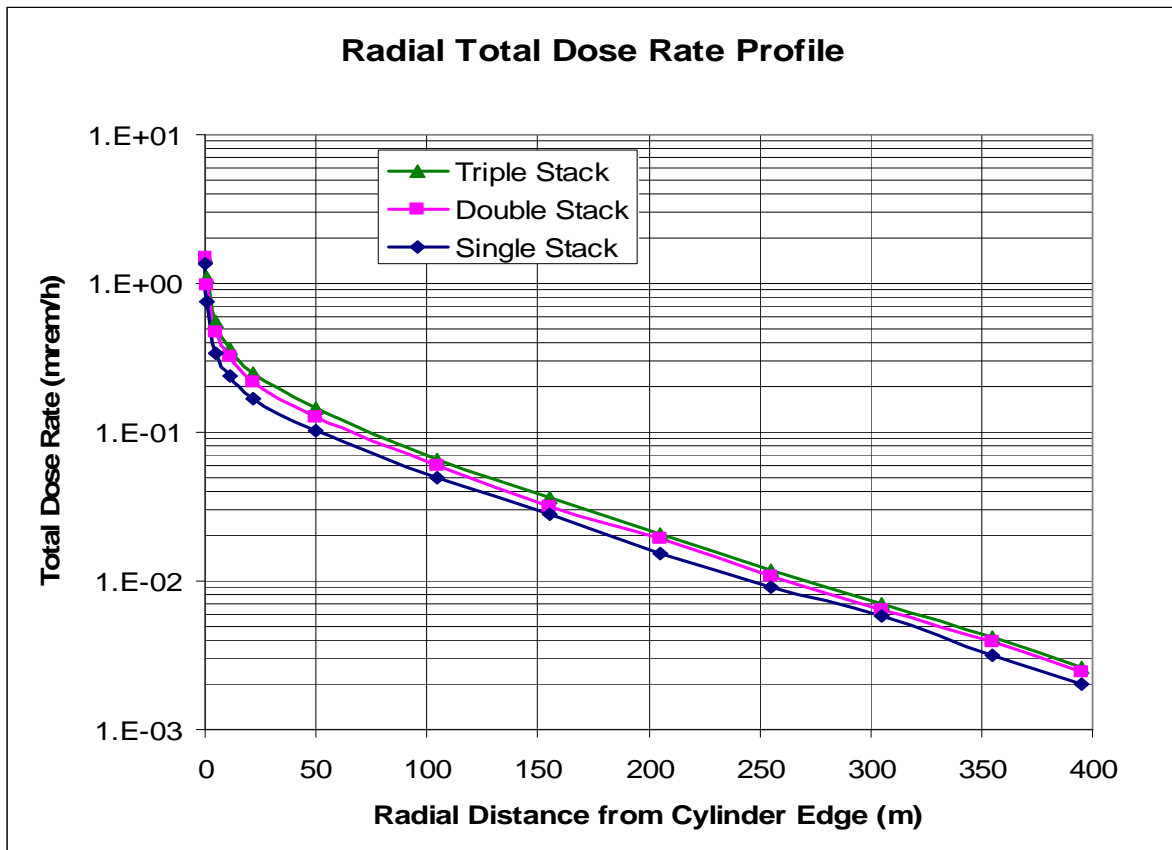


Figure 6-9 Radial Total Dose Rate Profile for 100x100 Array

6.4 DOSE SENSITIVITY TO ARRAY SIZE AND STACKING

Both neutron and photon doses are sensitive to the array size and stacking configuration. Higher doses are apparent as the storage capacity increases with more cylinders placed on the storage pad. To illustrate the dose sensitivity, two representative environmental locations at 105 m and 205 m radially from the nearest cylinder edge were selected for plotting the dose change with the array size and stacking.

For the filled feed cylinders, Figures 6-10 and 6-11 display the neutron dose sensitivity to the array size and stacking at 105 m and 205 m, respectively. The corresponding plots for the photon dose sensitivity are given in Figures 6-12 and 6-13 at 105 m and 205 m, respectively. The dose sensitivity exhibits a similar trend at 105 and 205 m for both neutrons and photons.

The array size affects the neutron dose more than the photon dose, as more cylinders make contributions to the neutron dose because of less self-shielding by UF_6 for neutrons. With respect to stacking, the neutron and photon sensitivity characteristics exhibit similar behavior. The dose increase factor from double stacking to triple stacking is less significant than that from single stacking to double stacking, demonstrating that triple stacking is beneficial to save the storage pad footprint.

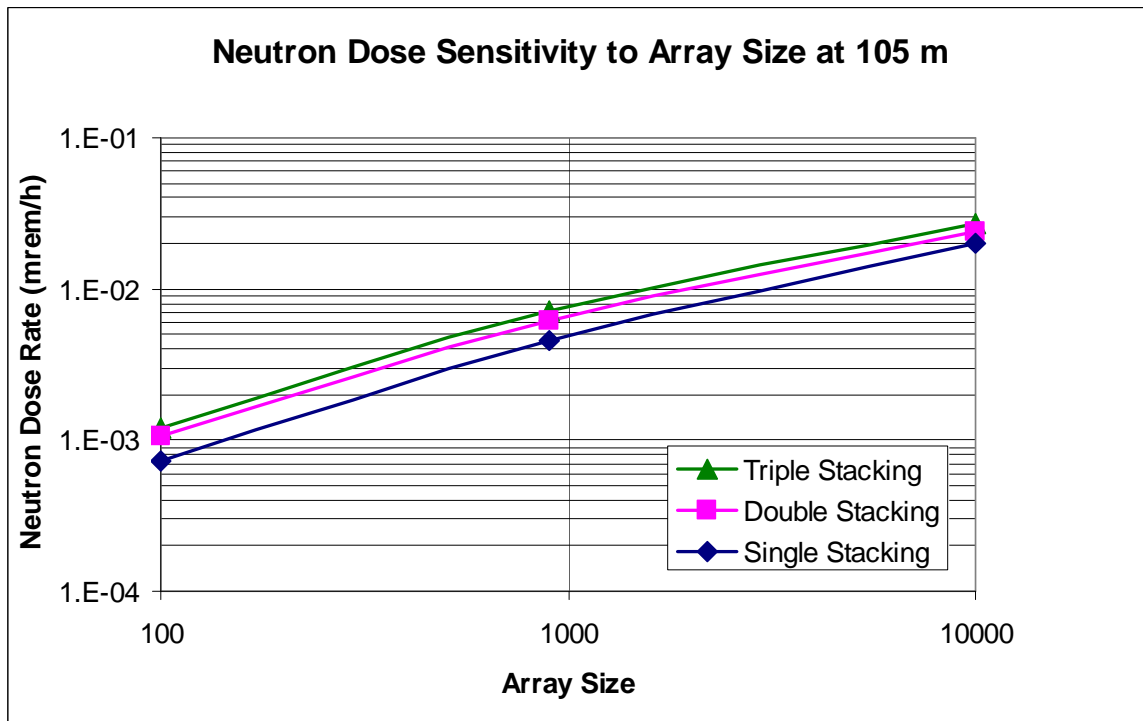
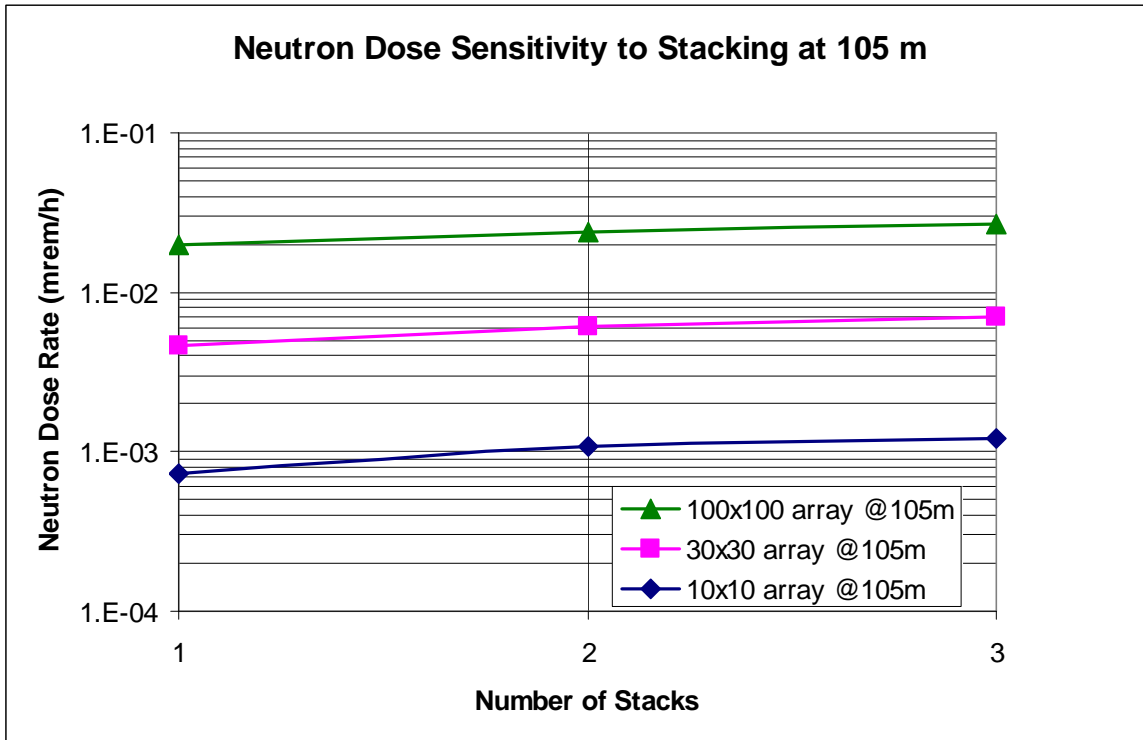


Figure 6-10 Neutron Dose Sensitivity to Array Size and Stacking at 105 m

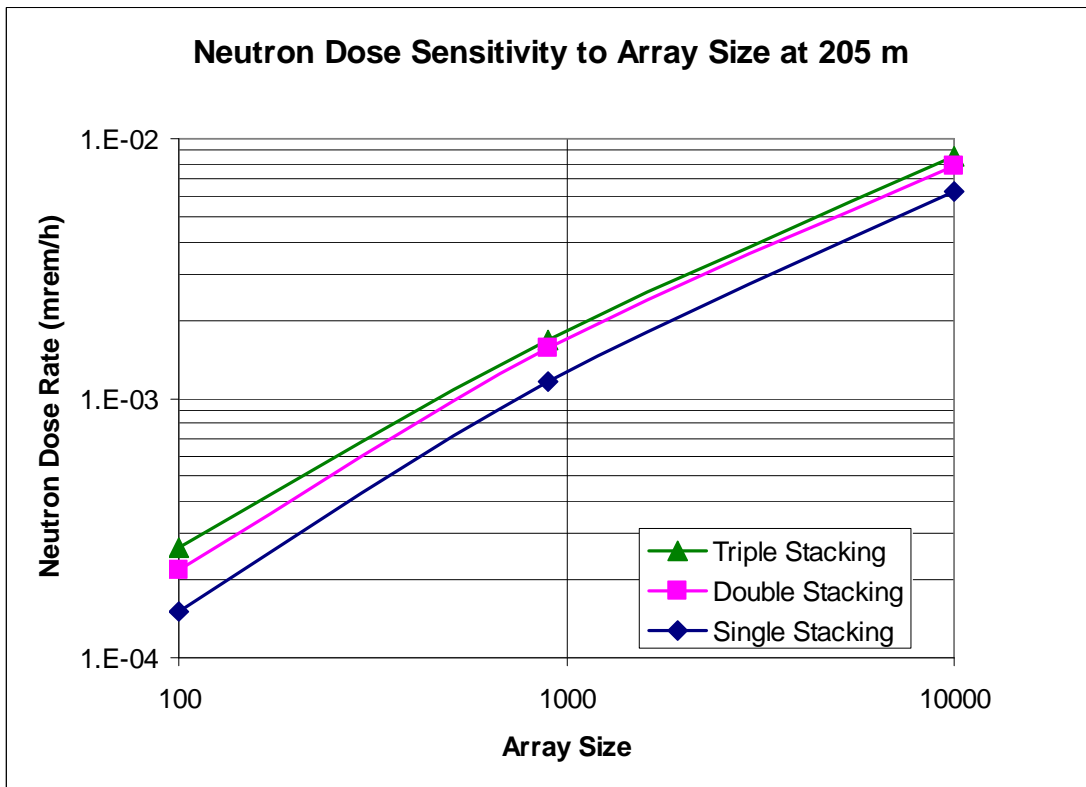
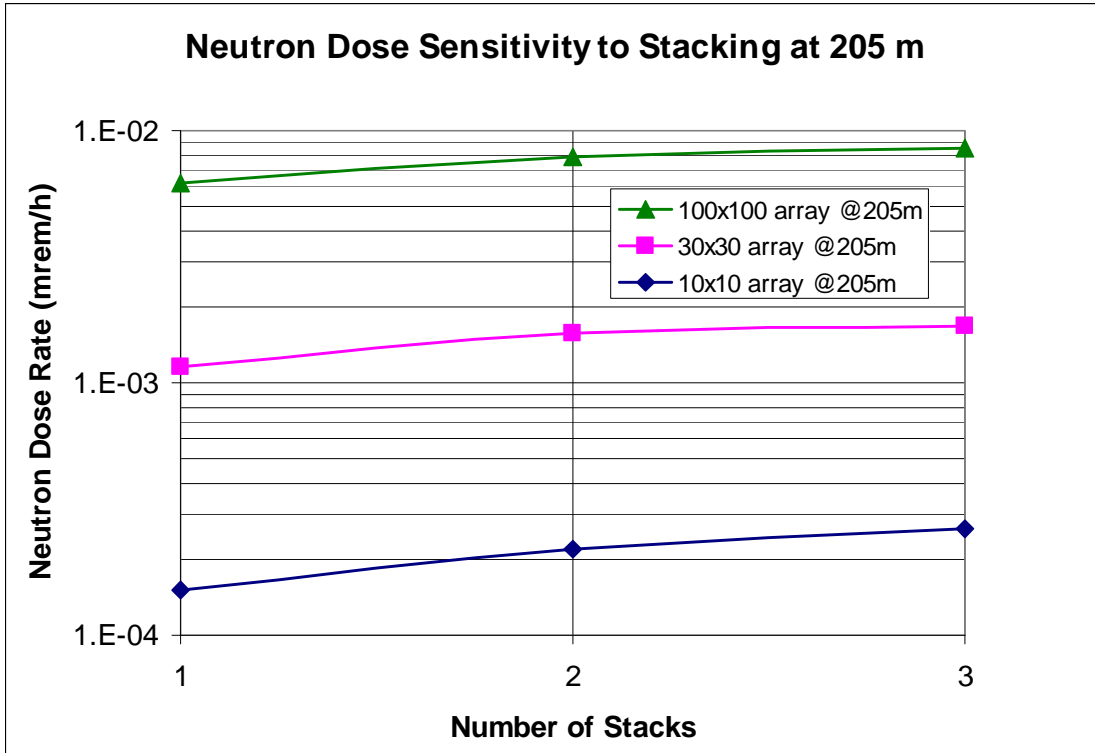


Figure 6-11 Neutron Dose Sensitivity to Array Size and Stacking at 205 m

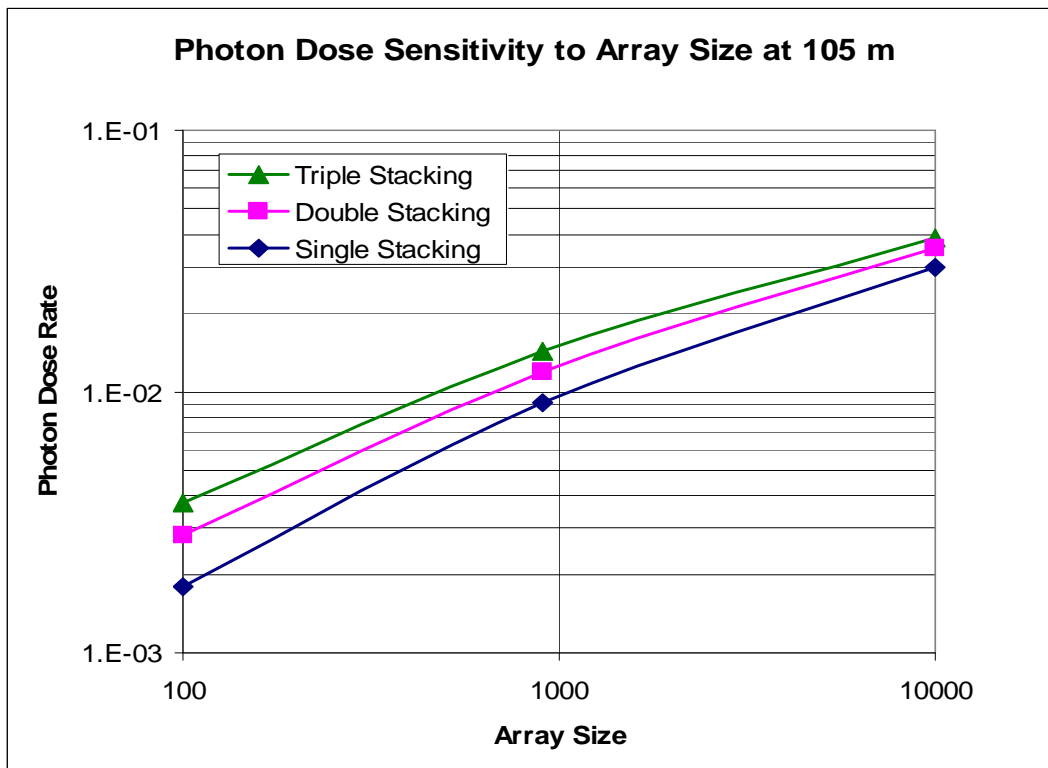
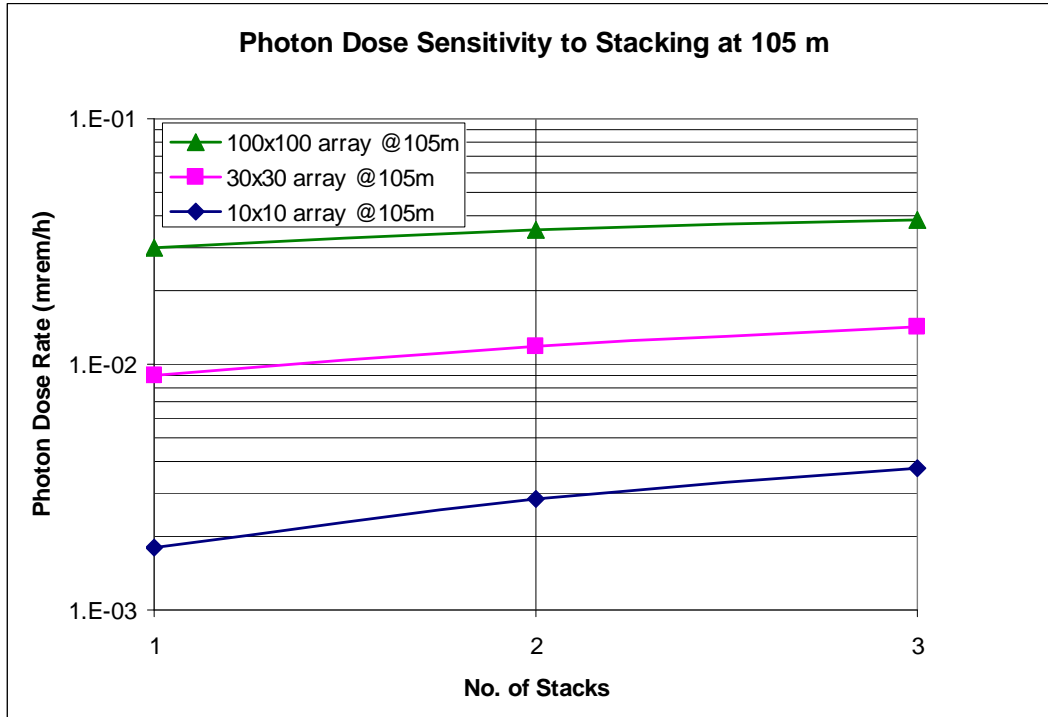


Figure 6-12 Photon Dose Sensitivity to Array Size and Stacking at 105 m

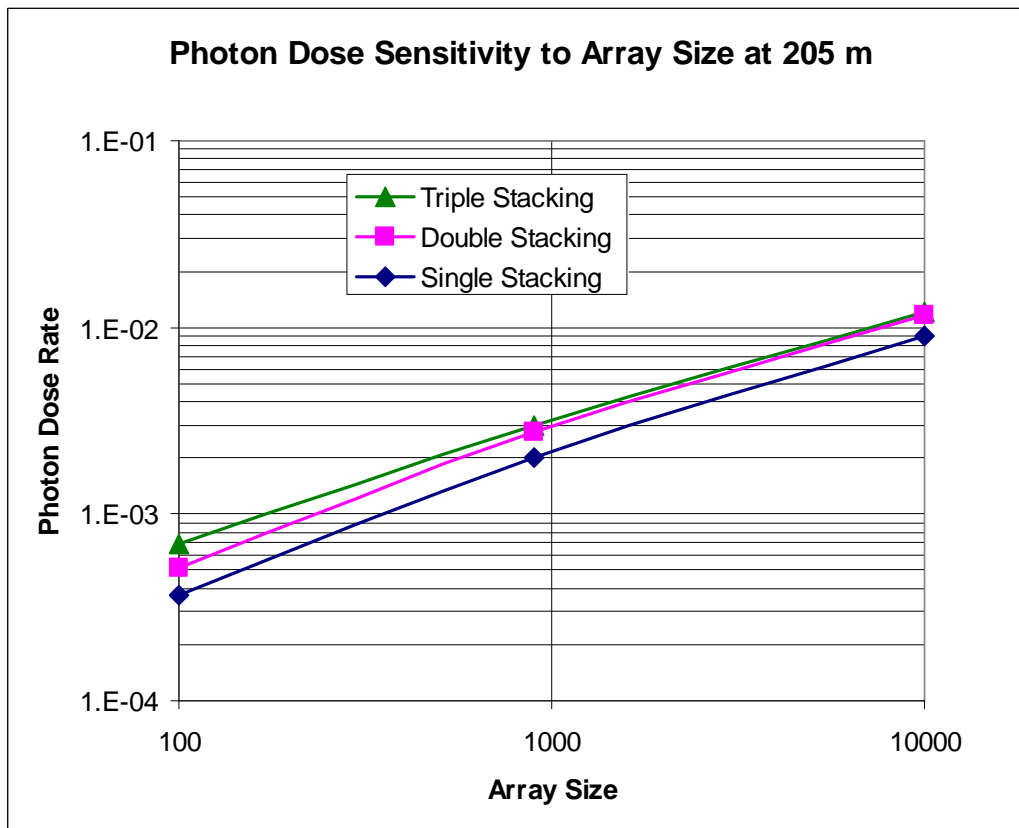
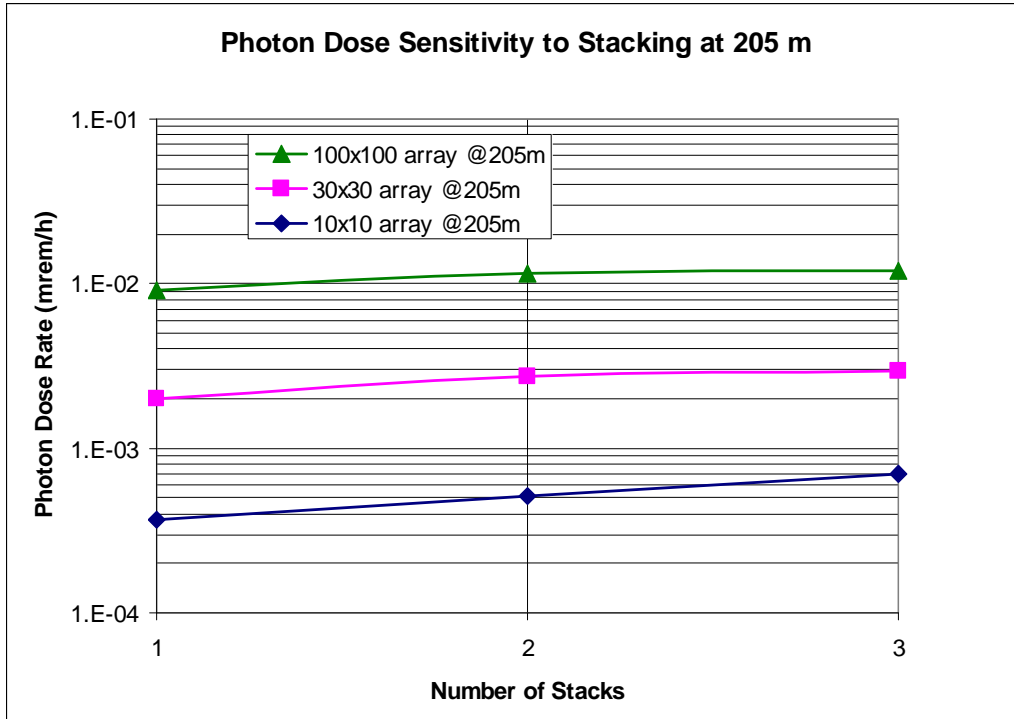


Figure 6-13 Photon Dose Sensitivity to Array Size and Stacking at 205 m

6.5 DOSE IMPACTS FOR FILLED FEED CYLINDERS

To maximize the cylinder storage capacity or minimize the required footprint, the dose impacts need to be considered in storage management. Beneficial considerations include:

- Minimal cylinder spacing in both radial and axial directions
- Maximum stacking up to three high
- Minimal setback distances from the site boundary

The case study described in Chapter 5 for the cylinder arrays used typical cylinder spacing to allow for personnel and equipment access between adjacent cylinders. Undoubtedly the closely packed arrangements would not only use less space and reduce the footprint requirement, but lessen radiation streaming around cylinders with somewhat lower dose consequences. Since cylinder spacing must meet the personnel and equipment access requirements, there may be little or no flexibility in changing the cylinder spacing without equipment redesign or modification at the existing facility. For new facilities, it will be worthwhile to incorporate minimal cylinder spacing in equipment design specifications.

As discussed in Section 6.4, stacking was proven to be beneficial to increase the storage capacity within a given footprint without appreciable dose impacts, because stacking would not cause the dose to double or triple from a single stack. The use of Model 48Y cylinders with a thicker wall than Model 48G provides stronger structural support for cylinder stacking and permits the triple-stacked arrangement to increase the storage capacity. Triple stacking is a unique storage configuration proposed for use at the UUSA Enrichment Facility [UUSA 2010, UUSA 2012c, and UUSA 2013c].

The setback distances from the site boundary depend on the dose levels. A lower dose would result in a shorter distance and lead to more footprint available for cylinder storage use. A reasonably accurate dose assessment without undue conservatism plays a vital role in the setback distance and footprint requirement to avoid unnecessary economic penalty.

The total dose rates presented in Section 6.3 are useful in determining the setback distance for the storage pad from the site boundary. For an annual dose limit of 25 mrem based on 2,000 hours occupancy, the allowable dose rate is 12.5 μ rem/h. To account for additional dose contributions from the cylinders housed inside the building, the dose rate limit for the contributions from the outdoor cylinders was reduced to 10 μ rem/h or 20 mrem/year [AREVA 2003d, §4]. Using the limit of 10 μ rem/h, the required setback distances in the radial direction are provided in Table 6-10 for the nine configurations (10x10, 30x30 and 100x100 in one, two and three high) considered in the case study.

Table 6-10 Storage Pad Setback Distance Requirements

Array Size	Setback Distance from Site Boundary (m)		
	Single Stacking	Double Stacking	Triple Stacking
10x10	52	70	80
30x30	120	140	150
100x100	240	260	270

The results prove that stacking provides an efficient storage management of UF₆ cylinders with only a small increase in the setback distance required – about 20 m from single to double stacking and another 10 m to triple stacking. These increments due to stacking are fairly insensitive to the array size. With this observation, the additional setback distances due to stacking may be applicable to any array size or shape (square or rectangular) as a first order of approximations.

It is also interesting to note that the increase in the array size from 10x10 to 30x30 requires an additional 70 m of setback, regardless of the stacking configuration. The additional setback requirement from the 30x30 to 100x100 array is 120 m for all stacking configurations. These results are useful for comparing with, and checking against, future calculations for a rectangular storage array used at the UUSA Enrichment Facility.

The setback distance of 270 m required for the triple-stacked 100x100 storage array (30,000 cylinders total) is less than 366 m to the east site boundary and 488 m to the north boundary from the UBC Storage Pad at the UUSA Enrichment Facility (Section 2.3). Although the UUSA Storage Pad was designed to accommodate a rectangular rather than square storage array, the case study in this research shows that there is a sufficient margin in the setback distance for facilitating a different storage array design and expansion of the storage capacity.

Mitigative measures such as a concrete shield wall or berm, if feasible and beneficial, may be considered to reduce the setback requirements. Additional dose assessment will be required for the shielded case. The indirect Monte Carlo simulation approach developed from this research is applicable and beneficial to the shielded case.

6.6 MANAGEMENT OF EMPTY FEED CYLINDER STORAGE

The number of empty cylinders stored on the pad is small in comparison to the total pad inventory, but their dose contribution is large because all the radioactivity of a full cylinder is present (the “heel”), but the UF₆ is not present to provide shielding [AREVA 2003d, §7]. Storage of the empty feed cylinders warrants special attention and management, especially for freshly emptied cylinders which are associated with much higher dose rates than those for filled feed cylinders by about one order of magnitude (see Section

4.7.2). Random placement on the storage pad without consideration of the dose impacts could potentially cause non-compliance with the regulations or violation of the ALARA principal. This section specifically addresses the treatment of empty feed cylinders and their dose impacts.

6.6.1 Equivalent Number of Freshly Emptied Cylinders

Unlike a filled feed cylinder, the dose rate from an empty feed cylinder decreases with time after emptying (see Section 4.7.2). The dose calculations for filled cylinders could conservatively assume the same maximum source term for every cylinder, making the doses time-independent. However, the condition is different for empty cylinders, as the source term changes with time. Instead of tracking the time-dependent source term for each individual cylinder, an alternative approach was taken by determining an equivalent number of the freshly emptied cylinders based on the cylinder production rate and source-term decay rate. For a 3-million SWU capacity, the production rate is 627 cylinders per year [AREVA 2003d, §7] or 1.72 cylinders per day, which can be linearly scaled to 5.72 cylinders per day for a 10-million SWU capacity.

The equivalent number of fresh empty cylinders was determined by accumulating the average surface dose rate from the decayed empty cylinders and relating the sum to the dose rate from a single fresh cylinder. The average contact dose rate on the external surface of an empty feed cylinder is given in Table 4-6 and plotted in Figure 4-5 in Chapter 4 as a function of time. With the contact dose rate normalized to 1.0 mrem/h, the relative time-dependent dose rate profile from the time of emptying to one year is shown in Figure 6-14 with the following Excel-generated trend-line:

$$y = 0.9898e^{-10.454x}$$

where y is the relative dose rate and x is the decay time in years.

The cumulative dose rate increases with time as more empty cylinders are produced and stored. For a base production rate of one cylinder per day, the calculation of the cumulative relative dose is provided in Table I-1 with the results displayed in Figure 6-15. From Figure 6-15, the cumulative relative dose rate from the decayed empty cylinders reaches an equivalent number of 35 freshly emptied feed cylinders at a production rate of one cylinder per day. For the 3-million SWU capacity with 1.72 cylinders per day, the equivalent number is $35 \times 1.72 = 60$ freshly emptied cylinders. The corresponding equivalent number for the 10-million SWU capacity is $35 \times 5.72 = 200$ freshly emptied cylinders.

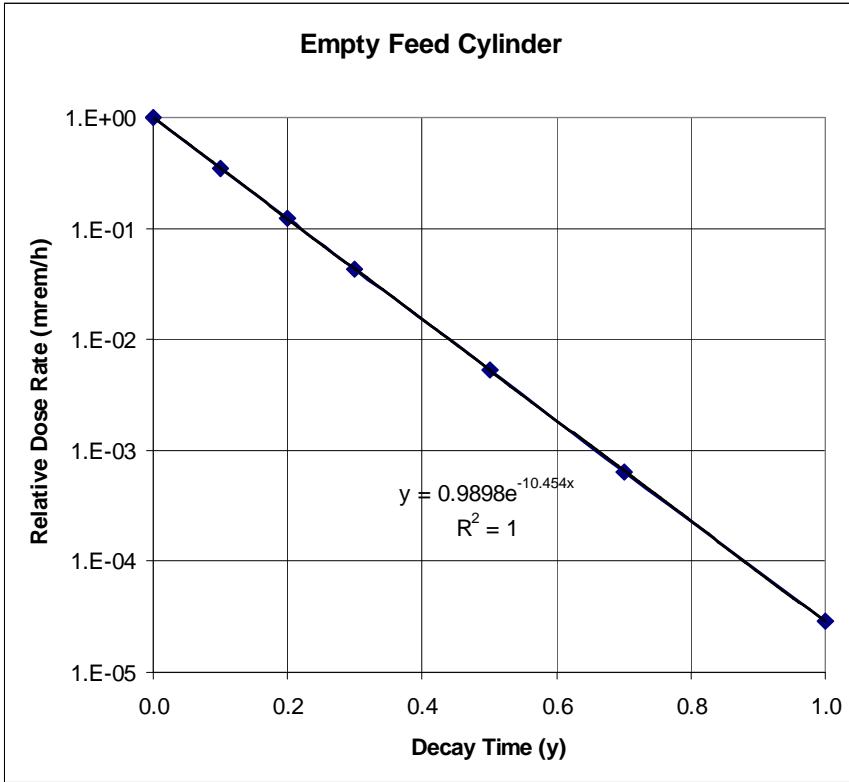


Figure 6-14 Time-dependent Photon Dose Rate Profile for an Empty Feed Cylinder

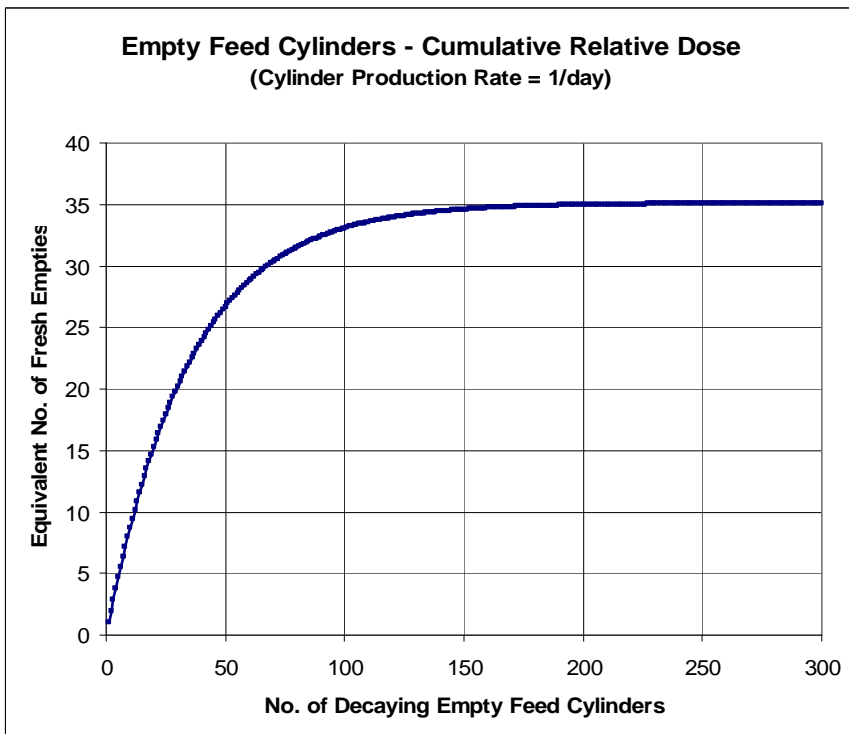


Figure 6-15 Number of Freshly Emptied Cylinders Needed for Equivalent Dose

6.6.2 Dose Assessment for Empty Feed Cylinders

To carry out the dose assessment for the empty feed cylinders, the 10x10 storage array was used in single, double and triple stacking. These arrangements provided sufficient storage space in double stacking for 200 freshly emptied feed cylinders discussed in Section 6.6.1 for the 10-million SWU capacity. The inclusion of single and triple stacking in the dose assessment would provide the results for comparison with the cases for filled feed cylinders from the case study described in Section 5.4.2.

As for the filled feed cylinders, the indirect Monte Carlo simulation approach with the two-step process was utilized for the empty feed cylinders. One difference in the approach between the filled and empty cylinders was that no photon source position biasing was applied to the empty cylinder cases because of the relatively small quantity of empty cylinders and absence of UF₆ in empty cylinders. The empty case was modeled in the same manner as the corresponding filled case minus UF₆ inside the cylinders. Table I-2 in Appendix I lists the MCNP input and output files from the first and second steps of the simulation. The sample input listing is also provided in Appendix I for the selected triple-stacked cases of *t10x10e1.txt* in the first-step process, and *t10x10e2.txt* in the second-step process.

The MCNP-calculated photon dose rates are presented in Table 6-11 and plotted in Figure 6-16 with comparison against the corresponding results for the filled feed cylinders. In the table and figure, E denotes “Empty” cylinders and F means “Filled” cylinders.

Similar to the dose rates for a single cylinder case, the dose rates from the 10x10 array of empty feed cylinders are considerably higher than those from the same array of filled feed cylinders. Management of empty feed cylinders is discussed in Section 6.6.3.

Table 6-11 Radial Photon Dose Rates for Empty Feed Cylinders

Filled and Empty Feed Cylinder Storage - 10x10 Array Photon Dose Rate (mrem/h) Comparison						
Distance (m)	Filled Photon Dose Rate (mrem/h)			Empty Photon Dose Rate (mrem/h)		
	Single Stack-F	Double Stack-F	Triple Stack-F	Single Stack-E	Double Stack-E	Triple Stack-E
0	1.13E+00	1.19E+00	1.21E+00	1.71E+01	1.88E+01	1.95E+01
1	5.26E-01	7.23E-01	8.26E-01	8.18E+00	1.16E+01	1.36E+01
5	1.56E-01	2.59E-01	3.41E-01	2.44E+00	4.28E+00	5.83E+00
11	7.09E-02	1.24E-01	1.71E-01	1.11E+00	2.05E+00	2.90E+00
22	2.95E-02	5.38E-02	7.52E-02	4.68E-01	8.63E-01	1.24E+00
50	8.19E-03	1.39E-02	1.85E-02	1.25E-01	2.19E-01	3.10E-01
105	1.80E-03	2.84E-03	3.77E-03	2.94E-02	4.98E-02	6.53E-02
155	7.50E-04	1.13E-03	1.45E-03	1.14E-02	1.88E-02	2.58E-02
205	3.66E-04	5.13E-04	6.96E-04	5.76E-03	8.48E-03	1.19E-02
255	1.73E-04	2.53E-04	3.70E-04	2.91E-03	4.46E-03	6.09E-03
305	1.04E-04	1.37E-04	2.07E-04	1.61E-03	2.40E-03	3.26E-03
355	6.02E-05	7.97E-05	1.09E-04	9.14E-04	1.30E-03	1.87E-03
395	3.70E-05	5.14E-05	7.54E-05	6.01E-04	8.34E-04	1.22E-03

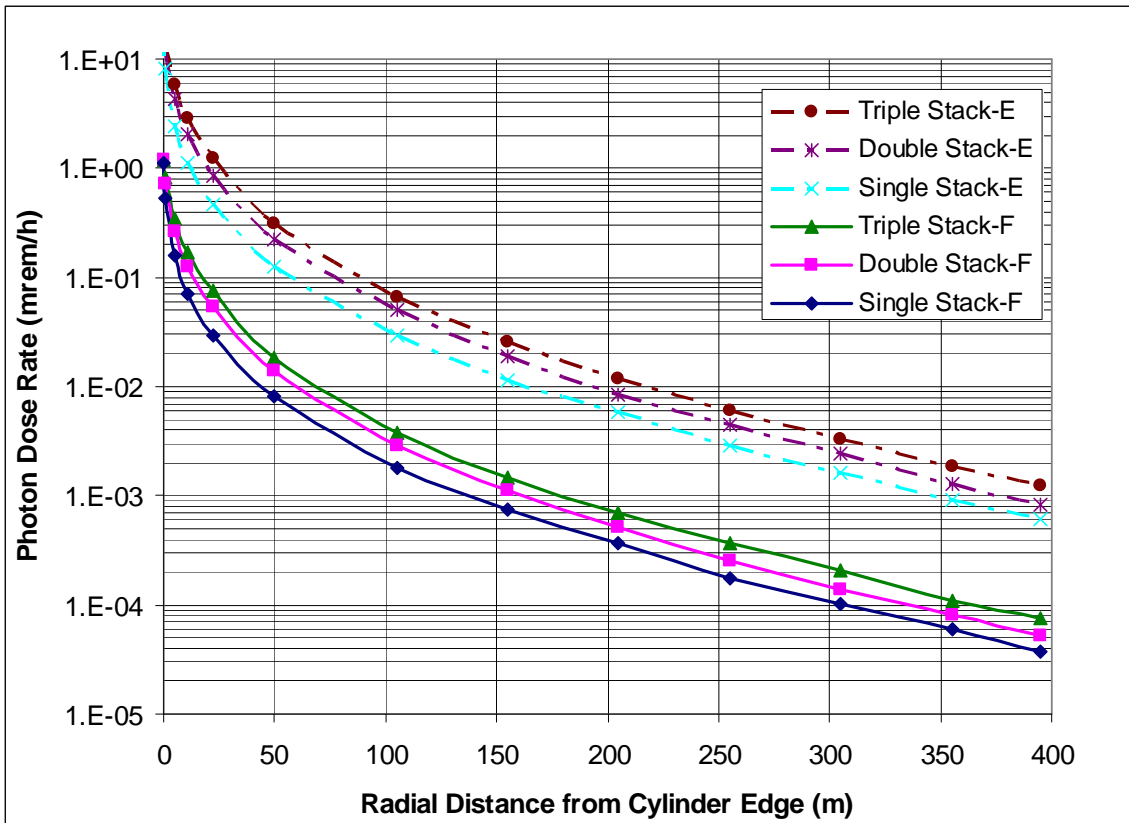


Figure 6-16 Photon Dose Rate Profile Comparison for Empty and Filled Cylinders

6.6.3 Storage Management Considerations

The higher doses from empty feed cylinders require special attention in their storage management. Viable options are available to manage empty feed cylinders at the enrichment facilities, including:

- Washing – An empty feed cylinder can be cleaned by washing down and removing the residual radioactivity inside the cylinder. Washing would certainly eliminate its dose impact. However, this option needs an onsite or offsite washing facility which would conceivably generate liquid effluents, requiring additional radwaste treatment measures.
- Return to customers – After three-month cooling for decay of the residual radioactivity to an acceptable level, the empty feed cylinders can be sent back to the utility customers for future use at the conversion facilities to fill natural UF₆. This option would reduce the long-term storage requirement for empties but still require consideration of onsite storage for three months after emptying.
- Reuse for tails – Since both feed and tails materials use the same model of cylinder (48Y), the empty feed cylinders can be reused at the enrichment facilities for tails withdrawal. In any event, short-term storage is still required for three months after emptying, and the cylinders need to be prepared to meet the vacuum and contamination requirements for connection to the enrichment process system. This option would reuse about 90% of empty cylinders discharged from the enrichment process, as one filled feed cylinder yields about 0.9 filled tails cylinders after enrichment. Onsite storage is still necessary for the remaining 10% of empty cylinders, if not washed or returned to the customers.

Regardless of the management option chosen, there is always a need for onsite storage of empty feed cylinders. The empties can be stored indoor or outdoor. Storage inside a building will occupy premium space that may be reserved for other purposes such as storage of product cylinders. Therefore, indoor storage of empties is generally undesirable. For outdoor storage, empties can be co-located on the storage pad with filled feed and tails cylinders, or segregated in a separate storage area where environmental dose impacts are minimal or inconsequential. If co-located, the dose impacts from empties must be evaluated, as a small quantity of empties would contribute significantly to the overall dose.

To illustrate the significance of the dose contribution from a small number of empties, the radial photon dose rate profiles for the 10x10 array of freshly emptied feed cylinders in single, double and triple stacking are compared with the corresponding profiles for the 100x100 array of filled feed cylinders in Table 6-12 and Figure 6-17. In comparison, the 10x10 array of empties constitutes merely 1% of the 100x100 array of filled cylinders, but gives higher dose rates at close-in distances (less than 100 m). Its contribution becomes less beyond 100 m, but is still significant and cannot be ignored. Hence, placement of empty feed cylinders will affect doses to onsite workers and the general public. For environmental considerations, additional setback distance will be required to account for additional dose contributions from empties to meet the regulatory dose limit at the site boundary.

Dose impacts from empties can be minimized by means of strategic placement of empties on the storage pad with sufficient shielding by the surrounding filled cylinders. In so doing, the dose contributions from empties would become negligible. A site-specific dose assessment (outside the scope of this research) would be still required to determine the proper locations of empties and confirm the negligible dose consequences due to empties.

Table 6-12 Dose Rate Comparison for Empty and Filled Feed Cylinder Storage Arrays

Filled Feed Cylinder Storage - 100x100 Array (Triple) Empty Feed Cylinder Storage - 10x10 Array (Triple)						
Distance (m)	Filled Total Dose Rate (mrem/h)			Empty Photon Dose Rate (mrem/h)		
	Single Stack-F	Double Stack-F	Triple Stack-F	Single Stack-E	Double Stack-E	Triple Stack-E
0	1.37E+00	1.50E+00	1.53E+00	1.71E+01	1.88E+01	1.95E+01
1	7.46E-01	9.85E-01	1.10E+00	8.18E+00	1.16E+01	1.36E+01
5	3.40E-01	4.72E-01	5.56E-01	2.44E+00	4.28E+00	5.83E+00
11	2.38E-01	3.23E-01	3.62E-01	1.11E+00	2.05E+00	2.90E+00
22	1.68E-01	2.18E-01	2.50E-01	4.68E-01	8.63E-01	1.24E+00
50	1.02E-01	1.27E-01	1.45E-01	1.25E-01	2.19E-01	3.10E-01
105	4.96E-02	5.92E-02	6.57E-02	2.94E-02	4.98E-02	6.53E-02
155	2.78E-02	3.18E-02	3.62E-02	1.14E-02	1.88E-02	2.58E-02
205	1.53E-02	1.94E-02	2.05E-02	5.76E-03	8.48E-03	1.19E-02
255	9.15E-03	1.08E-02	1.17E-02	2.91E-03	4.46E-03	6.09E-03
305	5.76E-03	6.44E-03	7.01E-03	1.61E-03	2.40E-03	3.26E-03
355	3.19E-03	3.90E-03	4.17E-03	9.14E-04	1.30E-03	1.87E-03
395	2.03E-03	2.45E-03	2.59E-03	6.01E-04	8.34E-04	1.22E-03

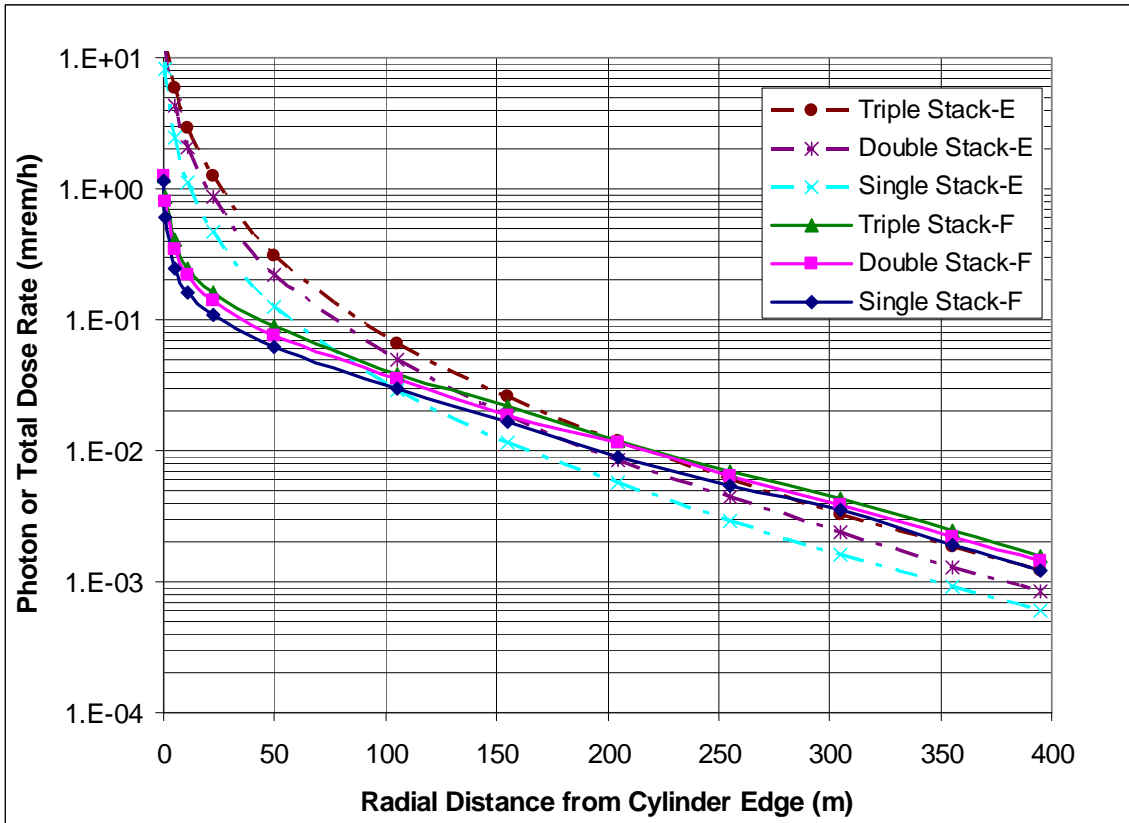


Figure 6-17 Dose Rate Comparison for Empty and Filled Feed Cylinder Storage Arrays

7. VALIDATION OF COMPUTATIONAL EFFICIENCY

This chapter presents the validation of the computational efficiency of the indirect Monte Carlo simulation approach developed and applied in this research. The computational efficiency is expressed in terms of the figure of merit (FOM) for comparison purposes. The most challenging case of the 100x100 storage array in triple stacking was selected for comparing the computational efficiency between the direct and indirect Monte Carlo methods. This comparison covers both neutron and photon calculations.

7.1 NEUTRON CALCULATIONS

The neutron calculations for the triple-stacked 100x100 storage array included the following cases:

- Unbiased two-step case – indirect approach
- Biased two-step case – indirect approach
- Unbiased one-step case – direct approach

The context of “unbiased” as used in this research means no source position or energy biasing and “biased” is with source position and energy biasing. For neutrons, the unbiased two-step case actually included energy biasing with minor effects on computational efficiency. The simple and convenient built-in direction biasing as described in Section 5.3.3 was included in all three cases.

The calculation for the unbiased two-step case is covered in Section 5.4 with the results presented in Table 6-3. For the biased two-step case, source position biasing was applied to the cylinder locations, using the importance data generated with MAVRIC in a manner similar to the photon case (see Section 5.3.1). The unbiased one-step case carried out

the calculation similar to the unbiased two-step case but in a single once-through process without generating a surface source file. All the calculations used the same mesh tally structure for consistent comparison.

Table 7-1 presents the comparison of the neutron dose rate results and the associated FOMs for the three cases of interest. The FOM was determined as follows [LANL 2008, Eq. 2.21a]:

$$\text{FOM} = 1/(\text{R}^2\text{T})$$

where R is the relative error or one fractional standard deviation, and T is the CPU time.

As can be seen from Table 7-1, the unbiased two-step case exhibits the best FOM, showing a significant improvement in computational efficiency over the unbiased one-step case by over one order of magnitude at environmental distances of greater than 150 m. The biased two-step case is better than the unbiased one-step case, but is worse than the unbiased two-step case, because of poor over-biasing for the weak neutron attenuator of UF₆ and detector-dependent adjoint calculations for source importance. The comparison demonstrates that poor biasing is worse than no biasing, as bad data do more harm than good to the random walk process in the Monte Carlo simulation.

Table 7-1 Neutron Computational Efficiency for Triple-stacked 100x100 Array

Neutron Dose Rate (mrem/h)						
Distance (m)	Dose Rate (mrem/h)			Relative Error		
	Biased Two-Step	Unbiased Two-Step	Unbiased One-Step	Biased Two-Step	Unbiased Two-Step	Unbiased One-Step
1	2.08E-01	2.24E-01	2.31E-01	0.0085	0.0336	0.0542
5	1.37E-01	1.43E-01	1.42E+00	0.0178	0.028	0.0508
11	1.11E-01	1.15E-01	1.08E-01	0.0231	0.0309	0.0550
22	8.51E-02	8.95E-02	8.06E-02	0.0217	0.0288	0.0619
50	5.38E-02	5.56E-02	5.02E-02	0.0356	0.0292	0.0609
105	2.58E-02	2.71E-02	2.56E-02	0.0284	0.0315	0.0821
155	1.45E-02	1.42E-02	1.30E-02	0.0335	0.0297	0.1058
205	8.43E-03	8.54E-03	6.88E-03	0.0470	0.0355	0.1328
255	5.11E-03	4.67E-03	4.45E-03	0.0592	0.0302	0.1804
305	2.87E-03	2.66E-03	2.20E-03	0.0549	0.0322	0.1606
355	1.61E-03	1.70E-03	2.19E-03	0.0639	0.0403	0.2852
395	1.26E-03	1.04E-03	8.64E-04	0.0789	0.0413	0.2802
CPU Time Consumed (min)						
Code	Biased Two-Step	Unbiased Two-Step	Unbiased One-Step			
MAVRIC	54.27	N/A	N/A			
MCNP 1 st step	307.34	102.00	100.20			
MCNP 2 nd step	98.03	16.47	N/A			
Total	459.64	118.47	100.20			
Figure of Merit (FOM)						
Distance (m)	Biased Two-Step FOM (1)	Unbiased Two-Step FOM (2)	Unbiased One-Step FOM (3)	FOM Ratio (2)/(1)	FOM Ratio (2)/(3)	
1	30.42	7.48	3.39	0.25	2.20	
5	6.83	10.77	3.87	1.58	2.78	
11	4.08	8.84	3.30	2.17	2.68	
22	4.61	10.18	2.61	2.21	3.91	
50	1.71	9.90	2.69	5.78	3.68	
105	2.70	8.51	1.48	3.15	5.75	
155	1.93	9.57	0.89	4.95	10.74	
205	0.99	6.70	0.57	6.79	11.83	
255	0.62	9.26	0.31	14.89	30.17	
305	0.72	8.14	0.39	11.29	21.05	
355	0.53	5.20	0.12	9.74	42.36	
395	0.35	4.95	0.13	14.15	38.92	

7.2 PHOTON CALCULATIONS

The Photon calculations for the triple-stacked 100x100 storage array also included the same cases as the neutron calculations. Table 7-2 presents the corresponding results of the dose rates, relative errors, CPU times consumed and FOMs.

Unlike the neutron calculations which did not require source position biasing, the photon calculations benefited from source biasing in addition to the advantage of the two-step process. For photons, the FOM is most favorable for the biased two-step process. The application of both source biasing and two-step calculations resulted in substantial improvement in the computational efficiency by two orders of magnitude at some locations. This observation shows that the indirect Monte Carlo simulation approach with source biasing is efficient and beneficial for application to the UF₆ cylinder array photon dose calculations.

The biased two-step process for the photon calculations in the case study primarily dealt with the radial direction. Separate photon calculations would be required for the axial direction, obviously consuming additional computer times similar to the radial calculations. Despite the additional axial calculations for photons, the improvement in the computational efficiency with the indirect Monte Carlo simulation is still substantial over the direct, unbiased approach.

Table 7-2 Photon Computational Efficiency for Triple-stacked 100x100 Array

Photon Dose Rate (mrem/h)						
Distance (m)	Dose Rate (mrem/h)			Relative Error		
	Biased Two-Step	Unbiased Two-Step	Unbiased One-Step	Biased Two-Step	Unbiased Two-Step	Unbiased One-Step
1	8.71E-01	9.32E-01	9.09E-01	0.0085	0.0263	0.0612
5	4.13E-01	4.47E-01	4.55E-01	0.0163	0.0540	0.1044
11	2.47E-01	2.25E-01	2.35E-01	0.0113	0.0811	0.1008
22	1.60E-01	1.48E-01	1.37E-01	0.0212	0.0710	0.1175
50	8.89E-02	7.74E-02	8.35E-02	0.0461	0.0807	0.1409
105	3.86E-02	3.75E-02	6.17E-02	0.0301	0.0667	0.2418
155	2.20E-02	2.20E-02	2.43E-02	0.0423	0.0577	0.2157
205	1.20E-02	1.28E-02	1.57E-02	0.0305	0.0571	0.2933
255	6.99E-03	6.64E-03	5.31E-03	0.0325	0.0753	0.2956
305	4.35E-03	4.40E-03	6.73E-03	0.0394	0.0911	0.5590
355	2.47E-03	3.10E-03	2.94E-03	0.0820	0.0960	0.6399
395	1.55E-03	1.87E-03	2.50E-03	0.0443	0.2375	0.5289
CPU Time Consumed (min)						
Code	Biased Two-Step	Unbiased Two-Step	Unbiased One-Step			
MAVRIC	13.97	N/A	N/A			
MCNP 1 st step	305.35	300.57	300.57			
MCNP 2 nd step	51.24	2.50	N/A			
Total	370.56	303.07	300.57			
Figure of Merit (FOM)						
Distance (m)	Biased Two-Step FOM (1)	Unbiased Two-Step FOM (2)	Unbiased One-Step FOM (3)	FOM Ratio (1)/(2)	FOM Ratio (1)/(3)	
1	37.73	1.13	0.889	33.34	42.45	
5	10.19	0.50	0.305	20.33	33.37	
11	21.04	0.65	0.327	32.15	64.32	
22	5.98	0.51	0.241	11.79	24.81	
50	1.27	0.74	0.168	1.71	7.57	
105	2.99	0.99	0.057	3.01	52.47	
155	1.51	1.01	0.072	1.49	21.07	
205	2.90	0.58	0.039	4.98	74.98	
255	2.56	0.40	0.038	6.44	67.25	
305	1.73	0.36	0.011	4.85	162.90	
355	0.40	0.06	0.008	6.86	49.37	
395	1.38	0.09	0.012	14.58	115.63	

7.3 DOSE ESTIMATES FROM SINGLE-STACK CALCULATIONS

An alternative approach may be used to save computational efforts by estimating the dose rates from the single-stack calculations. If proven acceptable, the calculations just need to be performed for the single-stack case. No detailed calculations would be necessary for the double- and triple-stack cases. Such derivation is a cost-effective approach, as no additional computer run or time is consumed to run MCNP for the double- and triple-stack cases, further enhancing the efficiency by saving resources (labor and computer).

As stated in Section 5.4, the dose contributions from the surface sources recorded in the first step of the MCNP calculation are separable. It would be curious and interesting to find out if the individual contribution from each surface for the single stacking configuration could be used to estimate the doses for the double and triple stacking configurations without further calculations.

For proof of concept, additional MCNP runs were made in the second step of the calculation to separate the contribution due to the top surface source from that due to the east and north surface sources (see Figure 5-8 in Chapter 5). Once separated, the dose at a given radial receptor for double and triple stacking was estimated as follows:

$$\text{Double Stacking} \quad D = D_T + 2(D_E + D_N)$$

$$\text{Triple Stacking} \quad D = D_T + 3(D_E + D_N)$$

where D_T is the dose contribution from the top surface source, and D_E and D_N are the dose contributions from the east and north surface sources for single stacking, respectively. In this estimate, the dose contribution from the top surface was assumed to be the same regardless of stacking (discussed later for validity). The factors of 2 and 3 in the estimate were simply

applied to account for double and triple stacking, respectively, as the dose contribution from the east and north surfaces would be approximately doubled or tripled.

Table 7-3 provides the estimated neutron dose results for double and triple stacking, based on the separable dose contributions for single stacking. Table 7-4 gives the corresponding estimates for photon doses.

At the locations near the storage array edge, the approximation method tends to overestimate the dose, as the dose effect from the east and north surface sources is not linear with the number of stacks. At the environmental locations away from the storage pad, the use of the results from the single-stack calculation appears to underestimate the doses, owing to the increase in the dose rates from the contributing top surface as the array size becomes larger. The top surface source is a principal dose contributor for the larger arrays such as 30x30 and 100x100, because of the association with a larger surface area (see Tables 7-5 and 7-6). The underestimate is more noticeable for neutrons than for photons, being in the neighborhood of 20% and 10%, respectively. This difference is attributable to the fact that the skyshine radiation contribution is more significant for neutrons than for photons and UF₆ provides less shielding for neutrons than for photons.

For a quick estimate without detailed calculations for double and triple stacking, one could perform a calculation for single stacking and use the results to predict the doses for other stacking configurations (double and triple). Since this approach would underestimate the doses at the environmental locations, a conservative multiplier of 1.2 for neutrons and 1.1 for photons could be applied to correct the estimated doses to be in line with the detailed calculations. These multipliers would account for the increase in the average dose rates on the top surface of the cylinder box with more stacking (see Tables 7-5 and 7-6).

The above process demonstrates that the results from the single-stack case are useful for making quick estimates of the doses for the double- and triple-stack cases with appropriate multipliers. Such a process also serves to check the detailed calculations for the double- and triple-stack cases.

Table 7-3 Neutron Dose Estimates from Single-stack Calculations

Distance (m)	Single-stack Dose Rate Contribution (mrem/h)		Estimated Dose Rate (mrem/h)		Estimate/Calculation	
	Top Surface	East & North Surfaces	Double Stacking	Triple Stacking	Double Stacking	Triple Stacking
10x10 Array						
1	2.24E-02	6.23E-02	1.47E-01	2.09E-01	1.20	1.46
5	1.01E-02	1.99E-02	4.99E-02	6.97E-02	0.98	1.03
11	6.82E-03	8.48E-03	2.38E-02	3.23E-02	0.89	0.93
22	4.16E-03	3.34E-03	1.08E-02	1.42E-02	0.85	0.82
50	1.76E-03	8.21E-04	3.40E-03	4.22E-03	0.86	0.85
105	5.56E-04	1.66E-04	8.88E-04	1.05E-03	0.83	0.88
155	2.57E-04	6.25E-05	3.81E-04	4.44E-04	0.81	0.79
205	1.21E-04	3.03E-05	1.81E-04	2.12E-04	0.83	0.80
255	6.72E-05	1.51E-05	9.74E-05	1.12E-04	0.84	0.81
305	3.84E-05	8.15E-06	5.48E-05	6.29E-05	0.80	0.79
355	2.31E-05	4.86E-06	3.29E-05	3.77E-05	0.92	0.92
395	1.44E-05	3.17E-06	2.08E-05	2.39E-05	0.96	0.89
30x30 Array						
1	3.97E-02	6.53E-02	1.70E-01	2.36E-01	1.20	1.42
5	2.96E-02	2.15E-02	7.26E-02	9.41E-02	0.99	1.05
11	2.43E-02	9.71E-03	4.37E-02	5.34E-02	0.90	0.88
22	1.85E-02	4.56E-03	2.77E-02	3.22E-02	0.85	0.82
50	1.06E-02	1.55E-03	1.36E-02	1.52E-02	0.82	0.81
105	4.14E-03	4.40E-04	5.02E-03	5.46E-03	0.81	0.77
155	2.09E-03	1.81E-04	2.45E-03	2.63E-03	0.81	0.80
205	1.07E-03	9.13E-05	1.25E-03	1.34E-03	0.80	0.80
255	5.83E-04	4.35E-05	6.69E-04	7.13E-04	0.79	0.79
305	3.27E-04	2.47E-05	3.77E-04	4.01E-04	0.84	0.79
355	1.87E-04	1.46E-05	2.17E-04	2.31E-04	0.80	0.79
395	1.17E-04	8.44E-06	1.33E-04	1.42E-04	0.81	0.82
100x100 Array						
1	7.34E-02	7.26E-02	2.19E-01	2.91E-01	1.16	1.30
5	7.32E-02	2.40E-02	1.21E-01	1.45E-01	0.94	1.02
11	6.73E-02	1.04E-02	8.81E-02	9.85E-02	0.86	0.86
22	5.61E-02	5.06E-03	6.63E-02	7.13E-02	0.85	0.80
50	3.82E-02	1.97E-03	4.22E-02	4.41E-02	0.83	0.79
105	1.91E-02	6.74E-04	2.05E-02	2.11E-02	0.86	0.78
155	1.07E-02	3.29E-04	1.13E-02	1.17E-02	0.86	0.82
205	6.05E-03	1.76E-04	6.41E-03	6.58E-03	0.82	0.77
255	3.63E-03	1.04E-04	3.83E-03	3.94E-03	0.88	0.84
305	2.13E-03	6.03E-05	2.25E-03	2.31E-03	0.86	0.87
355	1.25E-03	2.01E-05	1.29E-03	1.31E-03	0.76	0.77
395	7.91E-04	2.21E-05	8.35E-04	8.57E-04	0.84	0.82

Table 7-4 Photon Dose Estimates from Single-stack Calculations

Distance (m)	Single-stack Dose Rate Contribution (mrem/h)		Estimated Dose Rate (mrem/h)		Estimate/Calculation	
	Top Surface	East & North Surfaces	Double Stacking	Triple Stacking	Double Stacking	Triple Stacking
10x10 Array						
1	1.22E-01	4.04E-01	9.30E-01	1.33E+00	1.29	1.62
5	1.99E-02	1.36E-01	2.92E-01	4.28E-01	1.13	1.25
11	1.06E-02	6.03E-02	1.31E-01	1.92E-01	1.06	1.12
22	6.12E-03	2.34E-02	5.29E-02	7.64E-02	0.98	1.01
50	2.83E-03	5.37E-03	1.36E-02	1.89E-02	0.98	1.02
105	8.52E-04	9.48E-04	2.75E-03	3.70E-03	0.97	0.98
155	4.17E-04	3.33E-04	1.08E-03	1.42E-03	0.96	0.98
205	2.24E-04	1.42E-04	5.07E-04	6.49E-04	0.99	0.93
255	1.02E-04	7.10E-05	2.44E-04	3.15E-04	0.96	0.85
305	6.86E-05	3.54E-05	1.39E-04	1.75E-04	1.02	0.85
355	4.07E-05	1.95E-05	7.96E-05	9.91E-05	1.00	0.91
395	2.53E-05	1.17E-05	4.87E-05	6.04E-05	0.95	0.80
30x30 Array						
1	1.45E-01	4.02E-01	9.49E-01	1.35E+00	1.28	1.59
5	4.61E-02	1.35E-01	3.16E-01	4.50E-01	1.11	1.20
11	3.34E-02	6.32E-02	1.60E-01	2.23E-01	1.04	1.10
22	2.49E-02	2.81E-02	8.11E-02	1.09E-01	0.99	1.02
50	1.51E-02	9.03E-03	3.32E-02	4.22E-02	0.98	0.97
105	6.80E-03	2.24E-03	1.13E-02	1.35E-02	0.95	0.95
155	3.36E-03	8.63E-04	5.09E-03	5.95E-03	0.93	0.97
205	1.60E-03	4.05E-04	2.42E-03	2.82E-03	0.88	0.95
255	9.23E-04	1.96E-04	1.31E-03	1.51E-03	0.94	0.90
305	5.72E-04	1.05E-04	7.82E-04	8.87E-04	0.93	0.93
355	3.08E-04	5.68E-05	4.21E-04	4.78E-04	0.92	0.90
395	2.17E-04	3.40E-05	2.85E-04	3.19E-04	0.87	0.88
100x100 Array						
1	1.94E-01	4.06E-01	1.01E+00	1.41E+00	1.26	1.62
5	1.05E-01	1.38E-01	3.81E-01	5.18E-01	1.11	1.26
11	9.56E-02	6.46E-02	2.25E-01	2.89E-01	1.02	1.17
22	7.74E-02	3.00E-02	1.38E-01	1.68E-01	0.98	1.05
50	5.14E-02	1.05E-02	7.24E-02	8.29E-02	0.95	0.93
105	2.65E-02	3.36E-03	3.32E-02	3.65E-02	0.94	0.95
155	1.52E-02	1.56E-03	1.84E-02	1.99E-02	0.98	0.91
205	8.26E-03	7.93E-04	9.85E-03	1.06E-02	0.85	0.89
255	4.98E-03	4.39E-04	5.86E-03	6.30E-03	0.91	0.90
305	3.32E-03	2.51E-04	3.82E-03	4.07E-03	1.00	0.93
355	1.77E-03	1.46E-04	2.06E-03	2.21E-03	0.94	0.89
395	1.14E-03	8.37E-05	1.30E-03	1.39E-03	0.90	0.90

Table 7-5 Average Surface Neutron Dose Rates from First-Step MCNP Calculations

Array Size	Stacking (MCNP File)	Surface Source	Dose Rate (mrem/h)	Relative Error	Surface Area (m ²)
10x10	Single (s10x10n01)	East	0.165	0.0051	3.38E+01
		North	0.174	0.0065	2.12E+01
		Top	0.215	0.0010	3.60E+01
	Double (d10x10n01)	East	0.183	0.0064	6.33E+01
		North	0.209	0.0061	4.42E+01
		Top	0.240	0.0014	3.96E+02
	Triple (t10x10n01)	East	0.181	0.0074	9.30E+01
		North	0.216	0.0062	6.50E+01
		Top	0.240	0.0020	3.96E+02
30x30	Single (s30x30n01)	East	0.181	0.0100	1.02E+02
		North	0.189	0.0111	6.40E+01
		Top	0.249	0.0010	3.31E+03
	Double (d30x30n01)	East	0.200	0.0103	1.93E+02
		North	0.229	0.0118	1.25E+02
		Top	0.291	0.0015	3.42E+02
	Triple (t30x30n01)	East	0.215	0.0126	2.84E+03
		North	0.240	0.0102	1.84E+02
		Top	0.301	0.0020	3.42E+03
100x100	Single (s100x100n01)	East	0.209	0.0155	3.42E+02
		North	0.212	0.0198	2.14E+02
		Top	0.314	0.0012	3.70E+04
	Double (d100x100n01)	East	0.248	0.0216	6.46E+02
		North	0.245	0.0193	4.10E+02
		Top	0.371	0.0017	3.74E+04
	Triple (t100x100n01)	East	0.258	0.0205	9.50E+02
		North	0.271	0.0195	6.01E+02
		Top	0.389	0.0021	3.74E+04

Table 7-6 Average Surface Photon Dose Rates from First-Step MCNP Calculations

Array Size	Stacking (MCNP File)	Surface Source	Dose Rate (mrem/h)	Relative Error	Surface Area (m ²)
10x10	Single (s10x10p01)	East	1.128	0.0020	3.38E+01
		North	1.187	0.0100	2.12E+01
		Top	1.554	0.0019	3.60E+01
	Double (d10x10p01)	East	1.191	0.0020	6.33E+01
		North	1.321	0.0109	4.42E+01
		Top	1.617	0.0025	3.96E+02
	Triple (t10x10p01)	East	1.212	0.0042	9.30E+01
		North	1.350	0.0096	6.50E+01
		Top	1.581	0.0037	3.96E+02
30x30	Single (s30x30p01)	East	1.130	0.0023	1.02E+02
		North	1.240	0.0234	6.40E+01
		Top	1.620	0.0040	3.31E+03
	Double (d30x30p01)	East	1.209	0.0130	1.93E+02
		North	1.370	0.0191	1.25E+02
		Top	1.730	0.0027	3.42E+02
	Triple (t30x30p01)	East	1.234	0.0024	2.84E+03
		North	1.462	0.0189	1.84E+02
		Top	1.737	0.0027	3.42E+03
100x100	Single (s100x100p01)	East	1.155	0.0048	3.42E+02
		North	1.446	0.1372	2.14E+02
		Top	1.694	0.0037	3.70E+04
	Double (d100x100p01)	East	1.252	0.0092	6.46E+02
		North	1.389	0.0397	4.10E+02
		Top	1.847	0.0036	3.74E+04
	Triple (t100x100p01)	East	1.269	0.0046	9.50E+02
		North	1.464	0.0234	6.01E+02
		Top	1.871	0.0037	3.74E+04

7.4 COMPARISON WITH UUSA CALCULATION

A comparable MCNP case was selected from the UUSA calculation [UUSA 2012c] for comparison with this research (designated as the UNM calculation). The UUSA case is a triple-stacked configuration with a total of 25,380 cylinders. The UNM case is a triple-stacked configuration with a total of 30,000 cylinders. Table 7-7 compares the differences between the UUSA and UNM cases.

Although different computers were used for the UNM and UUSA calculations, the computer speeds appeared to be comparable based on the processors used and the capacity of random access memory (RAM). It is apparent from the comparison that the UNM case with the indirect simulation approach saves the number of input lines and computer times significantly. The UNM case is superior to the UUSA case with respect to the relative figure of merit or computational efficiency by a factor of about 500 or better at the selected environmental locations. These favorable results affirm that the indirect Monte Carlo approach as developed and used in this research is a valuable tool for future similar calculations.

Table 7-7 Comparison of Computational Efficiency between UNM and UUSA Cases

Description	UNM	UUSA
Computer	Toshiba Satellite C855	Dell PowerEdge 2900 III
CPU	Intel Core i3-3120 @2.5 GHz	Intel Xeon E5410 @2.33 GHz
Usable RAM	3.24 GB	3.89 GB
Operating System	Windows 8.1	Windows XP Pro
Array Shape	Square	Rectangular
Array Size	100x100	846x10
Stacking	Triple	Triple
No. of Cylinders	30,000	25,380
Monte Carlo Simulation	Indirect	Direct
Input Lines		
Neutron	118/83*	13,097
Photon	885/97*	13,061
Output	Mesh Tally	Limited Detectors
CPU (min)		
Neutron	118**	8431
Photon	371**	8503
Relative Error @ ~100 m		
Neutron	0.0315	0.0863
Photon	0.0301	0.1569
Relative Error @ ~200 m		
Neutron	0.0355	0.0860
Photon	0.0305	0.2180
FOM @ ~100 m		
Neutron	8.54	0.0159
Photon	2.97	0.0048
FOM @ ~200 m		
Neutron	6.72	0.0160
Photon	2.89	0.0025
Relative FOM @ ~100 m		
Neutron	536	1
Photon	621	1
Relative FOM @ ~200 m		
Neutron	419	1
Photon	1168	1

*First step/second step

**Total time for two steps

8. VALIDATION OF DOSE SIMULATIONS

This chapter presents the validation of the calculated dose rates from this research at the University of New Mexico (called the UNM calculations). The dose rate validation includes the comparisons with the field measurements and other calculations available for single and multiple cylinders. The validation focuses on the 48Y tails and feed cylinders, including filled tails, filled feed and empty feed cylinders.

8.1 MEASURED DOSE RATE DATA FOR SINGLE CYLINDERS

The measured dose rate data consist of the measurements for filled tails, filled feed and empty feed cylinders. The following subsections describe these field measurement data for use in the validation process.

8.1.1 Single Cylinder Measurements at UUSA

UUSA conducted radiation measurements for single cylinders using thermoluminescent dosimeters (TLD) and electronic alarming dosimeters (EAD) in September 2011. According to the presentation on *Electronic vs. Passive Dosimetry* by Neil Stanford [Stanford 2009], the TLD is a passive dosimeter, measuring the total dose (neutron and photon) and providing the dose of legal record. The EAD with its immediate readout and alarming capabilities is normally used as a secondary dosimeter for the purposes of radiation control and backup. Only the photon dose is measurable with the EAD.

For the legal doses, Tables 8-1 and 8-2 provide the TLD neutron and photon dose rate measurements at contact with the filled feed and tails cylinders on the UUSA UBC Storage Pad, respectively [Parish 2012a]. These tables include the EAD photon measurements [Parish 2012a] for comparison with the corresponding TLD measurements. The TLD and

EAD were placed at about 1.5 in. (3.81 cm) below the bottom surface of each cylinder at 6 o'clock position and approximately 2 ft (61 cm) from the end flange [Parish 2012b]. This placement hid the dosimeters from the adjacent cylinders, and minimized interference due to additional dose contributions. However, radiation scattering off the concrete pad contributes to the readings. Typical measurement uncertainties were quoted at around 10% [Parish 2012b], but could be higher to account for systematic and statistical errors.

For comparison, the calculated dose rates for a single filled feed cylinder and a single filled tails (0.3% U-235 used) cylinder were taken from the MCNP runs with the slumped source geometry and concrete pad/ground scattering in this research. The case for the slumped geometry is more appropriate than the case for the homogenized geometry for comparison with the measurements, because it is more representative of the actual source geometry. Detailed calculations were performed for the filled feed cylinder only (Sections 4.7.3 and 4.7.4), as the dose for the filled tails cylinder is scalable from that for the filled feed cylinder using the ratio of the average contact dose rates on the external cylinder dose derived from Table 4-5 in Chapter 4. The corresponding calculated results are included in Tables 8-1 and 8-2 as UNM Calculated in red.

The UUSA TLD measurement shows a higher photon reading, but a lower neutron reading than the UNM-calculated results for both feed and tails cylinders. Better agreement within 20% is shown for the total dose rate, indicating possible uncertainties in the TLD-based photon/neutron dose ratio. Since the cylinders were not isolated for measurements, minor contributions from the adjacent cylinders on the storage pad were conceivable. The difference is generally acceptable in the health physics community per discussion in Section

4.4.4 in Chapter 4. The use of the conservative homogenized source geometry in the dose assessment would adequately compensate for this difference.

Table 8-1 Comparison with TLD and EAD Measurements at UUSA for Filled 48Y Feed Cylinders

Description	Feed 1	Feed 2	Feed 3	Mean
Location on UBC Pad	UBC D90	UBC D90	UBC D90	N/A
TLD Total Dose Rate (mrem/d)	43.4	45.7	46.6	45.23
TLD Photon/Neutron Dose Ratio	15.56	9.97	11.64	12.39
Neutron Dose Rate (mrem/h)				
TLD Measured	0.11	0.17	0.15	0.14
UNM Calculated	N/A	N/A	N/A	0.26
Photon Dose Rate (mrem/h)				
TLD Measured	1.70	1.73	1.79	1.74
EAD Measured	1.57	1.57	N/A	1.57
UNM Calculated	N/A	N/A	N/A	1.39
Total Dose Rate (mrem/h)				
TLD Measured	□	□	□	1.84
UNM Calculated	□	□	□	1.65

Table 8-2 Comparison with TLD and EAD Measurements at UUSA for Filled 48Y Tails Cylinders

Description	Tails 1	Tails 2	Tails 3	Mean
Location on UBC Pad	UBC C5	UBC C5	UBC C5	N/A
TLD Total Dose Rate (mrem/d)	44	47	46.6	45.87
TLD Photon /Neutron Dose Ratio	24.93	16.93	15.35	19.07
Neutron Dose Rate (mrem/h)				
TLD Measured	0.07	0.11	0.12	0.10
UNM Calculated	N/A	N/A	N/A	0.17
Photon Dose Rate (mrem/h)				
TLD Measured	1.76	1.85	1.82	1.82
EAD Measured	1.60	1.63	N/A	1.62
UNM Calculated	N/A	N/A	N/A	1.39
Total Dose Rate (mrem/h)				
TLD Measured	□	□	□	1.92
UNM Calculated	□	□	□	1.56

8.1.2 Single Cylinder Radiation Surveys at UUSA

UUSA performed radiation surveys at their facility for the filled feed and tails cylinders and empty feed cylinders using the Thermo Scientific MicroRem Dose Rate Meter [TFSI 2007] to measure the photon dose rates. Table 8-3 provides the typical observed results from the UUSA radiation surveys, which represent photon dose rates at contact, 1 ft (30.48 cm) and 3 ft (91.44 cm) from the cylinder surface [Parish 2013b]. Measurement uncertainties were unavailable. It was unclear or unknown whether the contributions from the adjacent cylinders in storage were included in the readings. Comparison with the TLD and EAD measurements shows higher readings at contact from the radiation surveys, implying possible additional contributions from adjacent cylinders. Accordingly, these readings might not be characteristic of the dose rates for a single cylinder, and should be used with caution.

The UUSA radiation survey exhibits much higher photon readings as compared to the UNM calculation (included in Table 8-3 in red in parentheses) and other more reliable measurements. Without the knowledge of the exact survey conditions and reliability of the measurements, no conclusion could be drawn from the survey data.

In addition, there is a large discrepancy in the UUSA radiation survey for the filled tails cylinders. The photon dose rate is higher than that for a filled feed cylinder by a factor of about 2. This difference is possible only if the in-growth time for the feed cylinder is relatively short. As the radiation survey data are not the dose of legal record and its discrepancy from the calculation and other measurements cannot be quantified, they are included in Table 8-3 for information purposes only.

Table 8-3 Comparison with Photon Radiation Surveys at UUSA

(Black numbers – UUSA Surveys and Red Numbers in Parentheses – UNM Calculations*)

Description	Filled Feed	Filled Tails	Empty Feed
Dose Rate at Contact (mrem/h)	3.0 (1.33)	6.0 (1.33)	30 (21.6)
Dose Rate at 1 ft (mrem/h)	1.5 (0.69)	2.0 (0.69)	15 (12.8)
Dose Rate at 3 ft (mrem/h)	0.5 (0.33)	1.0 (0.33)	5 (6.1)

*UNM calculated dose rates (in red) from this research for the slumped source geometry

8.1.3 Single Tails Cylinder Measurements at Capenhurst

The URENCO Capenhurst site in the United Kingdom (UK) performed radiation measurements for an isolated single 48Y tails cylinder in 2003 [AREVA 2003c, §9]. The measured data were used in the derivation of the MCNP normalization factors for both neutrons and photons to account for uncertainties [AREVA 2003c]. For comparison, the measurement data for a single tails cylinder are provided in Table 8-4 at contact, 1 m and 2 m from the side of the cylinder and compared with the UNM calculated dose rates (in red) for the slumped source geometry. The tails assay was assumed to be the typical value of 0.3% U-235. The readings included ground scattering. Neutron measurement uncertainties with the NE Technology NM2B neutron dose rate meter were high – as much as $\pm 100\%$. The photon measurement detector and uncertainties were unavailable.

Table 8-4 Comparison with Single Tails Cylinder Measurements at Capenhurst

(Black numbers – UK Measurements and Red Numbers in Parentheses – UNM Calculations)

Description	Neutron*	Photon**
Dose Rate at Contact (mrem/h)	0.09 (0.10)	1.2 (1.33)
Dose Rate at 1 m (mrem/h)	0.03 (0.03)	0.65 (0.33)
Dose Rate at 2 m (mrem/h)	0.01 (0.014)	N/A

*UNM calculated neutron dose rate (in red) adjusted from the feed results in Table E-3 for Tails

**UNM calculated photon dose rate (in red) based on the feed results in Table E-8

The UNM calculated neutron dose rates are in excellent agreement with the Capenhurst measurements at contact and 1 m. The measured and calculated neutron dose rates at 2 m also agree to the second decimal place. Relative to a filled feed cylinder, the filled tails cylinder exhibits a lower neutron dose rate as expected, because of a lower U-235 concentration in wt %.

The Capenhurst measurements show a surface dose rate of 1.2 mrem/h photon which is fairly consistent with the UNM calculation. However, the Capenhurst measured photon dose rate of 0.65 mrem/h at 1 m appears to be overstated, based on the expected geometric attenuation factor from the surface to 1 m.

8.1.4 Single Feed Cylinder Measurements at Cameco

Measured neutron and photon dose rates are available for a test feed cylinder at the Cameco conversion facility. Cameco used the high sensitivity He-3 Meridian Neutron Monitor Model 5085 from Far West Technology Inc. for neutron measurements [Cameco 2009, §2.2], and a Bicron microsievert meter for photon measurements [Cameco 2009, §2.2.4]. Table 8-5 provides the measured data at contact, 1 m, 5 m and 10 m from the side and end of the cylinder [Cameco 2009, Table 2.2-2] along with the UNM calculated dose rates in parentheses in red. The readings included ground scattering. Measurement uncertainties were stated for the photon-to-neutron dose ratios at 20% or less at contact and 1 m, but larger uncertainties at greater distances with questionable reliability.

The UNM calculated dose rates agree reasonably well with, or are more conservative than, the Cameco measurements for both photons and neutrons at contact and 1 m. The photon readings at 5 m appear to be anomalous as the values are inconsistent with the expected dose reduction with distance when compared to other reliable measurements and

calculations. The larger discrepancy at greater distances (5 and 10 m) is attributable to the measurement uncertainties as stated in the Cameco report.

Table 8-5 Single Feed Cylinder Measurements at Cameco

(Black numbers – Cameco Measurements and Red Numbers in Parentheses – UNM Calculations)

Distance (m)	Dose Rate (mrem/h)		
	Neutron*	Photon**	P/N Ratio
From Side of Cylinder			
Contact (0.02)	0.163 (0.160)	1.04 (1.33)	6 (8.3)
1	0.052 (0.046)	0.387 (0.332)	7 (7.2)
5	0.0048 (0.0052)	0.0865 (0.0410)	18 (7.9)
10	0.0007 (0.0014)	0.0115 (0.0112)	16 (8.0)
From End of Cylinder			
Contact (0.02)	0.148 (0.163)	1.086 (1.46)	7 (9.0)
1	0.027 (0.027)	0.237 (0.249)	9 (9.2)
5	0.0024 (0.0021)	0.085 (0.0156)	3 (7.4)
10	<0.001 (<0.001)	<0.001 (0.0040)	N/A

*UNM calculated neutron dose rate from Table E-3 for the slumped source geometry

**UNM calculated photon dose rate from Table E-8 for the slumped source geometry

8.2 CALCULATED DOSE RATES FOR SINGLE CYLINDERS

There are three independent MCNP calculations of the dose response for a single cylinder performed at UUSA, Urenco Deutschland (UD) and Cameco. The following subsections describe the results of each calculation and comparison with the UNM calculation:

8.2.1 UUSA Calculation

CALC-S-142 [UUSA 2013c] documents the calculation of the dose rate as a function of distance from the surface of a single filled feed cylinder, including both neutron and photon components. The calculation used the ANSI/ANS-6.1.1-1977 flux-to-dose rate conversion

factors to convert the particle flux to the dose rate in units of mrem/h or rem/h. This version of the conversion factors is conservative (relative to the newer ANSI/ANS-6.1.1-1991), and compliant with 10 CFR 20 (Section 4.4.4 in Chapter 4).

Table 8-6 compares the nominal MCNP calculated dose rate results as a function of distance for a single filled feed cylinder between the UNM and UUSA calculations. The distance is measured from the side surface of the cylinder. For direct comparison, the calculations excluded scattering from the concrete pad, and the source model assumed a uniform distribution over the entire internal volume of the cylinder rather than the actual geometry with ~61% fill volume. In addition, an in-growth period of 1 year was assumed for the uranium progeny to reach secular equilibrium, consistent with other calculations.

Table 8-6 UNM and UUSA MCNP Calculated Dose Rates for a Single 48Y Filled Feed Cylinder

Distance (m)	Radial Dose Rate (mrem/h)				UNM/UUSA Ratio	
	UNM*		UUSA			
	Neutron	Photon	Neutron	Photon	Neutron	Photon
0	1.590E-01	1.375E+00	1.58E-01	1.47E+00	1.01	0.94
0.3	9.314E-02	8.442E-01	8.91E-02	8.89E-01	1.05	0.95
1	4.499E-02	4.308E-01	4.33E-02	4.51E-01	1.04	0.96
2	2.155E-02	2.140E-01	2.07E-02	2.24E-01	1.04	0.96
5	5.355E-03	5.304E-02	5.22E-03	5.59E-02	1.03	0.95
10	1.590E-03	1.498E-02	1.54E-03	1.58E-02	1.03	0.95
20	4.580E-04	3.855E-03	4.46E-04	4.18E-03	1.03	0.92
50	9.212E-05	6.101E-04	9.01E-05	6.77E-04	1.02	0.90
100	2.670E-05	1.389E-04	2.62E-05	1.59E-04	1.02	0.87
200	6.198E-06	2.594E-05	5.93E-06	3.05E-05	1.05	0.85

*From Table E-3 for neutrons and Table E-8 for photons for the homogenized geometry

The UNM calculation produced a slightly higher neutron dose rate but a lower photon dose rate than the UUSA calculation. Both UNM and UUSA calculations used the radiation source terms generated with ORIGEN-S in the SCALE 6.1.2 code package. However, the source terms were associated with different energy group structures for both neutrons and

photons, contributing to the minor differences in the dose rate results. These differences are within the typical calculational uncertainty.

8.2.2 UD Calculation

The UD calculation (UD 2002) was performed in a manner similar to the UNM calculation with the concrete scattering effect included, which is particularly significant for the neutron dose. Table 8-7 provides the UD calculated results on the side of the cylinder. The UNM calculated results are included in parentheses for comparison purposes.

The comparison shows that the UNM calculated photon dose rates are more conservative, especially for the empty feed cylinders. There is a large difference in the neutron dose rates, which could be attributable to the different neutron source strength/energy spectrum and dose conversion factors (ICRP 34 [similar to ICRP 74]) used in the UD calculation. Relative to the UNM calculations, the UD calculated neutron dose rates are more conservative but deviate from the measured data in Table 8-4 for the tail cylinder and Table 8-5 for the feed cylinder.

Table 8-7 UNM and UD MCNP Calculated Dose Rates for a Single 48Y Cylinder*

(Black numbers – UD Calculations and Red Numbers in Parentheses – UNM Calculations)

Distance (m)	Filled Feed (mrem/h)		Filled Tails (mrem/h)		Empty Feed (mrem/h)
	Neutron	Photon	Neutron	Photon	Photon
0.5	0.143 (0.084)	0.461 (0.76)	0.087 (0.055)	0.453 (0.76)	5.63 (11.0)
1	0.094 (0.059)	0.290 (0.46)	0.057 (0.039)	0.286 (0.46)	3.41 (6.11)
4	0.016 (0.012)	0.051 (0.094)	0.010 (0.008)	0.055 (0.094)	0.73 (1.20)

*Source: [UD 2002, §8] for UD calculation. Note – Values in parentheses are from the UNM calculation interpolated from Table E-3 for filled feed neutron, Table E-8 for filled feed photon and Table E-13 for empty photon. Tails doses were scaled from feed doses.

8.2.3 Cameco Calculation

The Cameco calculation (Cameco 2009) was performed in a manner similar to the UUSA calculation without concrete or ground scattering, but just for the neutron dose rates from a test feed cylinder. Table 8-8 provides the Cameco calculated neutron dose rates on the side of the cylinder, along with the corresponding UNM calculated results for comparison.

The UNM calculation is consistently more conservative (higher dose rates) than the Cameco calculation at all distances. The Cameco neutron source strength is 5.0×10^5 (also used by UD) vs. 4.98×10^5 n/s in the UNM calculation for a filled feed cylinder, a difference of only 0.4%, but the neutron source energy spectrum is unavailable for comparison. The lower Cameco neutron dose rates could be due to a different neutron source energy spectrum and the use of the ICRP 74 dose conversion. This comparison validates the conservatism that exists in the UNM neutron dose rate calculations.

Table 8-8 Comparison with Single Filled Feed Cylinder Neutron Dose Rates at Cameco*

Distance (m)	Neutron Dose Rate (mrem/h)		Dose Ratio UNM/Cameco
	UNM*	Cameco**	
0	1.59E-01	1.42E-01	1.12
1	4.50E-02	4.01E-02	1.12
5	5.36E-03	4.77E-03	1.12
10	1.59E-03	1.42E-03	1.12
20	4.58E-04	4.05E-04	1.13
50	9.21E-05	7.81E-05	1.18
100	2.67E-05	1.98E-05	1.35

*From Table E-5 in Appendix E without ground scattering

**Source: Cameco 2009, Table 4.2-1

8.3 SUMMARY OF SINGLE CYLINDER COMPARISON

For a filled feed cylinder, the UNM calculated dose rates agree reasonably well with the Cameco measurements for both photons and neutrons at contact and 1 m. The UUSA

TLD measurement shows a higher photon reading than the UNM calculated result possibly due to minor contributions from the adjacent cylinders, but within the uncertainties of 20% acceptable to the health physics community. It can be deduced from the comparison that the calculated and measured dose rates for a single filled feed cylinder are in good agreement for both photons and neutrons.

The filled tails cylinders should have approximately the same photon dose rates as the filled feed cylinders for a given in-growth time for the uranium progeny, as confirmed by the UNM calculation and UUSA TLD measurements. The Capenhurst measurements show a surface dose rate of 1.2 mrem/h photon which is fairly consistent with the UNM calculation. The UNM calculated neutron dose rates are in excellent agreement with the Capenhurst measurements, but more conservative than the UUSA TLD measurements. The dose rate of 0.46 mrem/h at 1 m from a single tails cylinder as reported in ANL/EAD/TM-112 [ANL 2001, Table 5.4] also supported the UNM calculation.

For an empty feed cylinder, the UNM calculated dose rates are conservative as compared to the UD calculation and the values of 10 mrem/h at contact and 1 mrem/h at 1 m cited in the UUSA Safety Analysis Report [UUSA 2013a, Table 4.1-2]. In addition, the UNM calculation is in reasonable agreement with the UUSA radiation survey (excluding the possible peaking effect at contact due to local deposits of the uranium progeny).

In summary, the UNM calculation for a single filled feed cylinder and a single filled tails cylinder is in satisfactory agreement with the measurements and other reliable independent calculations. This agreement validates the physical model (geometry and material), neutron and photon source terms, dose conversion factors and nuclear data used. The UNM calculation for an empty feed cylinder is conservative relative to the UD

calculation and the UUSA SAR values, but fairly consistent with the UUSA radiation surveys after discounting localized peaks.

8.4 UUSA UBC STORAGE PAD MEASUREMENTS AND CALCULATION

The comparisons addressed in Sections 8.1 through 8.3 are limited to a single cylinder. The dose validation for a single cylinder confirms that the cylinder geometry, materials, radiation source terms, dose conversion factors nuclear data used in the calculations are appropriate and acceptable.

Additional validation is necessary to demonstrate that the indirect Monte Carlo simulation approach developed and used in this research is also favorable. For this purpose, field radiation measurements were made at the UUSA UBC Storage Pad, and a dose calculation was performed for comparison with the measurements. The measurements and calculation covered photons only, as the neutron dose is relatively small (see Table 4-5 in Chapter 4), especially for filled tails cylinders.

8.4.1 UBC Storage Pad Measurements

As part of the radiation monitoring program to maintain ALARA doses to workers and the general public, UUSA routinely conducts radiation surveys within and around the UBC Storage Pad on a monthly basis. The surveys are limited to photon doses, as the neutron dose level is relatively low at the current inventory.

For validation purposes, the author performed photon dose rate measurements at various locations outside the radiologically controlled area south of the restricted area boundary (RAB). The designation of the RAB is for the convenience of identifying the boundary and reference point for dimensional measurements rather than for actual posting as used at the UUSA site.

With the support from UUSA, the author conducted a field survey at the UUSA site in Eunice, New Mexico on April 16 and 17, 2014, using the Thermo Scientific Interceptor [TFSI 2009] checked out from the UNM and Thermo Scientific MicroRem Dose Rate Meter [TFSI 2007] available at UUSA. The UUSA detector was calibrated with records, while the UNM detector lacked the calibration data. Both detectors gave the photon dose rate readings in units of $\mu\text{rem/h}$. The background readings were negligible, amounting to $<1 \mu\text{rem/h}$ for the UNM detector and $0.3 \mu\text{rem/h}$ for the UUSA detector.

Preliminary readings were taken on April 16, 2014 using the UUSA MicroRem Dose Rate Meter. The measured photon dose rates were 90, 80 and 70 $\mu\text{rem/h}$ at three representative locations along the RAB.

The readings taken with the UNM and UUSA detectors on April 17, 2014 are presented in Table 8-9. Note that the UUSA detector is a meter type with readings rounded to the nearest fives, while digital readings are readily available from the UNM detector.

The UNM and UUSA readings are generally in good agreement, considering the reading round-off for the UUSA meter-type detector. The peak UNM reading of 78 $\mu\text{rem/h}$ near the centerline of the RAB is due to a large gap in the middle of the storage pad which causes more radiation streaming around the cylinders and a higher dose.

With the reasonable agreement between the UNM and UUSA readings, only the UNM readings are used for comparison with the calculated dose rates (Section 8.4.2).

Table 8-9 Photon Measurements at UUSA UBC Storage Pad

Detector Point	Distance from RAB (ft)	Distance from Centerline (ft)	UNM Reading (µrem/h)	UUSA Reading (µrem/h)
A	0	-220	55	50
B	0	-165	54	60
C	0	-110	56	50
D	0	-55	56	60
E	0	0	78	70
F	0	55	58	60
G	0	110	53	50
H	0	165	54	50
I	0	220	52	50
J	50	0	42	40
K	100	0	27	30
L	100	50	26	30
M	100	100	28	25
N	150	0	21	20
O	150	100	21	20

Row A									North Cylinder Edge
Row B									
Row C									
Row D	UBC Storage Pad								
Row E	100x8 Array - Approximate								
Row F	Double Stacking								
Row G									
Row H									South Cylinder Edge
45 ft Separation between South Cylinder Edge and RAB									
Restricted Area Boundary (RAB)									
A	B	C	D	E	F	G	H	I	
55/50	54/60	56/50	56/60	78/70	58/60	53/50	54/50	52/50	
				J					
				42/40	(50 ft from RAB)				
				K	L	M			
				27/30	26/30	28/25	(100 ft from RAB)		
A to O - Detector Locations									
UNM/UUSA Photon Dose Rate Readings (µrem/h)									
Not to Scale				N	O				
				21/20	21/20		(150 ft from RAB)		

8.4.2 UBC Storage Pad Dose Calculation

For comparison with the measured photon dose rates at the UUSA UBC Storage Pad, the indirect Monte Carlo simulation approach developed in Chapter 5 was applied here to calculate the corresponding dose rates. The calculation simulated the actual configuration and conditions of the UBC Storage Pad as closely as possible to make reasonable dose estimates. Table 8-10 compares the model and parameters used in this calculation with those selected for the case study in Chapter 5 including similarities and differences.

Figure 8-1 depicts the geometric model constructed for validation use. The total number of cylinders considered was 1,608 in a double-stacked array [101x8 (bottom) and 100x8 (top)], consistent with the approximate inventory at the time of measurements. This model closely simulated the quantity and arrangement of cylinders that existed at the time of measurements. The spacing (both radial and axial) between the cylinders reflected the field dimensional measurements. The ground clearance for the cylinders was measured to be 3.5 in. (~9 cm) which was used for the validation model versus 6 in. used in the case study (see Table 8-10). A reflective boundary was placed on the west side (Y axis) to take advantage of geometric symmetry and thus, only 804 cylinders were included in the model.

The UBC Storage Pad contains both filled feed and filled tails cylinders. For validation, all the cylinders were assumed to be filled feed cylinders. This assumption is reasonable, as the photon doses are practically the same for feed and tails material. Moreover, each cylinder was filled to a maximum content of 12,501 kg UF₆. In actuality, the cylinder fill content is typically less than the maximum capacity. A test MCNP run for a single feed cylinder with 10,000 kg UF₆ shows that there is no appreciable change in the

average contact dose rate on the external surface of the cylinder, as the smaller source due to less UF_6 is offset by the weaker self-shielding effect of less UF_6 .

The indirect Monte Carlo simulation approach described in Section 5.4 was applied here to calculate the photon dose rates at the detector locations. The source importance for source position biasing was based on the 30x30 array data provided in Table 5-2 in Chapter 5 for the radial direction. The radial source importance data are applicable to the axial direction after testing and experimentation. The use of the axial importance data tended to provide an over-biased distribution with negative impacts on statistics.

As for the case study, the MCNP5, v1.60 code was employed for dose calculations in two steps – the first step for writing a surface source file and the second step for producing a mesh tally. Appendix J lists the MCNP input and output files created plus other pertinent information such as CPU time taken, number of histories processed and tracks written. The input listing is also included in Appendix J.

Table 8-11 provides the MCNP calculated photon dose rate results together with comparison with the measurements from the UNM detector readings. At the RAB, the calculated dose rates are consistently higher than the measured values by a factor in the neighborhood of 2. The difference becomes smaller at 50 ft (~15 m) from the RAB and beyond. It needs to be pointed out that the readings at the RAB were at the cylinder centerlines where the doses could be lower. A preliminary measurement with the UUSA MicroRem Dose Rate Meter on April 16, 2014 showed an average photon dose rate of 80 $\mu\text{rem/h}$ at the RAB (average of 90, 80 and 70 $\mu\text{rem/h}$ at three representative locations along the RAB). This measurement was more suitable for direct comparison with the MCNP calculation which scored an average tally over a mesh element, resulting in a calculation-to-

measurement (C/M) ratio of approximately 1.5. This C/M ratio is consistent with the dose ratio between the homogenized and slumped source geometry for a single cylinder in the axial direction (Table E-8 in Appendix E). Correction of the calculated dose rates for the slumped source geometry would lead to a satisfactory agreement between the calculation and measurement for the cylinder array.

The comparison proves that the homogenized source geometry used in the validation model is conservative and the dose ratio decreases with distance as concluded from the single cylinder evaluation (Table E-8 in Appendix E). Furthermore, the indirect Monte Carlo simulation approach is efficient and suitable for the environmental dose assessment with reasonable confidence.

Table 8-10 Comparison between Case Study and UBC Storage Pad Calculation

Description	Case Study	UBC Calculation
Cylinder Array	Square	Rectangular
Array Size	10x10, 30x30 & 100x100	100x8
Stacking	Single, double & triple	Double
Cylinder End Orientation	North - south	Same
Receptor Direction	Radial (east side)	Axial (south side)
Cylinder Type	48Y filled feed cylinders	Same
Cylinder CTC* Radial Spacing	5 ft	5.5 ft (actual)
Cylinder CTC Axial Spacing	16 ft	14.5 ft (actual)
Aisle Way	No	Yes
Cylinder Ground Clearance	6 in.	3.5 in. (actual)
Vertical Overlap between Cylinders	None	Same
UF ₆ Source Geometry	Homogenized	Same
Concrete Pad	Simulated by soil	Same
Ground scattering	Included	Same
Photon Source Energy Spectrum	Partial (important groups)	Same
Flux-to-dose-rate Conversion Factors	ANSI/ANS-6.1.1-1977	Same
Source Position Biasing	Radial importance in Tables 5-1 & 5-2 used	Radial importance in Table 5-2 used (applicable to axial)
Source Energy Biasing	Biased distribution in Table 5-4 used	Same
Source Direction Biasing	See Section 5.3.3	Same
Monte Carlo Simulation	Two-step process	Same

*Center-to-Center



Figure 8-1 UUSA UBC Storage Pad Validation Model

Table 8-11 Comparison with Photon Measurements at UUSA UBC Storage Pad

Detector Point	Distance from RAB (ft)	Distance from Centerline (ft)	UNM Measured - M (µrem/h)	UNM Calculated - C (µrem/h)*	C/M
A	0	-220	55	116 (0.070)	2.11
B	0	-165	54	123 (0.030)	2.28
C	0	-110	56	123 (0.028)	2.20
D	0	-55	56	125 (0.029)	2.23
E	0	0	78	128 (0.045)	1.64
F	0	55	58	125 (0.029)	2.16
G	0	110	53	123 (0.028)	2.32
H	0	165	54	123 (0.030)	2.28
I	0	220	52	116 (0.070)	2.23
J	50	0	42	58 (0.041)	1.38
K	100	0	27	33 (0.053)	1.22
L	100	50	26	38 (0.058)	1.46
M	100	100	28	33 (0.050)	1.18
N	150	0	21	26 (0.070)	1.24
O	150	100	21	25 (0.098)	1.19

*Relative error in parentheses

Row A									North Cylinder Edge
Row B									
Row C									
Row D	UBC Storage Pad								
Row E	100x8 Array - Approximate								
Row F	Double Stacking								
Row G									
Row H									South Cylinder Edge
45 ft Separation between South Cylinder Edge and RAB									
Restricted Area Boundary (RAB)									
A	B	C	D	E	F	G	H	I	
55/116	54/123	56/123	56/125	78/128	58/125	53/123	54/123	52/116	
				J					
				42/58	(50 ft from RAB)				
				K	L	M			
				27/33	26/38	28/33	(100 ft from RAB)		
A to O - Detector Locations									
Measured/Calculated Photon Dose Rate (µrem/h)									
Not to Scale				N			O		
				21/26			21/25	(150 ft from RAB)	

9. CONCLUSIONS AND FUTURE WORK

This research completed the full scope of work in four sequential distinct phases as defined Section 1.2 – UF₆ source term development (Phase 1), single cylinder dose evaluation (Phase 2), multiple cylinder dose assessment (Phase 3), and validation (Phase 4). Based on the conclusions reached in this chapter, the efforts met the objectives of substantially improving the Monte Carlo computational efficiency for dose simulations, and supporting onsite storage management of UF₆ cylinders as set forth in Section 1.1. Future related work is recommended for further development and enhancement.

9.1 CONCLUSIONS ON SOURCE TERMS

UF₆ emits neutron and photon radiation. The neutron source arises from spontaneous fission of uranium isotopes and (α , n) reactions with fluorine, and the photon source comes from gamma-rays, X-rays and bremsstrahlung emitted from uranium isotopes and their decay products. As generated with the ORIGEN-S module in SCALE 6.1.2, these source terms are necessary for the single cylinder dose evaluation and multiple cylinder dose assessment. Both sources are dependent on the U-235 concentration with more sensitivity for neutrons than for photons because of the contributing (α , n) component.

The source terms are different for filled and empty cylinders. The former with both neutron and photon sources contains UF₆ filled at or near the allowable capacity, while the latter with the photon source only retains residual radioactivity of the progeny following separation from uranium. The neutron source is time independent, whereas the photon source changes with time. For filled cylinders, the buildup of the daughter products from the decay of uranium isotopes reaches an equilibrium photon source after an in-growth time of

one year. For empty cylinders, the photon source decays rapidly with time after emptying. However, the freshly emptied feed cylinders require special attention because of their dose impacts due to the absence of UF_6 for self-shielding.

9.2 CONCLUSIONS ON SINGLE CYLINDER DOSE EVALUATION

For a filled feed or tails cylinder, the typical average contact dose rate on the external surface is about 2 mrem/h (~90% photon). The use of filled feed cylinders is bounding for dose assessment, as the feed dose is slightly higher than the tails dose. A freshly emptied feed cylinder with residual activity from the uranium progeny gives a dose rate of about 20 mrem/h (100% photons) at contact. The dose difference by one order of magnitude between the filled and empty cylinders affects storage management, and must be addressed in the multiple cylinder dose assessment.

The single cylinder dose evaluation with MCNP5, v1.60 concludes that it is conservative to use the homogenized source geometry for dose calculations to satisfy the regulatory preference. The concrete pad can be simulated by dry soil with an inconsequential effect on the photon doses, but with conservative results for the neutron doses which are acceptable because of a relatively small neutron component of the total dose. Ground scattering may increase or decrease the resulting doses depending on distances, and needs to be considered in the model for dose calculations. Secondary photon contributions from neutron interactions are negligible, and thus can be ignored. The dose conversion factors from the ANSI/ANS-6.1.1-1977 standard are appropriate to use for regulatory compliance and for comparison of ambient dose equivalents with measurements.

9.3 CONCLUSIONS ON MULTIPLE CYLINDER DOSE ASSESSMENT

An efficient indirect Monte Carlo simulation approach using MCNP5, v1.60 was developed for multiple cylinder dose assessment, and applied to the case study and validation model for proof of viability. The indirect simulation involved a two-step process with the first step to write a surface source file for use as a starting source in the second step to produce a mesh tally of the dose results and associated relative errors. The first step modeled each individual cylinder explicitly using the repeated structure feature. The model for the second step was fairly simple, consisting of a black box containing all cylinders and the surrounding air and soil.

The first-step process incorporated source importance biasing for better computational efficiency. Source energy and direction biasing applied to both neutrons and photons. The photon source included an additional scheme for position biasing, which was found unnecessary for neutrons. The photon source importance data with respect to position were generated with MAVRIC for the 10x10 and 30x30 arrays in two-high geometry. These data are applicable to other arrays and stacking arrangements by approximations and extrapolations. The radial importance data are also useful for the axial direction to avoid over-biasing and consideration of detector-dependent importance data.

The case study using the indirect Monte Carlo simulation approach covered 10x10, 30x30 and 100x100 arrays of filled feed cylinders in one-, two- and three-high geometry to investigate the dose trend and sensitivity to storage capacity and arrangements. All the cases achieved satisfactory statistics within reasonable computer times. The neutron calculations required less time than the photon calculations by virtue of less UF_6 self-shielding effect.

The results of the case study for filled cylinders show that the dose is more sensitive to the array size than stacking, and stacking is highly beneficial for boosting the storage capacity within a given footprint from a dose impact perspective. The array size and stacking also affects the setback distance requirements from the site boundary for regulatory compliance. As deduced from the case study, there is a simple relation between cylinder number and stacking and the required boundary distance. Increasing the array size from 10x10 to 30x30 and 30x30 to 100x100 moves the allowed dose 70 m and 120 m, respectively further away from the edge of the array, regardless of the stacking configurations. Stacking will increase the setback distance by 20 m from one to two high, and another 10 m from two to three high (30 m total from one to three high), independent of the array size.

Co-location of empty feed cylinders with filled cylinders on the storage pad must consider their dose impacts. For dose assessment, an equivalent number of freshly emptied cylinders may be conservatively used in lieu of each individual cylinder with a time-dependent photon source to simplify the analytical model. The equivalent number of fresh empties is relatively small, typically representing less than 1% of the total inventory on the storage pad. However their dose contribution is significant. A comparison of a 10x10 array of fresh empties and 100x100 array of filled cylinder in triple stacking shows that the smaller empty array gives higher photon dose rates than the filled array at close-in distances (less than 100 m) with diminishing but still significant contributions beyond 100 m. Dose impacts from empties can be minimized by means of strategic placement of empties on the storage pad with sufficient shielding by the surrounding filled cylinders, or segregation in a separate storage area where environmental doses are not negatively impacted.

9.4 CONCLUSIONS ON VALIDATION

Comparison of the direct (once-through) and indirect (two-step) Monte Carlo simulation methods indicates that the two-step process is a powerful approach for problems with multiple sources even without specific source biasing. For the triple-stacked 100x100 filled cylinder array, the unbiased (no position biasing) two-step neutron calculation improved the computational efficiency in terms of the FOM over the once-through process by better than one order of magnitude at environmental locations. Source position biasing was unnecessary for neutrons because of poor neutron attenuation by UF_6 . The photon calculations required the source position biasing to further improve computational efficiency. The overall improvement in the FOM achieved with the biased two-step process for photons was one to two orders of magnitude, depending on distances. Comparison with the UUSA calculation for a triple-stacked array with over 25,000 cylinders also shows that the indirect Monte Carlo simulation approach improved the FOM substantially (on the order of 500) at the selected environmental locations.

Additional efficiency in terms of resource (labor and computer) utilization is achievable by using the results from the single-stack calculation to quickly estimate the doses for the double and triple stacks without detailed calculations. For accuracy, appropriate correction factors must be incorporated into the estimated doses to account for the increase in the dose contribution from the top surface of the cylinder-containing box. At typical environmental locations, the correction factor amounts to 1.2 for neutrons and 1.1 for photons.

On validation of the dose simulations, the UNM calculation for a single filled feed cylinder and a single filled tails cylinder is in satisfactory agreement with the measurements

and other reliable independent calculations. This agreement validates the physical model (geometry and material), neutron and photon source terms, dose conversion factors and nuclear data used. The UNM calculation for an empty feed cylinder is conservative relative to the UD calculation and the UUSA SAR values, but fairly consistent with the UUSA radiation surveys after discounting localized peaks.

The dose simulation with the indirect Monte Carlo approach for the UUSA UBC Storage Pad that existed as of April 2014 produced conservative (higher) photon results as compared to the field measurements. The conservatism is due mainly to the assumption of the homogenized source geometry for UF₆ in filled cylinders. Correction for the more realistic slumped source geometry brought the calculated photon dose rates in line with the measured data, validating the efficiency and accuracy of the approach and data used in the cylinder array dose assessment with reasonable confidence.

9.5 FUTURE WORK

As a result of this research, the following future related work is worthwhile and recommended to complement or supplement the accomplishments to date:

1. Neutron Measurements – This research validated the cylinder array dose for photons only, because of a relatively small neutron component of the total dose rate at the existing UUSA Enrichment facility. As more cylinders are added onto the storage pad, the neutron component may be still less than the photon component, but becomes increasingly important especially at the environmental locations where skyshine radiation is of concern. Neutron measurements with a calibrated neutron detector will be beneficial to obtain the data for validation of neutron dose calculations for a cylinder array.

2. Differential Measurements – The measured data used in Sections 8.1 and 8.4 for comparison with the calculations are from integral measurements of the doses for all energy groups. Differential measurements will provide the energy spectrum data for comparison with the calculated energy spectra, as the dose conversion factors are energy dependent and affect the resulting doses.
3. Case Study for Rectangular Array – The case study considered in this research used a square storage array (in terms of cylinder quantity) to explore the dose sensitivity to the array size and stacking arrangement, and determine the setback distances from the site boundary. Although the results for the square array are expected to be applicable to the rectangular array used at UUSA, confirmation by additional calculations is desirable and useful.
4. Dose Trending – The dose increase with more cylinders placed on the storage pad may not be appreciable from month to month, but should be noticeable from year to year. Validation of the dose simulations on a yearly basis is valuable to establish a clear dose trend as the storage inventory increases with time.
5. Areas of Applicability – The indirect Monte Carlo simulation approach is applicable to other shielding problems with multiple sources such as radwaste storage yards, spent nuclear fuel dry storage cask array and high-capacity nuclear fuel transportation casks. Extension of the application of this approach to other related areas is worth investigating.

APPENDICES

This document contains the following appendices:

APPENDIX A	ORIGEN-S COMPUTER FILES AND SAMPLE INPUT
APPENDIX B	NEUTRON AND PHOTON SOURCE DATA
APPENDIX C	FLUX-TO-DOSE RATE CONVERSION FACTORS
APPENDIX D	MCNP COMPUTER FILES FOR SINGLE CYLINDERS
APPENDIX E	CALCULATED DOSE RATES FOR SINGLE CYLINDERS
APPENDIX F	MAVRIC COMPUTER FILES AND INPUT LISTING
APPENDIX G	MCNP COMPUTER FILES FOR FILLED CYLINDER ARRAY
APPENDIX H	MCNP DOSE RATE MAPS AND RELATIVE ERRORS
APPENDIX I	EMPTY FEED CYLINDER DOSE ASSESSMENT
APPENDIX J	UUSA UBC STORAGE PAD DOSE CALCULATION

APPENDIX A ORIGEN-S COMPUTER FILES AND SAMPLE INPUT

A.1 ORIGEN-S CASES AND COMPUTER FILES

Table A-1 lists the ORIGEN-S computer files used to generate the UF₆ neutron and photon source terms for filled tails and feed cylinders. The ORIGEN-S cases for an empty feed cylinder are listed in Table A-2.

Table A-1 ORIGEN-S Case Description and Computer Files for Filled Tails and Feed Cylinders

Case	Description	Input File*	Output File*
1	Tails UF ₆ (0.2% U-235) with UO ₂ brem	du2.inp	du2.out
2	Tails UF ₆ (0.2% U-235) without brem	du2_n.inp	du2_n.out
3	Tails UF ₆ (0.3% U-235) with UO ₂ brem	du3.inp	du3.out
4	Tails UF ₆ (0.3% U-235) without brem	du3_n.inp	du3_n.out
5	Tails UF ₆ (0.4% U-235) with UO ₂ brem	du4.inp	du4.out
6	Tails UF ₆ (0.4% U-235) without brem	du4_n.inp	du4_n.out
7	Tails UF ₆ (0.5% U-235) with UO ₂ brem	du5.inp	du5.out
8	Tails UF ₆ (0.5% U-235) without brem	du5_n.inp	du5_n.out
9	Feed UF ₆ (0.711% U-235) with UO ₂ brem	nu.inp	nu.out
10	Feed UF ₆ (0.711% U-235) without brem	nu_n.inp	nu_n.out

*du denotes the symbol for depleted U, and nu for natural U.

Table A-2 ORIGEN-S Case Description and Computer Files for Empty Feed Cylinders

Case	Description	Input File	Output File
1	Progeny inventory calculation	nu1.inp	nu2.out
2	Progeny photon source calculation	nu2.inp	nu2.out

A.2 SAMPLE ORIGEN-S INPUT LISTING

The representative cases selected for listing of the sample ORIGEN-S input files include the following:

- File *nu.inp* – Feed UF₆ (0.711% U-235) with UO₂ brems (§A.2.1)
- File *nu_n.inp* – Feed UF₆ (0.711% U-235) without UO₂ brems (§A.2.2)
- File *nu1.inp* – Progeny inventory for empty feed cylinder (§A.2.3)
- File *nu2.inp* – Progeny photon source for empty feed cylinder (§A.2.4)

A.2.1 Input File *nu.inp* – Natural Uranium with UO₂ Bremsstrahlung

```
=origen
0$$$ a11 71 e
1$$$ 1 t
NATURAL UF6 RADIATION SOURCE TERMS PER KG OF UF6
3$$$ 21 0 1 -88 a16 2 a32 0 -88 e t
35$$$ 0 t
54$$$ a9 1 a11 2 e
56$$$ 0 2 a5 2 a13 5 5 3 0 2 1 e
95$$$ 0 t
NATURAL UF6 (0.711% U-235 in U) RADIATION SOURCE TERMS
PER KG OF UF6 (UO2 BREMSSTRAHLUNG)
60** 0 1
61** 2r1.0E+99 3r1.0E-40 2r1.0E+99
65$$$ 27z 1 0 0 0 0 0 e
73$$$ 922340 922350 922360 922380 90190
74** 3.6122E-02 4.8076E+00 2.2115E-02 6.7132E+02 3.2382E+02
75$$$ 4r2 1 e
81$$$ 2 0 26 1 e
82$$$ f 2 e
t
56$$$ f0 t
end
```

A.2.2 Input File *nu.inp* – Natural Uranium without UO₂ Bremsstrahlung

```
=origen
0$$$ a11 71 e
1$$$ 1 t
NATURAL UF6 RADIATION SOURCE TERMS PER KG OF UF6
3$$$ 21 0 1 -88 a16 2 a32 0 -88 e t
35$$$ 0 t
54$$$ a9 1 a11 2 e
56$$$ 0 2 a5 2 a13 5 5 3 0 2 1 e
95$$$ 0 t
NATURAL UF6 (0.711% U-235 in U) RADIATION SOURCE TERMS
```



```

PER KG OF UF6 (NO BREMSSTRAHLUNG)
60** 0 1
61** 2r1.0E+99 3r1.0E-40 2r1.0E+99
65$$ 27z 1 0 0 0 0 0 0 e
73$$ 922340      922350      922360      922380      90190
74** 3.6122E-02 4.8076E+00 2.2115E-02 6.7132E+02 3.2382E+02
75$$ 4r2 1 e
81$$ 2 0 23 1 e
82$$ f 2 e
t
56$$ f0 t
end

```

A.2.3 Input File *nu1.inp* – Progeny Inventory for Empty Feed Cylinder

```

=origen
0$$  a11 71 e
1$$  1 t
NATURAL UF6 RADIATION SOURCE TERMS PER 48Y CYLINDER (12501 KG UF6)
3$$  21 0 1 -88 a16 2 a32 0 -88 e t
35$$ 0 t
54$$ a9 1 a11 2 e
56$$ 0 2 a5 2 a13 5 5 3 0 2 1 e
95$$ 0 t
NATURAL UF6 (0.711% U-235 in U) RADIATION SOURCE TERMS
PER 48Y CYLINDER (12501 KG UF6 - UO2 BREM)
60** 0 1
61** 1.0E+99 4r1.0E-40 2r1.0E+99
65$$ 24z 1 1 1 1 1 1 0 0 0 0 e
73$$ 922340      922350      922360      922380      90190
74** 4.5156E+02 6.0100E+04 2.7646E+02 8.3921E+06 4.0481E+06
75$$ 4r2 1 e
81$$ 2 0 26 1 e
82$$ f 2 e
t
56$$ f0 t
End

```

A.2.4 Input File *nu.inp* – Progeny Photon Source for Empty Feed Cylinder

```

=origen
0$$  a11 71 e
1$$  1 t
NATURAL UF6 PHOTON SOURCE TERMS PER EMPTY 48Y CYLINDER
3$$  21 0 1 0 a16 2 a32 0 -88 e t
35$$ 0 t
54$$ a9 1 a11 2 e
56$$ 0 11 a5 2 a13 44 5 3 0 2 1 e
95$$ 0 t
NATURAL UF6 (0.711% U-235 in U) PHOTON SOURCE TERMS
PER EMPTY 48Y CYLINDER (H2O BREMSSTRAHLUNG)
60** 0 0.1 0.2 0.3 0.5 0.7 1.0 2.0 3.0 5.0 10.0
61** 2r1.0E+99 3r1.0E-40 2r1.0E+99
65$$ 27z 1 0 0 0 0 0 0 e
73$$ 812060      812070      812080      812100      822060

```

	822070	822080	822090	822100	822110
	822120	822140	832100	832110	832120
	832140	842100	842110	842120	842140
	842150	842160	842180	852180	862180
	862190	862200	862220	872230	882230
	882240	882260	882280	892270	892280
	902270	902280	902300	902310	902320
	902340	912310	912341	912340	
74**	3.510E-25	2.268E-16	6.923E-24	1.707E-21	1.553E-15
	5.132E-12	5.807E-19	2.168E-23	7.424E-13	1.754E-15
	4.105E-21	1.707E-16	4.589E-16	1.040E-16	3.894E-22
	1.268E-16	4.108E-15	1.153E-21	6.865E-29	1.062E-22
	1.470E-21	1.583E-26	2.011E-17	3.245E-23	7.571E-28
	3.329E-18	6.183E-24	3.639E-14	1.559E-17	8.453E-13
	3.581E-20	5.662E-09	1.874E-16	5.986E-10	2.287E-20
	1.387E-12	6.954E-18	1.253E-03	2.444E-07	8.044E-06
	1.219E-04	5.819E-05	4.070E-09	2.258E-09	
75\$\$	44r2 e				
81\$\$	2 0 24 1 e				
82\$\$	f 2 e				
t					
56\$\$	f0 t				
end					

APPENDIX B NEUTRON AND PHOTON SOURCE DATA

This appendix compiles the neutron and photon source data based on the calculations with the ORIGEN-S module in the SCALE 6.1.2 code package. The compilation includes the following:

- Neutron yield by uranium isotope (Table B-1)
- UF₆ Neutron Source Term per kg UF₆ (Tables B-2 through B-6)
- Uncorrected UF₆ Photon Source Term per kg UF₆ (Tables B-7 through B-11)
- Corrected UF₆ Photon Source Term kg UF₆ (Tables B-8 through B-16)
- Source Term Comparisons (Tables B-17 and B-18)

Table B-1 Neutron Yield by Isotope

Material	Contributor	Neutron Yield (n/s per kg of UF ₆)				
		U-234	U-235	U-236	U-238	U-total
Depleted U (0.2% U-235)	(α, n)	5.577E+00	1.486E-01	2.564E-02	8.047E+00	1.380E+01
	S. F.	6.246E-05	1.408E-05	2.673E-05	9.197E+00	9.197E+00
	Total	5.577E+00	1.486E-01	2.567E-02	1.724E+01	2.300E+01
Depleted U (0.3% U-235)	(α, n)	8.655E+00	2.229E-01	3.846E-02	8.039E+00	1.696E+01
	S. F.	9.693E-05	2.113E-05	4.010E-05	9.187E+00	9.187E+00
	Total	8.655E+00	2.229E-01	3.850E-02	1.723E+01	2.614E+01
Depleted U (0.4% U-235)	(α, n)	1.182E+01	2.973E-01	5.128E-02	8.031E+00	2.020E+01
	S. F.	1.324E-04	2.817E-05	5.347E-05	9.178E+00	9.178E+00
	Total	1.182E+01	2.973E-01	5.133E-02	1.721E+01	2.938E+01
Depleted U (0.5% U-235)	(α, n)	1.505E+01	3.716E-01	6.409E-02	8.023E+00	2.351E+01
	S. F.	1.686E-04	3.521E-05	6.683E-05	9.169E+00	9.169E+00
	Total	1.505E+01	3.716E-01	6.416E-02	1.719E+01	3.268E+01
Natural U (0.711% U-235)	(α, n)	2.205E+01	5.284E-01	9.114E-02	8.005E+00	3.067E+01
	S. F.	2.469E-04	5.007E-05	9.504E-05	9.149E+00	9.149E+00
	Total	2.205E+01	5.285E-01	9.124E-02	1.715E+01	3.982E+01

Table B-2 UF₆ Neutron Source Term at 0.2% U-235

Group	Energy Boundaries (MeV)	DU-0.2% Neutron Source Intensity (n/s per kg of UF ₆)		
		(α, n) Reaction	Spontaneous Fission	Total
1	1.00E-11 - 1.00E-08	0.000E+00	2.444E-17	2.444E-17
2	1.00E-08 - 3.00E-08	0.000E+00	6.917E-17	6.917E-17
3	3.00E-08 - 5.00E-08	0.000E+00	1.742E-11	1.742E-11
4	5.00E-08 - 1.00E-07	0.000E+00	7.353E-11	7.353E-11
5	1.00E-07 - 2.25E-07	0.000E+00	3.021E-10	3.021E-10
6	2.25E-07 - 3.25E-07	0.000E+00	4.665E-10	4.665E-10
7	3.25E-07 - 4.14E-07	0.000E+00	2.055E-10	2.055E-10
8	4.14E-07 - 8.00E-07	0.000E+00	1.930E-09	1.930E-09
9	8.00E-07 - 1.00E-06	0.000E+00	1.474E-09	1.474E-09
10	1.00E-06 - 1.13E-06	0.000E+00	5.982E-10	5.982E-10
11	1.13E-06 - 1.30E-06	0.000E+00	1.254E-09	1.254E-09
12	1.30E-06 - 1.86E-06	0.000E+00	4.884E-09	4.884E-09
13	1.86E-06 - 3.06E-06	1.616E-09	1.201E-08	1.362E-08
14	3.06E-06 - 1.07E-05	1.154E-08	1.295E-07	1.411E-07
15	1.07E-05 - 2.90E-05	1.591E-07	5.334E-07	6.926E-07
16	2.90E-05 - 1.01E-04	1.399E-06	3.793E-06	5.192E-06
17	1.01E-04 - 5.83E-04	2.330E-05	5.736E-05	8.066E-05
18	5.83E-04 - 3.04E-03	2.514E-04	6.725E-04	9.240E-04
19	3.04E-03 - 1.50E-02	2.650E-03	7.337E-03	9.987E-03
20	1.50E-02 - 1.11E-01	8.763E-02	1.501E-01	2.377E-01
21	1.11E-01 - 4.08E-01	1.322E+00	8.620E-01	2.184E+00
22	4.08E-01 - 9.07E-01	5.461E+00	1.844E+00	7.305E+00
23	9.07E-01 - 1.42E+00	4.687E+00	1.790E+00	6.477E+00
24	1.42E+00 - 1.83E+00	1.708E+00	1.157E+00	2.865E+00
25	1.83E+00 - 3.01E+00	5.307E-01	2.114E+00	2.644E+00
26	3.01E+00 - 6.38E+00	0.000E+00	1.226E+00	1.226E+00
27	6.38E+00 - 2.00E+01	0.000E+00	4.655E-02	4.655E-02
Total	1.00E-11 - 2.00E+01	1.380E+01	9.197E+00	2.300E+01

*Associated ORIGEN-S output file – du2.out

Table B-3 UF₆ Neutron Source Term at 0.3% U-235

Group	Energy Boundaries (MeV)	DU-0.3% Neutron Source Intensity (n/s per kg of UF ₆)		
		(α, n) Reaction	Spontaneous Fission	Total
1	1.00E-11 - 1.00E-08	0.000E+00	3.666E-17	3.666E-17
2	1.00E-08 - 3.00E-08	0.000E+00	1.038E-16	1.038E-16
3	3.00E-08 - 5.00E-08	0.000E+00	1.740E-11	1.740E-11
4	5.00E-08 - 1.00E-07	0.000E+00	7.345E-11	7.345E-11
5	1.00E-07 - 2.25E-07	0.000E+00	3.018E-10	3.018E-10
6	2.25E-07 - 3.25E-07	0.000E+00	4.660E-10	4.660E-10
7	3.25E-07 - 4.14E-07	0.000E+00	2.053E-10	2.053E-10
8	4.14E-07 - 8.00E-07	0.000E+00	1.928E-09	1.928E-09
9	8.00E-07 - 1.00E-06	0.000E+00	1.472E-09	1.472E-09
10	1.00E-06 - 1.13E-06	0.000E+00	5.976E-10	5.976E-10
11	1.13E-06 - 1.30E-06	0.000E+00	1.253E-09	1.253E-09
12	1.30E-06 - 1.86E-06	0.000E+00	4.879E-09	4.879E-09
13	1.86E-06 - 3.06E-06	2.507E-09	1.200E-08	1.451E-08
14	3.06E-06 - 1.07E-05	1.790E-08	1.294E-07	1.473E-07
15	1.07E-05 - 2.90E-05	2.440E-07	5.329E-07	7.769E-07
16	2.90E-05 - 1.01E-04	1.859E-06	3.789E-06	5.648E-06
17	1.01E-04 - 5.83E-04	2.998E-05	5.730E-05	8.728E-05
18	5.83E-04 - 3.04E-03	3.190E-04	6.719E-04	9.909E-04
19	3.04E-03 - 1.50E-02	3.249E-03	7.329E-03	1.058E-02
20	1.50E-02 - 1.11E-01	1.018E-01	1.499E-01	2.517E-01
21	1.11E-01 - 4.08E-01	1.493E+00	8.611E-01	2.354E+00
22	4.08E-01 - 9.07E-01	6.375E+00	1.842E+00	8.217E+00
23	9.07E-01 - 1.42E+00	5.902E+00	1.788E+00	7.690E+00
24	1.42E+00 - 1.83E+00	2.267E+00	1.156E+00	3.423E+00
25	1.83E+00 - 3.01E+00	8.121E-01	2.111E+00	2.923E+00
26	3.01E+00 - 6.38E+00	0.000E+00	1.224E+00	1.224E+00
27	6.38E+00 - 2.00E+01	0.000E+00	4.650E-02	4.650E-02
Total	1.00E-11 - 2.00E+01	1.696E+01	9.188E+00	2.615E+01

*Associated ORIGEN-S output file – du3.out

Table B-4 UF₆ Neutron Source Term at 0.4% U-235

Group	Energy Boundaries (MeV)	DU-0.4% Neutron Source Intensity (n/s per kg of UF ₆)		
		(α , n) Reaction	Spontaneous Fission	Total
1	1.00E-11 - 1.00E-08	0.000E+00	4.888E-17	4.888E-17
2	1.00E-08 - 3.00E-08	0.000E+00	1.383E-16	1.383E-16
3	3.00E-08 - 5.00E-08	0.000E+00	1.738E-11	1.738E-11
4	5.00E-08 - 1.00E-07	0.000E+00	7.338E-11	7.338E-11
5	1.00E-07 - 2.25E-07	0.000E+00	3.015E-10	3.015E-10
6	2.25E-07 - 3.25E-07	0.000E+00	4.656E-10	4.656E-10
7	3.25E-07 - 4.14E-07	0.000E+00	2.050E-10	2.050E-10
8	4.14E-07 - 8.00E-07	0.000E+00	1.926E-09	1.926E-09
9	8.00E-07 - 1.00E-06	0.000E+00	1.471E-09	1.471E-09
10	1.00E-06 - 1.13E-06	0.000E+00	5.970E-10	5.970E-10
11	1.13E-06 - 1.30E-06	0.000E+00	1.251E-09	1.251E-09
12	1.30E-06 - 1.86E-06	0.000E+00	4.874E-09	4.874E-09
13	1.86E-06 - 3.06E-06	3.424E-09	1.198E-08	1.540E-08
14	3.06E-06 - 1.07E-05	2.443E-08	1.293E-07	1.537E-07
15	1.07E-05 - 2.90E-05	3.312E-07	5.324E-07	8.636E-07
16	2.90E-05 - 1.01E-04	2.332E-06	3.785E-06	6.117E-06
17	1.01E-04 - 5.83E-04	3.684E-05	5.725E-05	9.409E-05
18	5.83E-04 - 3.04E-03	3.884E-04	6.712E-04	1.060E-03
19	3.04E-03 - 1.50E-02	3.864E-03	7.322E-03	1.119E-02
20	1.50E-02 - 1.11E-01	1.163E-01	1.498E-01	2.661E-01
21	1.11E-01 - 4.08E-01	1.669E+00	8.602E-01	2.529E+00
22	4.08E-01 - 9.07E-01	7.315E+00	1.840E+00	9.155E+00
23	9.07E-01 - 1.42E+00	7.151E+00	1.786E+00	8.937E+00
24	1.42E+00 - 1.83E+00	2.842E+00	1.155E+00	3.997E+00
25	1.83E+00 - 3.01E+00	1.102E+00	2.109E+00	3.211E+00
26	3.01E+00 - 6.38E+00	0.000E+00	1.223E+00	1.223E+00
27	6.38E+00 - 2.00E+01	0.000E+00	4.645E-02	4.645E-02
Total	1.00E-11 - 2.00E+01	2.020E+01	9.178E+00	2.938E+01

*Associated ORIGEN-S output file – du4.out

Table B-5 UF₆ Neutron Source Term at 0.5% U-235

Group	Energy Boundaries (MeV)	DU-0.5% Neutron Source Intensity (n/s per kg of UF ₆)		
		(α, n) Reaction	Spontaneous Fission	Total
1	1.00E-11 - 1.00E-08	0.000E+00	6.109E-17	6.109E-17
2	1.00E-08 - 3.00E-08	0.000E+00	1.729E-16	1.729E-16
3	3.00E-08 - 5.00E-08	0.000E+00	1.736E-11	1.736E-11
4	5.00E-08 - 1.00E-07	0.000E+00	7.330E-11	7.330E-11
5	1.00E-07 - 2.25E-07	0.000E+00	3.012E-10	3.012E-10
6	2.25E-07 - 3.25E-07	0.000E+00	4.651E-10	4.651E-10
7	3.25E-07 - 4.14E-07	0.000E+00	2.048E-10	2.048E-10
8	4.14E-07 - 8.00E-07	0.000E+00	1.924E-09	1.924E-09
9	8.00E-07 - 1.00E-06	0.000E+00	1.469E-09	1.469E-09
10	1.00E-06 - 1.13E-06	0.000E+00	5.964E-10	5.964E-10
11	1.13E-06 - 1.30E-06	0.000E+00	1.250E-09	1.250E-09
12	1.30E-06 - 1.86E-06	0.000E+00	4.869E-09	4.869E-09
13	1.86E-06 - 3.06E-06	4.361E-09	1.197E-08	1.633E-08
14	3.06E-06 - 1.07E-05	3.111E-08	1.291E-07	1.602E-07
15	1.07E-05 - 2.90E-05	4.203E-07	5.318E-07	9.521E-07
16	2.90E-05 - 1.01E-04	2.815E-06	3.781E-06	6.596E-06
17	1.01E-04 - 5.83E-04	4.385E-05	5.719E-05	1.010E-04
18	5.83E-04 - 3.04E-03	4.593E-04	6.705E-04	1.130E-03
19	3.04E-03 - 1.50E-02	4.492E-03	7.314E-03	1.181E-02
20	1.50E-02 - 1.11E-01	1.311E-01	1.496E-01	2.807E-01
21	1.11E-01 - 4.08E-01	1.849E+00	8.593E-01	2.708E+00
22	4.08E-01 - 9.07E-01	8.274E+00	1.838E+00	1.011E+01
23	9.07E-01 - 1.42E+00	8.426E+00	1.785E+00	1.021E+01
24	1.42E+00 - 1.83E+00	3.430E+00	1.154E+00	4.584E+00
25	1.83E+00 - 3.01E+00	1.397E+00	2.107E+00	3.504E+00
26	3.01E+00 - 6.38E+00	0.000E+00	1.222E+00	1.222E+00
27	6.38E+00 - 2.00E+01	0.000E+00	4.641E-02	4.641E-02
Total	1.00E-11 - 2.00E+01	2.351E+01	9.169E+00	3.268E+01

*Associated ORIGEN-S output file – du5.out

Table B-6 UF₆ Neutron Source Term at 0.711% U-235

Group	Energy Boundaries (MeV)	NU Neutron Source Intensity (n/s per kg of UF ₆)		
		(α, n) Reaction	Spontaneous Fission	Total
1	1.00E-11 - 1.00E-08	0.000E+00	8.687E-17	8.687E-17
2	1.00E-08 - 3.00E-08	0.000E+00	2.459E-16	2.459E-16
3	3.00E-08 - 5.00E-08	0.000E+00	1.733E-11	1.733E-11
4	5.00E-08 - 1.00E-07	0.000E+00	7.315E-11	7.315E-11
5	1.00E-07 - 2.25E-07	0.000E+00	3.006E-10	3.006E-10
6	2.25E-07 - 3.25E-07	0.000E+00	4.641E-10	4.641E-10
7	3.25E-07 - 4.14E-07	0.000E+00	2.044E-10	2.044E-10
8	4.14E-07 - 8.00E-07	0.000E+00	1.920E-09	1.920E-09
9	8.00E-07 - 1.00E-06	0.000E+00	1.466E-09	1.466E-09
10	1.00E-06 - 1.13E-06	0.000E+00	5.951E-10	5.951E-10
11	1.13E-06 - 1.30E-06	0.000E+00	1.247E-09	1.247E-09
12	1.30E-06 - 1.86E-06	0.000E+00	4.859E-09	4.859E-09
13	1.86E-06 - 3.06E-06	6.386E-09	1.195E-08	1.834E-08
14	3.06E-06 - 1.07E-05	4.553E-08	1.289E-07	1.744E-07
15	1.07E-05 - 2.90E-05	6.130E-07	5.307E-07	1.144E-06
16	2.90E-05 - 1.01E-04	3.859E-06	3.773E-06	7.632E-06
17	1.01E-04 - 5.83E-04	5.901E-05	5.707E-05	1.161E-04
18	5.83E-04 - 3.04E-03	6.126E-04	6.691E-04	1.282E-03
19	3.04E-03 - 1.50E-02	5.850E-03	7.299E-03	1.315E-02
20	1.50E-02 - 1.11E-01	1.631E-01	1.493E-01	3.124E-01
21	1.11E-01 - 4.08E-01	2.237E+00	8.575E-01	3.095E+00
22	4.08E-01 - 9.07E-01	1.035E+01	1.834E+00	1.218E+01
23	9.07E-01 - 1.42E+00	1.118E+01	1.781E+00	1.296E+01
24	1.42E+00 - 1.83E+00	4.700E+00	1.151E+00	5.851E+00
25	1.83E+00 - 3.01E+00	2.036E+00	2.103E+00	4.139E+00
26	3.01E+00 - 6.38E+00	0.000E+00	1.219E+00	1.219E+00
27	6.38E+00 - 2.00E+01	0.000E+00	4.631E-02	4.631E-02
Total	1.00E-11 - 2.00E+01	3.067E+01	9.149E+00	3.982E+01

*Associated ORIGEN-S output file – nu.out

Table B-7 Uncorrected UF₆ Photon Source Term at 0.2% U-235

Group	Energy Boundaries (MeV)	DU-0.2% Photon Source Intensity (photons/s per kg of UF ₆)			
		Without Bremsstrahlung*		With UO ₂ Bremsstrahlung**	
		Initial (0 yr)	1 yr	Initial (0 yr)	1 yr
1	1.00E-02 - 4.50E-02	5.129E+05	8.595E+05	5.129E+05	3.521E+06
2	4.50E-02 - 1.00E-01	1.867E+04	7.751E+05	1.867E+04	1.897E+06
3	1.00E-01 - 2.00E-01	1.011E+05	1.250E+05	1.011E+05	8.095E+05
4	2.00E-01 - 3.00E-01	5.430E+03	1.512E+04	5.430E+03	2.435E+05
5	3.00E-01 - 4.00E-01	1.027E+02	1.302E+03	1.027E+02	1.687E+05
6	4.00E-01 - 6.00E-01	5.655E+00	4.812E+03	5.655E+00	1.150E+05
7	6.00E-01 - 8.00E-01	2.286E+01	5.338E+04	2.286E+01	1.013E+05
8	8.00E-01 - 1.00E+00	0.000E+00	5.533E+04	0.000E+00	7.471E+04
9	1.00E+00 - 1.33E+00	9.726E+00	3.389E+04	9.726E+00	4.442E+04
10	1.33E+00 - 1.66E+00	0.000E+00	4.901E+03	0.000E+00	6.646E+03
11	1.66E+00 - 2.00E+00	4.153E+00	7.384E+03	4.153E+00	7.653E+03
12	2.00E+00 - 2.50E+00	2.517E+00	3.042E+00	2.517E+00	1.511E+01
13	2.50E+00 - 3.00E+00	1.459E+00	1.459E+00	1.459E+00	1.459E+00
14	3.00E+00 - 4.00E+00	1.311E+00	1.311E+00	1.311E+00	1.311E+00
15	4.00E+00 - 5.00E+00	4.425E-01	4.425E-01	4.425E-01	4.425E-01
16	5.00E+00 - 6.50E+00	1.776E-01	1.776E-01	1.776E-01	1.776E-01
17	6.50E+00 - 8.00E+00	3.483E-02	3.483E-02	3.483E-02	3.483E-02
18	8.00E+00 - 1.00E+01	7.628E-03	7.628E-03	7.628E-03	7.628E-03
19	1.00E+01 - 2.00E+01	1.402E-04	1.402E-04	1.402E-04	1.402E-04
Total	1.00E-02 - 2.00E+01	6.383E+05	1.936E+06	6.383E+05	6.989E+06

*Associated ORIGEN-S output file – *du2_n.out*

**Associated ORIGEN-S output file – *du2.out*

Table B-8 Uncorrected UF₆ Photon Source Term at 0.3% U-235

Group	Energy Boundaries (MeV)	DU-0.3% Photon Source Intensity (photons/s per kg of UF ₆)			
		Without Bremsstrahlung*		With UO ₂ Bremsstrahlung**	
		Initial (0 yr)	1 yr	Initial (0 yr)	1 yr
1	1.00E-02 - 4.50E-02	5.920E+05	9.628E+05	5.920E+05	3.622E+06
2	4.50E-02 - 1.00E-01	2.618E+04	7.887E+05	2.618E+04	1.909E+06
3	1.00E-01 - 2.00E-01	1.513E+05	1.757E+05	1.513E+05	8.595E+05
4	2.00E-01 - 3.00E-01	8.134E+03	1.784E+04	8.134E+03	2.460E+05
5	3.00E-01 - 4.00E-01	1.541E+02	1.354E+03	1.541E+02	1.686E+05
6	4.00E-01 - 6.00E-01	8.539E+00	4.810E+03	8.539E+00	1.149E+05
7	6.00E-01 - 8.00E-01	2.290E+01	5.333E+04	2.290E+01	1.012E+05
8	8.00E-01 - 1.00E+00	0.000E+00	5.527E+04	0.000E+00	7.464E+04
9	1.00E+00 - 1.33E+00	9.719E+00	3.385E+04	9.719E+00	4.438E+04
10	1.33E+00 - 1.66E+00	0.000E+00	4.896E+03	0.000E+00	6.639E+03
11	1.66E+00 - 2.00E+00	4.150E+00	7.376E+03	4.150E+00	7.646E+03
12	2.00E+00 - 2.50E+00	2.515E+00	3.040E+00	2.515E+00	1.509E+01
13	2.50E+00 - 3.00E+00	1.458E+00	1.458E+00	1.458E+00	1.458E+00
14	3.00E+00 - 4.00E+00	1.310E+00	1.310E+00	1.310E+00	1.310E+00
15	4.00E+00 - 5.00E+00	4.421E-01	4.421E-01	4.421E-01	4.421E-01
16	5.00E+00 - 6.50E+00	1.774E-01	1.774E-01	1.774E-01	1.774E-01
17	6.50E+00 - 8.00E+00	3.480E-02	3.480E-02	3.480E-02	3.480E-02
18	8.00E+00 - 1.00E+01	7.621E-03	7.621E-03	7.621E-03	7.621E-03
19	1.00E+01 - 2.00E+01	1.400E-04	1.400E-04	1.400E-04	1.400E-04
Total	1.00E-02 - 2.00E+01	7.778E+05	2.106E+06	7.778E+05	7.155E+06

*Associated ORIGEN-S output file – *du3_n.out*

**Associated ORIGEN-S output file – *du3.out*

Table B-9 Uncorrected UF₆ Photon Source Term at 0.4% U-235

Group	Energy Boundaries (MeV)	DU-0.4% Photon Source Intensity (photons/s per kg of UF ₆)			
		Without Bremsstrahlung*		With UO ₂ Bremsstrahlung**	
		Initial (0 yr)	1 yr	Initial (0 yr)	1 yr
1	1.00E-02 - 4.50E-02	6.730E+05	1.068E+06	6.730E+05	3.726E+06
2	4.50E-02 - 1.00E-01	3.372E+04	8.024E+05	3.372E+04	1.922E+06
3	1.00E-01 - 2.00E-01	2.016E+05	2.264E+05	2.016E+05	9.095E+05
4	2.00E-01 - 3.00E-01	1.084E+04	2.056E+04	1.084E+04	2.485E+05
5	3.00E-01 - 4.00E-01	2.054E+02	1.406E+03	2.054E+02	1.685E+05
6	4.00E-01 - 6.00E-01	1.144E+01	4.808E+03	1.144E+01	1.148E+05
7	6.00E-01 - 8.00E-01	2.294E+01	5.327E+04	2.294E+01	1.011E+05
8	8.00E-01 - 1.00E+00	0.000E+00	5.521E+04	0.000E+00	7.456E+04
9	1.00E+00 - 1.33E+00	9.712E+00	3.382E+04	9.712E+00	4.433E+04
10	1.33E+00 - 1.66E+00	0.000E+00	4.891E+03	0.000E+00	6.632E+03
11	1.66E+00 - 2.00E+00	4.147E+00	7.368E+03	4.147E+00	7.638E+03
12	2.00E+00 - 2.50E+00	2.513E+00	3.038E+00	2.513E+00	1.508E+01
13	2.50E+00 - 3.00E+00	1.457E+00	1.457E+00	1.457E+00	1.457E+00
14	3.00E+00 - 4.00E+00	1.309E+00	1.309E+00	1.309E+00	1.309E+00
15	4.00E+00 - 5.00E+00	4.417E-01	4.417E-01	4.417E-01	4.417E-01
16	5.00E+00 - 6.50E+00	1.772E-01	1.772E-01	1.772E-01	1.772E-01
17	6.50E+00 - 8.00E+00	3.476E-02	3.476E-02	3.476E-02	3.476E-02
18	8.00E+00 - 1.00E+01	7.613E-03	7.613E-03	7.613E-03	7.613E-03
19	1.00E+01 - 2.00E+01	1.399E-04	1.399E-04	1.399E-04	1.399E-04
Total	1.00E-02 - 2.00E+01	9.194E+05	2.278E+06	9.194E+05	7.324E+06

*Associated ORIGEN-S output file – *du4_n.out*

**Associated ORIGEN-S output file – *du4.out*

Table B-10 Uncorrected UF₆ Photon Source Term at 0.5% U-235

Group	Energy Boundaries (MeV)	DU-0.5% Photon Source Intensity (photons/s per kg of UF ₆)			
		Without Bremsstrahlung*		With UO ₂ Bremsstrahlung**	
		Initial (0 yr)	1 yr	Initial (0 yr)	1 yr
1	1.00E-02 - 4.50E-02	7.556E+05	1.175E+06	7.556E+05	3.831E+06
2	4.50E-02 - 1.00E-01	4.129E+04	8.161E+05	4.129E+04	1.935E+06
3	1.00E-01 - 2.00E-01	2.518E+05	2.771E+05	2.518E+05	9.595E+05
4	2.00E-01 - 3.00E-01	1.354E+04	2.328E+04	1.354E+04	2.509E+05
5	3.00E-01 - 4.00E-01	2.568E+02	1.458E+03	2.568E+02	1.684E+05
6	4.00E-01 - 6.00E-01	1.435E+01	4.806E+03	1.435E+01	1.147E+05
7	6.00E-01 - 8.00E-01	2.299E+01	5.322E+04	2.299E+01	1.010E+05
8	8.00E-01 - 1.00E+00	0.000E+00	5.516E+04	0.000E+00	7.448E+04
9	1.00E+00 - 1.33E+00	9.705E+00	3.378E+04	9.705E+00	4.429E+04
10	1.33E+00 - 1.66E+00	0.000E+00	4.886E+03	0.000E+00	6.626E+03
11	1.66E+00 - 2.00E+00	4.144E+00	7.361E+03	4.144E+00	7.630E+03
12	2.00E+00 - 2.50E+00	2.512E+00	3.035E+00	2.512E+00	1.506E+01
13	2.50E+00 - 3.00E+00	1.456E+00	1.456E+00	1.456E+00	1.456E+00
14	3.00E+00 - 4.00E+00	1.308E+00	1.308E+00	1.308E+00	1.308E+00
15	4.00E+00 - 5.00E+00	4.413E-01	4.413E-01	4.413E-01	4.413E-01
16	5.00E+00 - 6.50E+00	1.771E-01	1.771E-01	1.771E-01	1.771E-01
17	6.50E+00 - 8.00E+00	3.473E-02	3.473E-02	3.473E-02	3.473E-02
18	8.00E+00 - 1.00E+01	7.606E-03	7.606E-03	7.606E-03	7.606E-03
19	1.00E+01 - 2.00E+01	1.398E-04	1.398E-04	1.398E-04	1.398E-04
Total	1.00E-02 - 2.00E+01	1.063E+06	2.452E+06	1.063E+06	7.494E+06

*Associated ORIGEN-S output file – *du5_n.out*

**Associated ORIGEN-S output file – *du5.out*

Table B-11 Uncorrected UF₆ Photon Source Term at 0.711% U-235

Group	Energy Boundaries (MeV)	NU Photon Source Intensity (photons/s per kg of UF ₆)			
		Without Bremsstrahlung*		With UO ₂ Bremsstrahlung**	
		Initial (0 yr)	1 yr	Initial (0 yr)	1 yr
1	1.00E-02 - 4.50E-02	9.337E+05	1.404E+06	9.337E+05	4.057E+06
2	4.50E-02 - 1.00E-01	5.732E+04	8.450E+05	5.732E+04	1.962E+06
3	1.00E-01 - 2.00E-01	3.579E+05	3.841E+05	3.579E+05	1.065E+06
4	2.00E-01 - 3.00E-01	1.925E+04	2.902E+04	1.925E+04	2.562E+05
5	3.00E-01 - 4.00E-01	3.651E+02	1.568E+03	3.651E+02	1.681E+05
6	4.00E-01 - 6.00E-01	2.054E+01	4.802E+03	2.054E+01	1.145E+05
7	6.00E-01 - 8.00E-01	2.308E+01	5.310E+04	2.308E+01	1.008E+05
8	8.00E-01 - 1.00E+00	0.000E+00	5.504E+04	0.000E+00	7.432E+04
9	1.00E+00 - 1.33E+00	9.690E+00	3.371E+04	9.690E+00	4.419E+04
10	1.33E+00 - 1.66E+00	0.000E+00	4.875E+03	0.000E+00	6.611E+03
11	1.66E+00 - 2.00E+00	4.138E+00	7.345E+03	4.138E+00	7.614E+03
12	2.00E+00 - 2.50E+00	2.508E+00	3.031E+00	2.508E+00	1.503E+01
13	2.50E+00 - 3.00E+00	1.453E+00	1.453E+00	1.453E+00	1.453E+00
14	3.00E+00 - 4.00E+00	1.305E+00	1.305E+00	1.305E+00	1.305E+00
15	4.00E+00 - 5.00E+00	4.405E-01	4.405E-01	4.405E-01	4.405E-01
16	5.00E+00 - 6.50E+00	1.767E-01	1.767E-01	1.767E-01	1.767E-01
17	6.50E+00 - 8.00E+00	3.466E-02	3.466E-02	3.466E-02	3.466E-02
18	8.00E+00 - 1.00E+01	7.590E-03	7.590E-03	7.590E-03	7.590E-03
19	1.00E+01 - 2.00E+01	1.395E-04	1.395E-04	1.395E-04	1.395E-04
Total	1.00E-02 - 2.00E+01	1.369E+06	2.823E+06	1.369E+06	7.857E+06

*Associated ORIGEN-S output file – *nu_n.out*

**Associated ORIGEN-S output file – *nu.out*

Table B-12 Corrected UF₆ Photon Source Term at 0.2% U-235

(one-year in-growth with corrected bremsstrahlung for UF₆)

Group	Photon Energy (MeV)	Photons/s-kg UF ₆				
		with UO ₂ Brem	No Brem	Net UO ₂ Brem	Net UF ₆ Brem	Adjusted Total
1	1.00E-02 - 4.50E-02	3.521E+06	8.595E+05	2.662E+06	2.129E+06	2.989E+06
2	4.50E-02 - 1.00E-01	1.897E+06	7.751E+05	1.122E+06	8.975E+05	1.673E+06
3	1.00E-01 - 2.00E-01	8.095E+05	1.250E+05	6.845E+05	5.476E+05	6.726E+05
4	2.00E-01 - 3.00E-01	2.435E+05	1.512E+04	2.284E+05	1.827E+05	1.978E+05
5	3.00E-01 - 4.00E-01	1.687E+05	1.302E+03	1.674E+05	1.339E+05	1.352E+05
6	4.00E-01 - 6.00E-01	1.150E+05	4.812E+03	1.102E+05	8.815E+04	9.296E+04
7	6.00E-01 - 8.00E-01	1.013E+05	5.338E+04	4.792E+04	3.834E+04	9.172E+04
8	8.00E-01 - 1.00E+00	7.471E+04	5.533E+04	1.938E+04	1.550E+04	7.083E+04
9	1.00E+00 - 1.33E+00	4.442E+04	3.389E+04	1.053E+04	8.424E+03	4.231E+04
10	1.33E+00 - 1.66E+00	6.646E+03	4.901E+03	1.745E+03	1.396E+03	6.297E+03
11	1.66E+00 - 2.00E+00	7.653E+03	7.384E+03	2.690E+02	2.152E+02	7.599E+03
12	2.00E+00 - 2.50E+00	1.511E+01	3.042E+00	1.207E+01	9.654E+00	1.270E+01
13	2.50E+00 - 3.00E+00	1.459E+00	1.459E+00	0.000E+00	0.000E+00	1.459E+00
14	3.00E+00 - 4.00E+00	1.311E+00	1.311E+00	0.000E+00	0.000E+00	1.311E+00
15	4.00E+00 - 5.00E+00	4.425E-01	4.425E-01	0.000E+00	0.000E+00	4.425E-01
16	5.00E+00 - 6.50E+00	1.776E-01	1.776E-01	0.000E+00	0.000E+00	1.776E-01
17	6.50E+00 - 8.00E+00	3.483E-02	3.483E-02	0.000E+00	0.000E+00	3.483E-02
18	8.00E+00 - 1.00E+01	7.628E-03	7.628E-03	0.000E+00	0.000E+00	7.628E-03
19	1.00E+01 - 2.00E+01	1.402E-04	1.402E-04	0.000E+00	0.000E+00	1.402E-04
Total	1.00E-02 - 2.00E+01	6.989E+06	1.936E+06	5.053E+06	4.043E+06	5.979E+06

Table B-13 Corrected UF₆ Photon Source Term at 0.3% U-235

(one-year in-growth with corrected bremsstrahlung for UF₆)

Group	Photon Energy (MeV)	Photons/s-kg UF ₆				
		with UO ₂ Brem	No Brem	Net UO ₂ Brem	Net UF ₆ Brem	Adjusted Total
1	1.00E-02 - 4.50E-02	3.622E+06	9.628E+05	2.659E+06	2.127E+06	3.090E+06
2	4.50E-02 - 1.00E-01	1.909E+06	7.887E+05	1.120E+06	8.962E+05	1.685E+06
3	1.00E-01 - 2.00E-01	8.595E+05	1.757E+05	6.838E+05	5.470E+05	7.227E+05
4	2.00E-01 - 3.00E-01	2.460E+05	1.784E+04	2.282E+05	1.825E+05	2.004E+05
5	3.00E-01 - 4.00E-01	1.686E+05	1.354E+03	1.672E+05	1.338E+05	1.352E+05
6	4.00E-01 - 6.00E-01	1.149E+05	4.810E+03	1.101E+05	8.807E+04	9.288E+04
7	6.00E-01 - 8.00E-01	1.012E+05	5.333E+04	4.787E+04	3.830E+04	9.163E+04
8	8.00E-01 - 1.00E+00	7.464E+04	5.527E+04	1.937E+04	1.550E+04	7.077E+04
9	1.00E+00 - 1.33E+00	4.438E+04	3.385E+04	1.053E+04	8.424E+03	4.227E+04
10	1.33E+00 - 1.66E+00	6.639E+03	4.896E+03	1.743E+03	1.394E+03	6.290E+03
11	1.66E+00 - 2.00E+00	7.646E+03	7.376E+03	2.700E+02	2.160E+02	7.592E+03
12	2.00E+00 - 2.50E+00	1.509E+01	3.040E+00	1.205E+01	9.640E+00	1.268E+01
13	2.50E+00 - 3.00E+00	1.458E+00	1.458E+00	0.000E+00	0.000E+00	1.458E+00
14	3.00E+00 - 4.00E+00	1.310E+00	1.310E+00	0.000E+00	0.000E+00	1.310E+00
15	4.00E+00 - 5.00E+00	4.421E-01	4.421E-01	0.000E+00	0.000E+00	4.421E-01
16	5.00E+00 - 6.50E+00	1.774E-01	1.774E-01	0.000E+00	0.000E+00	1.774E-01
17	6.50E+00 - 8.00E+00	3.480E-02	3.480E-02	0.000E+00	0.000E+00	3.480E-02
18	8.00E+00 - 1.00E+01	7.621E-03	7.621E-03	0.000E+00	0.000E+00	7.621E-03
19	1.00E+01 - 2.00E+01	1.400E-04	1.400E-04	0.000E+00	0.000E+00	1.400E-04
Total	1.00E-02 - 2.00E+01	7.155E+06	2.106E+06	5.049E+06	4.039E+06	6.145E+06

Table B-14 Corrected UF₆ Photon Source Term at 0.4% U-235

(one-year in-growth with corrected bremsstrahlung for UF₆)

Group	Photon Energy (MeV)	Photons/s-kg UF ₆				
		with UO ₂ Brem	No Brem	Net UO ₂ Brem	Net UF ₆ Brem	Adjusted Total
1	1.00E-02 - 4.50E-02	3.726E+06	1.068E+06	2.658E+06	2.126E+06	3.194E+06
2	4.50E-02 - 1.00E-01	1.922E+06	8.024E+05	1.120E+06	8.957E+05	1.698E+06
3	1.00E-01 - 2.00E-01	9.095E+05	2.264E+05	6.831E+05	5.465E+05	7.729E+05
4	2.00E-01 - 3.00E-01	2.485E+05	2.056E+04	2.279E+05	1.824E+05	2.029E+05
5	3.00E-01 - 4.00E-01	1.685E+05	1.406E+03	1.671E+05	1.337E+05	1.351E+05
6	4.00E-01 - 6.00E-01	1.148E+05	4.808E+03	1.100E+05	8.799E+04	9.280E+04
7	6.00E-01 - 8.00E-01	1.011E+05	5.327E+04	4.783E+04	3.826E+04	9.153E+04
8	8.00E-01 - 1.00E+00	7.456E+04	5.521E+04	1.935E+04	1.548E+04	7.069E+04
9	1.00E+00 - 1.33E+00	4.433E+04	3.382E+04	1.051E+04	8.408E+03	4.223E+04
10	1.33E+00 - 1.66E+00	6.632E+03	4.891E+03	1.741E+03	1.393E+03	6.284E+03
11	1.66E+00 - 2.00E+00	7.638E+03	7.368E+03	2.700E+02	2.160E+02	7.584E+03
12	2.00E+00 - 2.50E+00	1.508E+01	3.038E+00	1.204E+01	9.634E+00	1.267E+01
13	2.50E+00 - 3.00E+00	1.457E+00	1.457E+00	0.000E+00	0.000E+00	1.457E+00
14	3.00E+00 - 4.00E+00	1.309E+00	1.309E+00	0.000E+00	0.000E+00	1.309E+00
15	4.00E+00 - 5.00E+00	4.417E-01	4.417E-01	0.000E+00	0.000E+00	4.417E-01
16	5.00E+00 - 6.50E+00	1.772E-01	1.772E-01	0.000E+00	0.000E+00	1.772E-01
17	6.50E+00 - 8.00E+00	3.476E-02	3.476E-02	0.000E+00	0.000E+00	3.476E-02
18	8.00E+00 - 1.00E+01	7.613E-03	7.613E-03	0.000E+00	0.000E+00	7.613E-03
19	1.00E+01 - 2.00E+01	1.399E-04	1.399E-04	0.000E+00	0.000E+00	1.399E-04
Total	1.00E-02 - 2.00E+01	7.324E+06	2.278E+06	5.046E+06	4.036E+06	6.314E+06

Table B-15 Corrected UF₆ Photon Source Term at 0.5% U-235

(one-year in-growth with corrected bremsstrahlung for UF₆)

Group	Photon Energy (MeV)	Photons/s-kg UF ₆				
		with UO ₂ Brem	No Brem	Net UO ₂ Brem	Net UF ₆ Brem	Adjusted Total
1	1.00E-02 - 4.50E-02	3.831E+06	1.175E+06	2.656E+06	2.125E+06	3.300E+06
2	4.50E-02 - 1.00E-01	1.935E+06	8.161E+05	1.119E+06	8.951E+05	1.711E+06
3	1.00E-01 - 2.00E-01	9.595E+05	2.771E+05	6.824E+05	5.459E+05	8.230E+05
4	2.00E-01 - 3.00E-01	2.509E+05	2.328E+04	2.276E+05	1.821E+05	2.054E+05
5	3.00E-01 - 4.00E-01	1.684E+05	1.458E+03	1.669E+05	1.336E+05	1.350E+05
6	4.00E-01 - 6.00E-01	1.147E+05	4.806E+03	1.099E+05	8.792E+04	9.272E+04
7	6.00E-01 - 8.00E-01	1.010E+05	5.322E+04	4.778E+04	3.822E+04	9.144E+04
8	8.00E-01 - 1.00E+00	7.448E+04	5.516E+04	1.932E+04	1.546E+04	7.062E+04
9	1.00E+00 - 1.33E+00	4.429E+04	3.378E+04	1.051E+04	8.408E+03	4.219E+04
10	1.33E+00 - 1.66E+00	6.626E+03	4.886E+03	1.740E+03	1.392E+03	6.278E+03
11	1.66E+00 - 2.00E+00	7.630E+03	7.361E+03	2.690E+02	2.152E+02	7.576E+03
12	2.00E+00 - 2.50E+00	1.506E+01	3.035E+00	1.203E+01	9.620E+00	1.266E+01
13	2.50E+00 - 3.00E+00	1.456E+00	1.456E+00	0.000E+00	0.000E+00	1.456E+00
14	3.00E+00 - 4.00E+00	1.308E+00	1.308E+00	0.000E+00	0.000E+00	1.308E+00
15	4.00E+00 - 5.00E+00	4.413E-01	4.413E-01	0.000E+00	0.000E+00	4.413E-01
16	5.00E+00 - 6.50E+00	1.771E-01	1.771E-01	0.000E+00	0.000E+00	1.771E-01
17	6.50E+00 - 8.00E+00	3.473E-02	3.473E-02	0.000E+00	0.000E+00	3.473E-02
18	8.00E+00 - 1.00E+01	7.606E-03	7.606E-03	0.000E+00	0.000E+00	7.606E-03
19	1.00E+01 - 2.00E+01	1.398E-04	1.398E-04	0.000E+00	0.000E+00	1.398E-04
Total	1.00E-02 - 2.00E+01	7.494E+06	2.452E+06	5.042E+06	4.033E+06	6.485E+06

Table B-16 Corrected UF₆ Photon Source Term at 0.711% U-235

(one-year in-growth with corrected bremsstrahlung for UF₆)

Group	Photon Energy (MeV)	Photons/s-kg UF ₆				
		with UO ₂ Brem	No Brem	Net UO ₂ Brem	Net UF ₆ Brem	Adjusted Total
1	1.00E-02 - 4.50E-02	4.057E+06	1.404E+06	2.653E+06	2.122E+06	3.526E+06
2	4.50E-02 - 1.00E-01	1.962E+06	8.450E+05	1.117E+06	8.936E+05	1.739E+06
3	1.00E-01 - 2.00E-01	1.065E+06	3.841E+05	6.809E+05	5.447E+05	9.288E+05
4	2.00E-01 - 3.00E-01	2.562E+05	2.902E+04	2.272E+05	1.817E+05	2.108E+05
5	3.00E-01 - 4.00E-01	1.681E+05	1.568E+03	1.665E+05	1.332E+05	1.348E+05
6	4.00E-01 - 6.00E-01	1.145E+05	4.802E+03	1.097E+05	8.776E+04	9.256E+04
7	6.00E-01 - 8.00E-01	1.008E+05	5.310E+04	4.770E+04	3.816E+04	9.126E+04
8	8.00E-01 - 1.00E+00	7.432E+04	5.504E+04	1.928E+04	1.542E+04	7.046E+04
9	1.00E+00 - 1.33E+00	4.419E+04	3.371E+04	1.048E+04	8.384E+03	4.209E+04
10	1.33E+00 - 1.66E+00	6.611E+03	4.875E+03	1.736E+03	1.389E+03	6.264E+03
11	1.66E+00 - 2.00E+00	7.614E+03	7.345E+03	2.690E+02	2.152E+02	7.560E+03
12	2.00E+00 - 2.50E+00	1.503E+01	3.031E+00	1.200E+01	9.599E+00	1.263E+01
13	2.50E+00 - 3.00E+00	1.453E+00	1.453E+00	0.000E+00	0.000E+00	1.453E+00
14	3.00E+00 - 4.00E+00	1.305E+00	1.305E+00	0.000E+00	0.000E+00	1.305E+00
15	4.00E+00 - 5.00E+00	4.405E-01	4.405E-01	0.000E+00	0.000E+00	4.405E-01
16	5.00E+00 - 6.50E+00	1.767E-01	1.767E-01	0.000E+00	0.000E+00	1.767E-01
17	6.50E+00 - 8.00E+00	3.466E-02	3.466E-02	0.000E+00	0.000E+00	3.466E-02
18	8.00E+00 - 1.00E+01	7.590E-03	7.590E-03	0.000E+00	0.000E+00	7.590E-03
19	1.00E+01 - 2.00E+01	1.395E-04	1.395E-04	0.000E+00	0.000E+00	1.395E-04
Total	1.00E-02 - 2.00E+01	7.856E+06	2.823E+06	5.033E+06	4.027E+06	6.850E+06

Table B-17 Neutron Source Term Comparison for Filled Cylinders

Cylinder Type	Contributor	Neutron Source Strength (n/s per cylinder)	
		UUSA* (Hand-calculation)	UNM Calculation (ORIGEN-S)
48Y for Tails (0.34% U-235)	(α , n) Reaction	1.62E+05	2.28E+05
	Spontaneous Fission	1.15E+05	1.15E+05
	Total	2.77E+05	3.43E+05
48Y for Feed (0.711% U-235)	(α , n) Reaction	2.69E+05	3.84E+05
	Spontaneous Fission	1.15E+05	1.14E+05
	Total	3.84E+05	4.98E+05

*Reference: AREVA 2003a

Table B-18 Photon Source Term Comparison for Filled Cylinders

Group	Energy Boundaries (MeV)	Photon Source Strength (p/s-cylinder)			
		48Y Tails (0.34%)		48Y Feed (0.711%)	
		UUSA ORINGEN-2	UNM ORINGEN-S	UUSA ORINGEN-2	UNM ORINGEN-S
1	0.00E+00 - 2.00E-02	8.791E+10	7.552E+10	9.712E+10	8.850E+10
2	2.00E-02 - 3.00E-02	1.161E+10	8.919E+09	1.196E+10	9.319E+09
3	3.00E-02 - 4.50E-02	7.404E+09	6.702E+09	7.390E+09	6.691E+09
4	4.50E-02 - 7.00E-02	1.541E+10	1.164E+10	1.544E+10	1.168E+10
5	7.00E-02 - 1.00E-01	1.387E+10	1.057E+10	1.424E+10	1.105E+10
6	1.00E-01 - 1.50E-01	5.090E+09	4.898E+09	5.496E+09	5.343E+09
7	1.50E-01 - 3.00E-01	7.342E+09	6.258E+09	8.690E+09	7.695E+09
8	3.00E-01 - 4.50E-01	2.665E+09	2.142E+09	2.658E+09	2.136E+09
9	4.50E-01 - 7.00E-01	1.436E+09	1.029E+09	1.431E+09	1.026E+09
10	7.00E-01 - 1.00E+00	9.358E+08	1.617E+09	9.324E+08	1.611E+09
11	1.00E+00 - 1.50E+00	6.635E+08	5.460E+08	6.610E+08	5.439E+08
12	1.50E+00 - 2.00E+00	1.023E+08	1.280E+08	1.019E+08	1.275E+08
13	2.00E+00 - 2.50E+00	2.957E+04	1.640E+05	2.949E+04	1.634E+05
14	2.50E+00 - 3.00E+00	1.689E+04	1.823E+04	1.684E+04	1.816E+04
15	3.00E+00 - 4.00E+00	1.511E+04	1.636E+04	1.505E+04	1.631E+04
16	4.00E+00 - 6.00E+00	6.490E+03	7.021E+03	6.470E+03	6.997E+03
17	6.00E+00 - 8.00E+00	7.475E+02	8.084E+02	7.450E+02	8.056E+02
18	8.00E+00 - 1.10E+01	8.597E+01	9.298E+01	8.563E+01	9.264E+01
Total	0.00E+00 - 1.10E+01	1.545E+11	1.299E+11	1.661E+11	1.457E+11

*Reference: AREVA 2003b

APPENDIX C FLUX-TO-DOSE RATE CONVERSION FACTORS

This appendix contains the flux-to-dose rate conversion factors derived from the ANSI/ANS-6.1.1-1977 and 6.1.1-1991 standards as given in Tables C-1 and C-2, respectively. Photon energies above 2 MeV are irrelevant to this research as the cutoff energy for dose calculations is 2 MeV.

Table C-1 ANSI/ANS-6.1.1-1977 Dose Conversion Factors

Neutron Energy (MeV)	Neutron Dose Conversion Factors (mrem/hr)/(neutron/cm ² -s) ^a	Photon Energy (MeV)	Photon Dose Conversion Factors (mrem/hr)/(photon/cm ² -s) ^b
2.50E-08	3.67E-03	0.01	3.96E-03
1.00E-07	3.67E-03	0.03	5.82E-04
1.00E-06	4.46E-03	0.05	2.90E-04
1.00E-05	4.54E-03	0.07	2.58E-04
1.00E-04	4.18E-03	0.1	2.83E-04
1.00E-03	3.76E-03	0.15	3.79E-04
1.00E-02	3.56E-03	0.2	5.01E-04
1.00E-01	2.17E-02	0.25	6.31E-04
5.00E-01	9.26E-02	0.3	7.59E-04
1.0	1.32E-01	0.35	8.78E-04
2.5	1.25E-01	0.4	9.85E-04
5.0	1.56E-01	0.45	1.08E-03
7.0	1.47E-01	0.5	1.17E-03
10.0	1.47E-01	0.55	1.27E-03
14.0	2.08E-01	0.6	1.36E-03
20.0	2.27E-01	0.65	1.44E-03
		0.7	1.52E-03
		0.8	1.68E-03
		1.0	1.98E-03
		1.4	2.51E-03
		1.8	2.99E-03
		2.2	3.42E-03
		2.6	3.82E-03
		2.8	4.01E-03
		3.25	4.41E-03
		3.75	4.83E-03
		4.25	5.23E-03
		4.75	5.60E-03
		5.0	5.80E-03

^a Derived from ANSI/ANS-6.1.1-1977, p.4

^b Derived from ANSI/ANS-6.1.1-1977, p.5

Table C-2 ANSI/ANS-6.1.1-1991 Dose Conversion Factors

Neutron Energy (MeV)	Neutron Dose Conversion Factors (mrem/hr)/(neutron/cm ² -s) ^a	Photon Energy (MeV)	Photon Dose Conversion Factors (mrem/hr)/(photon/cm ² -s) ^b
2.50E-08	1.44E-03	0.010	2.23E-05
1.00E-07	1.58E-03	0.015	5.65E-05
1.00E-06	1.74E-03	0.020	8.57E-05
1.00E-05	1.61E-03	0.030	1.18E-04
1.00E-04	1.49E-03	0.040	1.31E-04
1.00E-03	1.38E-03	0.050	1.38E-04
1.00E-02	1.63E-03	0.060	1.44E-04
2.00E-02	2.11E-03	0.080	1.62E-04
5.00E-02	3.92E-03	0.100	1.92E-04
1.00E-01	7.13E-03	0.150	2.80E-04
2.00E-01	1.39E-02	0.200	3.71E-04
5.00E-01	3.13E-02	0.300	5.62E-04
1.0	5.15E-02	0.400	7.42E-04
1.5	6.59E-02	0.500	9.14E-04
2.0	7.70E-02	0.600	1.08E-03
3.0	9.50E-02	0.800	1.38E-03
4.0	1.08E-01	1.000	1.66E-03
5.0	1.18E-01	1.500	2.25E-03
6.0	1.25E-01	2.000	2.76E-03
7.0	1.31E-01	3.000	3.67E-03
8.0	1.37E-01	4.000	4.50E-03
10.0	1.48E-01	5.000	5.29E-03
14.0	1.73E-01		

^a Derived from ANSI/ANS-6.1.1-1991, Table 4 for anterior-posterior (AP) orientation

^b Derived from ANSI/ANS-6.1.1-1991, Table 3 for AP orientation

APPENDIX D MCNP COMPUTER FILES FOR SINGLE CYLINDERS

D.1 MCNP CASES AND COMPUTER FILES FOR SINGLE CYLINDERS

Table D-1 lists the MCNP computer files created for calculations of neutron and photon dose rates from a single filled or empty feed cylinder.

Table D-1 MCNP Case Description and Computer Files for a Single Feed Cylinder

Case	Description	Input File	Output File	CTME (minutes)
Neutron Cases for Filled Feed Cylinder				
n1	Radial & axial neutron dose rate profiles for homogenized geometry	feed_n1.txt	feed_n1.out	200
n2	Radial & axial neutron dose rate profiles for slumped geometry	feed_n2.txt	feed_n2.out	200
n3	Effect of concrete pad (radial only)	feed_n3.txt	feed_n3.out	100
n4	Effect of ground scattering (radial only)	feed_n4.txt	feed_n4.out	100
n5	Secondary photon contribution (radial only)	feed_n5.txt	feed_n5.out	100
n6	Effect of ANSI-ANS-6.1.1-1991 standard (radial only)	feed_n6.txt	feed_n6.out	100
Photon Cases for Filled Feed Cylinder				
p1	Radial & axial photon dose rate profiles for homogenized geometry	feed_p1.txt	feed_p1.out	100
p2	Radial & axial photon dose rate profiles for slumped geometry	feed_p2.txt	feed_p2.out	100
p3	Effect of concrete pad (radial only)	feed_p3.txt	feed_p3.out	50
p4	Effect of ground scattering (radial only)	feed_p4.txt	feed_p4.out	50
p5	Effect of full photon energy spectrum (radial only)	feed_p5c.txt	feed_p5.out	50
p6	Effect of ANSI-ANS-6.1.1-1991 standard (radial only)	feed_p6.txt	feed_p6.out	50
Photon Cases for Filled Empty Cylinder				
e1	Radial & axial photon dose rate profiles for homogenized geometry	empty_p1.txt	empty_p1.out	50

D.2 SAMPLE MCNP INPUT LISTING

The representative cases selected for listing of the sample MCNP input files include the following:

- File *feed_n1.txt* – Radial & axial neutron dose rate profiles for homogenized geometry for a single filled feed cylinder (§D.2.1)
- File *feed_p1.txt* – Radial & axial photon dose rate profiles for homogenized geometry for a single filled feed cylinder (§D.2.2)
- File *empty_p1.txt* – Radial & axial photon dose rate profiles for homogenized geometry for a single empty feed cylinder (§D.2.3)

D.2.1 Input File *feed_n1.txt*

```
Dose from Single Filled 48Y Feed Cylinder
c Neutron - homogenized source geometry - ANSI/ANS-6.1.1-1977
c
11 1 -2.897 103 -104 -401 imp:n=1 $UF6 inside
12 2 -7.8500 102 -105 -402 (-103 :104 :401) imp:n=2 $Steel shell
13 4 -2.35 110 -111 112 -113 -114 115 imp:n=1 $Concrete pad
14 3 -0.0012 114 -501 (-102 :105 :402) imp:n=2 $Air inside
15 5 -1.60 -114 -501 #13 imp:n=0.5 $Ground soil
16 0 501 imp:n=0 $Outer void

C Planes
c
102 px -186.3725 $ Outside of end plate
103 px -184.7850 $ Inside of end plate
104 px 184.7850 $ Inside of end plate
105 px 186.3725 $ Outside of end plate
c
110 px -30000.0 $ Concrete pad -x
111 px 30000.0 $ Concrete pad +x
112 py -30000.0 $ Concrete pad -y
113 py 30000.0 $ Concrete pad +y
114 pz -77.80 $ Concrete pad upper z
115 pz -108.30 $ Concrete pad lower z
C Cylinders
401 cx 60.9600 $ Inside of cylinder
402 cx 62.5475 $ Outside of cylinder
C Spheres
501 so 40000.00 $ Problem Boundary

prdmp j j j 4
m1 9019.70c 6.00 92238.70c 0.9928 92235.70c 0.0072 $ UF6
m2 26054.70c 0.05845 26056.70c 0.91754 26057.70c 0.02119 $ Iron
26058.70c 0.00282
m3 6000.70c -0.00014 7014.70c -0.75521 8016.70c -0.23177 $ Air
```

```

18040.70c -0.01288
m4 1001.70c -0.0055 8016.70c -0.4983 11023.70c -0.0170 $ Concrete
ANS6.4-1997
13027.70c -0.0455 12024.70c -0.0020 12025.70c -0.0003
12026.70c -0.0003 14028.70c -0.2900 14029.70c -0.0153
14030.70c -0.0104 16032.70c -0.0013 19039.70c -0.0178
19041.70c -0.0013 20040.70c -0.0826 26056.70c -0.0123
m5 8016.70c -0.465 11023.70c -0.0245 13027.70c -0.080 $ Ground soil
12024.70c -0.0117 12025.70c -0.0015 12026.70c -0.0018
14028.70c -0.2664 14029.70c -0.0140 14030.70c -0.0096
19039.70c -0.0209 19041.70c -0.0016 20040.70c -0.040
26056.70c -0.060
mode n
sdef erg=d1 axs=1 0 0 rad=d2 ext=d3 pos=0 0 0
C Neutron Spectrum
# sil spl sb1
0.015 0.0 0.0
0.111 7.849E-03 1.521E-03
0.408 7.776E-02 2.645E-02
0.907 3.060E-01 2.152E-01
1.42 3.256E-01 3.662E-01
1.83 1.470E-01 1.886E-01
3.01 1.040E-01 1.477E-01
6.38 3.063E-02 5.125E-02
20.0 1.163E-03 2.945E-03
si2 0.0 60.96 $ radial distribution, equal volume weighting
sp2 -21 1
si3 -184.785 184.785 $ axial distribution, equal along length
sp3 0.0 1.0
c neutron dose conversion factors (mrem/h)/(n/cm^2-s)}
c from MCNP Manual, ANSI/ANS-6.1.1-1977
DE0 LOG 2.5-8 1.0-7 1.0-6 1.0-5 1.0-4 1.0-3 1.0-2 1.0-1
5.0-1 1.0 2.5 5.0 7.0 10.0 14.0 20.0
DF0 LOG 3.67-3 3.67-3 4.46-3 4.54-3 4.18-3 3.76-3 3.56-3 2.17-2
9.26-2 1.32-1 1.25-1 1.56-1 1.47-1 1.47-1 2.08-1 2.27-1
c Energy bins for tally
e0 0.015 0.111 0.408 0.907 1.42 1.83 3.01 6.38 20.0
c Point detector tallies
c Radial neutron dose rates on side at 0.02/0.305/1/2/5/10/20/50/100/200m
f5:n 0.0 64.55 0.0 0.1
f15:n 0.0 93.05 0.0 0.3
f25:n 0.0 162.55 0.0 5.0
f35:n 0.0 262.55 0.0 5.0
f45:n 0.0 562.55 0.0 5.0
f55:n 0.0 1062.55 0.0 10.0
f65:n 0.0 2062.55 0.0 10.0
f75:n 0.0 5062.55 0.0 10.0
f85:n 0.0 10062.55 0.0 10.0
f95:n 0.0 20062.55 0.0 10.0
c Tally multiplier (n/s per feed cylinder)
fm5 4.976E+05
fm15 4.976E+05
fm25 4.976E+05
fm35 4.976E+05
fm45 4.976E+05
fm55 4.976E+05
fm65 4.976E+05
fm75 4.976E+05
fm85 4.976E+05
fm95 4.976E+05

```



```

c Axial neutron dose rates on end at 0.02/0.305/1/2/5/10/20/50/100/200m
f105:n 188.4 0.0 0.0 0.1
f115:n 216.9 0.0 0.0 0.3
f125:n 286.4 0.0 0.0 5.0
f135:n 386.4 0.0 0.0 5.0
f145:n 686.4 0.0 0.0 5.0
f155:n 1186.4 0.0 0.0 10.0
f165:n 2186.4 0.0 0.0 10.0
f175:n 5186.4 0.0 0.0 10.0
f185:n 10186.4 0.0 0.0 10.0
f195:n 20186.4 0.0 0.0 10.0
fm105 4.976E+05
fm115 4.976E+05
fm125 4.976E+05
fm135 4.976E+05
fm145 4.976E+05
fm155 4.976E+05
fm165 4.976E+05
fm175 4.976E+05
fm185 4.976E+05
fm195 4.976E+05
c Neutron dose rate at contact on cylindrical surface (bottom)
f205:n -95.4 0.0 -66.4 0.1
fm205 4.976E+05
c
ctme 200.0

```

D.2.2 Input File *feed_p1.txt*

Dose Rates from Single Filled 48Y Feed Cylinder

```

c Photon - homogenized source geometry - ANSI/ANS-6.1.1-1977
c
11 1 -2.897 103 -104 -401 imp:p=1 $UF6 inside
12 2 -7.8500 102 -105 -402 (-103 :104 :401) imp:p=2 $Steel shell
13 4 -2.35 110 -111 112 -113 -114 115 imp:p=1 $Concrete pad
14 3 -0.0012 114 -501 (-102 :105 :402) imp:p=2 $Air inside
15 5 -1.60 -114 -501 #13 imp:p=0.5 $Ground soil
16 0 501 imp:p=0 $Outer void

C Y planes
c
102 px -186.3725 $ Outside of end plate
103 px -184.7850 $ Inside of end plate
104 px 184.7850 $ Inside of end plate
105 px 186.3725 $ Outside of end plate
c
110 px -30000.0 $ Concrete pad -x
111 px 30000.0 $ Concrete pad +x
112 py -30000.0 $ Concrete pad -y
113 py 30000.0 $ Concrete pad +y
114 pz -77.80 $ Concrete pad upper z
115 pz -108.30 $ Concrete pad lower z
C Cylinders
401 cx 60.9600 $ Inside of cylinder
402 cx 62.5475 $ Outside of cylinder
C Spheres
501 so 40000.00 $ Problem Boundary

prdmp j j j 4

```

```

m1      9019  6.00    92238  0.9928  92235  0.0072  $ UF6
m2      26000  1.00
m3       6000 -0.00014  7014 -0.75521  8016 -0.23177  $ Air
        18000 -0.01288
m4       1001 -0.0055   8016 -0.4983  11023 -0.0170  $ Concrete ANS6.4-1997
        13027 -0.0455  12000 -0.0026  14000 -0.3157
        16000 -0.0013  19000 -0.0191  20000 -0.0826
        26000 -0.0123
m5       8016 -0.465   11023 -0.0245  13027 -0.080  $ Ground bulk soil
        12000 -0.015   14000 -0.290   19000 -0.0225
        20000 -0.040   26000 -0.060

phys:p 10          $ detailed physics, brems., coherent
mode  p
sdef  erg=d1  axs=1 0 0  rad=d2  ext=d3  pos=0 0 0
C Photon Spectrum
#      sil      spl      sb1
      4.50E-02  0.0      0.0
      1.00E-01  5.232E-01  7.933E-05
      2.00E-01  2.795E-01  1.494E-03
      3.00E-01  6.343E-02  1.378E-02
      4.00E-01  4.056E-02  3.645E-02
      6.00E-01  2.785E-02  8.181E-02
      8.00E-01  2.746E-02  1.927E-01
      1.00E+00  2.120E-02  2.608E-01
      1.33E+00  1.266E-02  2.593E-01
      1.66E+00  1.885E-03  5.885E-02
      2.00E+00  2.275E-03  9.479E-02
si2     0.0      60.96      $ radial distribution, equal volume weighting
sp2    -21      1
si3    -184.785  184.785  $ axial distribution, equal along length
sp3     0.0      1.0
c ANSI/ANS-6.1.1-1977 photon dose conversion factors (mrem/h)/(photon/cm^2-s)
de0    LOG    0.01  0.03  0.05  0.07  0.1  0.15  0.2
        0.25  0.3  0.35  0.4  0.45  0.5  0.55  0.6
        0.65  0.7  0.8  1.0  1.4  1.8  2.2  2.6
        2.8  3.25  3.75  4.25  4.75  5.0  5.25  5.75
        6.25  6.75  7.5  9.0  11.0  13.0  15.0
df0    LOG    3.96-3  5.82-4  2.90-4  2.58-4  2.83-4  3.79-7  5.01-4
        6.31-4  7.59-4  8.78-4  9.85-4  1.08-3  1.17-3  1.27-3  1.36-3
        1.44-3  1.52-3  1.68-3  1.98-3  2.51-3  2.99-3  3.42-3  3.82-3
        4.01-3  4.41-3  4.83-3  5.23-3  5.60-3  5.80-3  6.01-3  6.37-3
        6.74-3  7.11-3  7.66-3  8.77-3  1.03-2  1.18-2  1.33-2
c Energy bins for tally
e0     0.0  0.045  0.10  0.2  0.3  0.4  0.6  0.8  1.0  1.33  1.66  2.0
c Point detector tallies
c Radial photon dose rates on side at at 0.02/0.305/1/2/5/10/20/50/100/200m
f5:p   0.0    64.55  0.0    0.1
f15:p  0.0    93.05  0.0    0.3
f25:p  0.0   162.55  0.0    5.0
f35:p  0.0   262.55  0.0    5.0
f45:p  0.0   562.55  0.0    5.0
f55:p  0.0  1062.55  0.0   10.0
f65:p  0.0  2062.55  0.0   10.0
f75:p  0.0  5062.55  0.0   10.0
f85:p  0.0 10062.55  0.0   10.0
f95:p  0.0 20062.55  0.0   10.0
c Tally multiplier (p/s per feed cylinder)
fm5    4.155E+10
fm15   4.155E+10
fm25   4.155E+10

```

```

fm35      4.155E+10
fm45      4.155E+10
fm55      4.155E+10
fm65      4.155E+10
fm75      4.155E+10
fm85      4.155E+10
fm95      4.155E+10
c Axial photon dose rates on end at at 0.02/0.305/1/2/5/10/20/50/100/200m
f105:p    188.4  0.0  0.0  0.1
f115:p    216.9  0.0  0.0  0.3
f125:p    286.4  0.0  0.0  5.0
f135:p    386.4  0.0  0.0  5.0
f145:p    686.4  0.0  0.0  5.0
f155:p    1186.4 0.0  0.0  10.0
f165:p    2186.4 0.0  0.0  10.0
f175:p    5186.4 0.0  0.0  10.0
f185:p   10186.4 0.0  0.0  10.0
f195:p   20186.4 0.0  0.0  10.0
fm105     4.155E+10
fm115     4.155E+10
fm125     4.155E+10
fm135     4.155E+10
fm145     4.155E+10
fm155     4.155E+10
fm165     4.155E+10
fm175     4.155E+10
fm185     4.155E+10
fm195     4.155E+10
c Photon dose rate at contact on cylindrical surface (bottom)
f205:p   -95.4  0.0 -66.4  0.1
fm205    4.155E+10
c
ctme     100.0

```

D.2.3 Input File *empty_p1.txt*

Dose Rates from Single Empty 48Y Feed Cylinder

```

c Photon - homogenized source geometry - ANSI/ANS-6.1.1-1977
c
11      0          103 -104 -401          imp:p=1  $Void-no UF6
12      2  -7.8500  102 -105 -402 (-103 :104 :401) imp:p=2  $Steel shell
13      4  -2.35    110 -111  112 -113 -114 115  imp:p=1  $Concrete pad
14      3  -0.0012  114 -501  (-102 :105 :402) imp:p=2  $Air inside
15      5  -1.60    -114 -501  #13          imp:p=0.5 $Ground soil
16      0          501          imp:p=0   $Outer void

```

C Y planes

```

c
102  px  -186.3725          $ Outside of end plate
103  px  -184.7850          $ Inside of end plate
104  px   184.7850          $ Inside of end plate
105  px   186.3725          $ Outside of end plate
c
110  px  -30000.0          $ Concrete pad -x
111  px   30000.0          $ Concrete pad +x
112  py  -30000.0          $ Concrete pad -y
113  py   30000.0          $ Concrete pad +y
114  pz  -77.80           $ Concrete pad upper z
115  pz  -108.30          $ Concrete pad lower z

```

```

C Cylinders
401 cx 60.9600 $ Inside of cylinder
402 cx 62.5475 $ Outside of cylinder
C Spheres
501 so 40000.00 $ Problem Boundary

prdmp j j j 4
m1 9019 6.00 92238 0.9928 92235 0.0072 $ UF6
m2 26000 1.00 $ Iron
m3 6000 -0.00014 7014 -0.75521 8016 -0.23177 $ Air
18000 -0.01288
m4 1001 -0.0055 8016 -0.4983 11023 -0.0170 $ Concrete ANS6.4-1997
13027 -0.0455 12000 -0.0026 14000 -0.3157
16000 -0.0013 19000 -0.0191 20000 -0.0826
26000 -0.0123
m5 8016 -0.465 11023 -0.0245 13027 -0.080 $ Ground bulk soil
12000 -0.015 14000 -0.290 19000 -0.0225
20000 -0.040 26000 -0.060

phys:p 10 $ detailed physics, brems., coherent
mode p
sdef erg=d1 axs=1 0 0 rad=d2 ext=d3 pos=0 0 0
C Photon Spectrum
# sil spl
4.50E-02 0.0
1.00E-01 1.116E+10
2.00E-01 1.165E+09
3.00E-01 4.135E+08
4.00E-01 2.394E+08
6.00E-01 2.186E+08
8.00E-01 7.389E+08
1.00E+00 7.219E+08
1.33E+00 4.427E+08
1.66E+00 6.539E+07
2.00E+00 9.267E+07
si2 0.0 60.96 $ radial distribution, equal volume weighting
sp2 -21 1
si3 -184.785 184.785 $ axial distribution, equal along length
sp3 0.0 1.0
c ANSI/ANS-6.1.1-1977 photon dose conversion factors (mrem/h)/(photon/cm^2-s)
de0 LOG 0.01 0.03 0.05 0.07 0.1 0.15 0.2
0.25 0.3 0.35 0.4 0.45 0.5 0.55 0.6
0.65 0.7 0.8 1.0 1.4 1.8 2.2 2.6
2.8 3.25 3.75 4.25 4.75 5.0 5.25 5.75
6.25 6.75 7.5 9.0 11.0 13.0 15.0
df0 LOG 3.96-3 5.82-4 2.90-4 2.58-4 2.83-4 3.79-7 5.01-4
6.31-4 7.59-4 8.78-4 9.85-4 1.08-3 1.17-3 1.27-3 1.36-3
1.44-3 1.52-3 1.68-3 1.98-3 2.51-3 2.99-3 3.42-3 3.82-3
4.01-3 4.41-3 4.83-3 5.23-3 5.60-3 5.80-3 6.01-3 6.37-3
6.74-3 7.11-3 7.66-3 8.77-3 1.03-2 1.18-2 1.33-2
c Energy bins for tally
e0 0.0 0.045 0.10 0.2 0.3 0.4 0.6 0.8 1.0 1.33 1.66 2.0
c Point detector tallies
c Radial photon dose rates on side at 0.02/0.305/1/2/5/10/20/50/100/200m
f5:p 0.0 64.55 0.0 0.1
f15:p 0.0 93.05 0.0 0.3
f25:p 0.0 162.55 0.0 5.0
f35:p 0.0 262.55 0.0 5.0
f45:p 0.0 562.55 0.0 5.0
f55:p 0.0 1062.55 0.0 10.0
f65:p 0.0 2062.55 0.0 10.0

```

```

f75:p  0.0  5062.55  0.0  10.0
f85:p  0.0 10062.55  0.0  10.0
f95:p  0.0 20062.55  0.0  10.0
c Tally multiplier (p/s per feed cylinder)
fm5    1.526E+10
fm15   1.526E+10
fm25   1.526E+10
fm35   1.526E+10
fm45   1.526E+10
fm55   1.526E+10
fm65   1.526E+10
fm75   1.526E+10
fm85   1.526E+10
fm95   1.526E+10
c Axial photon dose rates on end at 0.02/0.305/1/2/5/10/20/50/100/200m
f105:p  188.4  0.0  0.0  0.1
f115:p  216.9  0.0  0.0  0.3
f125:p  286.4  0.0  0.0  5.0
f135:p  386.4  0.0  0.0  5.0
f145:p  686.4  0.0  0.0  5.0
f155:p  1186.4 0.0  0.0  10.0
f165:p  2186.4 0.0  0.0  10.0
f175:p  5186.4 0.0  0.0  10.0
f185:p 10186.4 0.0  0.0  10.0
f195:p 20186.4 0.0  0.0  10.0
fm105   1.526E+10
fm115   1.526E+10
fm125   1.526E+10
fm135   1.526E+10
fm145   1.526E+10
fm155   1.526E+10
fm165   1.526E+10
fm175   1.526E+10
fm185   1.526E+10
fm195   1.526E+10
c Photon dose rate at contact on cylindrical surface (bottom)
f205:p -95.4  0.0 -66.4  0.1
fm205   1.526E+10
c
ctme    50.0

```

APPENDIX E CALCULATED DOSE RATES FOR SINGLE CYLINDERS

This appendix compiles the neutron and photon dose rates from the single cylinder dose evaluation for a single filled, and a single empty feed cylinder, based on the calculations with the MCNP5, v1.60 code. The compilation includes the following:

- Energy response factors for filled and empty cylinders (Tables E-1 through E-2)
- Neutron dose rate results for a single filled feed cylinder (Tables E-3 through E-7)
- Photon dose rate results for a single filled feed cylinder (Tables E-8 through E-12)
- Photon dose rate results for a single empty feed cylinder (Table E-13)

Table E-1 Neutron and Photon Energy Response Factors for a Filled Cylinder

Energy Bin (MeV)	Average Radial Surface Dose Rate (mrem/h per n/s or p/s)		MCNP Calculation	
	Inside Surface	Outside Surface	Input File	Output File
Neutron Factors				
1.50E-02 - 1.11E-01	1.508E-07 (0.0027)*	7.863E-08 (0.0029)	UF6_n1.txt	UF6_n1.out
1.11E-01 - 4.08E-01	2.552E-07 (0.0023)	1.380E-07 (0.0023)	UF6_n2.txt	UF6_n2.out
4.08E-01 - 9.07E-01	4.971E-07 (0.0023)	2.853E-07 (0.0021)	UF6_n3.txt	UF6_n3.out
9.07E-01 - 1.42E+00	7.570E-07 (0.0021)	4.563E-07 (0.0019)	UF6_n4.txt	UF6_n4.out
1.42E+00 - 1.83E+00	8.652E-07 (0.0020)	5.206E-07 (0.0018)	UF6_n5.txt	UF6_n5.out
1.83E+00 - 3.01E+00	9.623E-07 (0.0020)	5.764E-07 (0.0018)	UF6_n6.txt	UF6_n6.out
3.01E+00 - 6.38E+00	1.126E-06 (0.0019)	6.788E-07 (0.0017)	UF6_n7.txt	UF6_n7.out
6.38E+00 - 2.00E+01	1.662E-06 (0.0020)	1.027E-06 (0.0017)	UF6_n8.txt	UF6_n8.out
Photon Factors				
4.50E-02 - 1.00E-01	5.237E-12 (0.0063)	5.574E-15 (0.1233)	UF6_p1.txt	UF6_p1.out
1.00E-01 - 2.00E-01	7.705E-12 (0.0057)	1.965E-13 (0.0177)	UF6_p2.txt	UF6_p2.out
2.00E-01 - 3.00E-01	6.139E-11 (0.0027)	7.986E-12 (0.0036)	UF6_p3.txt	UF6_p3.out
3.00E-01 - 4.00E-01	1.655E-10 (0.0020)	3.304E-11 (0.0023)	UF6_p4.txt	UF6_p4.out
4.00E-01 - 6.00E-01	4.196E-10 (0.0016)	1.080E-10 (0.0016)	UF6_p5.txt	UF6_p5.out
6.00E-01 - 8.00E-01	8.593E-10 (0.0013)	2.580E-10 (0.0013)	UF6_p6.txt	UF6_p6.out
8.00E-01 - 1.00E+00	1.363E-09 (0.0012)	4.522E-10 (0.0011)	UF6_p7.txt	UF6_p7.out
1.00E+00 - 1.33E+00	2.067E-09 (0.0011)	7.527E-10 (0.0010)	UF6_p8.txt	UF6_p8.out
1.33E+00 - 1.66E+00	2.921E-09 (0.0011)	1.148E-09 (0.0009)	UF6_p9.txt	UF6_p9.out
1.66E+00 - 2.00E+00	3.708E-09 (0.0011)	1.532E-09 (0.0009)	UF6_p10.txt	UF6_p10.out

*Relative error in parentheses

Table E-2 Photon Energy Response Factors for an Empty Cylinder

Energy Bin (MeV)	Average Radial Surface Dose Rate (mrem/h per p/s)		MCNP Calculation	
	Inside Surface	Outside Surface	Input File	Output File
Photon Factors				
4.50E-02 - 1.00E-01	3.395E-09 (0.0003)*	2.358E-12 (0.0068)	UF6_e1.txt	UF6_e1.out
1.00E-01 - 2.00E-01	1.096E-09 (0.0009)	6.257E-11 (0.0025)	UF6_e2.txt	UF6_e2.out
2.00E-01 - 3.00E-01	7.542E-09 (0.0005)	1.164E-09 (0.0007)	UF6_e3.txt	UF6_e3.out
3.00E-01 - 4.00E-01	1.113E-08 (0.0005)	2.518E-09 (0.0006)	UF6_e4.txt	UF6_e4.out
4.00E-01 - 6.00E-01	1.546E-08 (0.0005)	4.357E-09 (0.0005)	UF6_e5.txt	UF6_e5.out
6.00E-01 - 8.00E-01	2.013E-08 (0.0006)	6.590E-09 (0.0005)	UF6_e6.txt	UF6_e6.out
8.00E-01 - 1.00E+00	2.394E-08 (0.0006)	8.651E-09 (0.0005)	UF6_e7.txt	UF6_e7.out
1.00E+00 - 1.33E+00	2.823E-08 (0.0006)	1.121E-08 (0.0005)	UF6_e8.txt	UF6_e8.out
1.33E+00 - 1.66E+00	3.304E-08 (0.0006)	1.419E-08 (0.0005)	UF6_e9.txt	UF6_e9.out
1.66E+00 - 2.00E+00	3.751E-08 (0.0006)	1.701E-08 (0.0005)	UF6_e10.txt	UF6_e10.out

*Relative error in parentheses

Table E-3 Neutron Dose Rate Results for a Single Filled Feed Cylinder

Distance (m)	MCNP Tally No.	Homogenized Geometry		Slumped Geometry		Dose Ratio (1)/(2)
		(1) Dose Rate (mrem/h) ^a	Relative Error ^a	(2) Dose Rate (mrem/h) ^b	Relative Error ^b	
Radial Neutron Dose Rate Profile						
Contact 0.02	5	1.768E-01	0.0171	1.597E-01	0.0214	1.11
0.305	15	1.123E-01	0.0034	8.885E-02	0.0039	1.26
1	25	5.920E-02	0.0019	4.587E-02	0.0034	1.29
2	35	2.905E-02	0.0019	2.203E-02	0.0022	1.32
5	45	7.043E-03	0.0036	5.162E-03	0.0028	1.36
10	55	1.924E-03	0.0034	1.412E-03	0.0044	1.36
20	65	5.039E-04	0.0071	3.690E-04	0.0060	1.37
50	75	8.240E-05	0.0112	6.484E-05	0.0224	1.27
100	85	1.872E-05	0.0146	1.612E-05	0.0514	1.16
200	95	3.335E-06	0.0532	3.112E-06	0.1378	1.07
Axial Neutron Dose Rate Profile						
0.02	105	1.973E-01	0.0153	1.626E-01	0.0204	1.21
0.305	115	1.145E-01	0.0038	8.441E-02	0.0046	1.36
1	125	3.515E-02	0.0029	2.700E-02	0.0034	1.30
2	135	1.270E-02	0.0031	9.941E-03	0.0039	1.28
5	145	2.623E-03	0.0039	2.072E-03	0.0045	1.27
10	155	7.557E-04	0.0063	5.899E-04	0.0079	1.28
20	165	2.287E-04	0.0104	1.832E-04	0.0132	1.25
50	175	4.831E-05	0.0186	3.853E-05	0.0137	1.25
100	185	1.371E-05	0.0359	1.159E-05	0.0372	1.18
200	195	2.565E-06	0.0396	2.130E-06	0.0755	1.20

^a Associated MCNP output file: *feed_n1.out*^b Associated MCNP output file: *feed_n2.out*

Table E-4 Effect of Concrete Pad on Neutron Dose Rates
(Homogenized Geometry – Single Filled Feed Cylinder)

Distance (m)	MCNP Tally No.	With Concrete Pad		Without Concrete Pad		Dose Ratio (2)/(1)
		(1) Dose Rate (mrem/h) ^a	Relative Error ^a	(2) Dose Rate (mrem/h) ^b	Relative Error ^b	
Radial Neutron Dose Rate Profile						
Contact 0.02	5	1.768E-01	0.0171	1.778E-01	0.0171	1.01
0.305	15	1.123E-01	0.0034	1.189E-01	0.0035	1.06
1	25	5.920E-02	0.0019	6.393E-02	0.0023	1.08
2	35	2.905E-02	0.0019	3.131E-02	0.0022	1.08
5	45	7.043E-03	0.0036	7.446E-03	0.0033	1.06
10	55	1.924E-03	0.0034	2.022E-03	0.0037	1.05
20	65	5.039E-04	0.0071	5.416E-04	0.0069	1.07
50	75	8.240E-05	0.0112	9.482E-05	0.0154	1.15
100	85	1.872E-05	0.0146	2.273E-05	0.0208	1.21
200	95	3.335E-06	0.0532	4.875E-06	0.0847	1.46

^a Associated MCNP output file: *feed_n1.out*

^b Associated MCNP output file: *feed_n3.out*

Table E-5 Effect of Ground Scattering on Neutron Dose Rates
(Homogenized Geometry – Single Filled Feed Cylinder)

Distance (m)	MCNP Tally No.	Without Ground Scatter		With Ground Scatter		Dose Ratio (2)/(1)
		(1) Dose Rate (mrem/h) ^a	Relative Error ^a	(2) Dose Rate (mrem/h) ^b	Relative Error ^b	
Radial Neutron Dose Rate Profile						
Contact 0.02	5	1.590E-01	0.0405	1.778E-01	0.0171	1.12
0.305	15	9.314E-02	0.0083	1.189E-01	0.0035	1.28
1	25	4.499E-02	0.0044	6.393E-02	0.0023	1.42
2	35	2.155E-02	0.0047	3.131E-02	0.0022	1.45
5	45	5.355E-03	0.0034	7.446E-03	0.0033	1.39
10	55	1.590E-03	0.0041	2.022E-03	0.0037	1.27
20	65	4.580E-04	0.0063	5.416E-04	0.0069	1.18
50	75	9.212E-05	0.0223	9.482E-05	0.0154	1.03
100	85	2.670E-05	0.0119	2.273E-05	0.0208	0.85
200	95	6.198E-06	0.0243	4.875E-06	0.0847	0.79

^a Associated MCNP output file: *feed_n4.out*

^b Associated MCNP output file: *feed_n3.out*

Table E-6 Secondary Photon Dose Rates due to Neutron Interactions
(Homogenized Geometry – Single Filled Feed Cylinder)

Distance (m)	MCNP Tally No.	Neutron		Secondary Photon		Dose Ratio (2)/(1)
		(1) Dose Rate (mrem/h) ^a	Relative Error ^a	(2) Dose Rate (mrem/h) ^b	Relative Error ^b	
Radial Neutron Dose Rate Profile						
Contact 0.02	5	1.768E-01	0.0171	9.228E-04	0.0366	0.01
0.305	15	1.123E-01	0.0034	6.830E-04	0.0041	0.01
1	25	5.920E-02	0.0019	3.935E-04	0.0030	0.01
2	35	2.905E-02	0.0019	1.853E-04	0.0031	0.01
5	45	7.043E-03	0.0036	4.176E-05	0.0090	0.01
10	55	1.924E-03	0.0034	1.207E-05	0.0099	0.01
20	65	5.039E-04	0.0071	3.683E-06	0.0205	0.01
50	75	8.240E-05	0.0112	7.685E-07	0.0312	0.01
100	85	1.872E-05	0.0146	2.363E-07	0.0588	0.01
200	95	3.335E-06	0.0532	4.746E-08	0.0715	0.01

^a Associated MCNP output file: *feed_n1.out*

^b Associated MCNP output file: *feed_n5.out*

Table E-7 Effect of ANSI/ANS-6.1.1-1991 Standard on Neutron Dose Rates
(Homogenized Geometry – Single Filled Feed Cylinder)

Distance (m)	MCNP Tally No.	ANSI/ANS-6.1.1-1977		ANSI/ANS-6.1.1-1991		Dose Ratio (2)/(1)
		(1) Dose Rate (mrem/h) ^a	Relative Error ^a	(2) Dose Rate (mrem/h) ^b	Relative Error ^b	
Radial Neutron Dose Rate Profile						
Contact 0.02	5	1.768E-01	0.0171	7.303E-02	0.0176	0.41
0.305	15	1.123E-01	0.0034	4.623E-02	0.0037	0.41
1	25	5.920E-02	0.0019	2.434E-02	0.0021	0.41
2	35	2.905E-02	0.0019	1.194E-02	0.0020	0.41
5	45	7.043E-03	0.0036	2.894E-03	0.0028	0.41
10	55	1.924E-03	0.0034	7.946E-04	0.0039	0.41
20	65	5.039E-04	0.0071	2.057E-04	0.0050	0.41
50	75	8.240E-05	0.0112	3.426E-05	0.0118	0.42
100	85	1.872E-05	0.0146	8.083E-06	0.0306	0.43
200	95	3.335E-06	0.0532	1.361E-06	0.0519	0.41

^a Associated MCNP output file: *feed_n1.out*

^b Associated MCNP output file: *feed_n6.out*

Table E-8 Photon Dose Rate Results for a Single Filled Feed Cylinder

Distance (m)	MCNP Tally No.	Homogenized Geometry		Slumped Geometry		Dose Ratio (1)/(2)
		(1) Dose Rate (mrem/h) ^a	Relative Error ^a	(2) Dose Rate (mrem/h) ^b	Relative Error ^b	
Radial Photon Dose Rate Profile						
Contact	5	1.386E+00	0.0180	1.329E+00	0.0198	1.04
0.02	15	8.718E-01	0.0043	6.872E-01	0.0094	1.27
1	25	4.580E-01	0.0055	3.318E-01	0.0050	1.38
2	35	2.327E-01	0.0036	1.657E-01	0.0046	1.40
5	45	5.909E-02	0.0022	4.099E-02	0.0031	1.44
10	55	1.631E-02	0.0023	1.119E-02	0.0070	1.46
20	65	4.013E-03	0.0028	2.719E-03	0.0037	1.48
50	75	5.597E-04	0.0048	3.820E-04	0.0057	1.47
100	85	1.118E-04	0.0114	7.746E-05	0.0114	1.44
200	95	1.602E-05	0.0177	1.146E-05	0.0232	1.40
Axial Photon Dose Rate Profile						
0.02	105	1.500E+00	0.0193	1.457E+00	0.0193	1.03
0.305	115	1.153E+00	0.0032	8.243E-01	0.0055	1.40
1	125	3.688E-01	0.0044	2.491E-01	0.0042	1.48
2	135	1.209E-01	0.0040	8.275E-02	0.0048	1.46
5	145	2.270E-02	0.0053	1.557E-02	0.0042	1.46
10	155	5.810E-03	0.0037	4.013E-03	0.0054	1.45
20	165	1.435E-03	0.0061	9.898E-04	0.0079	1.45
50	175	2.140E-04	0.0085	1.524E-04	0.0116	1.40
100	185	4.677E-05	0.0138	3.523E-05	0.0205	1.33
200	195	7.436E-06	0.0291	6.095E-06	0.0487	1.22

^a Associated MCNP output file: *feed_p1.out*

^b Associated MCNP output file: *feed_p2.out*

Table E-9 Effect of Concrete Pad on Photon Dose Rates
(Homogenized Geometry – Single Filled Feed Cylinder)

Distance (m)	MCNP Tally No.	With Concrete Pad		Without Concrete Pad		Dose Ratio (2)/(1)
		(1) Dose Rate (mrem/h) ^a	Relative Error ^a	(2) Dose Rate (mrem/h) ^b	Relative Error ^b	
Radial Photon Dose Rate Profile						
Contact 0.02	5	1.386E+00	0.0180	1.389E+00	0.0202	1.00
0.305	15	8.718E-01	0.0043	8.676E-01	0.0052	1.00
1	25	4.580E-01	0.0055	4.550E-01	0.0027	0.99
2	35	2.327E-01	0.0036	2.316E-01	0.0026	1.00
5	45	5.909E-02	0.0022	5.935E-02	0.0029	1.00
10	55	1.631E-02	0.0023	1.644E-02	0.0054	1.01
20	65	4.013E-03	0.0028	4.021E-03	0.0034	1.00
50	75	5.597E-04	0.0048	5.615E-04	0.0057	1.00
100	85	1.118E-04	0.0114	1.138E-04	0.0167	1.02
200	95	1.602E-05	0.0177	1.641E-05	0.0282	1.02

^a Associated MCNP output file: *feed_p1.out*

^b Associated MCNP output file: *feed_p3.out*

Table E-10 Effect of Ground Scattering on Photon Dose Rates
(Homogenized Geometry – Single Filled Feed Cylinder)

Distance (m)	MCNP Tally No.	Without Ground Scatter		With Ground Scatter		Dose Ratio (2)/(1)
		(1) Dose Rate (mrem/h) ^a	Relative Error ^a	(2) Dose Rate (mrem/h) ^b	Relative Error ^b	
Radial Photon Dose Rate Profile						
Contact 0.02	5	1.375E+00	0.0205	1.389E+00	0.0202	1.01
0.305	15	8.442E-01	0.0061	8.676E-01	0.0052	1.03
1	25	4.308E-01	0.0027	4.550E-01	0.0027	1.06
2	35	2.140E-01	0.0028	2.316E-01	0.0026	1.08
5	45	5.304E-02	0.0019	5.935E-02	0.0029	1.12
10	55	1.498E-02	0.0057	1.644E-02	0.0054	1.10
20	65	3.855E-03	0.0030	4.021E-03	0.0034	1.04
50	75	6.101E-04	0.0118	5.615E-04	0.0057	0.92
100	85	1.389E-04	0.0094	1.138E-04	0.0167	0.82
200	95	2.594E-05	0.0156	1.641E-05	0.0282	0.63

^a Associated MCNP output file: *feed_p4.out*

^b Associated MCNP output file: *feed_p3.out*

Table E-11 Comparison of Photon Dose Rates between Full and Partial Spectra
(Homogenized Geometry – Single Filled Feed Cylinder)

Distance (m)	MCNP Tally No.	Partial Spectrum		Full Spectrum		Dose Ratio (2)/(1)
		(1) Dose Rate (mrem/h) ^a	Relative Error ^a	(2) Dose Rate (mrem/h) ^b	Relative Error ^b	
Radial Photon Dose Rate Profile						
Contact 0.02	5	1.386E+00	0.0180	1.343E+00	0.0397	0.97
0.305	15	8.718E-01	0.0043	8.525E-01	0.0066	0.98
1	25	4.580E-01	0.0055	4.568E-01	0.0092	1.00
2	35	2.327E-01	0.0036	2.318E-01	0.0042	1.00
5	45	5.909E-02	0.0022	5.915E-02	0.0057	1.00
10	55	1.631E-02	0.0023	1.633E-02	0.0048	1.00
20	65	4.013E-03	0.0028	4.141E-03	0.0253	1.03
50	75	5.597E-04	0.0048	5.700E-04	0.0116	1.02
100	85	1.118E-04	0.0114	1.080E-04	0.0154	0.97
200	95	1.602E-05	0.0177	1.585E-05	0.0240	0.99

^a Associated MCNP output file: *feed_p1.out*

^b Associated MCNP output file: *feed_p5.out*

Table E-12 Effect of ANSI/ANS-6.1.1-1991 Standard on Photon Dose Rates
(Homogenized Geometry – Single Filled Feed Cylinder)

Distance (m)	MCNP Tally No.	ANSI/ANS-6.1.1-1977		ANSI/ANS-6.1.1-1991		Dose Ratio (2)/(1)
		(1) Dose Rate (mrem/h) ^a	Relative Error ^a	(2) Dose Rate (mrem/h) ^b	Relative Error ^b	
Radial Photon Dose Rate Profile						
Contact 0.02	5	1.386E+00	0.0180	1.157E+00	0.0205	0.83
0.305	15	8.718E-01	0.0043	7.262E-01	0.0051	0.83
1	25	4.580E-01	0.0055	3.828E-01	0.0026	0.84
2	35	2.327E-01	0.0036	1.947E-01	0.0027	0.84
5	45	5.909E-02	0.0022	4.968E-02	0.0029	0.84
10	55	1.631E-02	0.0023	1.377E-02	0.0056	0.84
20	65	4.013E-03	0.0028	3.400E-03	0.0039	0.85
50	75	5.597E-04	0.0048	4.786E-04	0.0058	0.86
100	85	1.118E-04	0.0114	9.757E-05	0.0146	0.87
200	95	1.602E-05	0.0177	1.396E-05	0.0312	0.87

^a Associated MCNP output file: *feed_p1.out*

^b Associated MCNP output file: *feed_p6.out*

Table E-13 Photon Dose Rate Results for a Single Empty Feed Cylinder

Distance (m)	MCNP Tally No.*	Radial Profile		Axial Profile		Dose Ratio (1)/(2)
		(1) Dose Rate (mrem/h) ^a	Relative Error ^a	(2) Dose Rate (mrem/h) ^b	Relative Error ^b	
Contact 0.02	5/105	2.161E+01	0.0188	2.104E+01	0.0166	1.03
0.305	15/115	1.276E+01	0.0038	1.295E+01	0.0024	0.99
1	25/125	6.133E+00	0.0017	4.967E+00	0.0026	1.23
2	35/135	2.947E+00	0.0025	2.102E+00	0.0021	1.40
5	45/145	7.465E-01	0.0017	5.287E-01	0.0020	1.41
10	55/155	2.092E-01	0.0025	1.581E-01	0.0026	1.32
20	65/165	5.252E-02	0.0050	4.184E-02	0.0057	1.26
50	75/175	7.423E-03	0.0047	6.190E-03	0.0048	1.20
100	85/185	1.483E-03	0.0126	1.256E-03	0.0097	1.18
200	95/195	2.194E-04	0.0363	1.840E-04	0.0230	1.19

*Tally numbers 5 through 95 for the radial profile and 105 through 195 for the axial profile

APPENDIX F MAVRIC COMPUTER FILES AND INPUT LISTING

F.1 MAVRIC CASES AND COMPUTER FILES

Table F-1 lists the MAVRIC computer files used to generate the photon source importance data for filled feed cylinders.

Table F-1 MAVRIC Case Description and Computer Files

Case	Description	Input File	Output File
1	10x10 array, double stacking	d10x10p.inp	d10x10p.out
2	30x30 array, double stacking	d30x30p.inp	d30x30p.out

F.2 MAVRIC INPUT LISTING

The cases for listing of the MAVRIC input files include the following:

- File *d10x10p.inp* (§F.2.1)
- File *d30x30p.inp* (§F.2.2)
- File *nu1.inp* – Progeny inventory for empty feed cylinder (§A.2.3)
- File *nu2.inp* – Progeny photon source for empty feed cylinder (§A.2.4)

F.2.1 Input File *d10x10p.inp*

```
=mavric
UF6 48Y cylinder storage - neutron dose - double stack (10x10)
v7-27n19g

read composition
  wtptUF6 1 2.73 3
           92235 0.481 92238 67.138 9019 32.381
           1.0 293.0 end
  dry-air 2 1.0 293.0 end
  wtptSoil 3 1.6 13
           8016 46.8 11023 2.45 13027 8.0
           12024 1.17 12025 0.15 12026 0.18
           14028 26.64 14029 1.40 14030 0.96
           19039 2.09 19041 0.16 20040 4.0
           26056 6.0
           1.0 293.0 end
end composition
```



```

read geometry
  unit 1
    cuboid 1 131.63 20.77 430.21 57.47 110.86 0.0
    cuboid 99 152.40 0.0 487.68 0.0 110.86 0.0
    media 1 1 1
    media 2 1 -1 99
    boundary 99
  global unit 2
    cuboid 1 1524.0 0.0 4876.8 0.0 221.72 0.0
    cuboid 2 5000.0 -100.0 5500.0 -500.0 500.0 0.0
    cuboid 3 5500.0 -100.0 6000.0 -500.0 0.0 -30.0
    cuboid 4 5500.0 -100.0 6000.0 -500.0 500.0 -30.0
    array 10 1 place 1 1 1 0.0 0.0 0.0
    media 2 1 -1 2
    media 3 1 3
    media 0 1 -2 -3 4
    boundary 4
end geometry

read array
  ara=10 nux=10 nuy=10 nuz=2 fill 200r1 end fill
end array

read definitions
  gridgeometry 11
    title="fine geometry for adjoint source"
    xplanes -100.0 0.00 20.77 131.63
      152.40 173.17 284.03 304.80 325.57 436.43
      457.20 477.97 588.83 609.60 630.37 741.23
      762.00 782.77 893.63 914.40 935.17 1046.03
      1066.80 1087.57 1198.43 1219.20 1239.97 1350.83
      1371.60 1392.37 1503.23 1524.00
      3000.00 4500.00 5400.00 5500.00 end
    yplanes -500.0 0.00 57.47 430.21
      487.68 545.15 917.89 975.36 1032.83 1405.57
      1463.04 1520.51 1893.25 1950.72 2008.19 2380.93
      2438.40 2495.87 2868.61 2926.08 2983.55 3356.29
      3413.76 3471.23 3843.97 3901.44 3958.91 4331.65
      4389.12 4446.59 4819.33 4876.80
      5000.00 6000.00 end
    zplanes -30.0 0.0 110.86 221.72 500.00 end
  end gridgeometry
  response 1 specialdose=9029 end response
  distribution 1
    title="UF6 neutron source energy spectrum @0.711% U-235"
    neutronGroups
    truePDF 1.163E-03 3.063E-02 1.040E-01 1.470E-01 3.256E-01
      3.060E-01 7.776E-02 7.849E-03 0.0 0.0
      0.0 0.0 0.0 0.0 0.0
      0.0 0.0 0.0 0.0 0.0
      0.0 0.0 0.0 0.0 0.0
      0.0 0.0 end
  end distribution
end definitions

read sources
  src 1

```

```

    title="neutron sources for 200 cylinders"
    strength=9.952E+07
    neutrons
    cuboid 1503.23  20.77  4819.33    57.47  221.72  0.0
    mixture=1
    eDistributionID=1
    end src
end sources

read importanceMap
  adjointSource 1
    boundingBox 5500.0 5400.0 4876.80 0.0 221.72  0.0
    responseID=1
  end adjointSource
  gridGeometry=11
  respWeighting
end importanceMap

read parmeters
  perBatch=10000 batches=200
  noFissions
  noSecondaries
end parameters

end data
end

```

F.2.2 Input File *d30x30p.inp*

```

=mavric
UF6 48Y cylinder storage - neutron dose - double stack (30x30)
v7-27n19g

read composition
  wtptUF6 1 2.73 3
    92235 0.481 92238 67.138  9019 32.381
    1.0 293.0 end
  dry-air 2 1.0 293.0 end
  wtptSoil 3 1.6 13
    8016 46.8  11023 2.45  13027 8.0
    12024 1.17  12025 0.15  12026 0.18
    14028 26.64  14029 1.40  14030 0.96
    19039 2.09  19041 0.16  20040 4.0
    26056 6.0
    1.0 293.0 end
end composition

read geometry
  unit 1
    cuboid 1 131.63 20.77 430.21 57.47 110.86 0.0
    cuboid 99 152.40 0.0 487.68 0.0 110.86 0.0
    media 1 1 1
    media 2 1 -1 99
    boundary 99
  global unit 2

```

```

cuboid 1 4572.00 0.0 14630.40 0.0 221.72 0.0
cuboid 2 9000.0 -100.0 15000.0 -500.0 500.0 0.0
cuboid 3 9600.0 -100.0 15500.0 -500.0 0.0 -30.0
cuboid 4 9600.0 -100.0 15500.0 -500.0 500.0 -30.0
array 10 1 place 1 1 1 0.0 0.0 0.0
media 2 1 -1 2
media 3 1 3
media 0 1 -2 -3 4
boundary 4
end geometry

read array
ara=10 nux=30 nuy=30 nuz=2 fill 1800r1 end fill
end array

read definitions
gridgeometry 11
title="fine geometry for adjoint source"
xplanes -100.0 0.00 20.77 131.63
152.40 173.17 284.03 304.80 325.57 436.43
457.20 477.97 588.83 609.60 630.37 741.23
762.00 782.77 893.63 914.40 935.17 1046.03
1066.80 1087.57 1198.43 1219.20 1239.97 1350.83
1371.60 1392.37 1503.23 1524.00 1544.77 1655.63
1676.40 1697.17 1808.03 1828.80 1849.57 1960.43
1981.20 2001.97 2112.83 2133.60 2154.37 2265.23
2286.00 2306.77 2417.63 2438.40 2459.17 2570.03
2590.80 2611.57 2722.43 2743.20 2763.97 2874.83
2895.60 2916.37 3027.23 3048.00 3068.77 3179.63
3200.40 3221.17 3332.03 3352.80 3373.57 3484.43
3505.20 3525.97 3636.83 3657.60 3678.37 3789.23
3810.00 3830.77 3941.63 3962.40 3983.17 4094.03
4114.80 4135.57 4246.43 4267.20 4287.97 4398.83
4419.60 4440.37 4551.23 4572.00
5000.00 7000.00 9000.00 9500.00 9600.00 end
yplanes -500.0 0.00 57.47 430.21
487.68 545.15 917.89 975.36 1032.83 1405.57
1463.04 1520.51 1893.25 1950.72 2008.19 2380.93
2438.40 2495.87 2868.61 2926.08 2983.55 3356.29
3413.76 3471.23 3843.97 3901.44 3958.91 4331.65
4389.12 4446.59 4819.33 4876.80 4934.27 5307.01
5364.48 5421.95 5794.69 5852.16 5909.63 6282.37
6339.84 6397.31 6770.05 6827.52 6884.99 7257.73
7315.20 7372.67 7745.41 7802.88 7860.35 8233.09
8290.56 8348.03 8720.77 8778.24 8835.71 9208.45
9265.92 9323.39 9696.13 9753.60 9811.07 10183.81
10241.28 10298.75 10671.49 10728.96 10786.43 11159.17
11216.64 11274.11 11646.85 11704.32 11761.79 12134.53
12192.00 12249.47 12622.21 12679.68 12737.15 13109.89
13167.36 13224.83 13597.57 13655.04 13712.51 14085.25
14142.72 14200.19 14572.93 14630.40
15000.00 15500.00 end
zplanes -30.0 0.0 110.86 221.72 500.00 end
end gridgeometry
response 1 specialdose=9029 end response
distribution 1
title="UF6 neutron source energy spectrum @0.711% U-235"

```

```

        neutronGroups
        truePDF 1.163E-03 3.063E-02 1.040E-01 1.470E-01 3.256E-01
                3.060E-01 7.776E-02 7.849E-03 0.0      0.0
                0.0      0.0      0.0      0.0      0.0
                0.0      0.0      0.0      0.0      0.0
                0.0      0.0      0.0      0.0      0.0
                0.0      0.0      end
    end distribution
end definitions

read sources
  src 1
  title="neutron sources for 1800 cylinders"
  strength=8.957E+08
  neutrons
  cuboid 4551.23 20.77 14572.93 57.47 221.72 0.0
  mixture=1
  eDistributionID=1
  end src
end sources

read importanceMap
  adjointSource 1
    boundingBox 9500.0 9600.0 14630.40 0.0 221.72 0.0
    responseID=1
  end adjointSource
  gridGeometry=11
  respWeighting
end importanceMap

read parmaters
  perBatch=10000 batches=1800
  noFissions
  noSecondaries
end parameters

end data
end

```

APPENDIX G MCNP COMPUTER FILES FOR FILLED CYLINDER ARRAY

G.1 MCNP CASES AND COMPUTER FILES

Table G-1 lists the MCNP computer files used in the first-step process for calculations of neutron and photon dose rates for different configurations of filled feed cylinder storage arrangements. The corresponding cases for the second-step process in the MCNP simulations are provided in Table G-2.

Table G-1 MCNP Cases in First-Step Process for Cylinder Arrays

Case	Case Description	Input File	Output File	CPU (m)	nps	Tracks
Neutron Cases						
1	10x10 Array - Single	s10x10n01.txt	s10x10n01.out	104.55	21.63M	45.63M
2	10x10 Array - Double	d10x10n01.txt	d10x10n01.out	102.44	15.31M	23.47M
3	10x10 Array - Triple	t10x10n01.txt	t10x10n01.out	101.69	12.98M	15.06M
4	30x30 Array - Single	s30x30n01.txt	s30x30n01.out	104.75	19.80M	47.81M
5	30x30 Array - Double	d30x30n01.txt	d30x30n01.out	102.58	13.90M	24.73M
6	30x30 Array - Triple	t30x30n01.txt	t30x30n01.out	101.74	11.75M	16.01M
7	100x100 Array - Single	s100x100n01.txt	s100x100n01.out	105.33	16.85M	53.71M
8	100x100 Array - Double	d100x100n01.txt	d100x100n01.out	102.94	12.24M	28.26M
9	100x100 Array - Triple	t100x100n01.txt	t100x100n01.out	102.00	10.49M	18.48M
Photon Cases						
1	10x10 Array - Single	s10x10p01.txt	s10x10p01.out	103.95	300.8M	42.44M
2	10x10 Array - Double	d10x10p01.txt	d10x10p01.out	215.27	628.3M	56.40M
3	10x10 Array - Triple	t10x10p01.txt	t10x10p01.out	305.56	907.8M	59.85M
4	30x30 Array - Single	s30x30p01.txt	s30x30p01.out	103.57	301.9M	38.17M
5	30x30 Array - Double	d30x30p01.txt	d30x30p01.out	215.07	624.9M	54.61M
6	30x30 Array - Triple	t30x30p01.txt	t30x30p01.out	305.48	900.4M	59.36M
7	100x100 Array - Single	s100x100p01.txt	s100x100p01.out	103.49	298.1M	37.40M
8	100x100 Array - Double	d100x100p01.txt	d100x100p01.out	214.94	620.8M	53.22M
9	100x100 Array - Triple	t100x100p01.txt	t100x100p01.out	305.35	888.7M	57.12M

Table G-2 MCNP Cases in Second-Step Process for Cylinder Arrays

Case	Case Description	Input File	Output File	Surface Source File	Mesh Tally File	CPU (m)
Neutron Cases						
1	10x10 - Single	s10x10n02.txt	s10x10n02.out	w100n	mt100n	38.00
2	10x10 - Double	d10x10n02.txt	d10x10n02.out	w210n	m_210n	19.17
3	10x10 - Triple	t10x10n02.txt	t10x10n02.out	w300n	mt300n	12.48
4	30x30 - Single	s30x30n02.txt	s30x30n02.out	w900n	mt900n	42.69
5	30x30 - Double	d30x30n02.txt	d30x30n02.out	w1830n	mt1830n	21.20
6	30x30 - Triple	t30x30n02.txt	t30x30n02.out	w2700n	mt2700n	13.78
7	100x100 - Single	s100x100n02.txt	s100x100n02.out	w10000n	mt10000n	46.96
8	100x100 - Double	d100x100n02.txt	d100x100n02.out	w20100n	mt20100n	24.33
9	100x100 - Triple	t100x100n02.txt	t100x100n02.out	w30000n	mt30000n	16.47
Photon Cases						
1	10x10 - Single	s10x10p02.txt	s10x10p02.out	w100p	mt100p	52.55
2	10x10 - Double	d10x10p02.txt	d10x10p02.out	w210p	mt210p	36.77
3	10x10 - Triple	t10x10p02.txt	t10x10p02.out	w300p	mt300p	70.07
4	30x30 - Single	s30x30p02.txt	s30x30p02.out	w900p	mt900p	48.41
5	30x30 - Double	d30x30p02.txt	d30x30p02.out	w1830p	mt1830p	37.57
6	30x30 - Triple	t30x30p02.txt	t30x30p02.out	w2700p	mt2700p	73.99
7	100x100 - Single	s100x100p02.txt	s100x100p02.out	w10000p	mt10000p	51.24
8	100x100 - Double	d100x100p02.txt	d100x100p02.out	w20100p	mt20100p	40.25
9	100x100 - Triple	t100x100p02.txt	t100x100p02.out	w30000p	mt30000p	76.14

G.2 SAMPLE MCNP INPUT LISTING

The cases for listing of the MAVRIC input files include the following:

- File *t100x100n01.txt* (§G.2.1)
- File *t100x100n02.txt* (§G.2.2)
- File *t100x100p01.txt* (§G.2.3)
- File *t100x100p02.txt* (§G.2.4)

G.2.1 Input File *t100x100n01.txt*

```
Dose Rates from Multiple Filled 48Y Tails Cylinder
c file t100x100n01 (30,000 cylinders total - 101x100, 100x100 & 99x100)
c 101x100, 100x100 & 99x100 array - double stack
c reflective boundary at Y mid-plane (i.e., 15,000 cylinders modeled)
c Neutron - homogenized source geometry - ANSI/ANS-6.1.1-1977
c center-to-center spacing=5' (radial) & 16' (axial)
c lattice center element at far right
c 1st step calculation to tally surface sources
c include built-in directional biasing (a=1)
c no cell source biasing
c
c CELL CARDS
c
11      1      -2.897   -11                u=1 imp:n=1 $Inside of cylinder (UF6)
12      2      -7.8500  11 -12            u=1 imp:n=2 $Steel shell
13      3      -0.0012  12                u=1 imp:n=3 $External to cylinder
14      0                -13  fill=1 lat=1  u=2 imp:n=3 $Lattice for bottom stack
15      0                -31  fill=2                imp:n=3 $Box to fill bottom stack
16  like 14 but trcl=(-76.2  0 125.095) u=3 imp:n=3 $Lattice for middle stack
17      0                -32  fill=3                imp:n=3 $Box to fill middle stack
18  like 14 but trcl=(-152.4 0 250.190) u=4 imp:n=3 $Lattice for top stack
19      0                -33  fill=4                imp:n=3 $Box to fill top stack
c
20      3      -0.0012  -34  31 32  33                imp:n=3 $Box for all cylinders
21      3      -0.0012  41 -42 43 -44 46 -47 34  imp:n=3 $Air space
22      4      -1.685   41 -42 43 -44 45 -46  imp:n=1 $Ground soil
23      0                -41:42:-43:44:-45:47  imp:n=0 $Outer void
c
c SURFACE CARDS
c
11      rcc  0.0 -184.7850 0.0 0.0 369.570 0.0 60.9600      $UF6 cylinder
12      rcc  0.0 -186.3725 0.0 0.0 372.745 0.0 62.5475      $steel cylinder
13      rpp  -76.2  76.2 -243.84 243.84 -62.5475 62.5475  $unit box
c Box to fill cylinders (bottom stack - 101x50 cylinders)
31      rpp  -15316.2 62.6 -243.84 24083.0 -62.5475 62.5475
c Box to fill cylinders (mid stack - 100x50 cylinders)
32      rpp  -15240.0 0.0 -243.84 24083.0 62.5475 187.6425
c Box to fill cylinders (top stack - 99x50 cylinders)
33      rpp  -15163.8 -76.2 -243.84 24083.0 187.6425 312.8
c Box to contain all cylinders
```

```

34   rpp  -15316.2  62.6 -243.84 24083.0 -77.7875 312.8
c   Air box
41   px   -15320.0  $-X boundary
42   px    20000.0  $+X boundary
43*  py   -244.0    $-Y boundary (reflective)
44   py    44000.0  $+Y boundary
45   pz   -108.0    $-Z boundary (soil bottom)
46   pz   -77.7875 $ground Z level or soil top
47   pz    20000.0  $+Z boundary
48   pz   -62.5475 $bottom of cylinder

c
c
c   DATA CARDS
c
m1    9019.70c  6.00    92238.70c  0.9928  92235.70c  0.0072  $ UF6
m2    26054.70c 0.05845 26056.70c  0.91754 26057.70c  0.02119  $ Iron
      26058.70c  0.00282
m3    6000.70c -0.00014  7014.70c -0.75521  8016.70c -0.23177  $ Air
      18040.70c -0.01288
m4    8016.70c -0.465   11023.70c -0.0245  13027.70c -0.080   $ Ground soil
      12024.70c -0.0117  12025.70c -0.0015  12026.70c -0.0018
      14028.70c -0.2664  14029.70c -0.0140  14030.70c -0.0096
      19039.70c -0.0209  19041.70c -0.0016  20040.70c -0.040
      26056.70c -0.060

mode  n
c   Write surface source file
ssw   31.1 31.3 33.5
c   Source definition card with the following distributions:
c   d1=distribution #1 for selection of the cell (i.e., cylinder)
c   d2=distribution #2 for selection of x position
c   d3=distribution #3 for selection of y position
c   d4=distribution #4 for selection of z position
c   d5=distribution #5 for photon source energy spectrum
c   d6=distribution #6 for directional biasing w.r.t. +x axis
sdef  cel=d1 x=d2 y=d3 z=d4 erg=d5 vec=1 0 0 dir=d6
si1   1 (-11<14[-100:0 0:49 0:0]<15)  $cell information (101x50 - bottom)
      (-11<16[-99:0 0:49 0:0]<17)    $cell information (100x50 - mid)
      (-11<18[-98:0 0:49 0:0]<19)    $cell information (99x50 - top)
sp1   1 14999r                          $cell unbiased probability (equal)
si2   -60.96  60.96                      $source position in x for center element
sp2   0.0     1.0                        $equal weighting along x
si3   -184.7850 184.7850                $source position in y for center element
sp3   0.0     1.0                        $equal weighting along y
si4   -60.96  60.96                      $source position in z for center element
sp4   0.0     1.0                        $equal weighting along z
c   Neutron Spectrum (partial from SCALE 27 groups)
c   si5 - energy boundary information
c   sp5 - unbiased energy spectrum
c   sb5 - biased energy spectrum based on dose response
c   vertical input format used for si5, sp5 and sb5
#     si5    sp5    sb5
      0.015  0.0    0.0
      0.111  7.849E-03 1.521E-03
      0.408  7.776E-02 2.645E-02
      0.907  3.060E-01 2.152E-01
      1.42   3.256E-01 3.662E-01
      1.83   1.470E-01 1.886E-01
      3.01   1.040E-01 1.477E-01
      6.38   3.063E-02 5.125E-02

```



```

20.0 1.163E-03 2.945E-03
c Directional sampling with bias for forward direction
si6 -1.0 1.0 $direction cosine from -1 to 1
sb6 -31 1 $biased directional distribution for sampling
c neutron dose conversion factors (mrem/h)/(n/cm^2-s)}
c from MCNP Manual, ANSI/ANS-6.1.1-1977
DE0 LOG 2.5-8 1.0-7 1.0-6 1.0-5 1.0-4 1.0-3 1.0-2 1.0-1
5.0-1 1.0 2.5 5.0 7.0 10.0 14.0 20.0
DF0 LOG 3.67-3 3.67-3 4.46-3 4.54-3 4.18-3 3.76-3 3.56-3 2.17-2
9.26-2 1.32-1 1.25-1 1.56-1 1.47-1 1.47-1 2.08-1 2.27-1
c Energy bins for tally (same as for source energy groups)
e0 0.0 0.015 0.111 0.408 0.907 1.42 1.83 3.01 6.38 20.0
f2:n 31.1 31.3 33.5 $average dose rate on these facets
fm2 7.464E+09 $total source strength for 15,000 cylinders (n/s)
ctme 100.0
print

```

G.2.2 Input File *t100x100n02.txt*

```

Dose Rates from Multiple Filled 48Y Feed Cylinder
c file t100x100n02 (30,000 cylinders total)
c 101x100, 100x100 & 99x100 array - triple stack
c reflective boundary at Y mid-plane (i.e., 15,000 cylinders modeled)
c neutron - homogenized source geometry - ANSI/ANS-6.1.1-1977
c center-to-center spacing=5' (radial) & 16' (axial)
c 2nd step calculation with mesh tally
c
21 0 -31 32 imp:n=1 $Box around cylinders
22 0 -32 imp:n=0 $Black box for all
cylinders
23 3 -0.0012 41 -50 43 -44 46 -47 31 imp:n=1 $Air space
24 4 -1.60 41 -50 43 -44 45 -46 imp:n=1 $Ground soil
25 0 -41:42:-43:44:-45:47 imp:n=0 $Outer void
c Air importance cells
51 3 -0.0012 50 -51 43 -44 46 -47 imp:n=1 $1st air cell
52 3 -0.0012 51 -52 43 -44 46 -47 imp:n=2 $2nd air cell
53 3 -0.0012 52 -53 43 -44 46 -47 imp:n=4 $3rd air cell
54 3 -0.0012 53 -54 43 -44 46 -47 imp:n=8 $4th air cell
55 3 -0.0012 54 -42 43 -44 46 -47 imp:n=16 $5th air cell
c Soil importance cells
61 4 -1.60 50 -51 43 -44 45 -46 imp:n=1 $1st soil cell
62 4 -1.60 51 -52 43 -44 45 -46 imp:n=1 $2nd soil cell
63 4 -1.60 52 -53 43 -44 45 -46 imp:n=2 $3rd soil cell
64 4 -1.60 53 -54 43 -44 45 -46 imp:n=3 $4th soil cell
65 4 -1.60 54 -42 43 -44 45 -46 imp:n=5 $5th soil cell
c
c Box to fill cylinders (triple stack-15000 cylinders with reflective
boundary)
31 rpp -15378.8 0.0 -24326.84 0.0 -77.7875 312.8
c Black Box to contain all cylinders (to avoid round-off errors)
32 rpp -15378.8 -0.1 -24326.84 -0.1 -77.7875 312.7
c Air box
41 px -15380.0 $-X boundary
42 px 50000.0 $+X boundary
43* py -24327.0 $-Y boundary (reflective)
44 py 30000.0 $+Y boundary

```

```

45 pz -108.0 $-Z boundary (soil bottom)
46 pz -77.7875 $ground level or soil top)
47 pz 30000.0 $+Z boundary
48 pz -62.5475 $bottom of cylinder
c Cell importance division plane
50 px 0.0
51 px 10000.0
52 px 20000.0
53 px 30000.0
54 px 40000.0

m1 9019.70c 6.00 92238.70c 0.9928 92235.70c 0.0072 $ UF6
m2 26054.70c 0.05845 26056.70c 0.91754 26057.70c 0.02119 $ Iron
26058.70c 0.00282
m3 6000.70c -0.00014 7014.70c -0.75521 8016.70c -0.23177 $ Air
18040.70c -0.01288
m4 8016.70c -0.465 11023.70c -0.0245 13027.70c -0.080 $ Ground soil
12024.70c -0.0117 12025.70c -0.0015 12026.70c -0.0018
14028.70c -0.2664 14029.70c -0.0140 14030.70c -0.0096
19039.70c -0.0209 19041.70c -0.0016 20040.70c -0.040
26056.70c -0.060

mode n
c Coordinate transformation from previous to current problem
tr1 -62.6 -24083.0 0.0
c read source file
ssr old=31.1 31.3 33.5 new=31.1 31.3 31.5 tr=1
c neutron dose conversion factors (mrem/h)/(n/cm^2-s)
c from MCNP Manual, ANSI/ANS-6.1.1-1977
DE0 LOG 2.5-8 1.0-7 1.0-6 1.0-5 1.0-4 1.0-3 1.0-2 1.0-1
5.0-1 1.0 2.5 5.0 7.0 10.0 14.0 20.0
DF0 LOG 3.67-3 3.67-3 4.46-3 4.54-3 4.18-3 3.76-3 3.56-3 2.17-2
9.26-2 1.32-1 1.25-1 1.56-1 1.47-1 1.47-1 2.08-1 2.27-1
c Energy bins for tally (same as for source energy groups)
e0 0.0 0.015 0.111 0.408 0.907 1.42 1.83 3.01 6.38 20.0
c Mesh tally
fmesh4:n geom=xyz origin=-15378.8 -24326.84 -77.7875
imesh=-0.1 0.0 2000.0 10000.0 50000.0
iints=15 1 10 20 40
jmesh=-0.1 0.0 20000.0
jints=5 1 20
kmesh=166.0 $8 ft off ground for personnel height
kints=1
fm4 7.464E+09 $total source strength for 15,000 cylinders (n/s)
c
ctme 150.0
print

```

G.2.3 Input File *t100x100p01.txt*

```

Dose Rates from Multiple Filled 48Y Feed Cylinder
c file t100x100p01 (30,000 cylinders total - 101x100, 100x100 & 99x100)
c 101x100, 100x100 & 99x100 array - double stack
c reflective bounday at Y mid-plane (i.e., 15,000 cylinders modeled)
c Photon - homogenized source geometry - ANSI/ANS-6.1.1-1977
c center-to-center spacing=5' (radial) & 16' (axial)
c lattice center element at far right
c 1st step calculation to tally surface sources
c include built-in directional biasing (a=1)
c

```

```

c CELL CARDS
c
11 1 -2.897 -11 u=1 imp:p=1 $Inside of cylinder (UF6)
12 2 -7.8500 11 -12 u=1 imp:p=4 $Steel shell
13 3 -0.0012 12 u=1 imp:p=6 $External to cylinder
14 0 -13 fill=1 lat=1 u=2 imp:p=6 $Infinite lattice for
stack
15 0 -31 fill=2 imp:p=6 $Box to fill bottom stack
16 like 14 but trcl=(-76.2 0 125.095) u=3 imp:p=6 $Infinite lattice for mid
stack
17 0 -32 fill=3 imp:p=6 $Box to fill mid stack
18 like 14 but trcl=(-152.4 0 250.190) u=4 imp:p=6 $Infinite lattice for top
stack
19 0 -33 fill=4 imp:p=6 $Box to fill top stack
c
20 3 -0.0012 -34 31 32 33 imp:p=6 $Box to contain all
cylinders
21 3 -0.0012 41 -42 43 -44 46 -47 34 imp:p=6 $Air space
22 4 -1.60 41 -42 43 -44 45 -46 imp:p=1 $Ground soil
23 0 -41:42:-43:44:-45:47 imp:p=0 $Outer void

c
c SURFACE CARDS
c
11 rcc 0.0 -184.7850 0.0 0.0 369.570 0.0 60.9600 $UF6 cylinder
12 rcc 0.0 -186.3725 0.0 0.0 372.745 0.0 62.5475 $steel cylinder
13 rpp -76.2 76.2 -243.84 243.84 -62.5475 62.5475 $unit box
c Box to fill cylinders (bottom stack - 101x50 cylinders with reflective
boundary)
31 rpp -15316.2 62.6 -243.84 24083.0 -62.5475 62.5475
c Box to fill cylinders (mid stack - 100x50 cylinders)
32 rpp -15240.0 0.0 -243.84 24083.0 62.5475 187.6425
c Box to fill cylinders (top stack - 99x50 cylinders)
33 rpp -15163.8 -76.2 -243.84 24083.0 187.6425 312.8
c Box to contain all cylinders
34 rpp -15316.2 62.6 -243.84 24083.0 -77.7875 312.8
c Air box
41 px -15320.0 $-X boundary
42 px 20000.0 $+X boundary
43* py -244.0 $-Y boundary (reflective)
44 py 44000.0 $+Y boundary
45 pz -108.0 $-Z boundary (soil bottom)
46 pz -77.7875 $ground Z level or soil top
47 pz 20000.0 $+Z boundary
48 pz -62.5475 $bottom of cylinder

c
c DATA CARDS
c
m1 9019 6.00 92238 0.9928 92235 0.0072 $ UF6
m2 26000 1.00 $ Iron
m3 6000 -0.00014 7014 -0.75521 8016 -0.23177 $ Air
18000 -0.01288
m4 8016 -0.465 11023 -0.0245 13027 -0.080 $ Ground bulk soil
12000 -0.015 14000 -0.290 19000 -0.0225
20000 -0.040 26000 -0.060
phys:p 10 $ detailed physics, brems., coherent
mode p
c Write surface source file
ssw 31.1 31.3 33.5

```

```

c Source definition card with the following distributions:
c d1=distribution #1 for selection of the cell (i.e., cylinder)
c d2=distribution #2 for selection of x position
c d3=distribution #3 for selection of y position
c d4=distribution #4 for selection of z position
c d5=distribution #5 for photon source energy spectrum
c d6=distribution #6 for directional biasing w.r.t. +x axis
sdef cel=d1 x=d2 y=d3 z=d4 erg=d5 vec=1 0 0 dir=d6
sil 1 (-11<14[-100:0 0:49 0:0]<15) $cell information
(101x50 - bottom)
(-11<16[-99:0 0:49 0:0]<17) $cell information
(100x50 - mid)
(-11<18[-98:0 0:49 0:0]<19) $cell information (99x50
- top)
spl 1 14999r $cell unbiased
probability (equal)
c Biased source sampling probability based on MAVRIC-generated data (relative
to 1)
c MAVRIC biased sampling probability (101 or 100 or 99 cylinders/row in X
direction)
sb1 1.0E-03 81r 1.1E-03 $row 1 - bot
1.3E-03 1.5E-03 1.7E-03 2.0E-03 2.3E-03 2.7E-03
3.1E-03 3.5E-03 4.1E-03 4.8E-03 5.6E-03 6.8E-03
8.6E-03 1.2E-02 1.7E-02 2.8E-02 8.6E-02 9.9E-01
1.0E-03 81r 1.1E-03 $row 2 - bot
1.3E-03 1.5E-03 1.7E-03 2.0E-03 2.3E-03 2.7E-03
3.1E-03 3.5E-03 4.1E-03 4.8E-03 5.6E-03 6.8E-03
8.6E-03 1.2E-02 1.7E-02 2.8E-02 8.6E-02 9.9E-01
1.0E-03 81r 1.1E-03 $row 3 - bot
1.3E-03 1.5E-03 1.7E-03 2.0E-03 2.3E-03 2.7E-03
3.1E-03 3.5E-03 4.1E-03 4.8E-03 5.6E-03 6.8E-03
8.6E-03 1.2E-02 1.7E-02 2.8E-02 8.6E-02 9.9E-01
1.0E-03 81r 1.1E-03 $row 4 - bot
1.3E-03 1.5E-03 1.7E-03 2.0E-03 2.3E-03 2.7E-03
3.1E-03 3.5E-03 4.1E-03 4.8E-03 5.6E-03 6.8E-03
8.6E-03 1.2E-02 1.7E-02 2.8E-02 8.6E-02 9.9E-01
1.0E-03 81r 1.1E-03 $row 5 - bot
1.3E-03 1.5E-03 1.7E-03 2.0E-03 2.3E-03 2.7E-03
3.1E-03 3.5E-03 4.1E-03 4.8E-03 5.6E-03 6.8E-03
8.6E-03 1.2E-02 1.7E-02 2.8E-02 8.6E-02 9.9E-01
1.0E-03 81r 1.1E-03 $row 6 - bot
1.3E-03 1.5E-03 1.7E-03 2.0E-03 2.3E-03 2.7E-03
3.1E-03 3.5E-03 4.1E-03 4.8E-03 5.6E-03 6.8E-03
8.6E-03 1.2E-02 1.7E-02 2.8E-02 8.6E-02 9.9E-01
1.0E-03 81r 1.1E-03 $row 7 - bot
1.3E-03 1.5E-03 1.7E-03 2.0E-03 2.3E-03 2.7E-03
3.1E-03 3.5E-03 4.1E-03 4.8E-03 5.6E-03 6.8E-03
8.6E-03 1.2E-02 1.7E-02 2.8E-02 8.6E-02 9.9E-01
1.0E-03 81r 1.1E-03 $row 8 - bot
1.3E-03 1.5E-03 1.7E-03 2.0E-03 2.3E-03 2.7E-03
3.1E-03 3.5E-03 4.1E-03 4.8E-03 5.6E-03 6.8E-03
8.6E-03 1.2E-02 1.7E-02 2.8E-02 8.6E-02 9.9E-01
1.0E-03 81r 1.1E-03 $row 9 - bot
1.3E-03 1.5E-03 1.7E-03 2.0E-03 2.3E-03 2.7E-03
3.1E-03 3.5E-03 4.1E-03 4.8E-03 5.6E-03 6.8E-03
8.6E-03 1.2E-02 1.7E-02 2.8E-02 8.6E-02 9.9E-01
1.0E-03 81r 1.1E-03 $row 10 - bot
1.3E-03 1.5E-03 1.7E-03 2.0E-03 2.3E-03 2.7E-03
3.1E-03 3.5E-03 4.1E-03 4.8E-03 5.6E-03 6.8E-03
8.6E-03 1.2E-02 1.7E-02 2.8E-02 8.6E-02 9.9E-01

```


7.8E-02	9.1E-02	1.1E-01	1.3E-01	2.0E-01	1.0E+00	
1.0E-03	61r	1.1E-03				\$row 44 - top
1.2E-03	1.4E-03	1.6E-03	1.8E-03	2.0E-03	2.2E-03	
2.5E-03	2.8E-03	3.2E-03	3.7E-03	4.3E-03	5.0E-03	
5.8E-03	6.7E-03	7.7E-03	8.9E-03	1.0E-02	1.2E-02	
1.4E-02	1.6E-02	1.8E-02	2.1E-02	2.4E-02	2.8E-02	
3.3E-02	3.8E-02	4.3E-02	5.0E-02	5.8E-02	6.7E-02	
7.8E-02	9.1E-02	1.1E-01	1.3E-01	2.0E-01	1.0E+00	
1.0E-03	61r	1.1E-03				\$row 45 - top
1.2E-03	1.4E-03	1.6E-03	1.8E-03	2.0E-03	2.2E-03	
2.5E-03	2.8E-03	3.2E-03	3.7E-03	4.3E-03	5.0E-03	
5.8E-03	6.7E-03	7.7E-03	8.9E-03	1.0E-02	1.2E-02	
1.4E-02	1.6E-02	1.8E-02	2.1E-02	2.4E-02	2.8E-02	
3.3E-02	3.8E-02	4.3E-02	5.0E-02	5.8E-02	6.7E-02	
7.8E-02	9.1E-02	1.1E-01	1.3E-01	2.0E-01	1.0E+00	
1.0E-03	61r	1.1E-03				\$row 46 - top
1.2E-03	1.4E-03	1.6E-03	1.8E-03	2.0E-03	2.2E-03	
2.5E-03	2.8E-03	3.2E-03	3.7E-03	4.3E-03	5.0E-03	
5.8E-03	6.7E-03	7.7E-03	8.9E-03	1.0E-02	1.2E-02	
1.4E-02	1.6E-02	1.8E-02	2.1E-02	2.4E-02	2.8E-02	
3.3E-02	3.8E-02	4.3E-02	5.0E-02	5.8E-02	6.7E-02	
7.8E-02	9.1E-02	1.1E-01	1.3E-01	2.0E-01	1.0E+00	
1.0E-03	61r	1.1E-03				\$row 47 - top
1.2E-03	1.4E-03	1.6E-03	1.8E-03	2.0E-03	2.2E-03	
2.5E-03	2.8E-03	3.2E-03	3.7E-03	4.3E-03	5.0E-03	
5.8E-03	6.7E-03	7.7E-03	8.9E-03	1.0E-02	1.2E-02	
1.4E-02	1.6E-02	1.8E-02	2.1E-02	2.4E-02	2.8E-02	
3.3E-02	3.8E-02	4.3E-02	5.0E-02	5.8E-02	6.7E-02	
7.8E-02	9.1E-02	1.1E-01	1.3E-01	2.0E-01	1.0E+00	
1.0E-03	61r	1.1E-03				\$row 48 - top
1.2E-03	1.4E-03	1.6E-03	1.8E-03	2.0E-03	2.2E-03	
2.5E-03	2.8E-03	3.2E-03	3.7E-03	4.3E-03	5.0E-03	
5.8E-03	6.7E-03	7.7E-03	8.9E-03	1.0E-02	1.2E-02	
1.4E-02	1.6E-02	1.8E-02	2.1E-02	2.4E-02	2.8E-02	
3.3E-02	3.8E-02	4.3E-02	5.0E-02	5.8E-02	6.7E-02	
7.8E-02	9.1E-02	1.1E-01	1.3E-01	2.0E-01	1.0E+00	
1.0E-03	61r	1.1E-03				\$row 49 - top
1.2E-03	1.4E-03	1.6E-03	1.8E-03	2.0E-03	2.2E-03	
2.5E-03	2.8E-03	3.2E-03	3.7E-03	4.3E-03	5.0E-03	
5.8E-03	6.7E-03	7.7E-03	8.9E-03	1.0E-02	1.2E-02	
1.4E-02	1.6E-02	1.8E-02	2.1E-02	2.4E-02	2.8E-02	
3.3E-02	3.8E-02	4.3E-02	5.0E-02	5.8E-02	6.7E-02	
7.8E-02	9.1E-02	1.1E-01	1.3E-01	2.0E-01	1.0E+00	
1.0E-03	61r	1.1E-03				\$row 50 - top
1.2E-03	1.4E-03	1.6E-03	1.8E-03	2.0E-03	2.2E-03	
2.5E-03	2.8E-03	3.2E-03	3.7E-03	4.3E-03	5.0E-03	
5.8E-03	6.7E-03	7.7E-03	8.9E-03	1.0E-02	1.2E-02	
1.4E-02	1.6E-02	1.8E-02	2.1E-02	2.4E-02	2.8E-02	
3.3E-02	3.8E-02	4.3E-02	5.0E-02	5.8E-02	6.7E-02	
7.8E-02	9.1E-02	1.1E-01	1.3E-01	2.0E-01	1.0E+00	
si2	-60.96	60.96				\$source position in x for center element
sp2	0.0	1.0				\$equal weighting along x
si3	-184.7850	184.7850				\$source position in y for center element
sp3	0.0	1.0				\$equal weighting along y
si4	-60.96	60.96				\$source position in z for center element
sp4	0.0	1.0				\$equal weighting along z
c	Photon Spectrum (partial from SCALE 19 groups)					
c	si5 - energy boundary information					
c	sp5 - unbiased energy spectrum					
c	sb5 - biased energy spectrum based on dose response					


```

c vertical input format used for si5, sp5 and sb5
#   si5      sp5      sb5
   4.50E-02  0.0      0.0
   1.00E-01  5.232E-01  7.933E-05
   2.00E-01  2.795E-01  1.494E-03
   3.00E-01  6.343E-02  1.378E-02
   4.00E-01  4.056E-02  3.645E-02
   6.00E-01  2.785E-02  8.181E-02
   8.00E-01  2.746E-02  1.927E-01
   1.00E+00  2.120E-02  2.608E-01
   1.33E+00  1.266E-02  2.593E-01
   1.66E+00  1.885E-03  5.885E-02
   2.00E+00  2.275E-03  9.479E-02
c Directional sampling with bias for forward direction
si6  -1.0  1.0      $direction cosine from -1 to 1
sb6  -31  1      $biased directional distribution for sampling
c ANSI/ANS-6.1.1-1977 photon dose conversion factors (mrem/h)/(photon/cm^2-s)
de0  LOG    0.01  0.03  0.05  0.07  0.1  0.15  0.2
      0.25  0.3  0.35  0.4  0.45  0.5  0.55  0.6
      0.65  0.7  0.8  1.0  1.4  1.8  2.2  2.6
      2.8  3.25  3.75  4.25  4.75  5.0  5.25  5.75
      6.25  6.75  7.5  9.0  11.0  13.0  15.0
df0  LOG    3.96-3  5.82-4  2.90-4  2.58-4  2.83-4  3.79-7  5.01-4
      6.31-4  7.59-4  8.78-4  9.85-4  1.08-3  1.17-3  1.27-3  1.36-3
      1.44-3  1.52-3  1.68-3  1.98-3  2.51-3  2.99-3  3.42-3  3.82-3
      4.01-3  4.41-3  4.83-3  5.23-3  5.60-3  5.80-3  6.01-3  6.37-3
      6.74-3  7.11-3  7.66-3  8.77-3  1.03-2  1.18-2  1.33-2
c Energy bins for tally (same as for source energy groups)
e0  0.0
     4.50E-02
     1.00E-01
     2.00E-01
     3.00E-01
     4.00E-01
     6.00E-01
     8.00E-01
     1.00E+00
     1.33E+00
     1.66E+00
     2.00E+00
f2:p  31.1 31.3 33.5  $average dose rate on these facets
fm2  6.231E+14      $total source strength for 15,000 cylinders (p/s)
c
ctme  300.0
print

```

G.2.4 Input File *t100x100p02.txt*

Dose Rates from Multiple Filled 48Y Feed Cylinder

```

c file t100x100p02 (30,000 cylinders total)
c 101x100, 100x100 & 99x100 array - triple stack
c reflective bounday at Y mid-plane (i.e., 15,000 cylinders modeled)
c Photon - homogenized source geometry - ANSI/ANS-6.1.1-1977
c center-to-center spacing=5' (radial) & 16' (axial)
c 2nd step calculation with mesh tally
c
21  0      -31  32      imp:p=1  $Box around cylinders

```

```

22      0          -32          imp:p=0  $Black box for all
cylinders
23      3  -0.0012  41 -50 43 -44 46 -47 31 imp:p=1  $Air space
24      4  -1.60    41 -50 43 -44 45 -46    imp:p=1  $Ground soil
25      0          -41:42:-43:44:-45:47    imp:p=0  $Outer void
c Air importance cells
51      3  -0.0012  50 -51 43 -44 46 -47    imp:p=1  $1st air cell
52      3  -0.0012  51 -52 43 -44 46 -47    imp:p=3  $2nd air cell
53      3  -0.0012  52 -53 43 -44 46 -47    imp:p=9  $3rd air cell
54      3  -0.0012  53 -54 43 -44 46 -47    imp:p=27 $4th air cell
55      3  -0.0012  54 -42 43 -44 46 -47    imp:p=81 $5th air cell
c Soil importance cells
61      4  -1.60    50 -51 43 -44 45 -46    imp:p=1  $1st soil cell
62      4  -1.60    51 -52 43 -44 45 -46    imp:p=1  $2nd soil cell
63      4  -1.60    52 -53 43 -44 45 -46    imp:p=3  $3rd soil cell
64      4  -1.60    53 -54 43 -44 45 -46    imp:p=9  $4th soil cell
65      4  -1.60    54 -42 43 -44 45 -46    imp:p=27 $5th soil cell

c
c Box to fill cylinders (triple stack - 15000 cylinders with reflective
boundary)
31      rpp -15378.8  0.0 -24326.84  0.0 -77.7875 312.8
c Black Box to contain all cylinders (to avoid round-off errors)
32      rpp -15378.8 -0.1 -24326.84 -0.1 -77.7875 312.7
c Air box
41      px -15380.0  $-X boundary
42      px  50000.0  $+X boundary
43*     py -24327.0  $-Y boundary (reflective)
44      py  30000.0  $+Y boundary
45      pz -108.0    $-Z boundary (soil bottom)
46      pz -77.7875 $ground level or soil top)
47      pz  30000.0  $+Z boundary
48      pz -62.5475 $bottom of cylinder
c Cell importance division plane
50      px  0.0
51      px 10000.0
52      px 20000.0
53      px 30000.0
54      px 40000.0

m1      9019  6.00    92238  0.9928  92235  0.0072  $ UF6
m2      26000 1.00
m3      6000 -0.00014  7014 -0.75521  8016 -0.23177  $ Air
        18000 -0.01288
m4      8016 -0.465  11023 -0.0245  13027 -0.080  $ Ground bulk soil
        12000 -0.015  14000 -0.290  19000 -0.0225
        20000 -0.040  26000 -0.060

phys:p 10          $ detailed physics, brems., coherent
mode p
c Coordinate transformation from previous to current problem
tr1     -62.6 -24083.0 0.0
c read source file
ssr     old=31.1 31.3 33.5 new=31.1 31.3 31.5 tr=1
c ANSI/ANS-6.1.1-1977 photon dose conversion factors (mrem/h)/(photon/cm^2-s)
de0     LOG  0.01  0.03  0.05  0.07  0.1  0.15  0.2
        0.25  0.3  0.35  0.4  0.45  0.5  0.55  0.6
        0.65  0.7  0.8  1.0  1.4  1.8  2.2  2.6
        2.8  3.25  3.75  4.25  4.75  5.0  5.25  5.75
        6.25  6.75  7.5  9.0  11.0  13.0  15.0
df0     LOG  3.96-3 5.82-4 2.90-4 2.58-4 2.83-4 3.79-7 5.01-4

```

```

6.31-4 7.59-4 8.78-4 9.85-4 1.08-3 1.17-3 1.27-3 1.36-3
1.44-3 1.52-3 1.68-3 1.98-3 2.51-3 2.99-3 3.42-3 3.82-3
4.01-3 4.41-3 4.83-3 5.23-3 5.60-3 5.80-3 6.01-3 6.37-3
6.74-3 7.11-3 7.66-3 8.77-3 1.03-2 1.18-2 1.33-2
c Energy bins for tally (same as for source energy group)
e0      0.0
        4.50E-02
        1.00E-01
        2.00E-01
        3.00E-01
        4.00E-01
        6.00E-01
        8.00E-01
        1.00E+00
        1.33E+00
        1.66E+00
        2.00E+00
fmesh4:p geom=xyz origin=-15378.8 -24326.84 -77.7875
        imesh=-0.1 0.0 2000.0 10000.0 50000.0
        iints=15  1  10  20  40
        jmesh=-0.1 0.0 20000.0
        jint=5  1  20
        kmesh=312.7 $top stack level
        kints=1
fm4      6.231E+14      $total source strength for 15,000 cylinders (p/s)
c
ctme     150.0
print

```

APPENDIX H MCNP DOSE RATE MAPS AND RELATIVE ERRORS

This appendix presents the neutron and photon dose rate maps and associated relative errors for different storage arrays and stacking of filled feed cylinders. The storage arrays include 10x10, 30x30 and 100x100 in one, two and three high. The neutron results are given in Figures H-1 through H-9, and the photon results are shown in Figures H-10 through H-18.

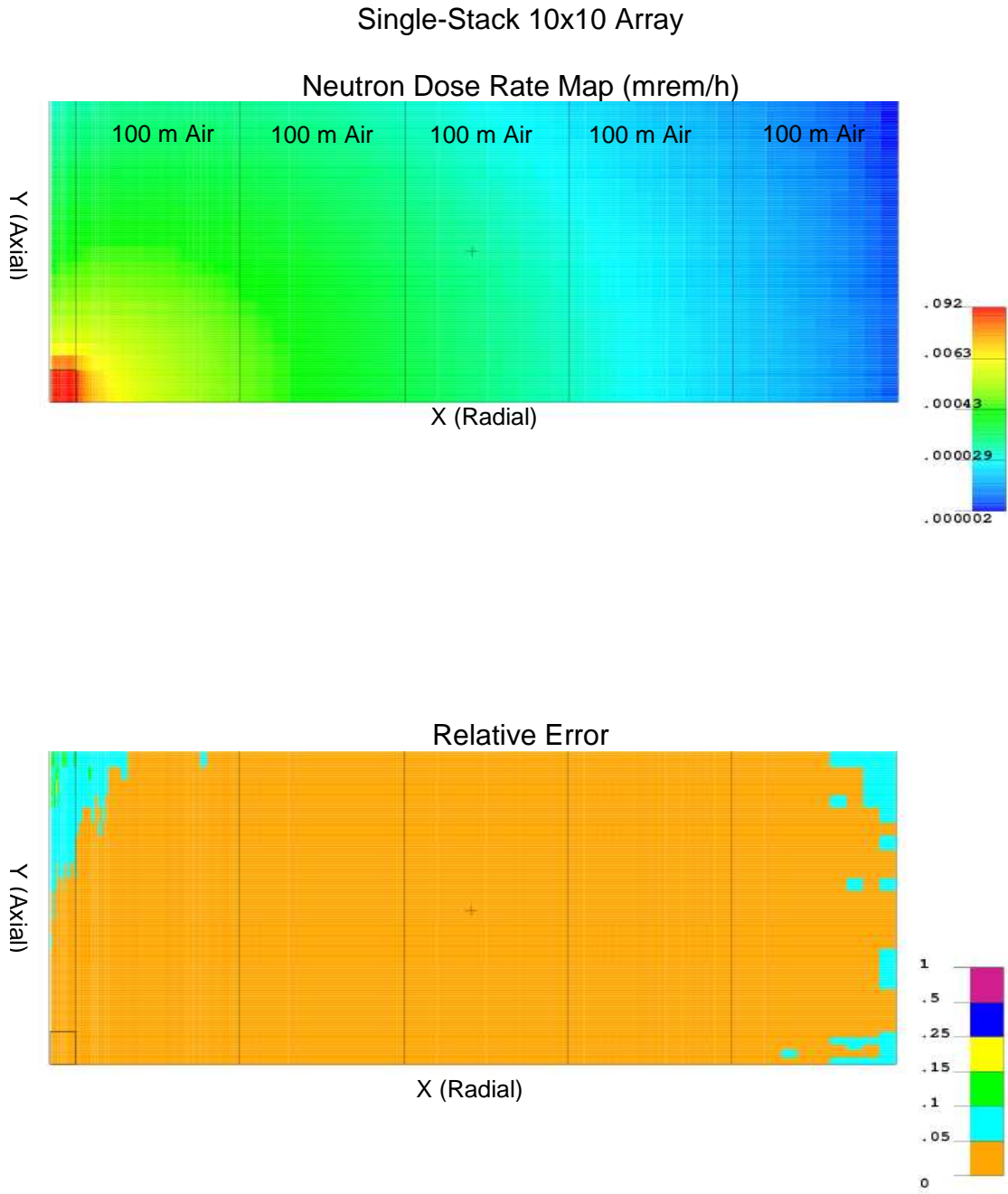
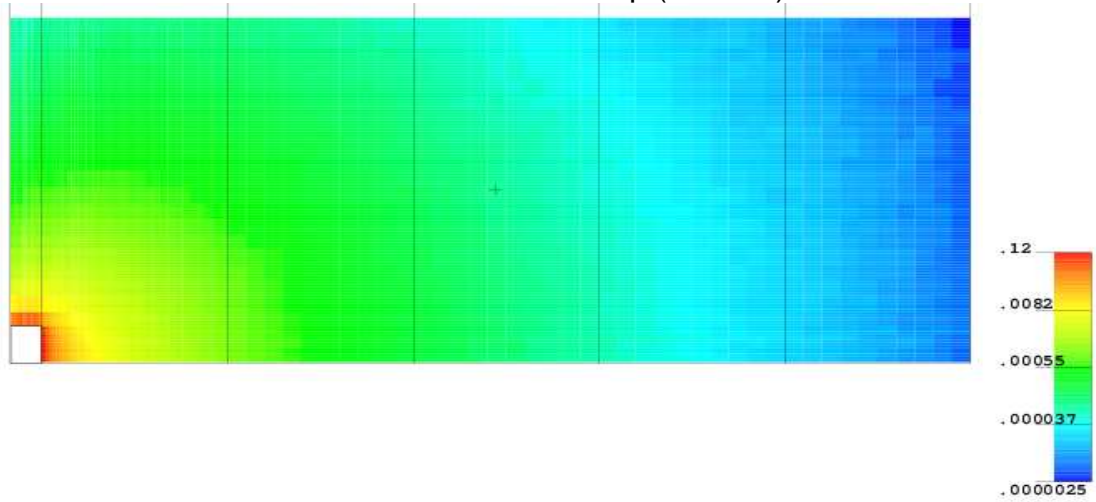


Figure H-1 Single-Stack 10x10 Array Neutron Dose Rate Map and Relative Error

Double-Stack 10x10 Array

Neutron Dose Rate Map (mrem/h)



Relative Error

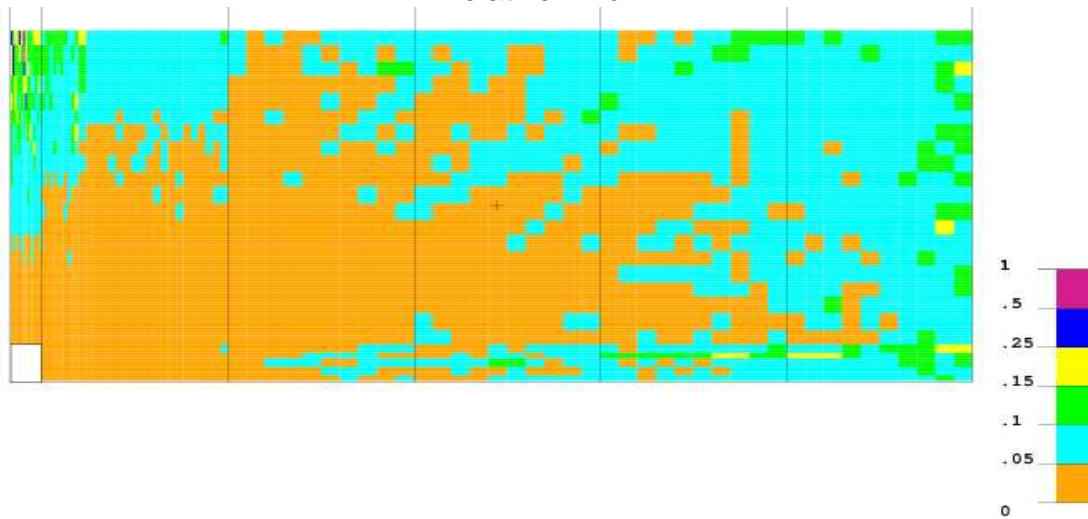
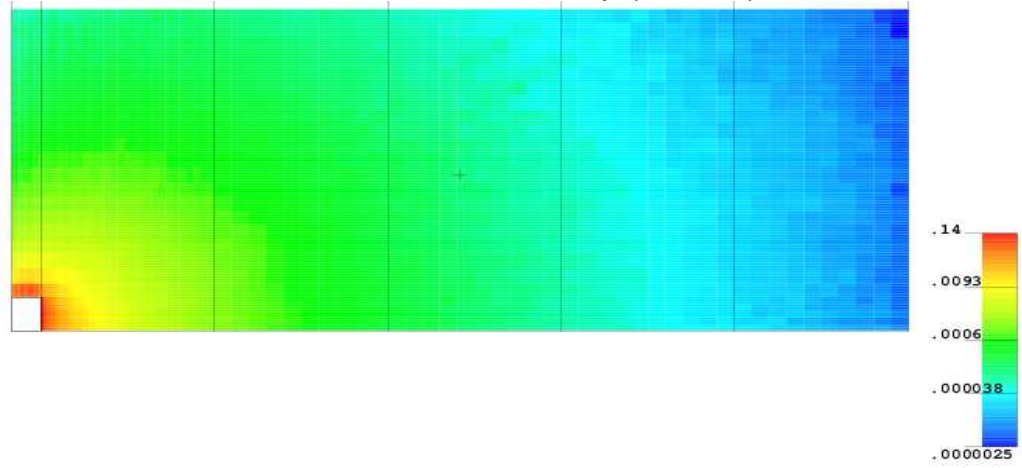


Figure H-2 Double-Stack 10x10 Array Neutron Dose Rate Map and Relative Error

Triple-Stack 10x10 Array

Neutron Dose Rate Map (mrem/h)



Relative Error

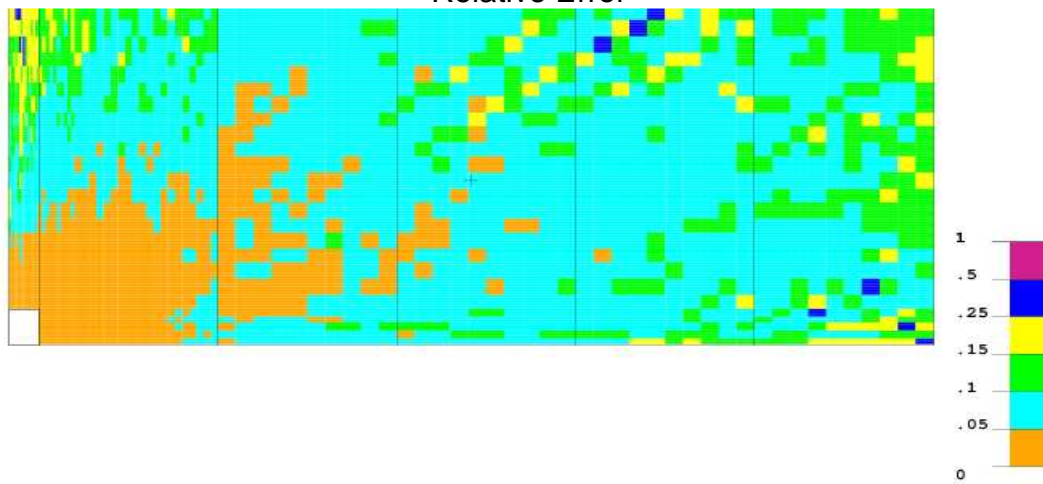
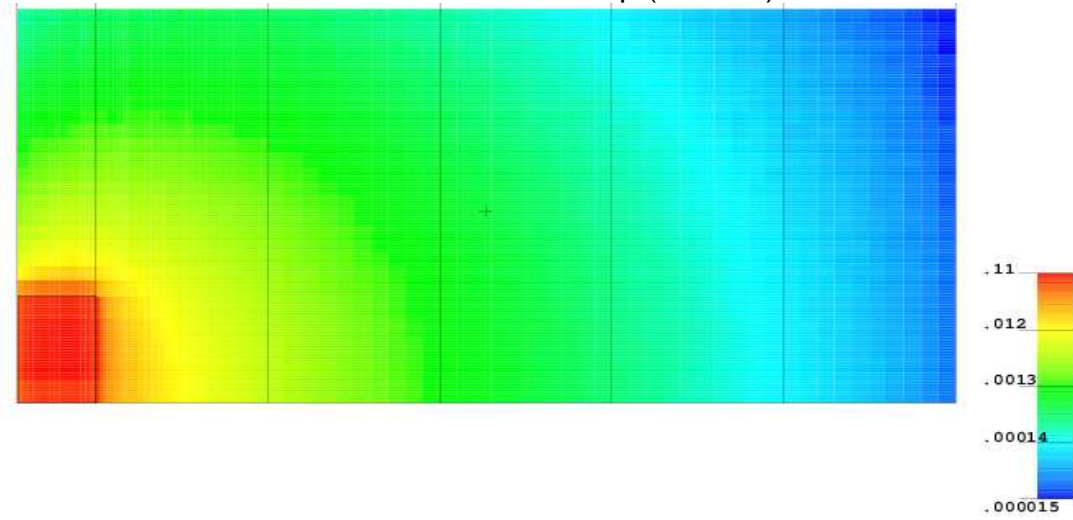


Figure H-3 Triple-Stack 10x10 Array Neutron Dose Rate Map and Relative Error

Single-Stack 30x30 Array

Neutron Dose Rate Map (mrem/h)



Relative Error

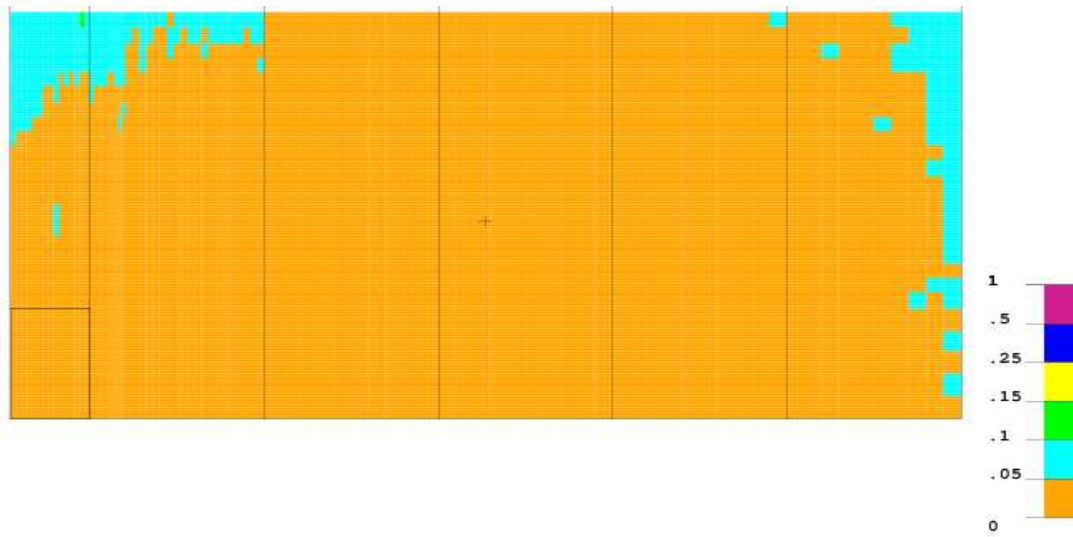
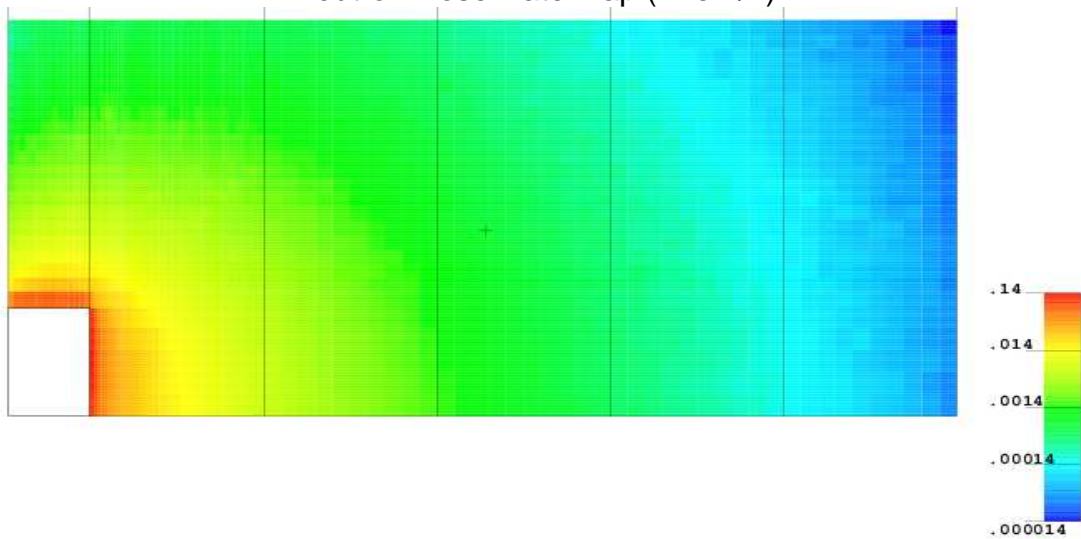


Figure H-4 Single-Stack 30x30 Array Neutron Dose Rate Map and Relative Error

Double-Stack 30x30 Array

Neutron Dose Rate Map (mrem/h)



Relative Error

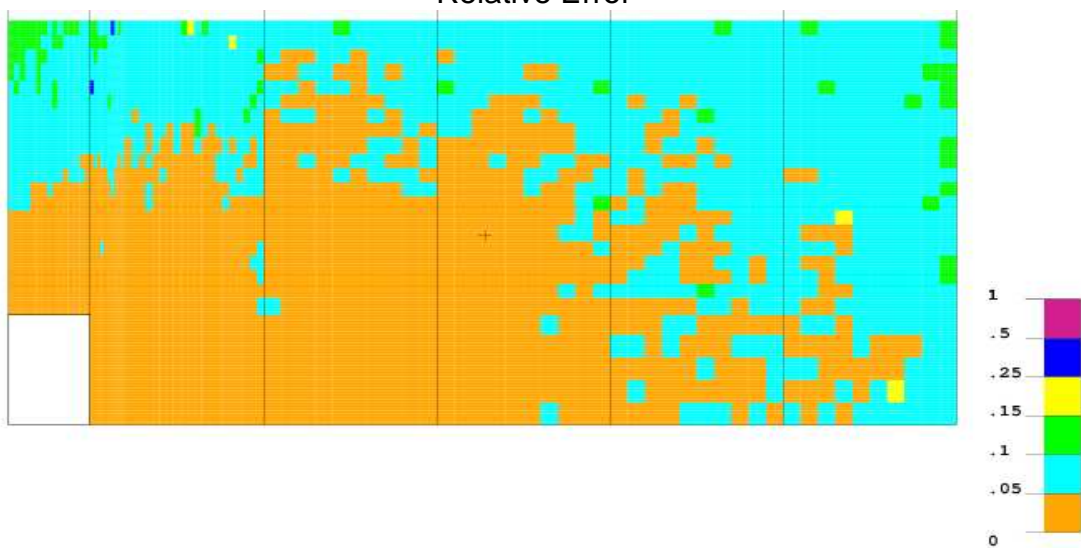
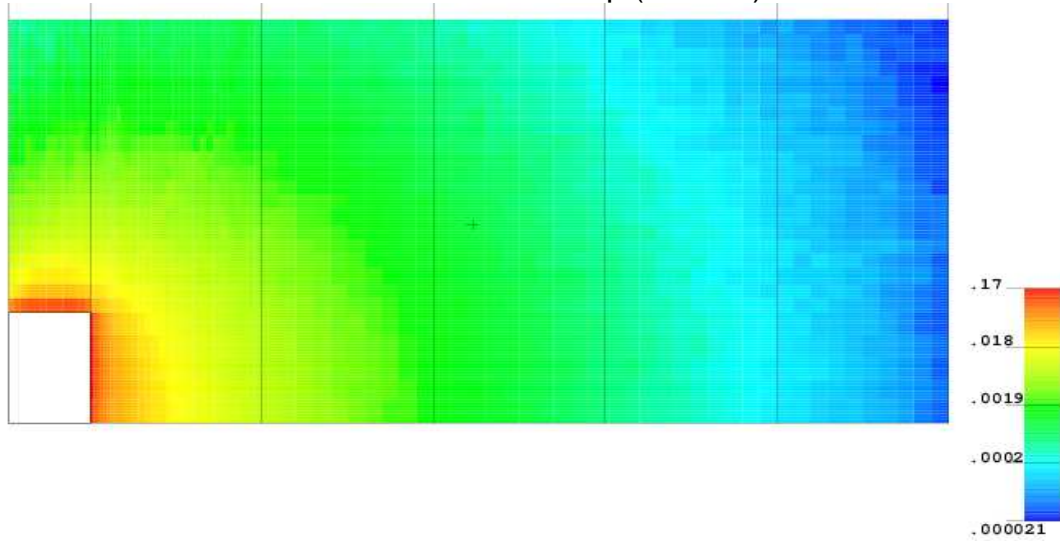


Figure H-5 Double-Stack 30x30 Array Neutron Dose Rate Map and Relative Error

Triple-Stack 30x30 Array

Neutron Dose Rate Map (mrem/h)



Relative Error

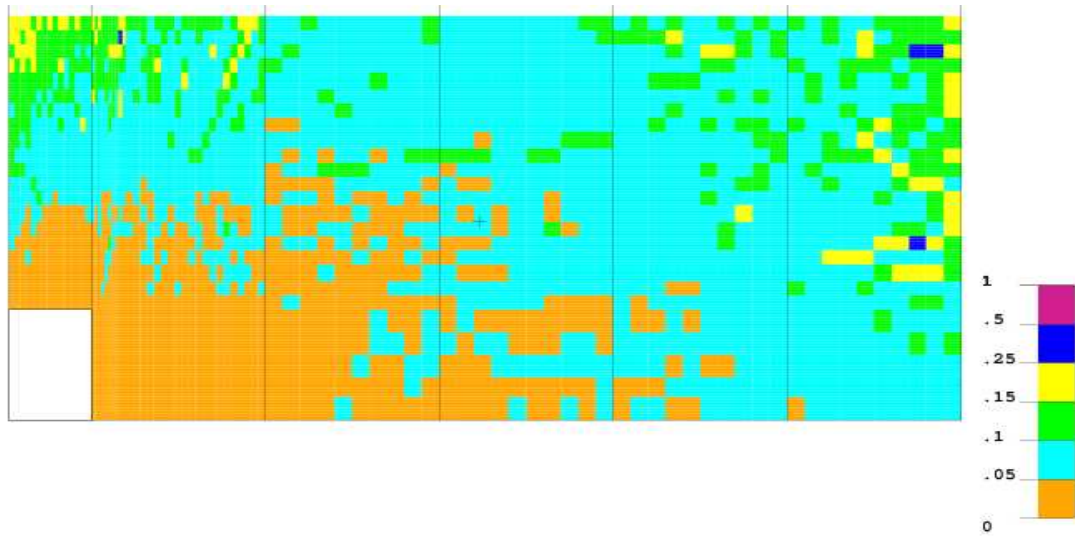
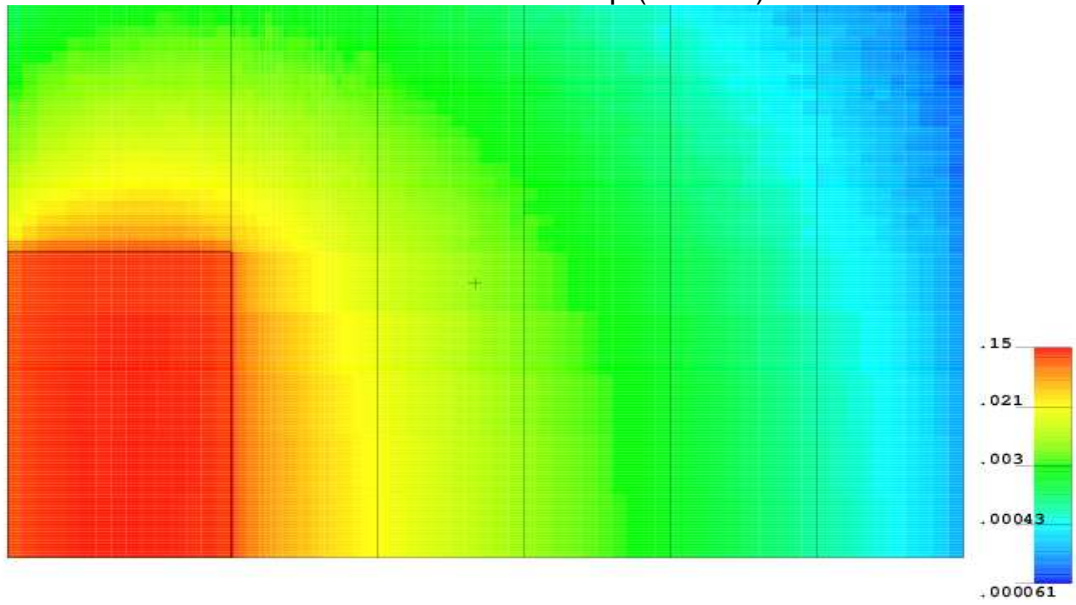


Figure H-6 Triple-Stack 30x30 Array Neutron Dose Rate Map and Relative Error

Single-Stack 100x100 Array

Neutron Dose Rate Map (mrem/h)



Relative Error

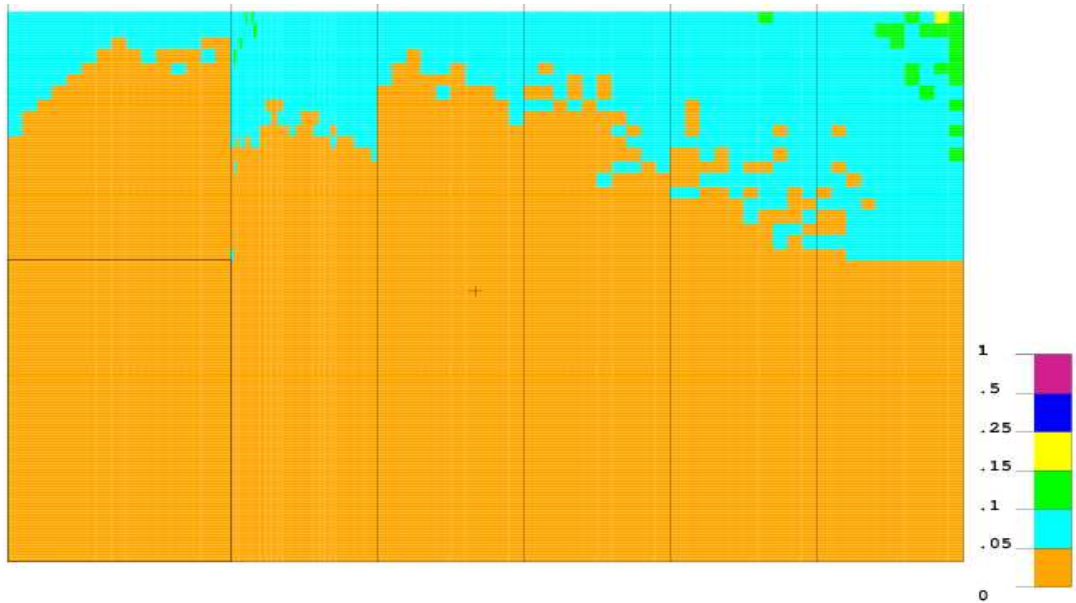
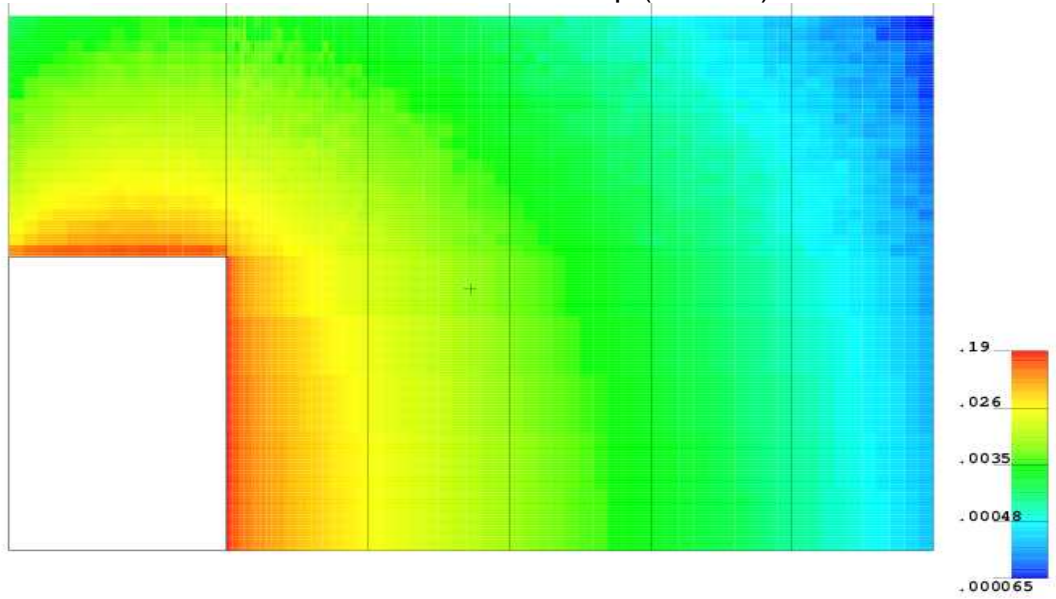


Figure H-7 Single-Stack 100x100 Array Neutron Dose Rate Map and Relative Error

Double-Stack 100x100 Array

Neutron Dose Rate Map (mrem/h)



Relative Error

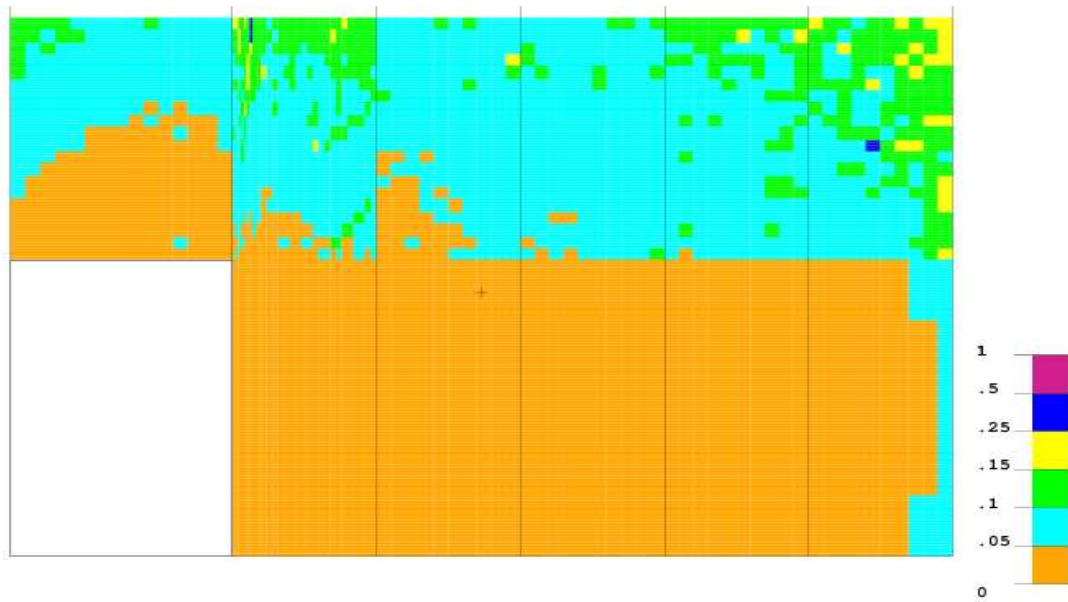
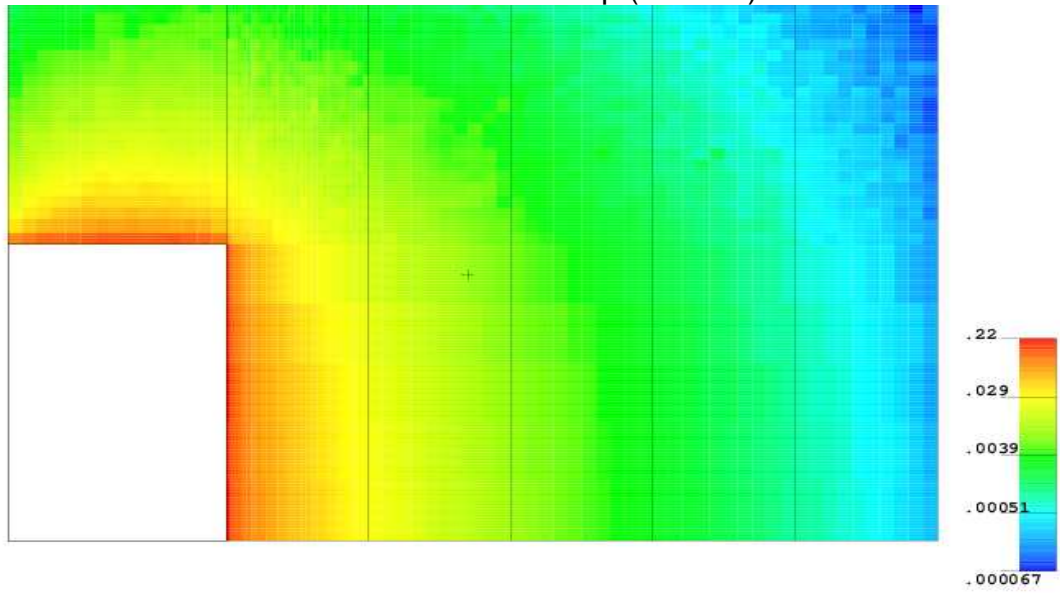


Figure H-8 Double-Stack 100x100 Array Neutron Dose Rate Map and Relative Error

Triple-Stack 100x100 Array

Neutron Dose Rate Map (mrem/h)



Relative Error

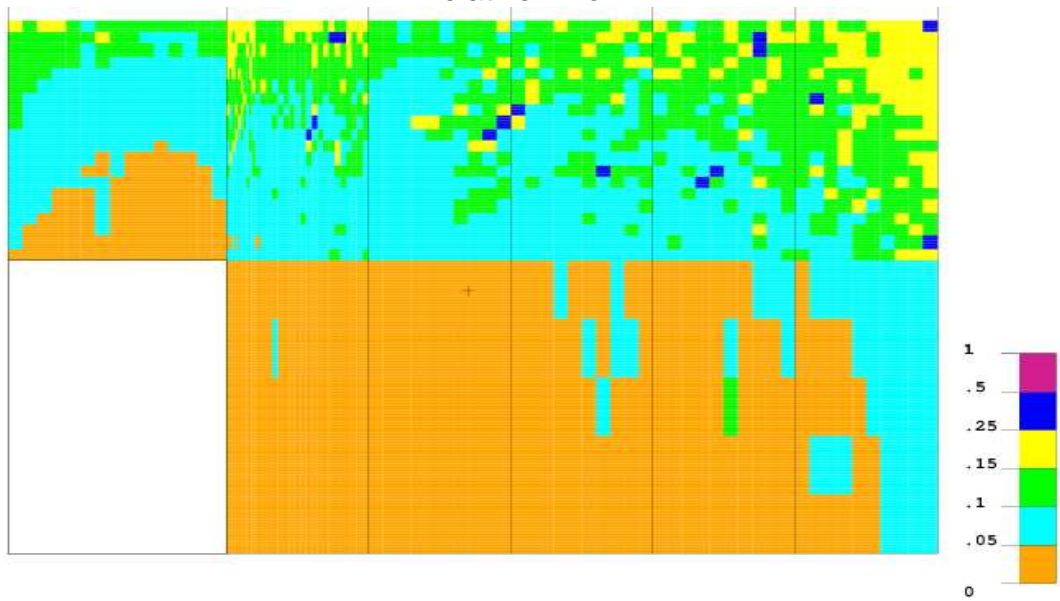


Figure H-9 Triple-Stack 100x100 Array Neutron Dose Rate Map and Relative Error

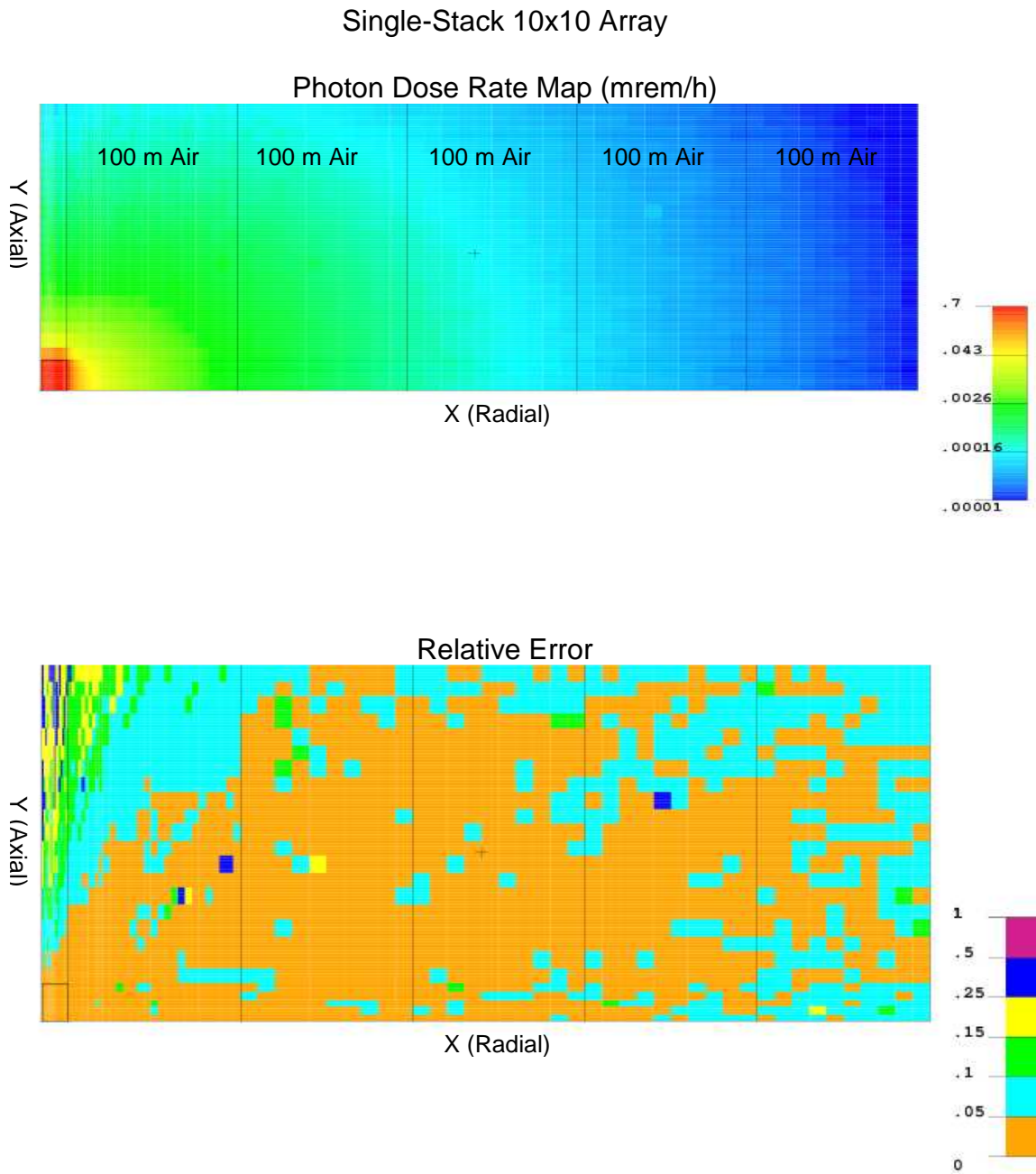
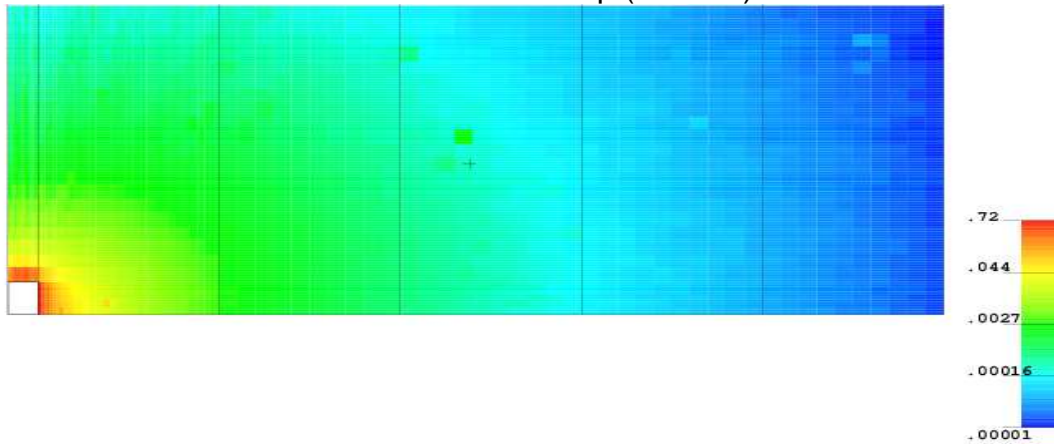


Figure H-10 Single-Stack 10x10 Array Photon Dose Rate Map and Relative Error

Double-Stack 10x10 Array

Photon Dose Rate Map (mrem/h)



Relative Error

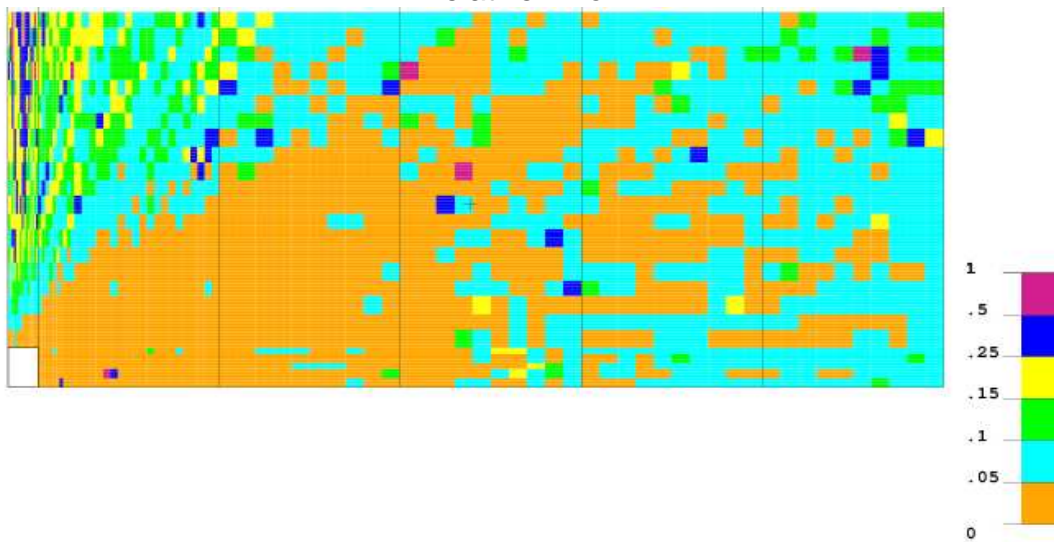
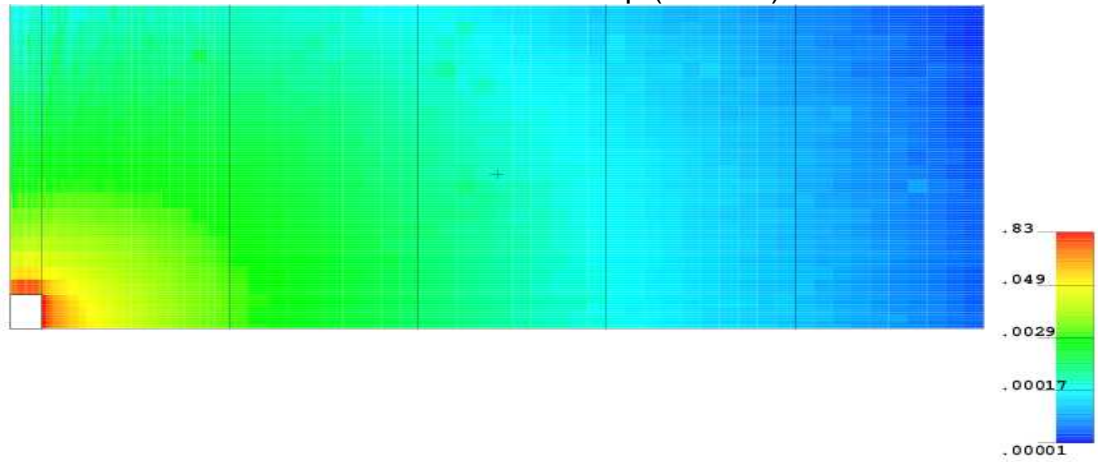


Figure H-11 Double-Stack 10x10 Array Photon Dose Rate Map and Relative Error

Triple-Stack 10x10 Array
Photon Dose Rate Map (mrem/h)



Relative Error

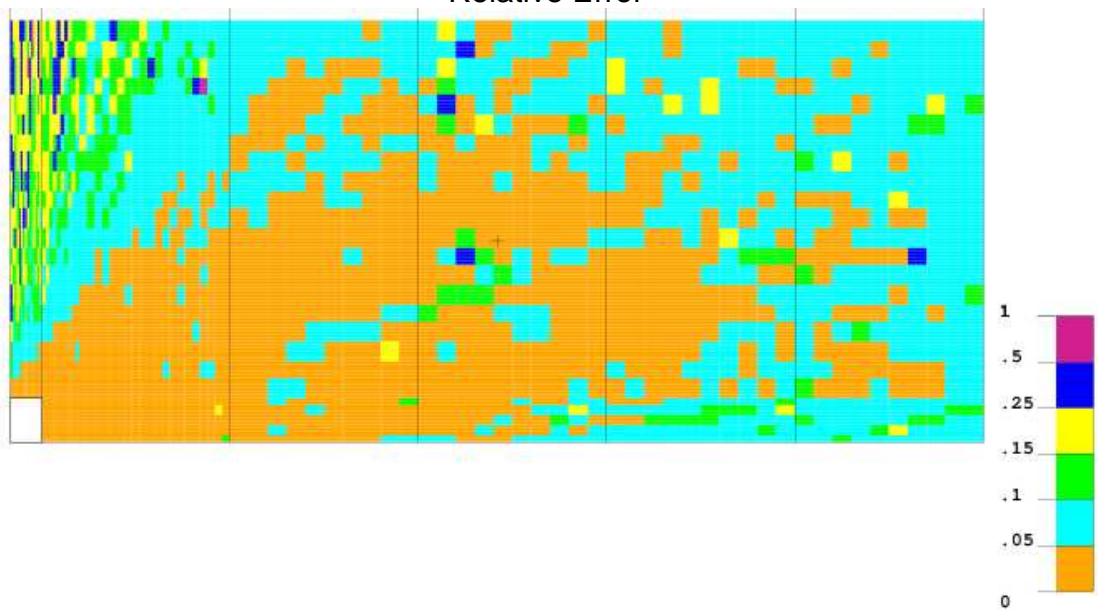
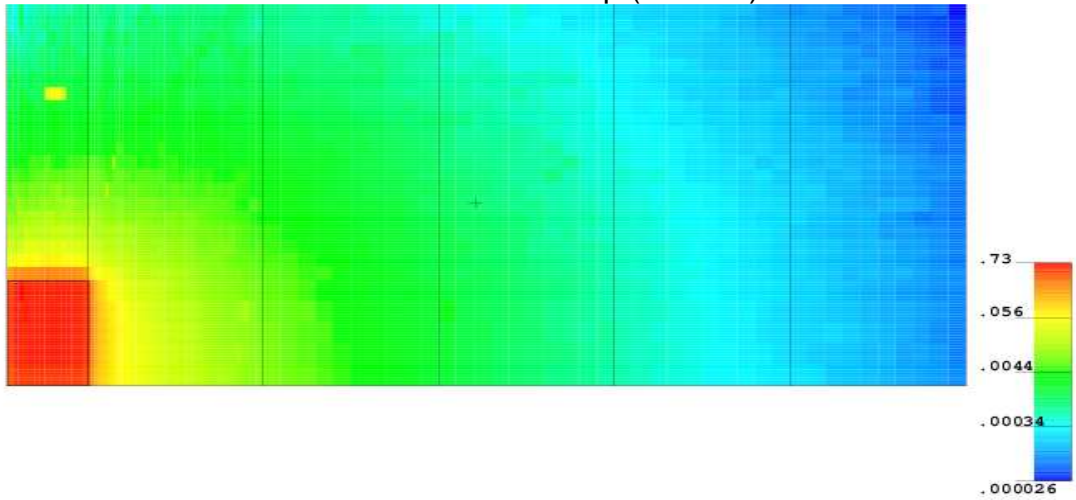


Figure H-12 Triple-Stack 10x10 Array Photon Dose Rate Map and Relative Error

Single-Stack 30x30 Array

Photon Dose Rate Map (mrem/h)



Relative Error

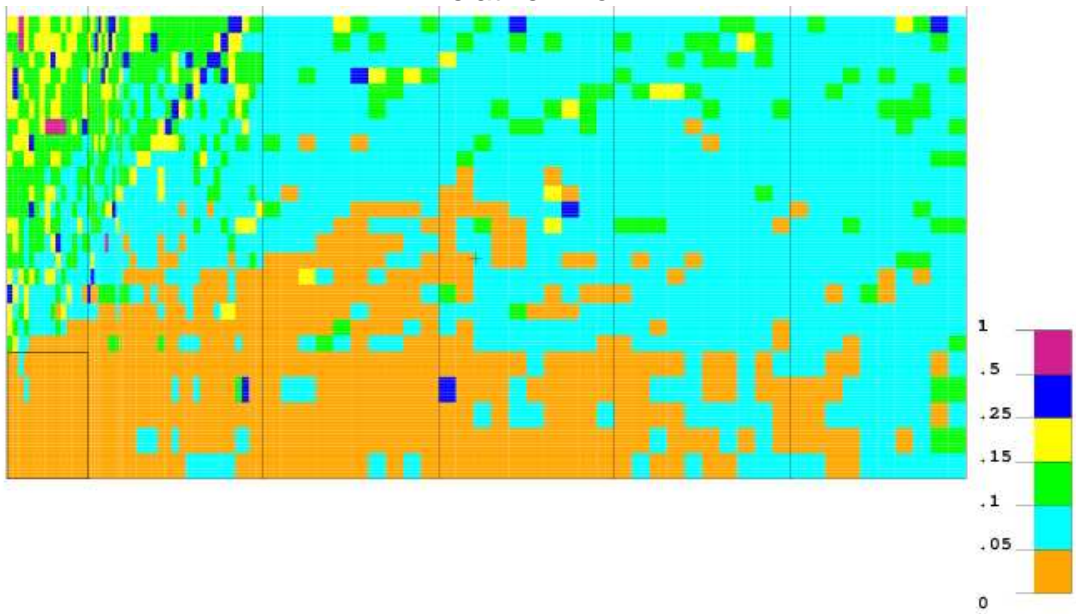
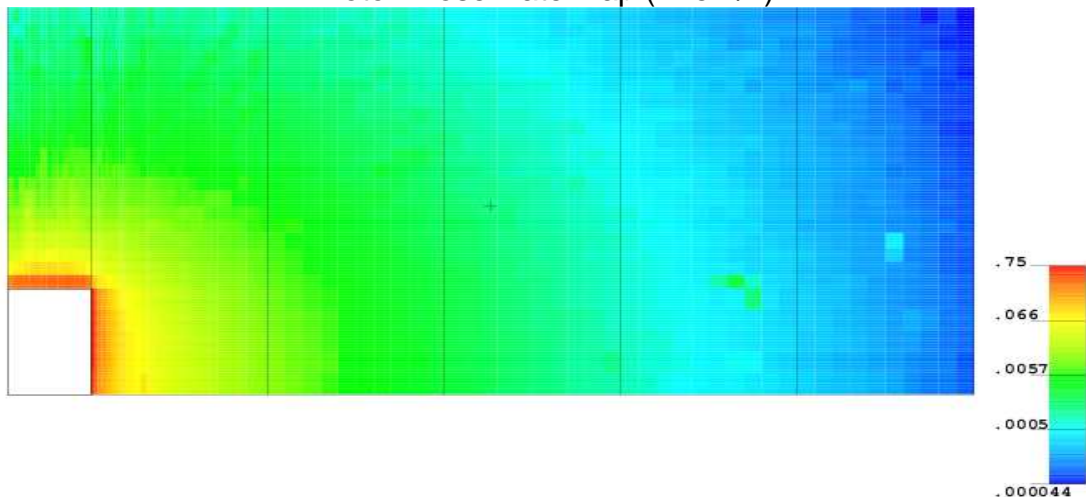


Figure H-13 Single-Stack 30x30 Array Photon Dose Rate Map and Relative Error

Double-Stack 30x30 Array

Photon Dose Rate Map (mrem/h)



Relative Error

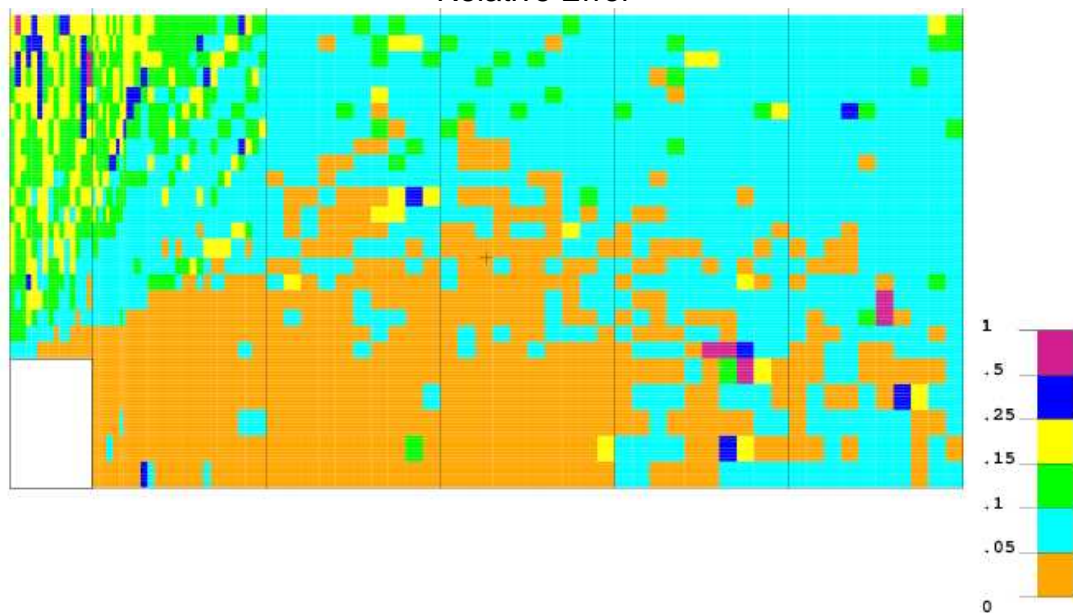
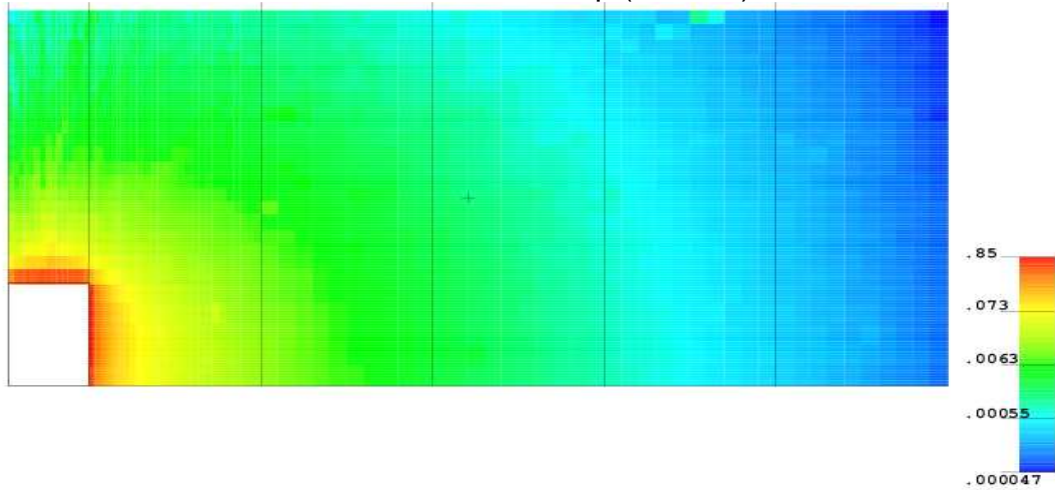


Figure H-14 Double-Stack 30x30 Array Photon Dose Rate Map and Relative Error

Triple-Stack 30x30 Array

Photon Dose Rate Map (mrem/h)



Relative Error

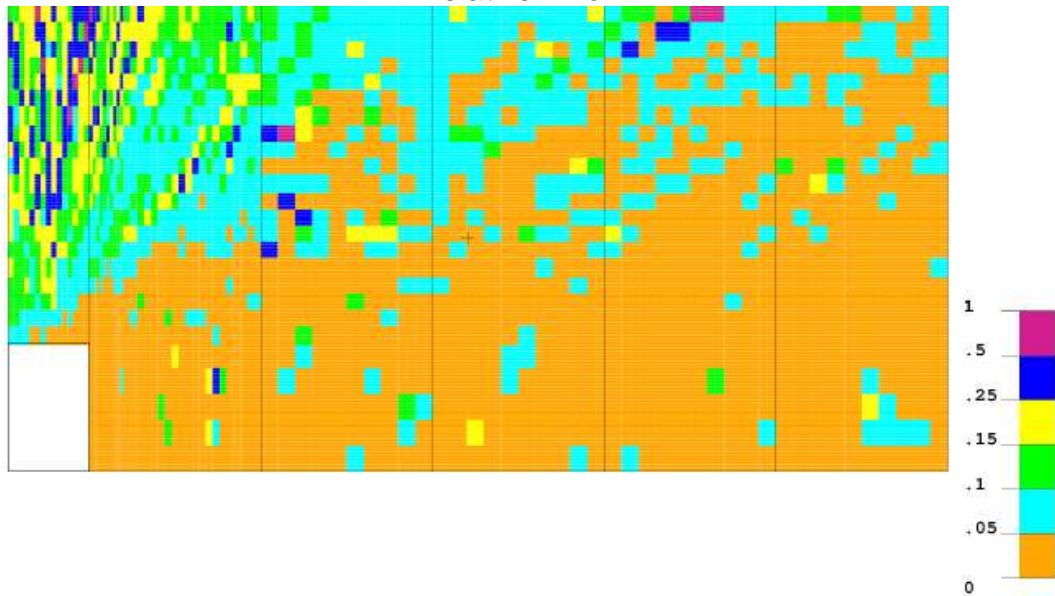
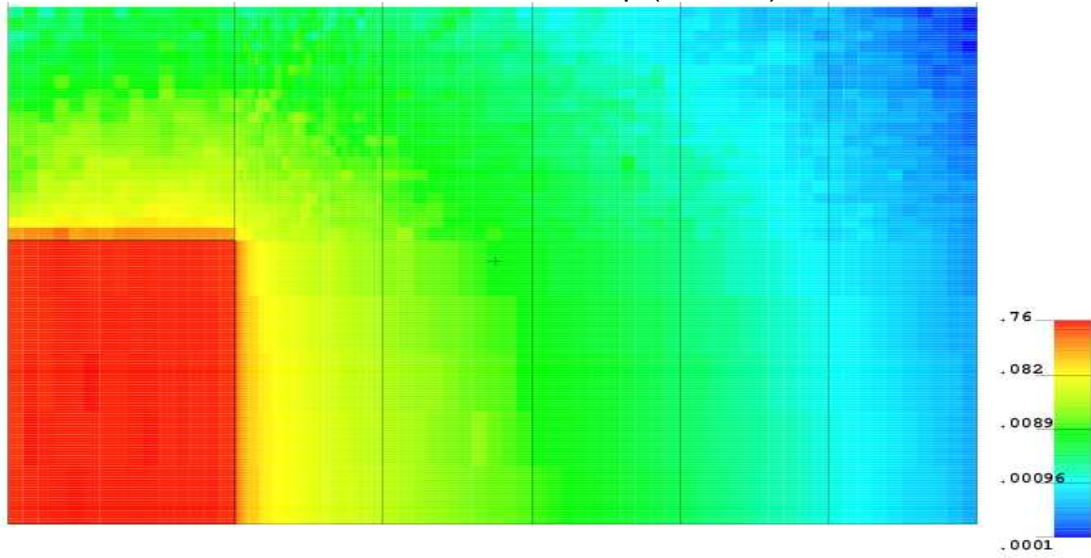


Figure H-15 Triple-Stack 30x30 Array Photon Dose Rate Map and Relative Error

Single-Stack 100x100 Array

Photon Dose Rate Map (mrem/h)



Relative Error

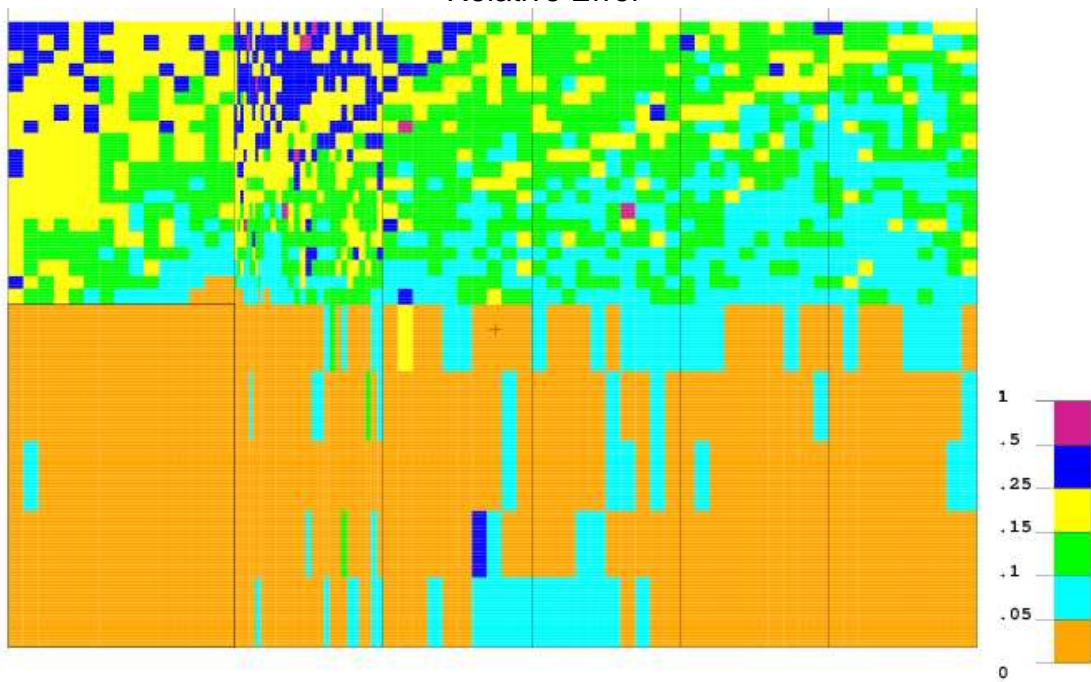
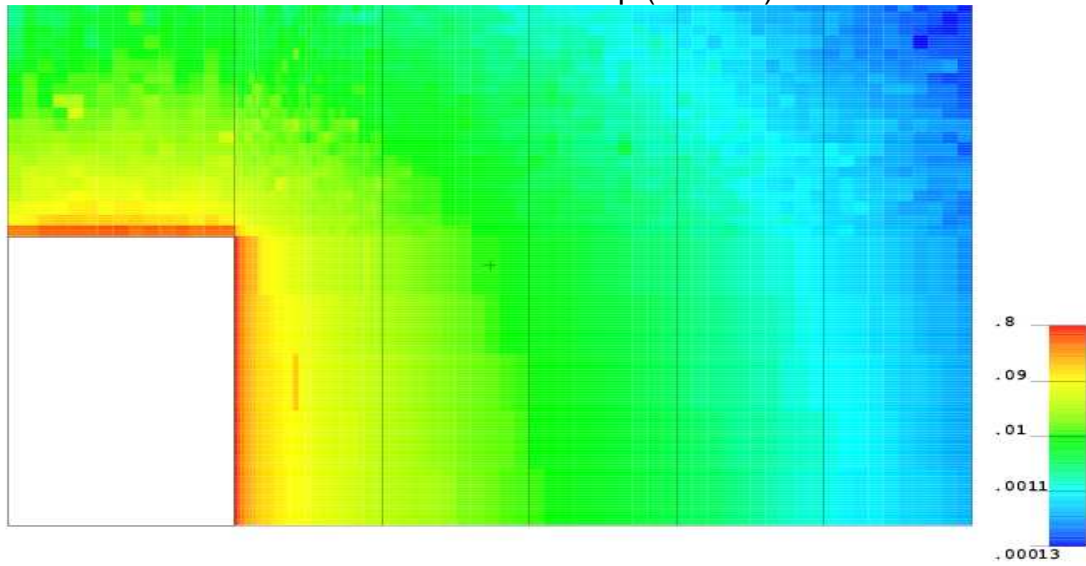


Figure H-16 Single-Stack 100x100 Array Photon Dose Rate Map and Relative Error

Double-Stack 100x100 Array

Photon Dose Rate Map (mrem/h)



Relative Error

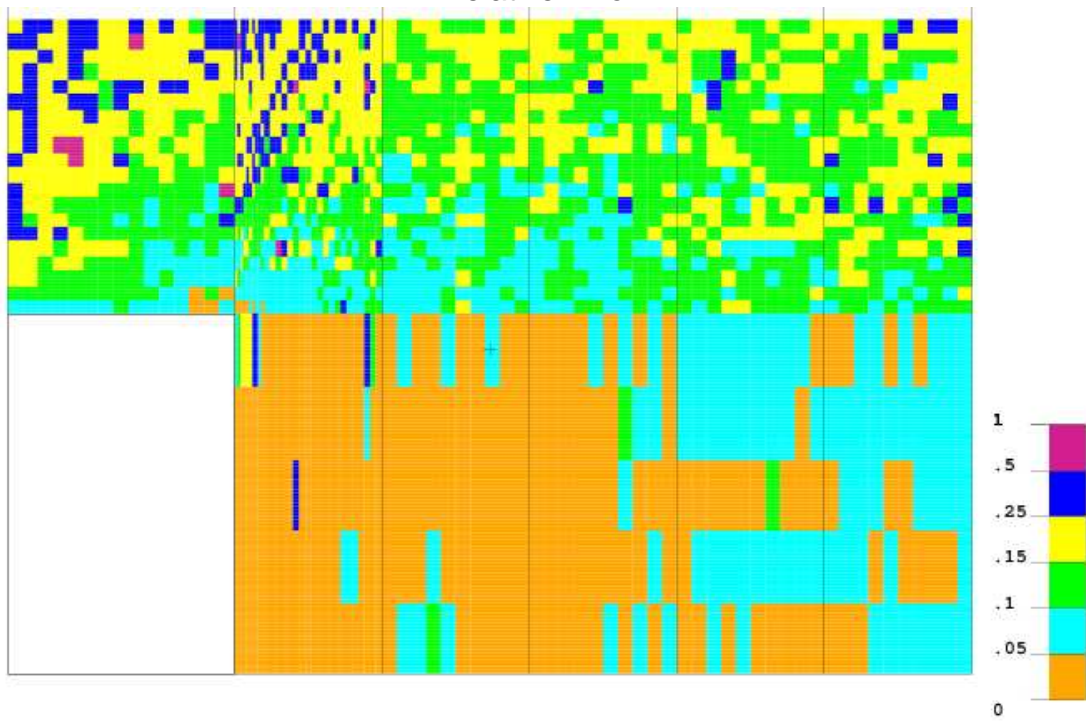
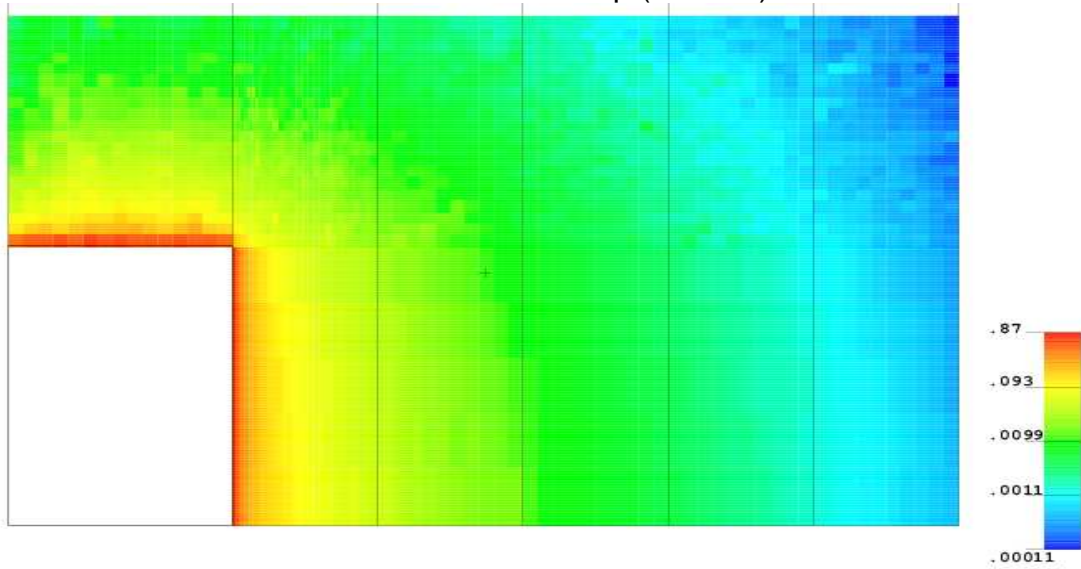


Figure H-17 Double-Stack 100x100 Array Photon Dose Rate Map and Relative Error

Triple-Stack 100x100 Array

Photon Dose Rate Map (mrem/h)



Relative Error

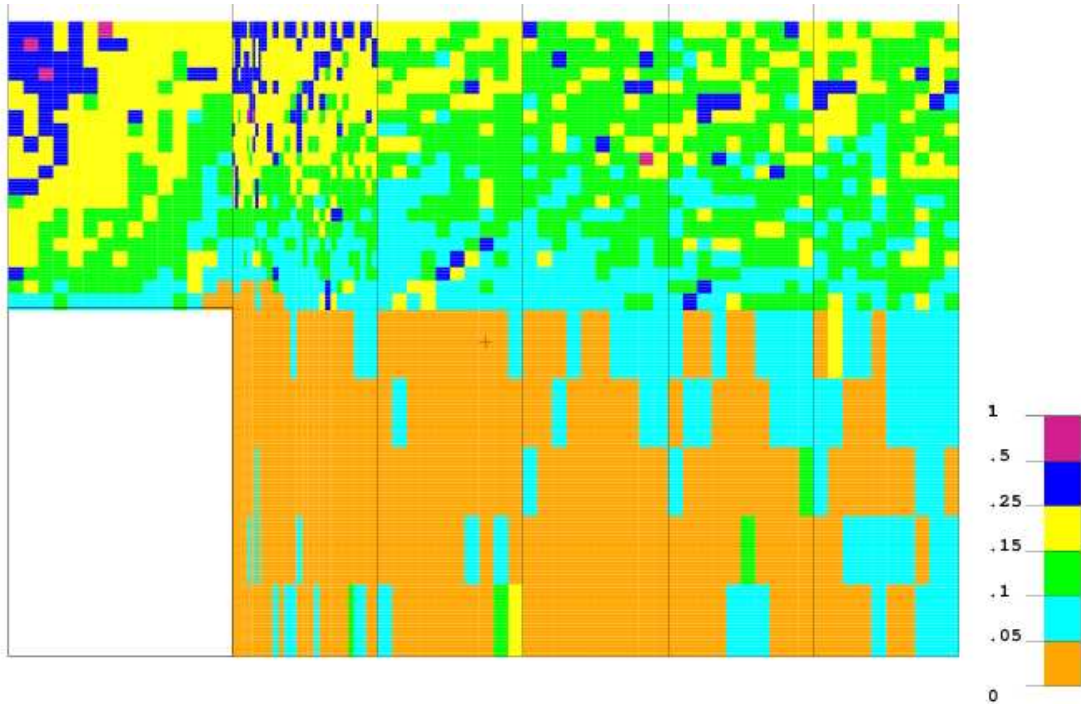


Figure H-18 Triple-Stack 100x100 Array Photon Dose Rate Map and Relative Error

APPENDIX I EMPTY FEED CYLINDER DOSE ASSESSMENT

This appendix contains the following supporting information for the empty feed cylinder dose assessment:

- Cumulative relative dose from empty feed cylinders (§I.1)
- MCNP cases and computer files for empty feed cylinders (§I.2)
- Sample MCNP input listing (§I.3)

I.1 CUMULATIVE RELATIVE DOSE FROM EMPTY FEED CYLINDERS

The equivalent number of fresh empty cylinders can be found by accumulating the dose equivalent from the decayed empty cylinders and relating the sum to the dose from a single fresh cylinder. Table I-1 presents such calculation for a cylinder production rate of one per day. In other words, a new emptied cylinder is added every day. For instance, there is only one cylinder on the first day. On the second day, there are two empties – one freshly emptied on the second day and the other from day 1 with a decay time of 1 day. The results of the calculation are plotted in Figure 6-15 in Chapter 6 as a function of the number of cylinders added.

Table I-1 Cumulative Relative Dose from Empty Feed Cylinders

Cylinder	Age (d)	Relative Dose	Total Dose		Cylinder	Age (d)	Relative Dose	Total Dose
1	0	0.9898	0.990		51	50	0.2366	26.930
2	1	0.9619	1.952		52	51	0.2299	27.160
3	2	0.9347	2.886		53	52	0.2234	27.384
4	3	0.9084	3.795		54	53	0.2171	27.601
5	4	0.8827	4.677		55	54	0.2110	27.812
6	5	0.8578	5.535		56	55	0.2051	28.017
7	6	0.8336	6.369		57	56	0.1993	28.216
8	7	0.8101	7.179		58	57	0.1937	28.410
9	8	0.7872	7.966		59	58	0.1882	28.598
10	9	0.7650	8.731		60	59	0.1829	28.781
11	10	0.7434	9.475		61	60	0.1777	28.959
12	11	0.7225	10.197		62	61	0.1727	29.131
13	12	0.7021	10.899		63	62	0.1678	29.299
14	13	0.6823	11.582		64	63	0.1631	29.462
15	14	0.6630	12.245		65	64	0.1585	29.621
16	15	0.6443	12.889		66	65	0.1540	29.775
17	16	0.6261	13.515		67	66	0.1497	29.925
18	17	0.6085	14.123		68	67	0.1455	30.070
19	18	0.5913	14.715		69	68	0.1414	30.211
20	19	0.5746	15.289		70	69	0.1374	30.349
21	20	0.5584	15.848		71	70	0.1335	30.482
22	21	0.5426	16.390		72	71	0.1297	30.612
23	22	0.5273	16.918		73	72	0.1261	30.738
24	23	0.5125	17.430		74	73	0.1225	30.861
25	24	0.4980	17.928		75	74	0.1190	30.980
26	25	0.4839	18.412		76	75	0.1157	31.095
27	26	0.4703	18.882		77	76	0.1124	31.208
28	27	0.4570	19.339		78	77	0.1093	31.317
29	28	0.4441	19.784		79	78	0.1062	31.423
30	29	0.4316	20.215		80	79	0.1032	31.526
31	30	0.4194	20.635		81	80	0.1003	31.627
32	31	0.4076	21.042		82	81	0.0974	31.724
33	32	0.3961	21.438		83	82	0.0947	31.819
34	33	0.3849	21.823		84	83	0.0920	31.911
35	34	0.3740	22.197		85	84	0.0894	32.000
36	35	0.3635	22.561		86	85	0.0869	32.087
37	36	0.3532	22.914		87	86	0.0844	32.171
38	37	0.3433	23.257		88	87	0.0821	32.253
39	38	0.3336	23.591		89	88	0.0797	32.333
40	39	0.3242	23.915		90	89	0.0775	32.411
41	40	0.3150	24.230		91	90	0.0753	32.486
42	41	0.3061	24.536		92	91	0.0732	32.559
43	42	0.2975	24.834		93	92	0.0711	32.630
44	43	0.2891	25.123		94	93	0.0691	32.699
45	44	0.2809	25.404		95	94	0.0672	32.767
46	45	0.2730	25.677		96	95	0.0653	32.832
47	46	0.2653	25.942		97	96	0.0634	32.895
48	47	0.2578	26.200		98	97	0.0616	32.957
49	48	0.2506	26.450		99	98	0.0599	33.017
50	49	0.2435	26.694		100	99	0.0582	33.075

Table I-1 Cumulative Relative Dose from Empty Feed Cylinders (continued)

Cylinder	Age (d)	Relative Dose	Total Dose		Cylinder	Age (d)	Relative Dose	Total Dose
101	100	0.0566	33.132		151	150	0.0135	34.614
102	101	0.0550	33.187		152	151	0.0131	34.627
103	102	0.0534	33.240		153	152	0.0128	34.640
104	103	0.0519	33.292		154	153	0.0124	34.652
105	104	0.0504	33.342		155	154	0.0121	34.664
106	105	0.0490	33.391		156	155	0.0117	34.676
107	106	0.0476	33.439		157	156	0.0114	34.687
108	107	0.0463	33.485		158	157	0.0111	34.699
109	108	0.0450	33.530		159	158	0.0108	34.709
110	109	0.0437	33.574		160	159	0.0105	34.720
111	110	0.0425	33.616		161	160	0.0102	34.730
112	111	0.0413	33.658		162	161	0.0099	34.740
113	112	0.0401	33.698		163	162	0.0096	34.749
114	113	0.0390	33.737		164	163	0.0093	34.759
115	114	0.0379	33.775		165	164	0.0091	34.768
116	115	0.0368	33.812		166	165	0.0088	34.777
117	116	0.0358	33.847		167	166	0.0086	34.785
118	117	0.0348	33.882		168	167	0.0083	34.793
119	118	0.0338	33.916		169	168	0.0081	34.801
120	119	0.0328	33.949		170	169	0.0078	34.809
121	120	0.0319	33.981		171	170	0.0076	34.817
122	121	0.0310	34.012		172	171	0.0074	34.824
123	122	0.0301	34.042		173	172	0.0072	34.832
124	123	0.0293	34.071		174	173	0.0070	34.839
125	124	0.0285	34.100		175	174	0.0068	34.845
126	125	0.0277	34.127		176	175	0.0066	34.852
127	126	0.0269	34.154		177	176	0.0064	34.858
128	127	0.0261	34.180		178	177	0.0062	34.865
129	128	0.0254	34.206		179	178	0.0061	34.871
130	129	0.0247	34.230		180	179	0.0059	34.877
131	130	0.0240	34.254		181	180	0.0057	34.882
132	131	0.0233	34.277		182	181	0.0056	34.888
133	132	0.0226	34.300		183	182	0.0054	34.893
134	133	0.0220	34.322		184	183	0.0053	34.899
135	134	0.0214	34.343		185	184	0.0051	34.904
136	135	0.0208	34.364		186	185	0.0050	34.909
137	136	0.0202	34.384		187	186	0.0048	34.913
138	137	0.0196	34.404		188	187	0.0047	34.918
139	138	0.0191	34.423		189	188	0.0046	34.923
140	139	0.0185	34.442		190	189	0.0044	34.927
141	140	0.0180	34.460		191	190	0.0043	34.931
142	141	0.0175	34.477		192	191	0.0042	34.936
143	142	0.0170	34.494		193	192	0.0041	34.940
144	143	0.0165	34.511		194	193	0.0039	34.944
145	144	0.0161	34.527		195	194	0.0038	34.947
146	145	0.0156	34.542		196	195	0.0037	34.951
147	146	0.0152	34.557		197	196	0.0036	34.955
148	147	0.0147	34.572		198	197	0.0035	34.958
149	148	0.0143	34.587		199	198	0.0034	34.962
150	149	0.0139	34.600		200	199	0.0033	34.965

Table I-1 Cumulative Relative Dose from Empty Feed Cylinders (continued)

Cylinder	Age (d)	Relative Dose	Total Dose		Cylinder	Age (d)	Relative Dose	Total Dose
201	200	0.0032	34.968		251	250	0.0008	35.053
202	201	0.0031	34.971		252	251	0.0008	35.054
203	202	0.0031	34.975		253	252	0.0007	35.055
204	203	0.0030	34.977		254	253	0.0007	35.055
205	204	0.0029	34.980		255	254	0.0007	35.056
206	205	0.0028	34.983		256	255	0.0007	35.057
207	206	0.0027	34.986		257	256	0.0007	35.057
208	207	0.0026	34.989		258	257	0.0006	35.058
209	208	0.0026	34.991		259	258	0.0006	35.058
210	209	0.0025	34.994		260	259	0.0006	35.059
211	210	0.0024	34.996		261	260	0.0006	35.060
212	211	0.0024	34.998		262	261	0.0006	35.060
213	212	0.0023	35.001		263	262	0.0005	35.061
214	213	0.0022	35.003		264	263	0.0005	35.061
215	214	0.0022	35.005		265	264	0.0005	35.062
216	215	0.0021	35.007		266	265	0.0005	35.062
217	216	0.0020	35.009		267	266	0.0005	35.063
218	217	0.0020	35.011		268	267	0.0005	35.063
219	218	0.0019	35.013		269	268	0.0005	35.064
220	219	0.0019	35.015		270	269	0.0004	35.064
221	220	0.0018	35.017		271	270	0.0004	35.065
222	221	0.0018	35.019		272	271	0.0004	35.065
223	222	0.0017	35.020		273	272	0.0004	35.065
224	223	0.0017	35.022		274	273	0.0004	35.066
225	224	0.0016	35.024		275	274	0.0004	35.066
226	225	0.0016	35.025		276	275	0.0004	35.067
227	226	0.0015	35.027		277	276	0.0004	35.067
228	227	0.0015	35.028		278	277	0.0004	35.067
229	228	0.0015	35.030		279	278	0.0003	35.068
230	229	0.0014	35.031		280	279	0.0003	35.068
231	230	0.0014	35.032		281	280	0.0003	35.068
232	231	0.0013	35.034		282	281	0.0003	35.069
233	232	0.0013	35.035		283	282	0.0003	35.069
234	233	0.0013	35.036		284	283	0.0003	35.069
235	234	0.0012	35.038		285	284	0.0003	35.070
236	235	0.0012	35.039		286	285	0.0003	35.070
237	236	0.0012	35.040		287	286	0.0003	35.070
238	237	0.0011	35.041		288	287	0.0003	35.070
239	238	0.0011	35.042		289	288	0.0003	35.071
240	239	0.0011	35.043		290	289	0.0003	35.071
241	240	0.0010	35.044		291	290	0.0002	35.071
242	241	0.0010	35.045		292	291	0.0002	35.071
243	242	0.0010	35.046		293	292	0.0002	35.072
244	243	0.0009	35.047		294	293	0.0002	35.072
245	244	0.0009	35.048		295	294	0.0002	35.072
246	245	0.0009	35.049		296	295	0.0002	35.072
247	246	0.0009	35.050		297	296	0.0002	35.073
248	247	0.0008	35.051		298	297	0.0002	35.073
249	248	0.0008	35.051		299	298	0.0002	35.073
250	249	0.0008	35.052		300	299	0.0002	35.073

I.2 MCNP CASES AND COMPUTER FILES FOR EMPTY FEED CYLINDERS

Table I-2 lists the MCNP computer files created for calculations of photon dose rates from different arrays of empty feed cylinders. The table also contains relevant information such as the CPU time consumed, number of histories processed, and number of tracks created for the surface source.

Table I-2 MCNP Photon Cases for Empty Feed Cylinders

Case	Case Description	Input File	Output File	CPU (m)	nps	Tracks
First Step						
1	10x10 Array - Single	s10x10e01.txt	s10x10e01.out	22.52	22.89M	20.80M
2	10x10 Array - Double	d10x10e01.txt	d10x10e01.out	42.57	44.54M	25.52M
3	10x10 Array - Triple	t10x10e01.txt	t10x10e01.out	62.60	63.43M	26.25M
Second Step						
1	10x10 Array - Single	s10x10e02.txt	s10x10e02.out	12.51	N/A	N/A
2	10x10 Array - Double	d10x10e02.txt	d10x10e02.out	25.24	N/A	N/A
3	10x10 Array - Triple	t10x10e02.txt	t10x10e02.out	25.19	N/A	N/A

I.3 SAMPLE MCNP INPUT LISTING

The representative cases selected for listing of the sample MCNP input files include the following:

- File *t10x10e01.txt* (§I.3.1)
- File *t10x10e02.txt* (§I.3.2)

I.3.1 Input File *t10x10e01.txt*

```

Dose Rates from Multiple Empty 48Y Feed Cylinder
c file t10x10e01 (300 cylinders total - 11x10, 10x10 & 9x10)
c 11x10, 10x10 & 9x10 array - triple stack
c reflective bounday at Y mid-plane (i.e., 150 cylinders modeled)
c Photon - homogenized source geometry - ANSI/ANS-6.1.1-1977
c center-to-center spacing=5' (radial) & 16' (axial)
c lattice center element at far right
c 1st step calculation to tally surface sources
c include built-in directional biasing (a=1)
c no cell source biasing
c
c CELL CARDS
c
11      3      -0.0012  -11                u=1 imp:p=1 $Inside of cylinder (air)

```

```

12      2   -7.8500   11 -12                u=1 imp:p=2 $Steel shell
13      3   -0.0012   12                    u=1 imp:p=3 $External to cylinder
14      0                -13 fill=1 lat=1    u=2 imp:p=3 $Lattice for bottom stack
15      0                -31 fill=2          imp:p=3 $Box to fill bottom stack
16      like 14 but trcl=(-76.2  0 125.095) u=3 imp:p=3 $Lattice for mid stack
17      0                -32 fill=3          imp:p=3 $Box to fill middle stack
18      like 14 but trcl=(-152.4 0 250.190) u=4 imp:p=3 $Lattice for top stack
19      0                -33 fill=4          imp:p=3 $Box to fill top stack
c
20      3   -0.0012  -34  31 32  33          imp:p=3 $Box for all cylinders
21      3   -0.0012  41 -42 43 -44 46 -47 34 imp:p=3 $Air space
22      4   -1.60     41 -42 43 -44 45 -46    imp:p=1 $Ground soil
23      0                -41:42:-43:44:-45:47 imp:p=0 $Outer void

```

c

c SURFACE CARDS

c

```

11      rcc  0.0 -184.7850  0.0 0.0 369.570  0.0 60.9600      $UF6 cylinder
12      rcc  0.0 -186.3725  0.0 0.0 372.745  0.0 62.5475      $steel cylinder
13      rpp   -76.2   76.2 -243.84  243.84 -62.5475 62.5475  $unit box
c Box to fill cylinders (bottom stack - 11x5 cylinders with refl. boundary)
31      rpp -1600.2  62.6 -243.84 2138.00 -62.5475 62.5475
c Box to fill cylinders (middle stack - 10x10 cylinders)
32      rpp -1524.0   0.0 -243.84 2138.00  62.5475 187.6425
c Box to fill cylinders (top stack - 9x10 cylinders)
33      rpp -1447.8 -76.2 -243.84 2138.00 187.6425 312.8
c Box to contain all cylinders
34      rpp -1600.2  62.6 -243.84 2138.00 -77.7875 312.8
c Air box
41      px  -1700.0   $-X boundary
42      px   20000.0  $+X boundary
43*     py  -244.0    $-Y boundary (reflective)
44      py   22000.0  $+Y boundary
45      pz  -108.0    $-Z boundary (soil bottom)
46      pz  -77.7875 $ground Z level or soil top
47      pz   23000.0  $+Z boundary
48      pz  -62.5475 $bottom of cylinder

```

c

c DATA CARDS

c

```

m1      9019  6.00      92238  0.9928  92235  0.0072  $ UF6
m2      26000  1.00
m3      6000 -0.00014  7014 -0.75521  8016 -0.23177  $ Air
        18000 -0.01288
m4      8016 -0.465     11023 -0.0245  13027 -0.080  $ Ground soil
        12000 -0.015     14000 -0.290   19000 -0.0225
        20000 -0.040     26000 -0.060

```

phys:p 10 \$ detailed physics, brems., coherent

mode p

c Write surface source file

ssw 31.1 31.3 33.5

c Source definition card with the following distributions:

c d1=distribution #1 for selection of the cell (i.e., cylinder)

c d2=distribution #2 for selection of x position

c d3=distribution #3 for selection of y position

c d4=distribution #4 for selection of z position

c d5=distribution #5 for photon source energy spectrum

c d6=distribution #6 for directional biasing w.r.t. +x axis

sdef cel=d1 x=d2 y=d3 z=d4 erg=d5 vec=1 0 0 dir=d6

```

si1  1 (-11<14[-10:0 0:4 0:0]<15)    $cell information (11x5 - bottom)
      (-11<16[-9:0 0:4 0:0]<17)    $cell information (10x5 - middle)
      (-11<18[-8:0 0:4 0:0]<19)    $cell information (9x5 - top)
sp1   1 149r                          $cell unbiased probability (equal)
si2  -60.96 60.96                      $source position in x for center element
sp2   0.0 1.0                          $equal weighting along x
si3  -184.7850 184.7850                $source position in y for center element
sp3   0.0 1.0                          $equal weighting along y
si4  -60.96 60.96                      $source position in z for center element
sp4   0.0 1.0                          $equal weighting along z
c Photon Spectrum (partial from SCALE 19 groups)
c si5 - energy boundary information
c sp5 - unbiased energy spectrum
c sb5 - biased energy spectrum based on dose response
c vertical input format used for si5, sp5 and sb5
#    si5      sp5      sb5
    4.50E-02  0.0      0.0
    1.00E-01  7.314E-01  1.270E-03
    2.00E-01  7.635E-02  3.518E-03
    3.00E-01  2.710E-02  2.323E-02
    4.00E-01  1.569E-02  2.910E-02
    6.00E-01  1.433E-02  4.598E-02
    8.00E-01  4.843E-02  2.350E-01
    1.00E+00  4.732E-02  3.015E-01
    1.33E+00  2.901E-02  2.395E-01
    1.66E+00  4.286E-03  4.479E-02
    2.00E+00  6.074E-03  7.609E-02
c Directional sampling with bias for forward direction
si6  -1.0 1.0                          $direction cosine from -1 to 1
sb6  -31 1                              $biased directional distribution for sampling
c ANSI/ANS-6.1.1-1977 photon dose conversion factors (mrem/h)/(photon/cm^2-s)
de0  LOG  0.01  0.03  0.05  0.07  0.1  0.15  0.2
      0.25  0.3  0.35  0.4  0.45  0.5  0.55  0.6
      0.65  0.7  0.8  1.0  1.4  1.8  2.2  2.6
      2.8  3.25  3.75  4.25  4.75  5.0  5.25  5.75
      6.25  6.75  7.5  9.0  11.0  13.0  15.0
df0  LOG  3.96-3 5.82-4 2.90-4 2.58-4 2.83-4 3.79-7 5.01-4
      6.31-4 7.59-4 8.78-4 9.85-4 1.08-3 1.17-3 1.27-3 1.36-3
      1.44-3 1.52-3 1.68-3 1.98-3 2.51-3 2.99-3 3.42-3 3.82-3
      4.01-3 4.41-3 4.83-3 5.23-3 5.60-3 5.80-3 6.01-3 6.37-3
      6.74-3 7.11-3 7.66-3 8.77-3 1.03-2 1.18-2 1.33-2
c Energy bins for tally (same as for source energy groups)
e0   0.0
      4.50E-02
      1.00E-01
      2.00E-01
      3.00E-01
      4.00E-01
      6.00E-01
      8.00E-01
      1.00E+00
      1.33E+00
      1.66E+00
      2.00E+00
f2:p  31.1 31.3 33.5 $average dose rate on these facets
fm2   2.289E+12      $total source strength for 150 cylinders (p/s)
c
ctme  60.0
print

```

I.3.2 Input File *t10x10e02.txt*

```

Dose Rates from Multiple Empty 48Y Feed Cylinder
c file t10x10e02 (300 cylinders total)
c 11x10, 10x10 & 9x10 array - triple stack
c reflective bounday at Y mid-plane (i.e., 150 cylinders modeled)
c Photon - homogenized source geometry - ANSI/ANS-6.1.1-1977
c center-to-center spacing=5' (radial) & 16' (axial)
c 2nd step calculation with mesh tally
c
21      0          -31  32          imp:p=1  $Box around cylinders
22      0          -32          imp:p=0  $Black box for all
cylinders
23      3  -0.0012  41 -50 43 -44 46 -47 31 imp:p=1  $Air space
24      4  -1.60    41 -50 43 -44 45 -46  imp:p=1  $Ground soil
25      0          -41:42:-43:44:-45:47  imp:p=0  $Outer void
c Air importance cells
51      3  -0.0012  50 -51 43 -44 46 -47  imp:p=1  $1st air cell
52      3  -0.0012  51 -52 43 -44 46 -47  imp:p=3  $2nd air cell
53      3  -0.0012  52 -53 43 -44 46 -47  imp:p=9  $3rd air cell
54      3  -0.0012  53 -54 43 -44 46 -47  imp:p=27 $4th air cell
55      3  -0.0012  54 -42 43 -44 46 -47  imp:p=81 $5th air cell
c Soil importance cells
61      4  -1.60    50 -51 43 -44 45 -46  imp:p=1  $1st soil cell
62      4  -1.60    51 -52 43 -44 45 -46  imp:p=1  $2nd soil cell
63      4  -1.60    52 -53 43 -44 45 -46  imp:p=3  $3rd soil cell
64      4  -1.60    53 -54 43 -44 45 -46  imp:p=9  $4th soil cell
65      4  -1.60    54 -42 43 -44 45 -46  imp:p=27 $5th soil cell
c
c Box to fill cylinders (3 stacks - 150 cylinders with reflective boundary)
31      rpp -1662.6  0.0 -2381.84  0.0 -77.7875 312.8
c Black Box to contain all cylinders (to avoid round-off errors)
32      rpp -1662.6 -0.1 -2381.84 -0.1 -77.7875 312.7
c Air box
41      px  -1700.0  $-X boundary
42      px   50000.0  $+X boundary
43*     py  -2382.0  $-Y boundary (reflective)
44      py   30000.0  $+Y boundary
45      pz  -108.0   $-Z boundary (soil bottom)
46      pz  -77.7875 $ground level or soil top)
47      pz   30000.0  $+Z boundary
48      pz  -62.5475 $bottom of cylinder
c Cell importance division plane
50      px    0.0
51      px  10000.0
52      px  20000.0
53      px  30000.0
54      px  40000.0

m1      9019  6.00    92238  0.9970  92235  0.0030  $ UF6
m2      26000  1.00
m3      6000 -0.00014  7014 -0.75521  8016 -0.23177  $ Air
        18000 -0.01288
m4      8016 -0.465   11023 -0.0245  13027 -0.080   $ Ground soil
        12000 -0.015   14000 -0.290   19000 -0.0225
        20000 -0.040   26000 -0.060

phys:p 10          $ detailed physics, brems., coherent
mode   p

```

```

c Coordinate transformation from previous to current problem
tr1 -62.6 -2138.0 0.0
c read source file
ssr old=31.1 31.3 33.5 new=31.1 31.3 31.5 tr=1
c ANSI/ANS-6.1.1-1977 photon dose conversion factors (mrem/h)/(photon/cm^2-s)
de0 LOG 0.01 0.03 0.05 0.07 0.1 0.15 0.2
0.25 0.3 0.35 0.4 0.45 0.5 0.55 0.6
0.65 0.7 0.8 1.0 1.4 1.8 2.2 2.6
2.8 3.25 3.75 4.25 4.75 5.0 5.25 5.75
6.25 6.75 7.5 9.0 11.0 13.0 15.0
df0 LOG 3.96-3 5.82-4 2.90-4 2.58-4 2.83-4 3.79-7 5.01-4
6.31-4 7.59-4 8.78-4 9.85-4 1.08-3 1.17-3 1.27-3 1.36-3
1.44-3 1.52-3 1.68-3 1.98-3 2.51-3 2.99-3 3.42-3 3.82-3
4.01-3 4.41-3 4.83-3 5.23-3 5.60-3 5.80-3 6.01-3 6.37-3
6.74-3 7.11-3 7.66-3 8.77-3 1.03-2 1.18-2 1.33-2
c Energy bins for tally (same as for source energy group)
e0 0.0
4.50E-02
1.00E-01
2.00E-01
3.00E-01
4.00E-01
6.00E-01
8.00E-01
1.00E+00
1.33E+00
1.66E+00
2.00E+00
fmesh4:p geom=xyz origin=-1662.6 -2381.84 -77.7875
imesh=-0.1 0.0 2000.0 10000.0 50000.0
iints=15 1 10 20 40
jmesh=-0.1 0.0 20000.0
jints=5 1 20
kmesh=312.7 $top stack level
kints=1
fm4 2.289E+12 $total source strength for 150 cylinders (p/s)
c
ctme 50.0
print

```

APPENDIX J UUSA UBC STORAGE PAD DOSE CALCULATION

This appendix contains the following supporting information for the calculation of the photon dose rates from the UUSA UBC Storage Pad for comparison with the field measurements:

- MCNP cases and computer files for empty feed cylinders (§J.1)
- MCNP input listing (§J.2)

J.1 MCNP CASES AND COMPUTER FILES FOR VALIDATION USE

Table J-1 lists the MCNP computer files created for calculations of photon dose rates from the UUSA UBC Storage Pad. The table also contains relevant information such as the CPU time consumed, number of histories processed, and number of tracks created for the surface source.

Table J-1 MCNP Photon Cases for Empty Feed Cylinders

Case	Case Description	Input File	Output File	CPU (m)	nps	Tracks
First Step						
1	100x8 Array - Double	d100x8p01.txt	d100x8p01.out	200.17	602M	1.38M
Second Step						
1	100x8 Array - Double	d100x8p02.txt	d100x8p02.out	0.52	N/A	N/A

J.2 MCNP INPUT LISTING

The listing of the MCNP input files include the following:

- File *d100x8p01.txt* (§J.2.1)
- File *d100x8p02.txt* (§J.2.2)

J.2.1 Input File *d100x8p01.txt*

```
Dose Rates from Multiple Filled 48Y Feed Cylinder
c file d100x8p01 (1,608 cylinders total - 101x8 & 100x8)
c 101x8 & 100x8 array - double stack
c reflective boundary at X mid-plane (i.e., 804 cylinders modeled)
c Photon - homogenized source geometry - ANSI/ANS-6.1.1-1977
c center-to-center spacing=5.5' (radial) & 14.52' (axial per section)
c lattice center element at far left
c 1st step calculation to tally surface sources
c include built-in directional biasing (a=1)
c
c CELL CARDS
c
1      1      -2.897  -1                u=1 imp:p=1 $Inside of cylinder (UF6)
2      2      -7.8500  1 -2            u=1 imp:p=4 $Steel shell
3      3      -0.0012  2                u=1 imp:p=6 $External to cylinder
c 1st two-row section
11     0                -3  fill=1 lat=1  u=2 imp:p=6 $Lattice for bot stack
12     0                -11 fill=2        imp:p=6 $Box to fill bottom stack
13     like 11 but trcl=(83.82 0 125.095) u=3 imp:p=6 $Lattice for top stack
14     0                -12 fill=3        imp:p=6 $Box to fill top stack
c 2nd two-row section
15     like 11 but trcl=(0 1097.2 0)      u=4 imp:p=6 $Lattice for bot stack
16     0                -13 fill=4        imp:p=6 $Box to fill bot stack
17     like 11 but trcl=(83.82 1097.2 125.095)
                                           u=5 imp:p=6 $Lattice for top stack
                                           imp:p=6 $Box to fill top stack
18     0                -14 fill=5        imp:p=6 $Box to fill top stack
c 3rd two-row section
19     like 11 but trcl=(0 2194.4 0)      u=6 imp:p=6 $Lattice for bot stack
20     0                -15 fill=6        imp:p=6 $Box to fill bot stack
21     like 11 but trcl=(83.82 2194.4 125.095)
                                           u=7 imp:p=6 $Lattice for top stack
                                           imp:p=6 $Box to fill top stack
22     0                -16 fill=7        imp:p=6 $Box to fill top stack
c 4th two-row section
23     like 11 but trcl=(0 3291.6 0)      u=8 imp:p=6 $Lattice for bot stack
24     0                -17 fill=8        imp:p=6 $Box to fill bot stack
25     like 11 but trcl=(83.82 3291.6 125.095)
                                           u=9 imp:p=6 $Lattice for top stack
                                           imp:p=6 $Box to fill top stack
26     0                -18 fill=9        imp:p=6 $Box to fill top stack
c
31     3      -0.0012  -31 11 12 13 14 15 16 17 18
                                           imp:p=6 $Box for all cylinders
41     3      -0.0012  41 -42 43 -44 46 -47 31 imp:p=6 $Air space
42     4      -1.60    41 -42 43 -44 45 -46    imp:p=1 $Ground soil
43     0                -41:42:-43:44:-45:47 imp:p=0 $Outer void
c
c SURFACE CARDS
c
1      rcc  0.0 -184.7850 0.0 0.0 369.570 0.0 60.9600    $UF6 cylinder
2      rcc  0.0 -186.3725 0.0 0.0 372.745 0.0 62.5475    $steel cylinder
3      rpp  -83.82 83.82 -221.4 221.4 -62.5475 62.5475    $unit box
c 1st section of two-row cylinders
c Box to fill cylinders (bot stack-51x8 cylinders with reflective boundary)
11     rpp  -0.0 8465.82 -221.3 663.9 -62.5475 62.5475
c Box to fill cylinders (top stack-50x8 cylinders)
```

```

12  rpp  -0.0 8382.00 -221.3 663.9 62.5475 187.6425
c 2nd section of two-row cylinders
13  rpp  -0.0 8465.82 875.9 1761.9 -62.5475 62.5475 $bottom
14  rpp  -0.0 8382.00 875.9 1761.9 62.5475 187.6425 $top
c 3rd section of two-row cylinders
15  rpp  -0.0 8465.82 1973.1 2858.3 -62.5475 62.5475 $bottom
16  rpp  -0.0 8382.00 1973.1 2858.3 62.5475 187.6425 $top
c 4th section of two-row cylinders
17  rpp  -0.0 8465.82 3070.3 3955.5 -62.5475 62.5475 $bottom
18  rpp  -0.0 8382.00 3070.3 3955.5 62.5475 187.6425 $top
c Box to contain all cylinders
31  rpp  -0.0 8466.00 -221.3 3955.6 -71.44 187.8
c Air box
41* px  -0.01  $-X boundary (reflective)
42  px  10400.0 $+X boundary
43  py  -221.4  $-Y boundary
44  py  6000.0  $+Y boundary
45  pz  -101.92 $-Z boundary (soil bottom)
46  pz  -71.44  $ground Z level or soil top
47  pz  20000.0 $+Z boundary
48  pz  -62.5475 $bottom of cylinder

c
c DATA CARDS
c
m1  9019 6.00 92238 0.9928 92235 0.0072 $ UF6
m2  26000 1.00 $ Iron
m3  6000 -0.00014 7014 -0.75521 8016 -0.23177 $ Air
    18000 -0.01288
m4  8016 -0.465 11023 -0.0245 13027 -0.080 $ Ground bulk soil
    12000 -0.015 14000 -0.290 19000 -0.0225
    20000 -0.040 26000 -0.060
phys:p 10 $ detailed physics, brems., coherent
mode p
c Write surface source file
ssw 31.1 31.3 31.5
c Source definition card with the following distributions:
c d1=distribution #1 for selection of the cell (i.e., cylinder)
c d2=distribution #2 for selection of x position
c d3=distribution #3 for selection of y position
c d4=distribution #4 for selection of z position
c d5=distribution #5 for photon source energy spectrum
c d6=distribution #6 for directional biasing w.r.t. +x axis
sdef cel=d1 x=d2 y=d3 z=d4 erg=d5 vec=0 1 0 dir=d6
si1 1 (-1<11[0:50 0:1 0:0]<12) (-1<13[0:49 0:1 0:0]<14) $1st cell information
    (-1<15[0:50 0:1 0:0]<16) (-1<17[0:49 0:1 0:0]<18) $2nd cell information
    (-1<19[0:50 0:1 0:0]<20) (-1<21[0:49 0:1 0:0]<22) $3rd cell information
    (-1<23[0:50 0:1 0:0]<24) (-1<25[0:49 0:1 0:0]<26) $4th cell information
sp1 1 807r $cell unbiased probability (equal)
c Biased source sampling probability based on MAVRIC-generated data
c MAVRIC biased sampling probability (51 or 50 cylinders/row in X direction)
sb1 5.6E-03 50r 6.8E-03 50r 5.8E-02 49r 6.7E-02 49r $1st section - bot & top
    8.6E-03 50r 1.2E-02 50r 7.8E-02 49r 9.1E-02 49r $2nd section - bot & top
    1.7E-02 50r 2.8E-02 50r 1.1E-01 49r 1.3E-03 49r $3rd section - bot & top
    8.6E-02 50r 9.9E-01 50r 2.0E-01 49r 1.0 49r $4th section - bot & top
si2 -60.96 60.96 $source position in x for center element
sp2 0.0 1.0 $equal weighting along x
si3 -184.7850 184.7850 $source position in y for center element
sp3 0.0 1.0 $equal weighting along y
si4 -60.96 60.96 $source position in z for center element

```

```

sp4      0.0      1.0      $equal weighting along z
c Photon Spectrum (partial from SCALE 19 groups)
c si5 - energy boundary information
c sp5 - unbiased energy spectrum
c sb5 - biased energy spectrum based on dose response
c vertical input format used for si5, sp5 and sb5
#      si5      sp5      sb5
      4.50E-02  0.0      0.0
      1.00E-01  5.232E-01  7.933E-05
      2.00E-01  2.795E-01  1.494E-03
      3.00E-01  6.343E-02  1.378E-02
      4.00E-01  4.056E-02  3.645E-02
      6.00E-01  2.785E-02  8.181E-02
      8.00E-01  2.746E-02  1.927E-01
      1.00E+00  2.120E-02  2.608E-01
      1.33E+00  1.266E-02  2.593E-01
      1.66E+00  1.885E-03  5.885E-02
      2.00E+00  2.275E-03  9.479E-02
c Directional sampling with bias for forward direction
si6     -1.0  1.0      $direction cosine from -1 to 1
sb6     -31  1      $biased directional distribution for sampling
c ANSI/ANS-6.1.1-1977 photon dose conversion factors (mrem/h)/(photon/cm^2-s)
de0     LOG     0.01  0.03  0.05  0.07  0.1  0.15  0.2
      0.25  0.3  0.35  0.4  0.45  0.5  0.55  0.6
      0.65  0.7  0.8  1.0  1.4  1.8  2.2  2.6
      2.8  3.25  3.75  4.25  4.75  5.0  5.25  5.75
      6.25  6.75  7.5  9.0  11.0  13.0  15.0
df0     LOG     3.96-3 5.82-4 2.90-4 2.58-4 2.83-4 3.79-7 5.01-4
      6.31-4 7.59-4 8.78-4 9.85-4 1.08-3 1.17-3 1.27-3 1.36-3
      1.44-3 1.52-3 1.68-3 1.98-3 2.51-3 2.99-3 3.42-3 3.82-3
      4.01-3 4.41-3 4.83-3 5.23-3 5.60-3 5.80-3 6.01-3 6.37-3
      6.74-3 7.11-3 7.66-3 8.77-3 1.03-2 1.18-2 1.33-2
c Energy bins for tally (same as for source energy groups)
e0      0.0
      4.50E-02
      1.00E-01
      2.00E-01
      3.00E-01
      4.00E-01
      6.00E-01
      8.00E-01
      1.00E+00
      1.33E+00
      1.66E+00
      2.00E+00
f2:p    31.1 31.3 31.5  $average dose rate on these facets
fm2     3.341E+13      $total source strength for 804 cylinders (p/s)
c
ctme    200.0
print

```

J.2.2 Input File *d100x8p02.txt*

```
Dose Rates from Multiple Filled 48Y Feed Cylinder
c file d100x8p02 (1608 cylinders total)
c 101x8 & 100x8 array - double stack
c reflective boundary at X mid-plane (i.e., 804 cylinders modeled)
c Photon - homogenized source geometry - ANSI/ANS-6.1.1-1977
c center-to-center spacing=5.5' (radial) & 14.52' (axial in section)
c 2nd step calculation with mesh tally
c
21      0          -31  32                      imp:p=1 $Box around cylinders
22      0          -32                          imp:p=0 $Black box for all cylinders
23      3  -0.0012  41 -42 43 -51 46 -47 31 imp:p=1 $Air space
24      4  -1.60    41 -42 43 -51 45 -46    imp:p=1 $Ground soil
25      0          -41:42:-43:44:-45:47    imp:p=0 $Outer void
c Air importance cells
51      3  -0.0012  41 -42 51 -52 46 -47    imp:p=1  $1st air cell
52      3  -0.0012  41 -42 52 -53 46 -47    imp:p=1  $2nd air cell
53      3  -0.0012  41 -42 53 -44 46 -47    imp:p=1  $3rd air cell
c Soil importance cells
61      4  -1.60    41 -42 51 -52 45 -46    imp:p=0.5 $1st soil cell
62      4  -1.60    41 -42 52 -53 45 -46    imp:p=0.5 $2nd soil cell
63      4  -1.60    41 -42 53 -44 45 -46    imp:p=0.5 $3rd soil cell

c
c Box to fill cylinders (double stack-51x8cylinders with reflective boundary)
31      rpp  0.0 8466.0 -221.3 3955.6 -71.44  187.8
c Black Box to contain all cylinders (to avoid round-off errors)
32      rpp  0.0 8465.9 -221.3 3955.5 -71.44  187.7
c Air box
41*     px  -0.01    $-X boundary (reflective)
42     px  10400.0  $+X boundary
43     py  -221.4    $-Y boundary
44     py  40000.0  $+Y boundary
45     pz  -101.92  $-Z boundary (soil bottom)
46     pz  -71.44  $ground Z level or soil top
47     pz  20000.0  $+Z boundary
48     pz  -62.5475 $bottom of cylinder
c Cell importance division plane in Y
51     py  13920.0
52     py  23920.0
53     py  33920.0

m1      9019  6.00    92238  0.9928  92235  0.0072  $ UF6
m2      26000  1.00                                $ Iron
m3      6000 -0.00014  7014 -0.75521  8016 -0.23177  $ Air
        18000 -0.01288
m4      8016 -0.465  11023 -0.0245  13027 -0.080  $ Ground soil
        12000 -0.015  14000 -0.290  19000 -0.0225
        20000 -0.040  26000 -0.060

phys:p 10                                $ detailed physics, brems., coherent
mode   p
c read source file
ssr   old=31.1 31.3 31.5 new=31.1 31.3 31.5
c ANSI/ANS-6.1.1-1977 photon dose conversion factors
c (mrem/h)/(photon/cm^2-s)
de0   LOG    0.01  0.03  0.05  0.07  0.1  0.15  0.2
        0.25  0.3  0.35  0.4  0.45  0.5  0.55  0.6
        0.65  0.7  0.8  1.0  1.4  1.8  2.2  2.6
```

```

2.8    3.25   3.75   4.25   4.75   5.0    5.25   5.75
6.25   6.75   7.5    9.0    11.0   13.0   15.0
df0    LOG    3.96-3 5.82-4 2.90-4 2.58-4 2.83-4 3.79-7 5.01-4
6.31-4 7.59-4 8.78-4 9.85-4 1.08-3 1.17-3 1.27-3 1.36-3
1.44-3 1.52-3 1.68-3 1.98-3 2.51-3 2.99-3 3.42-3 3.82-3
4.01-3 4.41-3 4.83-3 5.23-3 5.60-3 5.80-3 6.01-3 6.37-3
6.74-3 7.11-3 7.66-3 8.77-3 1.03-2 1.18-2 1.33-2
c Energy bins for tally (same as for source energy group)
e0     0.0
      4.50E-02
      1.00E-01
      2.00E-01
      3.00E-01
      4.00E-01
      6.00E-01
      8.00E-01
      1.00E+00
      1.33E+00
      1.66E+00
      2.00E+00
fmesh4:p geom=xyz origin=0.0 -221.3 -71.44
      imesh=8466.0
      iints=10
      jmesh=3920.0 13920.0
      jint=1 100
      kmesh=172.4 $8 ft off ground for personnel height
      kints=1
fm4    3.341E+13    $total source strength for 804 cylinders (p/s)
c
ctme  100.0
print

```

REFERENCES

ANL 2001, *Transportation Impact Assessment for Shipment of Uranium Hexafluoride (UF₆) from the East Tennessee Technology Park to the Portsmouth and Paducah Gaseous Diffusion Plants*, ANL/EAD/TM-112, Argonne National Laboratory, October 2001.

ANL 2013, *What does a cylinder storage yard look like?*, Argonne National Laboratory, <http://web.ead.anl.gov/uranium/faq/storage/faq18.cfm>, retrieved in 2013.

ANS 1977, *Neutron and Gamma-Ray Flux-to-Dose-Rate Factors*, ANSI/ANS-6.1.1-1977, La Grange Park, Illinois: American Nuclear Society, 1977.

ANS 1991, *Neutron and Gamma-Ray Fluence-to-Dose Factors*, ANSI/ANS-6.1.1-1991, La Grange Park, Illinois: American Nuclear Society, 1991.

ANS 1997 *Nuclear Analysis and Design of Concrete Radiation Shielding for Nuclear Power Plants*, ANSI/ANS-6.4-1997, La Grange Park, Illinois: American Nuclear Society, 1997.

ANSI 2001, *Uranium Hexafluoride – Packaging and Transport*, ANSI N14.1-2001, American National Standards Institute.

AREVA 2003a, *Neutron Source Strength and Spectra in UF₆ as a Function of Enrichment*, Document Identifier 32-2400526-00, Framatone ANP, November 2003.

AREVA 2003b, *Activity and Photon Spectra in UF₆ for Natural, Enriched and Depleted Uranium*, Document Identifier 32-2400524-00, Framatone ANP, October 2003.

AREVA 2003c, *Normalization of UF₆ MCNP Dose Equivalent Calculation*, Document Identifier 32-2400527-00, Framatome ANP, November 2003.

AREVA 2003d, *Dose Equivalent from the Uranium Byproduct Cylinder Storage Pad*, Document Identifier 32-2400507-00, Framatome ANP, November 2003.

ASM International 1990, *Properties and Selection: Nonferrous Alloys and Special-Purpose Materials*, Volume 2 of *ASM Handbook*. Formerly Tenth Edition, Metals Handbook. 5th Printing 1998. [Materials Park, Ohio]: ASM International.

Attix 1986, Attix, F. H., *Introduction to Radiological Physics and Radiation Dosimetry*, John Wiley & Sons, 1986.

Baum 2002, Baum E. M., et al, *Nuclides and Isotopes – Chart of the Nuclides*, 16th Edition, Knolls Atomic Power Laboratory, Lockheed Martin, 2002.

Bell 1970, Bell, G. I. and S. Glasstone, *Nuclear Reactor Theory*, Von Norstand Reinhold Company, New York, New York, 1970.

Cameco 2009, *Assessment of Neutron Dose from Cameco's Port Hope Conversion Facility*, Cameco Corporation, June 2009.

DOE 2001, *Overview of Depleted Uranium Hexafluoride Management Program*, U.S. Department of Energy, Office of Environmental Management, Fall 2001.

DOT, *Shippers – General Requirements for Shipments and Packaging*, 49 CFR 173, U.S. Department of Transportation.

Engineering ToolBox 2013, *Earth or Soil: Weight and Composition*, The Engineering ToolBox, http://www.engineeringtoolbox.com/earth-soil-weight-d_1349.html, retrieved in 2013.

EPA, *Environmental Radiation Protection Standards for Nuclear Power Operations*, 40 CFR 190, U.S. Environmental Protection Agency.

Groff 1991, Groff, G., *ORIGEN2.1 – Isotope Generation and Depletion Code – Matrix Exponential Method*, RSICC Computer Code Package CCC-371, August 1991.

ICRP 1971, *Data for Protection Against Ionizing Radiation*, ICRP Publication 21, Pergamon Press, Oxford, U.K., April 1971.

ICRP 1987, *Data for Use in Protection Against External Radiation*, ICRP Publication 51, Pergamon Press, Oxford, U.K., 1987.

ICRP 1997, *1997 Conversion Coefficients for Use in Radiological Protection Against External Radiation*, ICRP Publication 74, Pergamon Press, Oxford, U.K., 1997.

Jaeger 1975, Jaeger, R. G. (Editor-in-Chief), *Engineering Compendium on Radiation Shielding, Volume II Shielding Materials*, Springer-Verlag, Berlin, Heidelberg, New York 1975.

Kohrt 2014, Kohrt, R., *UBC Pad Inventory*, Email from R. Kohrt to S. Su, April 16, 2014.

Lang 2012, Lang, R., *GSview 5.0*, Ghostgum Software Pty Ltd., May 4, 2012.

LANL 2000, *Data Updates for the SOURCES-4A Computer Code*, Los Alamos National Laboratory, LA-UR-00-5016, October 2000. SOURCES-4B available from the Radiation Safety Information Computational Center (RSICC) as code package CCC.

LANL 2005, *MCNP5.1.40 RSICC Release Notes*, LA-UR-05-8617, Los Alamos National Laboratory, November 2005.

LANL 2008, *MCNP – A General Purpose N-Particle Transport Code, Version 5*, LA-UR-03-1987, Los Alamos National Laboratory, April 24, 2003 (Revised 2/1/2008).

LANL 2010, *MCNP5 1.60 RSICC Release Notes*, LA-UR-10-06235, Los Alamos National Laboratory, 2010.

LPES 2014, *Risk Assessment for the Transport of Radioactive Materials for the Proposed URENCO USA Facility Capacity Expansion, Lea County, New Mexico*, LPES Inc., January 2014.

Mair 2006, *Xming X Server for Windows*, Novel, November 22, 2006.

McGinnis 2009, McGinnis, B. R., et al, *Survey of Field Measurements on UF₆ Cylinders Using Electromechanically Cooled Systems*, Technical paper, 2009.

NCRP 1971, *Protection Against Neutron Radiation*, NCRP-38, National Council on Radiation Protection, January 1971.

NRCa, *Domestic Licensing of Special Nuclear Material*, 10 CFR 70, U.S. Nuclear Regulatory Commission.

NRCb, *Packaging and Transportation of Radioactive Material*, 10 CFR 71, U.S. Nuclear Regulatory Commission.

NRCc, *Physical Protection of Plants and Materials*, 10 CFR 73, U.S. Nuclear Regulatory Commission.

NRCd, *Standards for Protection Against Radiation*, 10 CFR 20, U.S. Nuclear Regulatory Commission.

NRC 2005, *Safety Evaluation Report for the National Enrichment Facility in Lea County, New Mexico*, NUREG-1827, U.S. Nuclear Regulatory Commission, June 2005.

NRC 2008, *Uranium Enrichment Processes, Module 7.0: Depleted Uranium*, Technical Training Center, U.S. Nuclear Regulatory Commission, September 2008.

NRC 2013, *Materials License*, SNM-2010, Condition 21, Amendment 59, U.S. Nuclear Regulatory Commission, October 30, 2013.

NSE 1993, *Benchmarking the MCNP Monte Carlo Code with a Photon Skyshine Experiment*, Nuclear Science and Engineering: 114, pp. 219-227, 1993.

OEPA 2004, *Modifications of Director's Final Findings and Orders of March 12, 2004*, Ohio Environmental Protection Agent, November 2, 2004.

ORNL 1995, *SCALE-4 Analysis of Pressurized Water Reactor Critical Configurations: Volume 2 – Sequoyah Unit 2 Cycle 3*, ORNL/TM-12294/V2, Oak Ridge National Laboratory, March 1995.

ORNL 2011a, *MAVRIC: MONACO with Automated Variance Reduction Using Importance Calculations*, ORNL/TM-2005/39, Version 6.1, Section S6, Oak Ridge National Laboratory, June 2011.

ORNL 2011b, *ORIGEN-S: Depletion Module to Calculate Neutron Activation, Actinide Transmutation, Fission Product Generation, and Radiation Source Terms*, ORNL/TM-2005/39, Version 6.1, Section F7, Oak Ridge National Laboratory, June 2011.

ORNL 2011c, *Scale: A Comprehensive Modeling and Simulation Suite for Nuclear Safety Analysis and Design*, ORNL/TM-2005/39, Version 6.1, Oak Ridge National Laboratory, June 2011.

ORNL 2013, *SCALE 6.1.2 Update*, Announcement from the SCALE group, Oak Ridge National Laboratory, February 2013.

Parish 2012a, Parish, W., *Neutron Gamma Study Results*, E-mail to R. Kohrt/S. Su, April 24, 2012.

Parish 2012b, Parish, W., *Neutron Gamma Study Results*, E-mail to S. Su, April 27, 2012.

RSICC 2000, *RSCII Computer Code Collection, MCNP4C Monte Carlo N-Particle Transport Code System*, Radiation Safety Information Computational Center, Oak Ridge National Laboratory, April 2000 (Revised July 2000).

RSICC 2013, *MCNP6.1/MCNP5/MCNPX – Monte Carlo N-Particle Transport Code Including MCNP6.1, MCNP5-1.60, MCNPX-2.7.0 and Data Libraries*, RSICC Code Package CCC-810, Radiation Safety Information Computational Center, Oak Ridge National Laboratory, August 2013.

Sanders 2010, Sanders, C. E. and S. Su, *UF₆ Cylinder Dose Assessment at URENCO USA*, Paper Presented at the ANS Radiation Protection and Shielding Division Topical Meeting in Las Vegas, April 2010.

Stanford 2009, *Stanford, N., Electronic vs Passive Dosimetry*, Presented at the 28th International Dosimetry and Records Symposium, June 2, 2009.

TFSI 2007, *Micro Rem / Micro Sievert Tissue Equivalent Survey Meters*, Thermal Fisher Scientific Inc., 2007.

TFSI 2009, *Interceptor User's Manual*, Thermal Fisher Scientific Inc., December 2009.

UD 2002, *Dose Rate Calculations for Uranium Hexafluoride Containers in UAG-2*, UPD/0002296C, Urenco Deutschland, May 2002.

USEC 1995, *Uranium Hexafluoride – A Manual of Good Handling Practice*, USEC-651 (Revision 7), USEC Inc., January 1995.

UUSA 2004, *NEF Safety Analysis Report, Rev. 3*, URENCO USA, September 2004.

UUSA 2005, *Integrated Safety Analysis Summary, Rev. 4*, URENCO USA, April 2005.

UUSA 2010, *UBC Storage Pad Radiation Dose Calculation*, CALC-S-00115, Rev. 0, URENCO USA, September 2010.

UUSA 2012a, *Emergency Preparedness Hazards Assessment, Rev. 1*, URENCO USA, April 2012.

UUSA 2012b, *License Amendment Request for Capacity Expansion at URENCO USA Facility*, LAR-12-10, URENCO USA, November 9, 2012.

UUSA 2012c, *Radiation Dose Calculation of the Site Boundary due to UBC Storage Pad Expansion*, CALC-S-00141, Rev. 1, URENCO USA, August 2012.

UUSA 2013a, *Safety Analysis Report, Rev. 33b*, URENCO USA, March 2013.

UUSA 2013b, *UF₆ Radiation Source Terms for Feed, Tails and Product Cylinders*, CALC-S-00142, Rev. 0, URENCO USA, July 2013.

UUSA 2013c, *Worker Dose Assessment for 10MSWU Site Expansion Activities*, CALC-S-00143, Rev. 0, URENCO USA, July 2013.

Weast 1985, Weast, R.C., ed, *CRC Handbook of Chemistry and Physics*. 66th Edition, Boca Raton, Florida: CRC Press, 1985.

Wilson 1981, Wilson, W. B., et al, *Neutron Production in UF₆ from the Decay of Uranium Nuclides*, Transactions of the American Nuclear Society 38, 176 (1981).